

SYMPOSIUM ON PYROLYSIS REACTIONS OF FOSSIL FUELS
PRESENTED BEFORE THE DIVISION OF PETROLEUM CHEMISTRY, INC.
AMERICAN CHEMICAL SOCIETY
PITTSBURGH MEETING, MARCH 23-26, 1966

SMALL CONTINUOUS UNIT FOR FLUIDIZED COAL CARBONIZATION

By

Robert T. Struck, Philip J. Dudt and Everett Gorin
Research Division
Consolidation Coal Company
Library, Pennsylvania

INTRODUCTION

Since the commercial development of the fluidized-bed technique in World War II, many individuals and groups have applied fluidization to low temperature carbonization of coal. (1-7, 9, 13, 14, 15) In addition to providing rapid heat transfer and good temperature control, the fluidized process produces much higher tar yields than a static carbonization in an oven or Fischer Assay. This is due to rapid heating and removal of vapors, minimizing secondary reactions to gas and coke. (10, 11)

A small-scale unit to study fluidized carbonization normally has two functions, one to determine yields and the other to define operability in a commercial unit. At constant temperature and residence time the yields, particularly of tar, are a function of the sweep gas rate used (volume of fluidizing gas per unit of coal fed), while operability is largely dictated by fluidizing velocity. To maintain both fluidizing velocity and sweep gas rate at commercial levels would require a bed of the same depth as a commercial unit. In a small unit, the resulting high depth-to-diameter ratio would result in severe slugging and a completely unrealistic simulation.

The dilemma was resolved here by designing a continuous unit with an internal stirrer so that it could be run at low gas rates corresponding to commercial sweep rates and still provide rapid heat transfer and mixing. This gives tar yields which match larger scale results and allows a study of tar yield as a function of sweep gas rate. It also permits tar yield information to be obtained from caking coals under conditions which cannot be used in a normal fluidized bed operation since operability is "forced" by the mechanical action of the stirrer.

Although high-volatile coking coals give the highest tar yields, they require preoxidation and/or thermal treatment to prevent agglomeration during normal fluidized carbonization. (3, 4, 5, 7, 9) When evaluating pretreated coals to determine their operability during carbonization (freedom from excessive size growth), it is desirable to match the commercial bed turbulence, i. e., the fluidizing velocity. This can be done with the carbonizer described here by removing the stirrer and operating with a normal fluidized bed. Thus, the unit can be operated either with normal fluidization (and high sweep gas rates) to test operability, or at normal sweep gas rates and sub-fluidization gas velocities, using the stirrer) to evaluate tar yields.

The use of a stirrer to simulate a fluidized bed has been reported by Lastovtsev, et al. (8) In mixing of pigments they report that at a critical blade tip velocity of 5 to 8 m/sec a bed motion similar to that obtained with flow of gases is produced. The blade tip speed used in the work reported here, however, was 0.9 m/sec and was combined with a low flow of gases.

DESCRIPTION OF CARBONIZATION UNIT

A flow sheet of the unit is given in Figure 1. Coal is picked up with recycle gas and conveyed into the side of the carbonizer. Additional recycle gas is fed to the bottom of the bed through a porous plate. Air may be added to either stream. The coal is carbonized and overflows the top of the bed into the char receiver. Gases and vapors pass overhead to either of two liquid recovery trains. The small quantity of char fines which do not settle out in the expanded section is caught by the filter. The clean gases from a recovery train pass through a back pressure control valve and to the inlet of the recycle compressor. Compressed gases are cleaned and sent to rotameters for return to the unit. Net make gases are removed between the pressure control valve and the compressor, either via a wet test meter or by automatic sampling.

The carbonizer itself is six inches in diameter and 20 inches deep in the lower bed section, increasing to 12 inches in diameter in the expanded section. The stirrer consists of a 7/8-inch

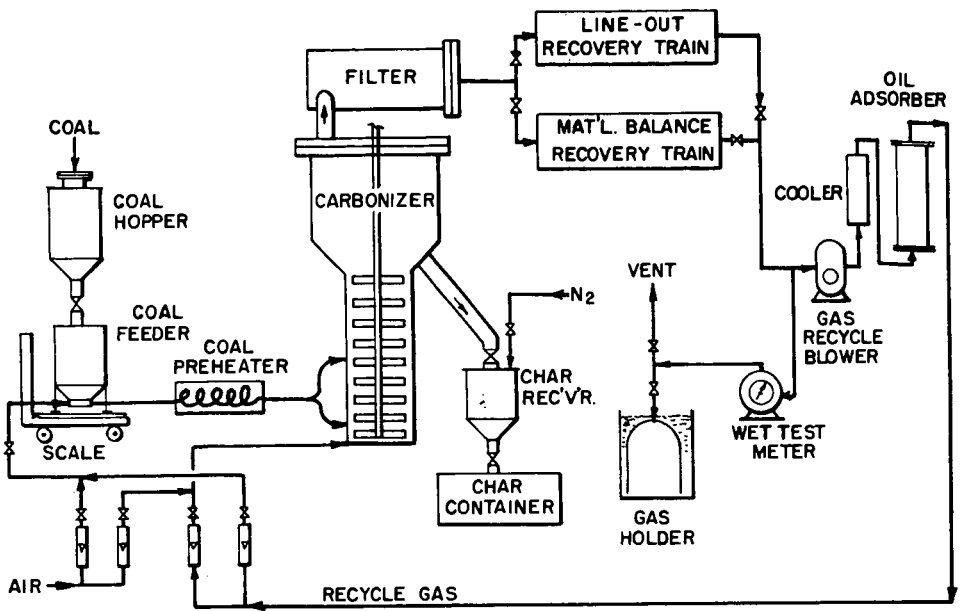
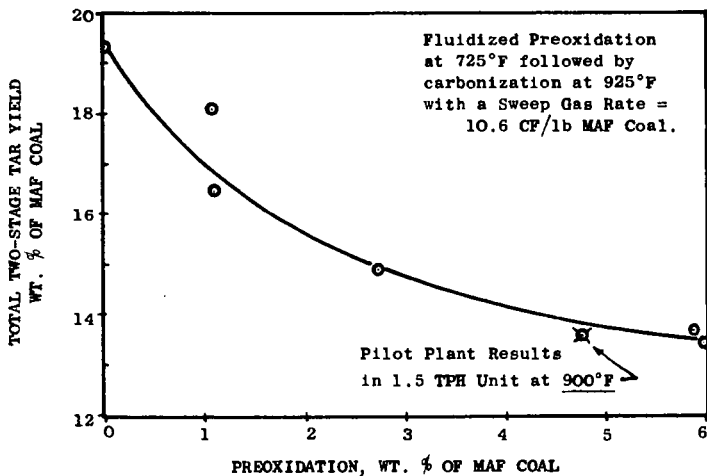


FIG. 1 STIRRED CARBONIZER UNIT

FIGURE 4

THE EFFECT OF PREOXIDATION ON TAR YIELD



shaft on which are mounted thirteen, three-bladed propellers with a left-hand helix. These blades were made from 8-inch blades machined to fit closely to the side walls and are mounted with a thermowell or other baffle extending two inches into the vessel between each blade. The stirrer is rotated at 112 rpm. Temperature is maintained by electrical windings on all sections of the carbonizer.

Coal is ground to pass a 28 mesh screen and charged to the lock-hopper above the feeder. The coal feeder is one developed by S. A. Jones in our laboratories and operates by squeezing coal between two rubber rolls. The rate is varied by changing roll speed and is measured by noting change in weight on a scale on which the feeder and lock hopper are mounted. After passing through the rolls, the coal is picked up by recycle carrier gas and transported through the pre-heater into the carbonizer. The coal preheater is a 16-foot coil of 1/4-inch O. D. tubing coiled to 3-inches O. D. and cast into an aluminum cylinder 5 inches in diameter and 15 inches long. The preheater is electrically wound and its temperature controlled to prevent coking in case the flow stops.

The solid product from carbonization (char) overflows and is lock-hoppered out. The small amount of very fine char elutriated with the gases is removed by a filter maintained at carbonization temperature. This filter is housed in a separate 6-inch vessel above the carbonizer and consists of a 3-1/2-inch O. D. cylinder of expanded metal, 18 inches long, on which about one-half inch of Pyrex wool is wrapped.

In order to provide accurate material balances in two shifts of operation, tar recovery is provided for via two similar trains--one to be used during line-out and the other for a material balance period. The latter train is constructed of aluminum and is taken down completely and weighed before washing out the tar. Both trains include: a) a bare 1-inch pipe cooler, b) an electrostatic precipitator, c) a water-cooled condenser, d) an electrostatic precipitator, and e) a silica gel trap to absorb light oil and water. The electrostatic precipitators consist of 0.0007-inch diameter tungsten wires centered in 2 or 2-1/2-inch pipes by means of spark plugs in the top flanges and weighted glass spiders near the bottom. The power supply is a Trion modified Type B Power Pack supplying up to 20,000 volts D. C.

PROCEDURE

The general procedure for a run is to charge the carbonizer with a start-up bed of char and turn on gas flows, using prepurified nitrogen for start-up. After adjusting pressure and flows, the heats are turned on and the reactor and lines brought up to operating temperature. The coal flow is started with products passing through the line-out recovery train. After the carbonizer has been at the desired temperature long enough to replace the bed three times, flows are switched to the material balance train and the char receiver emptied. At the end of the balance period (at least three inventory changes), the char receiver is again emptied and the flows switched back through the line-out train. Gas samples are taken at the beginning and end of the balance period as well as an integrated sample collected over the whole period. After switching from the balance period, the coal feed is normally stopped, but temperatures and flows maintained for another hour to complete carbonization of the bed inventory. Gas flows are continued as the unit cools down.

After a balance, the recovery train is removed, weighed, and cleaned with benzene. The benzene plus tar plus water is placed in a 5-liter flask and water removed by modified Dean-Stark azeotropic distillation. The recovery train pieces are then further cleaned with methyl ethyl ketone and the effluent combined with the water-free benzene solution. Solvents are then distilled off and the tar analyzed. Light products are recovered from the absorber by heating the trap while it is connected to a vacuum pump through a dry ice-acetone cold trap.

The amount of preoxidation is defined as the weight percent of oxygen consumed, based on moisture- and ash-free coal. All oxygen fed to the carbonizer was completely consumed. In preoxidation, a small breakthrough (ca. 1%) was obtained at lower temperatures and detected with a continuous Beckman Oxygen Analyzer operating on a side stream of overhead gas.

EXPERIMENTAL RESULTS

To illustrate the use of the 6-inch stirred carbonizer, a few results are given from the 1950-54 development of the Consolidation Fluidized Carbonization Process. (1, 13) The coals used were high volatile bituminous coals from the Montour No. 10 and Arkwright mines operating in the Pittsburgh Seam of Western Pennsylvania. Properties of these coals are given in Table 1. All of the results reported here except in Table 4 were obtained with Montour No. 10 coal.

The sweep gas rate as used here is the volume of all gases entering the carbonizer bed at reaction conditions (usually 925°F, 10 psig) per pound of moisture- and ash-free coal fed.

FIGURE 2
THE EFFECT OF SWEEP GAS ON YIELDS FROM
UNTREATED COAL

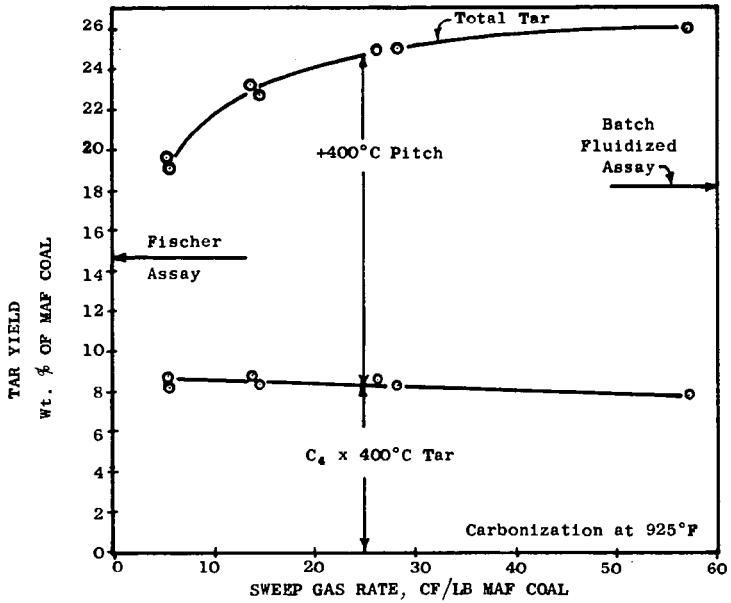
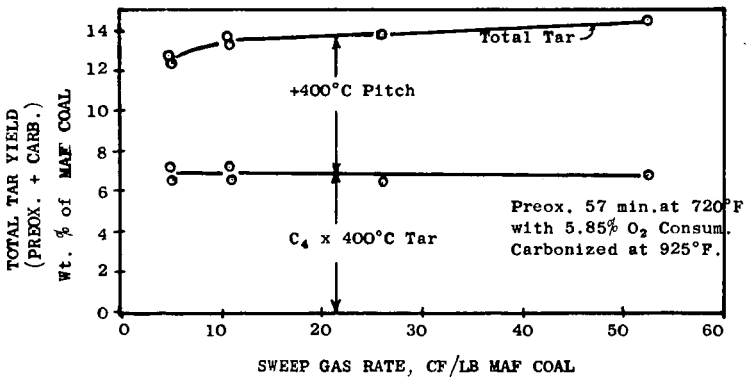


FIGURE 3
THE EFFECT OF SWEEP GAS ON YIELDS WITH
PREOXIDIZED COAL



The exit gas volume is larger by 3 to 5 CF/lb due to gases and water produced. The sweep gas rate in a commercial carbonizer is determined by the coal feed rate per unit of cross-sectional area, the operating pressure and temperature, and the fluidizing velocity (usually 0.8-1.5 ft/sec). The designer thus has some latitude in choosing sweep rate. Generally, they will fall in the range of 5 to 15 CF/lb of coal fed. The effect of sweep gas rate on tar yield was therefore studied over the range of 5 to 60 CF/lb.

The effect of sweep gas rate on tar yield from carbonization of untreated coal at 925°F is shown in Figure 2. The retort pressure was held constant at 10 psig throughout this series of runs, and the solids residence times were long enough so that essentially all available tar was evolved (45-120 minutes).

It can be seen that the total tar yield increased with sweep gas rate, particularly at low sweep gas rates. Note, however, that the increased tar is entirely in the +400°C pitch fraction, and the incentive to increase its yield would depend upon an economic balance between increased value and increased cost. It is clear, therefore, that the major effect of higher sweep gas rates is to aid in the evaporation of high molecular weight pitch molecules. The pitch yield apparently is controlled by saturation of the gas with pitch vapor. On this basis the controlling variable at constant temperature would be the sweep rate as defined above.

Results of two batch carbonization assays are also shown on Figure 1. One is the familiar Fischer Assay in which coal is heated without gas injection in a static retort. The fluidized assay is a method developed by G. P. Curran of our laboratories to assay coals for fluidized carbonization. A 400 gram charge of coal or coal diluted with coke is fluidized in a 2-inch diameter retort at 0.3 ft/sec with nitrogen. Both assays heat to a final temperature of 932°F (500°C) and the heating rates over the last 80°F are similar (4°F/min.). It will be noted that these two assays represent opposite extremes in sweep gas rate. Thus, the difference between them must be a measure of the effect of increased sweep gas rate for batch carbonization. The fluidized assay gives about 24 percent higher tar yield than the Fischer Assay (18.2 vs. 14.7%) with this coal. The tar yield from the continuous unit is, however, 42% higher than the fluidized assay yield (25.9 vs. 18.2%). This represents the effect of rapid heating in the continuous unit. It is obvious, moreover, that the increase due to rapid heating is also some function of sweep gas rate since the upper curve as it approaches zero sweep rate will fall considerably below the Fischer Assay value plus 42 percent. The ratio of yield in continuous carbonization to that from batch Fluidized Assay varies with the coal used. Table 4 shows that for coals from the same seam this effect is small, but much larger variations can be expected from widely different coals. (11b)

It is interesting to note that Peters (11b) reported about the same tar yield at 1112°F (600°C) in the Lurgi-Ruhrgas unit with no sweep gas as was obtained here at 925°F (496°C) at high sweep rates. Although different coals were used, they had the same Fischer Assay values.

Figure 3 shows the effect of sweep gas rate on tar yield from a coal which was preoxidized before carbonization. Preoxidation and carbonization were conducted separately to provide accurate balances, but the tar yields shown are the sums for both steps. The sweep rate is slightly distorted since preoxidation products did not pass through the carbonizer, but the effect is very minor since the preoxidation tar yield is less than 2 percent absolute.

The effect of sweep rate on tar yield is less pronounced with the preoxidized coal, due to the lower tar yield. Note that the percentage yield loss in the case of distillate is considerably less than the loss in the pitch fraction.

The decrease in tar yield with extent of preoxidation is illustrated in Figure 4. The shape of this curve is typical, but the extent of loss of tar varies widely with the coal used, the preoxidation temperature and residence time, coal size and oxygen partial pressure as well as sweep rate. The amount of preoxidation required to result in an operable carbonizer also varies greatly with the feed coal—for Montour 10 coal it is approximately 4 percent for an unstirred fluidized carbonizer. The fact that preoxidation decreases tar yield has been reported previously (3, 5, 7, 14), but it is difficult to find such a curve as Figure 4. It should be noted that the tar yield of 19.3% at zero oxidation takes into account the reduction in tar yield due to thermal treatment at 725°F without added oxygen. With no pretreatment at 725°F, the yield at this sweep rate is 22 percent as shown in Figure 2.

Also shown in Figure 4 is the result of a run with Montour 10 coal in the pilot plant operating at 1.5 tons/hour feed rate. The point falls below the line for the 6-inch unit since the pilot plant was carbonizing at 900°F instead of 925°F. This and later work with other coals confirm that the 6-inch stirred unit gives a reliable assay of tar yields when sweep gas rates are equal.

TABLE 1
TYPICAL COAL PROPERTIES

Source:	Montour No. 10 Mine Library, Pa.	Arkwright Mine Morgantown, W. Va.
<u>Proximate Analysis (MF)</u>		
Volatile Matter	38.70	38.26
Fixed Carbon	56.00	53.69
Ash	5.30	8.05
<u>Ultimate Analysis</u>		
Hydrogen	5.31	5.17
Carbon	78.96	77.29
Nitrogen	1.60	1.55
Oxygen (By Diff.)	7.57	5.29
Sulfur	1.26	2.65
BTU/LB (Gross)	13,900	14,000

TABLE 2
EFFECT OF AIR INJECTION POINT ON TAR YIELD

Results of a Number of Runs with 5.8 to 6.1% Oxygen Consumed and Carbonized at 925°F with Sweep Gas Rate of 10.5 CF/LB MAF Coal

	Loss of Tar Yield, Lb. Tar/Lb. Oxygen
<u>With Preoxidation</u>	
at 725°F, 1 hr. residence time.	
Loss due to preoxidation.	1.0*
<u>Without Preoxidation</u>	
Air and Coal Enter Carbonizer Together	1.2
Air Enters Above Bed - Sees Vapors Only	0.94
Air Enters Bed Above Coal Feed Point	0.36
Air Enters Bed 4" Below Coal Feed Point	0.0

*With preoxidation, there is a loss due to thermal treatment at 725°F in addition to the loss due to oxidation.

TABLE 3
EFFECT OF VAPOR RESIDENCE TIME ON TAR YIELD AT 925°F.

Run Number	Vapor Residence Time, Seconds			Solids Residence Time (Min.)	Sweep Gas CF/LB MAF	Tar Yield Wt. % of MAF Coal
	In Bed	Above Bed	Total			
29	3	19	22	121	28	25.1
14	7	45	52	44.5	26	24.9
17	5	34	39	58	15	22.7
16	11	73	84	127	14	23.2

TABLE 4
RATIO OF TAR YIELDS FOR DIFFERENT PITTSBURGH SEAM COALS
AT 925°F.

Coal	Continuous Unit		Fluid Assay Tar Yield Wt. % MAF Coal	Yield Ratio Continuous Assay
	Sweep Rate CF/LB MAF	Tar Yield Wt. % MAF Coal		
Montour 10 Mine	28	25.1	18.2	1.38
Arkwright Mine	27	26.2	20.7	1.27

Effect of Carbonizer Air on Tar Yield

The 6-inch stirred unit with its flexibility and accurate material balances proved to be useful for a study of where the carbonizer air should be added for maximum tar yield. Tar yields were determined for runs in which the air was injected: (1) directly above the porous support plate, (2) 4 inches higher, entering with the coal, (3) in the upper part of the bed, and (4) above the bed where it contacted tar vapors only. The results of these runs feeding untreated coal to 925°F carbonization are compared in Table 2 with normal preoxidation plus carbonization with no additional air. All runs consumed approximately 6% oxygen with carbonization at a sweep gas rate of 10.6 CF/lb.

When preoxidation is conducted within the plastic range of the coal, there is a decrease in tar producing molecules due to thermal reactions in addition to the effect of oxygen. The thermal effect varies with temperature and residence time and can be as much as that produced by the oxidation. The loss due to oxygen alone is about 1 lb. tar/lb. oxygen consumed.

The loss due to preoxidation is similar to that obtained in direct carbonization of untreated coal with oxygen injected with the coal. This loss is apparently due to reaction of oxygen with tar or tar producing molecules since injection of oxygen above the carbonizer bed results in approximately the same tar loss. The decreased tar yield when the air is injected into the carbonizer along with the coal has been reported by several investigators. (2, 6)

When oxygen is introduced into the carbonizer bed at some distance above the coal feed point, the loss of tar is considerably reduced. This confirms the report by Lang, et al. (7) that oxygen preferentially attacks char rather than tar vapors where both are present. The best situation occurs where the oxygen is introduced sufficiently below the coal feed point to be largely consumed before it encounters tar vapors. In this stirred unit tar loss was reduced to zero when oxygen was injected four inches below the coal feed point. In a normal fluidized bed with its greater degree of solids and gas backmixing, tar loss is not reduced so completely unless baffles are used to promote it.

Vapor Residence Time

A few runs showing the effect of vapor residence time on tar yield at 925°F are shown in Table 3. Separate control could not be effected over solids and vapor residence times. Work not reported here, however, showed that tar yields were independent of solids residence time within the range given in Table 3. The first two runs shown, at a sweep rate of 27 CF/lb show similar tar yields even though the total residence time of tar vapors varied from 22 to 52 seconds. Similarly the last two runs at a sweep rate of about 14 SCF/lb show similar tar yields with residence times of 39 and 84 seconds. Since commercial vapor residence times would be less, one can be confident that there would be no influence on tar yield at 925°F.

Other work has shown that vapor residence time in the stirred carbonizer can reduce tar yield at higher temperatures. The maximum tar yield from this unit is therefore obtained in the range of 900-950°F. In the Lurgi-Ruhrgas unit where very short residence times prevail, the maximum tar yield is achieved at temperatures as high as 1150-1220°F. (11)

LITERATURE CITED

- (1) Anon., Chem. Eng. News, 34, 1318-20, 1397 (1956).
- (2) Bowling, K. McG., et al., J. Inst. Fuel, 36, 99-107 (1961).
- Bowling, K. McG., and Waters, P. L., Brit. Chem. Eng. 7, 98-101 (1962).
- (3) Boyer, A. F., Ann. mines Belg. 1956, 908-12.
- (4) Bunte, K., et al., Fuel, 12, 222-32 (1933).
- (5) Channabasappa, K. C., and Linden, H. R., Ind. Eng. Chem., 50, 637 (1958).
- (6) INICHAR, Bull. tech. houille derives, No. 14, 449-84 (1957).
- (7) Lang, E. W., et al., Ind. Eng. Chem., 49, 355-9 (1957).
- (8) Lastovtsev, A. M., et al., Khim. Prom. 1962 (11), 815-18.
- (9) Minet, R. G., and Mirkus, J. D., Chem. Eng. Prog., 52, 531-4 (1956).
- (10) Parry, V. F., et al., U. S. Bur. Mines, Rep't. Invest. No. 4954, 43 pp (1953).
- (11a) Peters, W., and Bertling, H., Preprints Am. Chem. Soc. Div. Fuel Chemistry, Vol. 8, No. 3, 77 (1964).
- (11b) Peters, W., Gas und Wasserfach, 99, 1045-54 (1958).
- (12) Petit, D., A.I.M.E. Proceedings, Blast Furnace, Coke Oven and Raw Materials Committee, 11, 209-13 (1952).
- (13) Pursglove, J. (Jr.), Coal Age, 62, No. 1, 70-3 (1957).
- (14) Singh, A. D., and Kane, L. J., Paper to A.S.M.E. Meeting, June, 1947.
- (15) Wilson, P. L. (Jr.), and Clendenin, J. D., Chemistry of Coal Utilization, H. H. Lowry, Ed., Supplementary Volume, p. 427-38, 1085, J. Wiley, 1963.

SYMPOSIUM ON PYROLYSIS REACTIONS OF FOSSIL FUELS
PRESENTED BEFORE THE DIVISION OF PETROLEUM CHEMISTRY, INC.
AMERICAN CHEMICAL SOCIETY
PITTSBURGH MEETING, MARCH 23-26, 1966

MAXIMIZING TAR YIELDS IN A TRANSPORT REACTOR

By

L. D. Friedman, E. Rau, and R. T. Eddinger
FMC Corporation
Central Research and Development Center
Princeton, New Jersey

INTRODUCTION

The objective of the Char Oil Energy Development (COED) project, sponsored by the Office of Coal Research, is to develop an economic process for converting coal to a gas, a liquid and a solid, and to upgrade the coal substance and decrease the delivered cost of coal energy. To achieve an economic process, a maximum amount of liquids and gases and a minimum amount of solid char had to be produced. One technique considered for possible scale up to a commercial process involved the transport of coal in a disperse phase through a hot-wall reactor. The transport reactor was consistent with our philosophy that we needed to heat coal rapidly to obtain maximum volatilization of coal. In addition, this type of reactor provided a ready means for removing pyrolysis products quickly from the hot zone.

The operation of a bench-scale transport reactor has already been described. (1) Those studies demonstrated that char yields decreased as reactor temperatures were raised to 2200°F. but increased at 2400°F. and higher temperatures. Investigation showed that the increased yield of char resulted from the decomposition of product tars and hydrocarbon gases to char and hydrogen. Because a maximum yield of tar was desired, the emphasis of these studies was changed from seeking maximum volatilization of coal at high heating rates to pyrolysis under conditions which avoided the loss of liquids to vapor-cracked carbon. Such operation involved pyrolysis with shorter residence times, so that tar vapors left the reactor before secondary cracking reactions occurred, or with lower temperatures and longer residence times. Most work was done with Elkol coal, a non-caking sub-bituminous C coal. However, some higher-rank coals were also processed to observe whether they would give larger tar yields on volatilization.

EXPERIMENTAL PROCEDURE AND RESULTS

1. Apparatus and Experimental Procedure

The first reactor used shown in Figure 1, had an 8-inch heating zone. This reactor has been discussed in detail. (1) Additional heating zones of one, two and four inches in length were attained with an induction furnace, the length of heating zone being controlled by the length of the inductor surrounding the ceramic reaction tube. The 12-foot reactor, shown in Figure 2, consisted of two 6-foot section of 1/4-inch stainless steel pipe. Each section was heated independently with 6-foot long electrical strip heaters. Coal could be introduced either at the middle or at the inlet of the reactor. When coal was charged at the center, the first half of the reactor was used to preheat the carrier gas. Unless stated otherwise, the carrier gas linear velocity at room temperature was 4.0 ft./sec.

Coking coals were processed in dilute phase in a 3-foot long, vertical 3-inch pipe. Coal was dropped into the reactor through an unheated, 1/4-inch ceramic tube. The sweep gas, either steam, helium, or nitrogen, was passed up the reactor at a linear velocity of less than one foot per second. The velocity was sufficient to extend the coal's residence time within the hot zone, but low enough to prevent turbulence inside the reactor. This technique prevented plastic coal particles from striking each other or the hot walls of the furnace. Char was collected in an 8-inch, unheated bottom section of the reactor, and volatiles left the reactor 6 inches from the top. The recovery section was similar to that shown in Figure 1. Most char entrained in the carrier gas was collected in a cyclone, the balance in a settling vessel, along with tar, or on glass-wool filters. A cold trap after the filters removed moisture from the gas. The gas was metered and sampled for mass-spectrographic analysis.

Chars collected after the cyclone were treated in one of two ways. Some were washed with acetone to remove condensed tar. The recovered char was dried at 220°F., mixed with char from the cyclone and analyzed. Tar was recovered by evaporating the wash acetone. With other chars, the adsorbed tar was determined by the quinoline-solubility technique used for determining free carbon in coal-tar pitch. (5)

The analyses of coals used in these studies are shown in Table 1.

TABLE I
ANALYSES OF COALS

Coal Mine Company	Elkol	Orient No. 3	Federal No. 1	Kopperston No. 2
	Kemmerer Coal Co. Adaville	Freeman Coal Mining Corp. Illinois No. 6	Eastern Associated Coal Corp. Pittsburgh Campbells Creek	
Seam				
State	Wyoming	Illinois	W. Va.	W. Va.
County	Lincoln	Jefferson	Marion	Wyoming
Moisture, %, as-received	12.8	9.4	2.5	2.9
Proximate Analysis, % dry basis				
Volatile Matter	40.7	34.6	37.7	31.6
Fixed Carbon	54.6	58.8	56.8	63.9
Ash	4.7	6.6	5.5	4.5
Ultimate Analysis, % dry basis				
Carbon	70.6	75.0	78.4	85.1
Hydrogen	5.4	4.8	4.9	6.2
Nitrogen	1.2	1.6	1.5	1.5
Sulfur	1.0	1.5	1.9	0.7
Oxygen	17.1	9.7	7.8	2.0
Ash	4.7	7.4	5.5	4.5

2. Results

Using an induction heating furnace, 1-, 2-, and 4-inch hot zones were obtained. These studies were made with a downflow reactor, as opposed to the horizontal reactor used principally in the previous work. The first three runs in Table II show how product distribution varied with shortening of the hot zone.

TABLE II
INDUCTION FURNACE RUNS

Coal Mesh Size	100- x 200-mesh			Minus 5-Micron	
	26	23	21	24	25
Run No.	26	23	21	24	25
Heating Zone, in.	4	2	1	1	1
Furnace Temp., °F.	2400	2400	2400	2400	3000
Coal Conversion, % dry					
Char	54.5	67.1	87.5	87.0	65.0
Tar	3.4	6.0	4.7	2.4	4.0
Water	-	-	-	0.3	3.0
Gases	42.1	26.7	7.8	10.3	28.0
Gas Comp., Mol %					
H ₂	13.6	42.4	-	12.2	37.6
CH ₄	12.3	12.9	-	16.3	6.7
C ₂ 's	16.4	13.7	-	17.0	6.7
CO	50.9	14.9	-	32.6	22.2
CO ₂	6.8	12.9	-	16.2	26.8
Char V. M., % dry	14.6	32.2	37.9	37.3	20.9

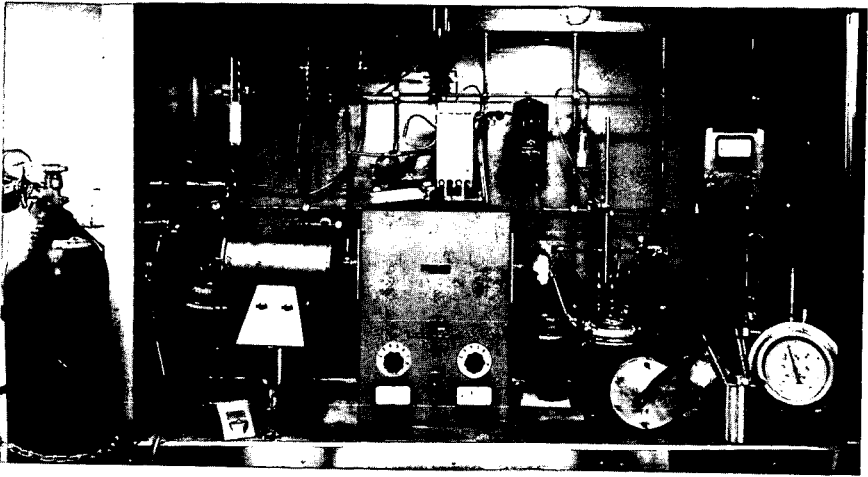


FIGURE 1

Transport Reactor Assembly - Original Reactor

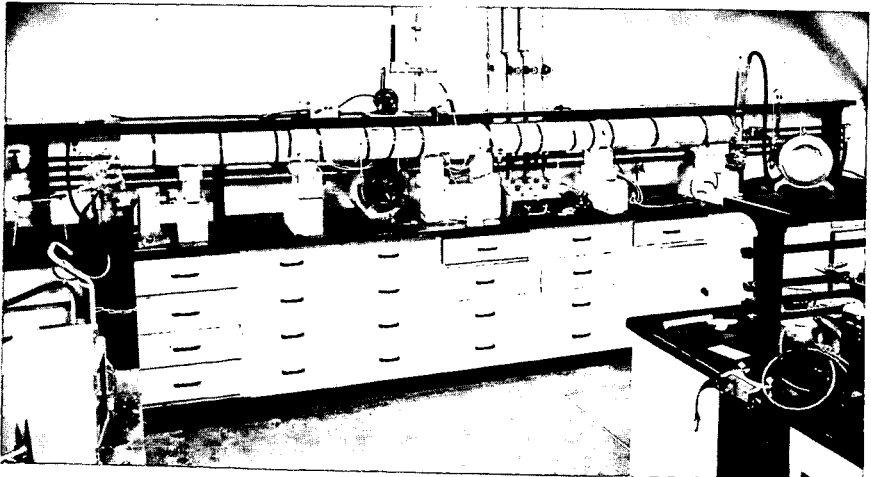


FIGURE 2

Twelve-Foot Transport Reactor

As the zone was shortened from 4 inches to 1 inch, at 2400°F. furnace temperature, the char yield rose from 54.5 to 87.5 percent, gas yields dropped from 42.1 to 7.8 percent, and the volatile-matter content of the char rose sharply. It is obvious that the maximum coal particle temperature was far lower than the indicated furnace temperature. The 6 percent tar yield in Run 23 with the 2-inch hot zone was especially interesting, since it was more than double that obtained at the same furnace temperature with an 8-inch hot zone. Note that some tar was recovered even at a 3000°F. furnace temperature with the 1-inch hot zone. All tars formed in these experiments appeared to be similar to low-temperature-carbonization tars, being brownish in color and quite sticky. Infrared analysis, however, indicated that these tars had a higher conjugated carbonyl-to-alkyl ratio than normal for LTC tar, and were virtually free of long methylene chains commonly found in low temperature tars. These data confirmed that with sufficiently short residence time, tar could be recovered from pyrolysis chambers operated at temperatures considerably higher than tar-cracking temperatures. Some vapor-cracked carbon was found in the run made with the 4-inch hot zone at 2400°F. furnace temperature, but none was found in the runs made with shorter heating zones. Use of the much finer coal in the last two runs did not increase the volatile products, nor was the product distribution different from that obtained with the coarser coal. This is also true when comparing these two differently sized coals in other work done using the 8-inch hot zone of the Lindberg furnace.

The 12-foot reactor gave residence times from 0.7 to 2.0 sec. at temperatures ranging from 500 to 1400°F. These compared with the 0.02 to 0.05 sec. residence times obtained using the 8-inch hot zone in the Lindberg furnace. Using preheated steam as the carrier gas and injecting the Elkol coal at the center of the reactor, tar yields of 16 weight percent of dry coal charge were obtained at temperatures ranging from 1100 to 1400°F. As the reactor temperatures were lowered, the char yields increased and the hydrogen content of the product gas dropped. These results are summarized in Table III. The residual volatile matter in these chars was much higher than in previous transport reactor studies cited, indicating that further processing would yield additional gas and perhaps some tar. Only 4 percent of tar was recovered at a reactor temperature of 825°F.

TABLE III
DEVOLATILIZATION OF ELKOL COAL IN TWELVE-FOOT REACTOR

Run No.	100- x 200-Mesh Coal			Vitrainoids
	Carrier Gas - Steam			
Preheat Temp., °F.	1400	1100	1400	1500
Reactor Temp., °F.	1400	1100	825	1100
<u>Coal Conv., %, dry</u>				
Char	59.0	67.9	91.0	60.0
Tar	16.0	16.2	4.1	20.4
Gas	<u>17.4</u>	<u>10.2</u>	<u>4.9</u>	<u>14.0</u>
Total	92.4	94.3	100.0	94.4
<u>Gas Anal., Mol %</u>				
H ₂	15.5	5.5	12.2	6.0
CH ₄	21.8	23.6	6.1	23.8
C ₂	15.7	12.2	2.2	11.4
C ₃ ⁺	6.6	8.0	1.2	10.0
CO	27.6	19.9	18.3	24.9
CO ₂	12.8	30.8	60.0	23.9
V. M. of Char, %, dry	21.0	27.4	37.5	27.3

The last column in Table III shows data obtained using a concentrate of vitrainoids from the same Elkol coal which was prepared by Bituminous Coal Research, Inc. Over 20 weight percent of tar was recovered from this run--the highest yield obtained from Elkol coal. The product char contained 27.3 percent volatile matter, indicating that additional tar might have been obtained by reprocessing the char at a higher reactor temperature. This run has interesting implications, in that concentration of specific coal macerals offers a way of obtaining more tar from coals by pyrolysis.

If thermal cracking destroyed tars, improved tar yields should result if tars were quenched before decomposition set in. This was the case in some 12-foot studies, as demonstrated in Runs C-970-97 and 98 in Table IV. The coal was introduced with helium as the carrier gas at the beginning of the reactor and steam was introduced at the mid-point of the reactor as the quenching medium. To reduce tar residence time within the hot zone, the helium velocity was raised to 8 ft./sec., twice the normal rate. A temperature profile showed that the steam cooled the center of the reactor 200 to 300°F., but the end of the reactor approached the prequench temperature. The indicated tar yields from these runs, 13.9 and 17.2 percent, respectively, were the highest obtained with helium as the carrier gas. Although sought in several ways, no quenching effects were found in any short reactor, high-temperature studies.

TABLE IV
INCREASE IN TAR YIELDS VIA QUENCHING

100- x 200-Mesh Coal				
Run No.	90	97	91	98
Reactor Temp., °F.	1400	1400	1100	1100
Carrier Gas	He	He	He	He
Quench	None	Steam	None	Steam
<u>Coal Conv., % dry</u>				
Char	48.5 ^a	56.9	57.0	69.5
Tar	11.2	13.9	11.0	17.2 ^b
Gas	21.5	24.2	26.4	6.0
Total	81.2	95.0	94.4	92.7
<u>Gas Anal., Mol %</u>				
H ₂	22.2	10.1	25.6	2.0
CH ₄	29.6	26.6	33.9	18.8
C ₂	15.4	15.0	8.8	15.8
C ₃ +	5.1	7.2	5.2	4.5
CO	15.4	24.3	10.5	18.8
CO ₂	12.3	16.8	16.0	40.1
V. M. of Char, %, dry	15.6	19.4	23.1	28.0

^aSome solids lost.

^b2% moisture may be included.

In the gas analyses presented in Tables III and IV, the CO:CO₂ ratio was less than 1.0 in runs made at or below 1100°F., but was over 1.0 in runs made at higher temperatures. Since this was the case when both steam and helium were used as carrier gas, this phenomenon must have been due to some temperature-dependent decomposition characteristic of this coal, rather than to a water-gas reaction.

Higher-rank coals were devolatilized in a 3-inch diameter vertical reactor. The coal-charging gas to the Syntron feeder was nitrogen, and steam was passed up the reactor to slow the rate at which the coal dropped and to entrain evolved volatiles. Some typical data for Federal coal are shown in Table V. These runs gave tar yields of between 28.5 and 31.5 weight percent of dry coal charged. These were the highest tar yields found throughout these studies. This mode of operation was the only one found suitable for handling strongly coking coals and this is believed to be the first time such coals were devolatilized in this manner.

The Syntron coal feeder was operated in Run 130 employing a minimum quantity of air as the coal-charging gas, about 0.1 cubic foot per minute. Although this amount of air caused the concentration of CO to double and that of CO₂ to increase by a factor of 5 to 10, it had no apparent effect of the yield of tar.

TABLE V
DEVOLATILIZATION OF FEDERAL COAL AT 1100°F.

Run No., C-970	130 ^a	139	144 ^c	149
Coal		Federal (Pittsburgh-Seam)		
Mesh Size	-100	-100	-100	-200
Coal Charged, gm.	43.6	53.0	52.5	148.9
Charge Rate, gm./hr.	101	206.0	105	270
Product Recovery, wt. %, dry coal basis				
Tar-free Solids	48.5	49.7	38.5	57.3
Tar	29.5	29.5 ^b	31.5	28.5
Gas	21.2	-	22.0	11.0
Total	99.2		92.0	96.8
<u>Gas Composition, Mol %</u>				
H ₂	5.0	18.6	17.1	28.6
CH ₄	10.0	40.3	42.9	35.1
C ₂ H ₂	0.0	0.0	0.0	0.0
C ₂	4.4	15.5	14.1	13.2
CO	20.2	12.4	9.5	6.6
CO ₂	58.5	6.2	9.5	8.8
C ₆ H ₆	0.0	6.2	2.3	0.0
C ₃ ⁺	1.9	0.8	2.6	7.7
% Ash in Char, dry basis	8.5	9.7	11.4	10.6

^a Air used as coal charging gas.

^b Gas leak due to plug in feed line.

^c Coal, steam and N₂ passed in bottom of reactor.

Data in Table VI show results obtained from the pyrolysis of Orient No. 3 and Kopperston No. 2 coals in the 3-inch downflow reactor. Both coals gave less tar than the Pittsburgh-seam coal from Federal. Raising the reactor temperature to 1300°F. in Run 40 caused some lowering of tar yields. This was also the case with Federal coal.

Because it contained more hydrogen and much less oxygen than any other coal investigated, it was thought that Kopperston No. 2 coal might give high yields of tar. Data for Run 42 in Table V showed no particular advantage for this low-oxygen coal as far as the tar yield was concerned.

TABLE VI
DEVOLATILIZATION OF ORIENT NO. 3 AND KOPPERSTON NO. 2 COALS

Run No.	39	40	42
Coal	Orient No. 3		Kopperston
Reactor Temp., °F.	1100	1300	1100
Coal Charged, gm.	104	77.5	140.4
Charge Rate, gm./hr.	147	86	210
Product Recovery, wt. %, dry coal basis			
Tar-free Solids	56.1	51.5	73.0
Tar	19.6	17.2	18.7
Gas	13.9 ^a	26.7	1.8 ^a
Total	89.6	95.4	93.5
<u>Gas Composition, Mol %</u>			
H ₂	23.0	47.0	19.4
CH ₄	40.7	31.8	24.7
C ₂ H ₂	0.0	0.0	0.0
C ₂	17.1	10.7	38.0
CO	0.0	0.0	3.6
CO ₂	11.7	7.0	9.2
C ₆ H ₆	0.0	0.2	0.0
C ₃ ⁺	7.5	2.3	5.1
% Ash in Char, dry basis	11.0	13.9	5.3

^aSome gas lost.

DISCUSSION

Throughout these studies it was obvious that chars were not heated to the indicated furnace temperatures. Based on a devolatilization correlation described previously (1), we estimated the temperatures to which chars were heated in the various reactors described. These data are summarized in Figure 3. According to this figure, char pyrolyzed in the 12-foot reactor almost reached the reactor temperature at 825°F., but only reached 1100°F. when the reactor temperature was 1400°F. As the furnace temperature was raised and the heating zone was shortened, the disparity between calculated particle temperatures and furnace temperatures grew. Thus, particle temperatures in a short transport reactor were far below the furnace temperatures, and the difference became greater as the residence time was cut. Increasing the furnace temperature gave sharper heating rates, as indicated by the slopes of the lines for runs made at 2000-2400°F.

No significant amount of vapor-cracked carbon was found in any char having an indicated char temperature of less than 1200°F. in this figure. No vapor-cracked carbon was found in chars from the 12-foot reactor and, as stated above, none was found in runs at 2000°F. in the Lindberg furnace. All these runs, according to Figure 3, had a maximum char temperature of only 1100°F. This temperature might seem low for the amount of volatilization which was obtained. However, other investigators (2, 3) indicated that in the rapid heating of coal, devolatilization was essentially completed at 600°C., or 1112°F.

The existence of a time-temperature relationship in the shock-heated Elkol coal pyrolysis experiments became apparent. Thus, a hot zone of 4 inches at 2400°F. was roughly comparable to 8 inches at 2000°F., and a 1 inch zone at 3000°F. was about as effective as 2 inches at 2400°F. in volatilizing coal. For a carrier gas velocity of 4 ft./sec. calculated at room temperature, an approximate expression for this relationship is

$$Y = 0.0084t + 3.75L$$

where

Y = percent volatilized
t = furnace temperature in degrees R
L = length of hot zone in inches.

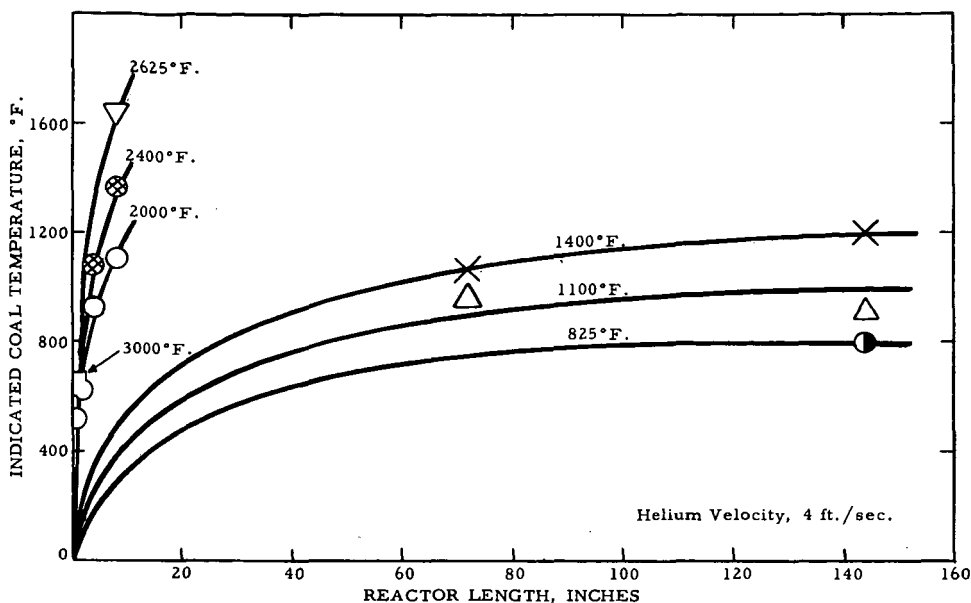
The quenching experiments showed that quenching was effective only when it initiated the cooling of the product vapors. This was the case inside the 12-foot reactor. In the Lindberg furnace, however, the volatilization products were cooled at the end of the furnace in the 5 to 20 milliseconds that elapsed between the time the particles left the hot zone and reached the quench zone. Further quenching at this point, however severe, had no effect on either the product yields or on the distribution of products. The initial cooling at the end of the furnace had already quenched the decomposition reactions.

The transport reactor was designed to permit scaling up to a commercial unit. The alternate approach to achieving the COED objectives employed a 3-inch multistage fluidized-bed system to process coals. (4) Data in Table VII compare transport reactor tar yields with those from the 3-inch fluidized-bed unit. (4) Tar yields from the transport reactor were only slightly lower than those from the fluidized-bed unit. The difference was attributed to the much shorter residence time for vapors in the transport reactor.

TABLE VII
COMPARISON OF TAR YIELDS FROM TRANSPORT
AND FLUIDIZED BED REACTORS

<u>Coal Feed</u>	<u>Transport Reactor</u>	<u>Fluidized-Bed Reactor</u>
Elkol	16.5%	17%
Illinois No. 6	19.6	23
Federal	28.5-31.5	32
<u>Av. Residence Time</u>		
Coal	2 sec.	20 min.
Vapors	0.01-0.7 sec.	1-2 sec.

FIGURE 3
Estimated Elkol Char Temperatures at Various Furnace Temperatures



SUMMARY

Transport reactors proved to be effective laboratory devices for shock-heating coals at rates in excess of 2000°F./sec. At such heating rates more coal was volatilized than was predicted from standard ASTM volatile matter determinations. Both coking and non-coking coals were processed in transport reactors. By controlling heating rates and residence times, yields of tars, chars and gases were varied over fairly wide limits. Highest yields of tars were achieved at reactor temperatures of about 1100°F. and relatively long (0.5 to 2.0 seconds) residence times.

ACKNOWLEDGMENT

The authors wish to thank the Office of Coal Research and the FMC Corporation for permission to present this information. They wish also to acknowledge the help and encouragements of other members of the project staff. All analyses were made by members of the Analytical Department.

LITERATURE CITED

- (1) Paper presented before the Division of Fuel Chemistry, American Chemical Society, Fall Meeting, Chicago, Illinois, September 1964.
- (2) Badzioch, S., B. C. U. R. A. Bulletin 25, (8), 285 (August 1961).
- (3) Peters, W., Chemie-Ing.-Techn. 32 (3) 178 (1960).
- (4) Jones, J. F., Schmid, M. R., and Eddinger, R. T., Chem. Eng. Progress 60 (6) 69 (1964).
- (5) FMC test method.

SYMPOSIUM ON PYROLYSIS REACTIONS OF FOSSIL FUELS
PRESENTED BEFORE THE DIVISION OF PETROLEUM CHEMISTRY, INC.
AMERICAN CHEMICAL SOCIETY
PITTSBURGH MEETING, MARCH 23-26, 1966

PYROLYSIS OF COAL PARTICLES IN PULVERIZED FUEL FLAMES

By

Jack B. Howard
Department of Chemical Engineering
Massachusetts Institute of Technology

and

Robert H. Essenhigh
Department of Fuel Science
The Pennsylvania State University

1. INTRODUCTION

Pyrolysis of coal converts the original material into volatile products and a solid residue. Both the formation of the volatiles and their mass transport out of the decomposing solid are usually included as parts of the pyrolysis process. The kinetics of pyrolysis, being concerned with the rate of the process, is an important consideration in dealing with pulverized coal flames since one mechanism of flame propagation depends upon the rate of appearance of combustible volatiles ahead of the flame front; and, also, heterogeneous combustion is influenced by the rate of pyrolysis behind the flame front. The need for a fundamental understanding of pulverized fuel combustion therefore places pyrolysis studies in a position of primary importance. In addition to this, further stimulation for such studies comes from other areas of current interest such as the investigation of fire spread in fundamental fire research.

This investigation was concerned with the pyrolysis of coal, and was designed to obtain information which would be directly applicable to real flames. To accomplish this end, the flame itself was chosen as the experimental system, thus eliminating potential difficulties with similitude. At the same time, the generality of the results obtained is believed to be even greater than is usually obtained in studies of coal pyrolysis.

The reason for performing this investigation is described best by considering its connection with other research in the field of pulverized fuel combustion. Considerable progress was made in this area, beginning about 1959, by performing measurements in a one-dimensional or flat flame. (7) However, in spite of the favorable capability of this technique, it had not been applied in any study of the region of the flame extending from the flame front to the point at which pyrolysis is essentially complete. Since some studies had been conducted in the regions lying on both sides of it, (1,5) this unexplored pyrolysis zone constituted a gap in the knowledge of the flame, the existence of which was both serious and surprising, in view of the assumed importance of the role of pyrolysis in the process of ignition and flame propagation. The present investigation employed a one-dimensional flame and was designed to fill this gap.

2. PREVIOUS INVESTIGATIONS

Previous investigations of the pyrolysis of coal have shown that the amount of volatile material produced by pyrolysis of a given coal depends upon the temperature to which the coal is heated and the duration of the process. In cases where the particle size is large enough to require a heating time for the center of the particle which is significantly large in comparison with the duration of the process, particle size is an important variable along with temperature and time. However, knowledge is not sufficiently advanced to permit specification of this critical size for a given time of heating.

Most investigators in this area fall into one of two broad categories depending upon their beliefs about the control of the rate of devolatilization. One group supports the proposition that the rate controlling step is the decomposition of the coal (e.g., 21, 16), while the other group advocates physical control, saying that decomposition is faster than diffusion of the volatiles to the surface of the particle (e.g., 4). The investigators in each group support their views with certain experimental observations, and a unifying theory has yet to be produced.

Although the lack of agreement among previous investigators is unfortunate in many ways, the very existence of disagreement has implicit value in indicating that the cause of lack of unification might be the use of many different experimental apparatuses and conditions. Since various types of retorts and flow systems, various particle sizes, and various heating rates have been employed, the disagreement probably results from the dependence of pyrolysis rate on such factors as heating rate, particle size, and type of experimental system. Thus, the use of previous results in a system differing markedly from the original experimental conditions appears questionable, especially in the case of extreme differences.

The pulverized coal flame differs enormously from systems in which pyrolysis has been studied. Instead of a particle size of around 5 mm, the flame employs an average size of about 0.03 mm; instead of a heating time of around 30 minutes, the time in the flame is around 0.5 seconds; and, instead of a heating rate of around $1^{\circ}\text{C}/\text{sec.}$, the rate in the flame is as high as $10^{4^{\circ}}\text{C}/\text{sec.}$ Therefore, to extrapolate specific results from previous experiments to conditions found in the flame would be with very little confidence, so the need for suitable data in this area is obvious.

3. OBJECT

The object of this investigation was to study the pyrolysis of coal particles in pulverized coal flames, and thus to fill a gap which was found to exist in the knowledge of pulverized fuel combustion. Preliminary measurements in the flame revealed that, contrary to our expectation, a significant amount of heterogeneous combustion occurs simultaneously with rapid pyrolysis so the flame cannot be separated into two distinct zones, one containing only heterogeneous combustion and one containing only devolatilization. Therefore, in addition to pyrolysis, the study was designed to include ignition and heterogeneous combustion as well, because of the expected interdependence of these three processes.

The immediate goal of the investigation was to measure the rates of both pyrolysis and heterogeneous combustion in the flame and to employ the results thus obtained to determine: (1) important characteristics of the kinetics of pyrolysis, such as activation energy; (2) whether pyrolysis is a surface or volume reaction in the case of particle sizes in the pulverized fuel range (0-200 microns); and (3) whether the rate of pyrolysis determines the rate of ignition, and thus the rate of flame propagation.

4. EXPERIMENTAL METHOD

The experimental method consisted primarily of passing a stoichiometric cloud of pulverized bituminous coal and air down through a vertical plug flow reactor in which the particles experienced a known temperature profile established and maintained by the combustion of the coal itself. Upon entering the reactor, the particles were heated rapidly and then pyrolyzed as they passed down through the flame. The decay of volatile matter was observed by withdrawing samples of solid material from several points appropriately spaced along the axis of propagation of the flame, and analyzing them for volatile matter, fixed carbon, and ash content. In addition to this, the temperature profile along the axis of propagation of the flame was measured. The data thus obtained consists of corresponding values of volatile content, fixed carbon content, time and temperature; this is the essential information required for studying pyrolysis kinetics.

5. EQUIPMENT

5.1 Equipment for Producing and Maintaining the Flame

5.1.1 Complete Unit - The equipment for producing and maintaining the flame included the furnace, the fuel-supply system, the air-supply system and the monitoring apparatus. This is described below though further fine detail on the system can be found elsewhere. (9) Figure 1 presents schematically the complete unit.

5.1.2 Furnace - The furnace consists of a "one dimensional", pulverized fuel burner, a vertical combustion chamber, and a flue connection (see Figure 2). The flue connection provides the necessary draft for maintaining flow through the flame. The combustion chamber is of square cross section (internal dimensions of 6.5 in. x 6.5 in.), stands about 6 ft. high, and has walls composed of an insulating fire brick lining (2.5 in. thick) encased with transite sheet (0.25 in. thick).

A row of observation and sampling ports are located along the center line of the front side of the chamber at intervals determined by preliminary measurements; the region in the flame where the rate of pyrolysis and temperature increase is most rapid requires the most closely spaced sampling points. This region occurs just below the "burner".

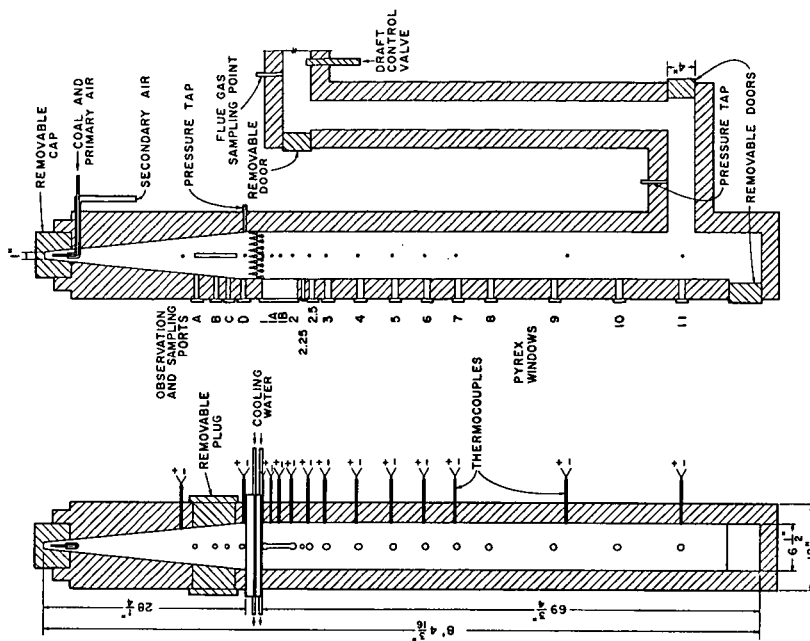


FIGURE 2
EXPERIMENTAL FURNACE

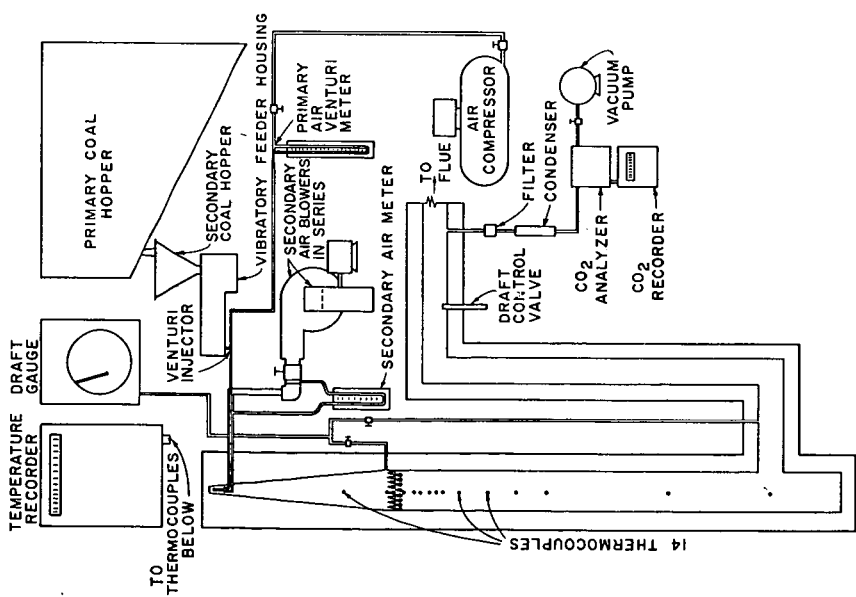


FIGURE 1
SCHEMATIC ARRANGEMENT OF EXPERIMENTAL EQUIPMENT
FOR PRODUCING AND MAINTAINING FLAME

The "burner", which has the geometry of a truncated pyramid of square cross section, sits on top of the combustion chamber and, receiving the supply of fuel and air at its truncation, utilizes the uniform expansion of its sides to supply the cloud to the combustion chamber in plug flow. The burner expands with a total angle of 10.6° between the center lines of its sides, from a cross section of 1 in. x 1 in. at the truncation to a cross section of 6.5 in. x 6.5 in. at the base. The base of the burner is fitted with a two-row bank of water-cooled tubes staggered in such a way that radiation from the flame below cannot pass into the burner, but the cloud can pass into the chamber; the burner and the dust cloud therein are thus maintained cold. Therefore, to reach ignition temperature, the material emerging from the burner must move a finite distance into the combustion chamber and the flame is thereby forced to stabilize a finite distance below the lower surface of the tube bank. In the absence of the tubes, the flame propagates into the pyramidal section and stabilizes at a point where the flame speed is balanced by the velocity of the incoming cloud.

Since the material emerging from the burner is in plug flow, the flame stabilizes with a flat front situated perpendicular to the axis of propagation and thus assumes one-dimensionality. Recirculation currents are absent, and the history of the material collected at a given sampling point can therefore be specified with accuracy. In this respect, the furnace is similar to one constructed and used for pulverized fuel research at the University of Sheffield, (2) the principal difference being that, in the Sheffield furnace, the flame was stabilized in the diverging nozzle or cone (as described above). In our furnace, with the flat flame stabilizing in a parallel sides duct, the system is much closer to the idealized model assumed for the mathematical analysis.

5.1.3 Fuel and Air Supply System - A system was developed for supplying fuel and air at adequately constant and controllable rates and mixture ratios (see Figures 1 and 3). A metered stream of compressed air (primary air) collects the coal from a small funnel fitted into the throat of an asymmetric venturi and injects it up against the truncation of the burner where mixing occurs with a second stream of metered air (secondary air). Utilizing two separate air supplies permits independent control of the supplies of fuel and air, and impinging both streams against the truncation of the burner creates enough turbulence to ensure dispersion of the dust in the resulting cloud.

The rate of coal feed is controlled by adjusting the intensity of vibration of a vibratory feeder enclosed with the venturi funnel in an air-tight box. The coal drops into the venturi funnel after traveling on the feeder tray from a small hopper designed to serve as a self-regulating valve between a larger primary hopper and the rest of the feed system. Continuous circulation of the bed in the primary hopper prevents packing. With this system, the average variation in the rate of coal feed during an experimental run was measured to be 2.8%, and the variation in the air supply rate was nil.

5.1.4 Monitoring Apparatus - Operation under steady conditions was ensured by monitoring the flame with three independent measuring and recording instruments (see Figures 1 and 2): (a) the temperature along the inside surface of one wall was sensed by fourteen sheathed Pt/Pt 10% Rh thermocouples appropriately spaced along the length of the flame, and continuously plotted by a 24-point potentiometer/recorder; (b) the content of carbon dioxide in the combustion gases was monitored by analyzing a continuous sample of flue gas with a thermal conductivity instrument; and (c) the pressure at each end of the combustion chamber was monitored by an oil type, inverted-bell draft gauge. Of the three, the first was by far the most useful; a significant change in the flame was reflected in the wall-temperature profile in a matter of seconds, and could then be corrected.

5.2 Equipment for Probing the Flame

5.2.1 Solid-Sampling Probe - A water-cooled suction instrument was built which collects a sample of particles representative of the material at a point in the flame and quenches it at a sufficiently rapid rate (see Figure 4). The probe is composed of three individually cooled units and is easily disassembled to facilitate cleaning. The requirement that the sampling operation exert no significant influence on the flame forced us to minimize the diameter of the part of the probe penetrating the flame; this resulted in the filter chamber being located outside the flame. In the zone of the flame where particles become sticky because of primary decomposition, clogging of the sampling tube is a menace which prevented us from using a smaller diameter probe.

When the probe is in sampling position, the nozzle points vertically upward and, given the proper suction velocity, collects particles without changing their flow direction until they are already inside the probe. A rotameter and valve in the suction line allowed the proper suction velocity/about five times the main stream velocity(11)/ to be obtained.

A substantial amount of the sample does not reach the filter chamber but instead collects on the cold walls of the probe. We were therefore careful to save the whole sample to avoid both selectivity and contamination.

5.2.2 Suction Pyrometer - A single-shield suction pyrometer was built for temperature measurement (see Figure 5). The instrument uses a Pt/Pt 10% Rh thermocouple, and its

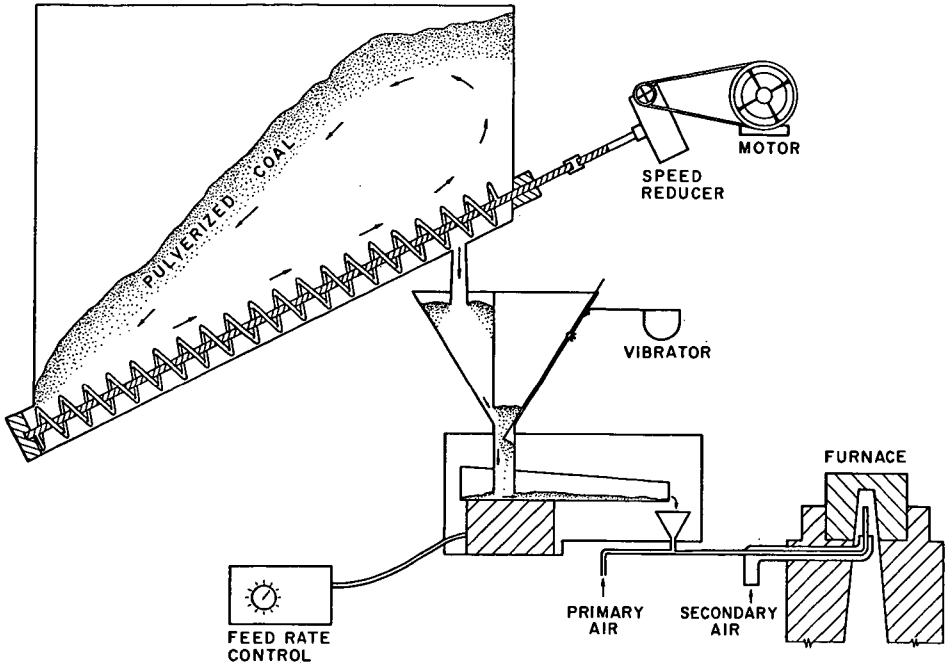


FIGURE 3
FUEL SUPPLY SYSTEM

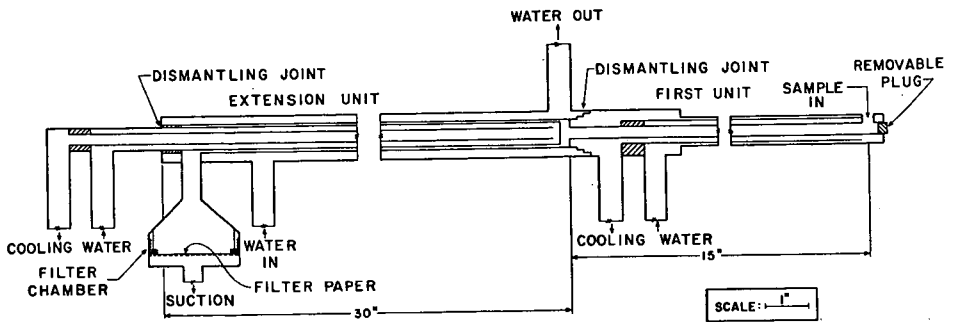


FIGURE 4
SOLID-SAMPLING PROBE

radiation shield and thermocouple protection sheath are made of either mullite or high temperature alumina. The pyrometer is composed of two individually cooled units and a filter chamber, and is easily disassembled for cleaning.

This type of instrument measures a temperature which lies somewhere between that of the particles and that of the gas. (12) However, according to our calculations, there is no significant difference between those two temperatures for particle sizes below about 200 microns, even in the region of the flame where the rate of heating is most rapid. Therefore, the temperature of the particles can be taken as the suction pyrometer temperature.

5.2.3 Probe Supporter and Positioner - Apparatus used for supporting the sampling probe and pyrometer consists of a frame which slides vertically in a track along the front of the furnace (see Figure 6). The track is graduated to permit precision in positioning the instruments: a given sampling point is located with an error of less than 0.5 mm in all three directions.

5.3 Equipment for Analyzing Samples

The equipment used for analyzing the solid samples obtained from the flame was basically the standard apparatus specified by the A. S. T. M. for the proximate analysis of coal. However, the A. S. T. M. directions are based on the availability of plenty of coal (2 gram samples) whereas, in this investigation, the collection of such a large quantity was impossible. The collection also was both time consuming and tedious, so the A. S. T. M. specifications were modified to suit the condition of a limited supply of material for each sample (down to 50 mg). Three alterations were introduced; (1) smaller containers were used for the samples in each test in order to attain the desired accuracy of weighing (Coors size 000 with size B lid); (2) the residue from the volatile matter test was used in the ash test in order to eliminate the need for two different samples; and (3) a small stream of dry nitrogen was passed through the volatile matter furnace to prevent combustion of samples which, either because of previous devolatilization or small size, produced insufficient volatiles to displace the surrounding air. The necessity for these alterations, and the desired effectiveness of each, were demonstrated by extensive preliminary testing. (9)

6. EXPERIMENTAL MEASUREMENTS

6.1 Preliminary Tests

Two important aspects of the experimental system were tested prior to performing the main measurements. These were (1) the absence of recirculation currents in the flame and (2) the quenching ability of the solid sampling probe. A description of each test is given below.

(i) Even before the tests were conducted the flame was believed to be adequately one-dimensional (and therefore free of recirculation currents) on the grounds that: (a) with regard to one-dimensionality, this system is very similar to one at the University of Sheffield which was shown experimentally (3) to produce a one-dimensional flame; and (b) the visually observed flame front was flat. Nevertheless, since our ability to specify the history of a given sample of solid material depends on the absence of recirculation currents, additional verification of this feature was essential. To attain this, the following tracer experiment was conducted. A stream of helium amounting to 7 per cent by volume of the total flow in the furnace was injected into the flame through a 1/4 inch ceramic tube positioned successively at various points along the axis of propagation of the flame and along the center lines of the inside surfaces of two adjacent walls. During injection at each point, a water-cooled probe was used to withdraw samples of flame gases at points displaced both horizontally and vertically from the seeding point. The samples collected were analyzed for helium content with a gas chromatograph capable of detecting traces of helium amounting to less than 0.01 per cent by volume.

The flame and the preignition region between the burner and the flame front were surveyed with this technique: at no point was helium found to be carried vertically upwards as would be expected if a recirculation current were present. Instead, the seeding stream always flowed downwards, spreading laterally at the slow rate expected from molecular diffusion. The conclusion was, therefore, that the flame is free of recirculation currents.

(ii) The quenching ability of the solid sampling probe was determined by measuring the temperature profile in the stream of sampled material flowing through the probe. This was accomplished with a narrow-shield suction pyrometer extending into the probe and positioned successively at several points from the inlet to the exit. As was expected, we found that the temperature of the material at a given position in the probe increases with both increasing suction velocity and increasing flame temperature. When sampling from the hottest point in the flame with the suction velocity employed in the actual experimental runs, the first unit of the probe (see Figure 4) was found to cool the sample from 1520°C (the flame temperature) down to 420°C in a period of 0.01 seconds, and the second, larger unit cooled the sample on down to about 25°C in

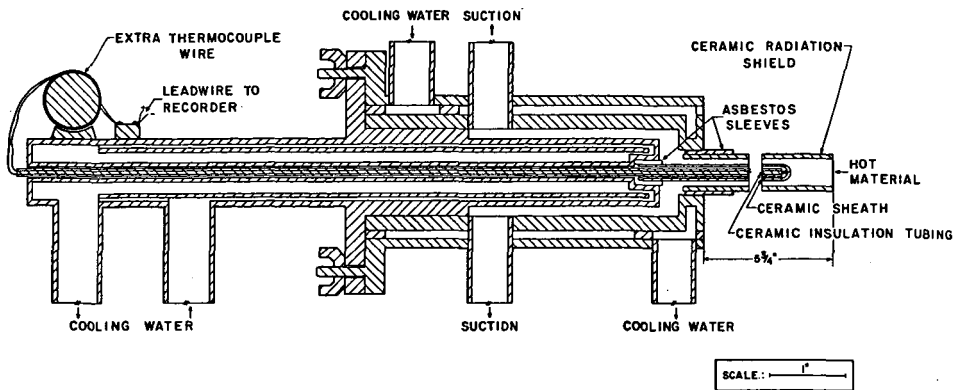


FIGURE 5
SUCTION PYROMETER

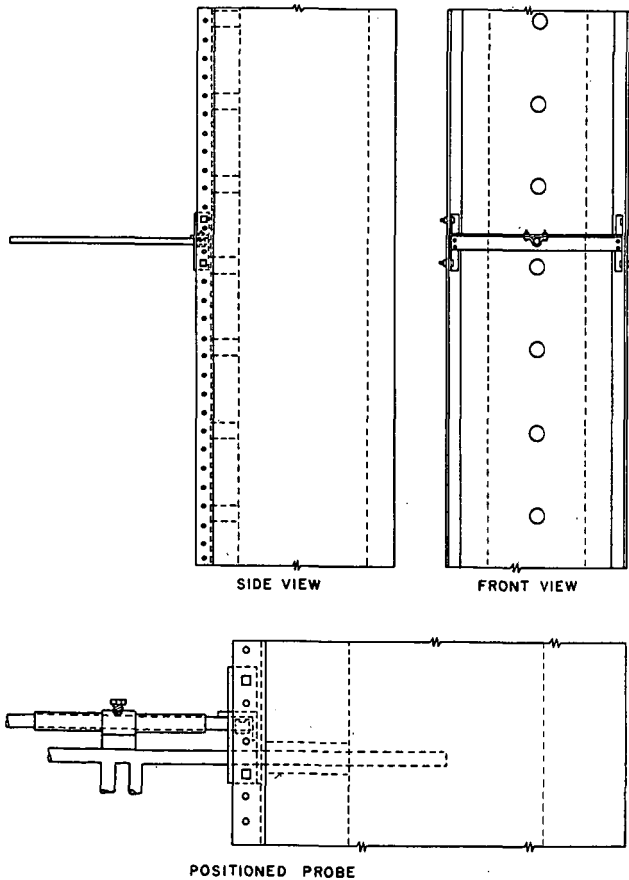


FIGURE 6
PROBE SUPPORTER AND POSITIONER

less than 0.1 seconds. The solid particles leaving the first unit of the probe can be regarded as quenched since the rate of pyrolysis is extremely slow at 420°C, and the time required to attain this inactive state is suitably small. Therefore, the quenching ability of the probe is acceptable.

6.2 Measurements in the Flame

6.2.1 Scope of the Measurements - A single set of experimental conditions was employed during the whole investigation and no attempt was made to study the effect produced on pyrolysis by varying a certain input quantity (feed rate or fuel/air ratio). Runs were repeated only for the purpose of increasing confidence in the observations.

In each experimental run, solid samples were taken and flame temperatures were measured along the flame axis by utilizing the ports in the furnace wall (see Figure 2). In addition to some preliminary exploratory runs, seven data producing runs, each lasting about sixteen hours, were conducted. The samples obtained were analyzed for ash, volatile matter, and fixed carbon.

6.2.2 Experimental Coal - The coal used (trade name, Grade E-5 Ground Coal) was purchased in the pulverized form from the Penn-Rilton Company. The coal came from the Mathies Mine where it is taken from the Pittsburgh seam and ground in a Raymond-Hammer-Screen Mill. The particle size distribution (see Figure 7) was measured with a Coulter Counter; some variation in the size of the coal used in the different runs was found, but this was small enough to be acceptable. The proximate analysis of the coal is as follows: Ash - 3.86% of dry coal; Moisture - 0.97% of raw coal; Volatile Matter - 37.35% of dry, ash-free coal; and Fixed Carbon - 62.65% of dry, ash-free coal.

6.2.3 Experimental Conditions - The flame studied in each run was produced under the following set of conditions:

(i) Coal feed rate	10 pounds per hour
(ii) Flow rate of primary air	6.9 SCFM (1 atm and 70°F)
(iii) Flow rate of secondary air	11.4 SCFM
(iv) Fuel-air ratio	0.135 grams/liter or oz/cu. ft. (at 1 atm and 0°C)

The procedure for stabilizing the flame included first preheating the furnace with a natural gas flame and then making a transition from gas to coal. When the change to coal was completed, a sufficient lapse of time was allowed to ensure stabilized flame conditions. The three monitoring devices described earlier were used to determine flame stability.

6.2.4 Experimental Procedure - The collection of solid samples and measurement of flame temperature followed a procedure in which the probe positioner was fixed at a given port and both instruments were used there before proceeding on to the next port. After collecting a sample of solid material (which required a suction time of about three minutes), the probe and filter chamber were disassembled, the sample was removed and the inside of the probe was thoroughly cleaned. The samples were placed in the same covered crucibles in which they were subsequently analyzed, and then stored in a desiccator.

In the temperature measurements, the thermocouple protection sheaths were replaced after two or three measurements because a coating of ash deposits soon became thick enough to affect the readings. Also, the instrument was disassembled and cleaned before the accumulation of solid material became large enough to affect seriously the flow past the thermocouple.

In each experimental run, three and sometimes four individual samples were collected at each sampled port, and at least 10 and sometimes up to 14 ports were sampled.

6.3 Analysis of Samples

The crucibles containing the samples from the probe were first placed in the moisture oven (with their lids off) for drying. The initial weight was not measured since the moisture content of the samples was not needed, though drying was required since any moisture left in the samples would appear later as apparent volatile material. After moisture removal, the covered samples were cooled in a desiccator, weighed, devolatilized in the volatile furnace (7 minutes at 95°C), cooled in the desiccator, and weighed for volatile loss, all without removing the lids.

Next, the samples, i. e., the remains from the volatile tests, were placed in the ash furnace with the lids removed from the crucibles. After complete burning of the samples, the lids were replaced on the crucibles and the samples were once again cooled in a desiccator. After cooling, the covered crucibles were weighed both with and without the ash remains of the samples.

These four weighings allowed calculation of the contents of volatile matter and ash, both expressed as a percentage of the original, dry sample. The percentage of fixed carbon was then determined by subtracting the sum of these two percentages from 100.

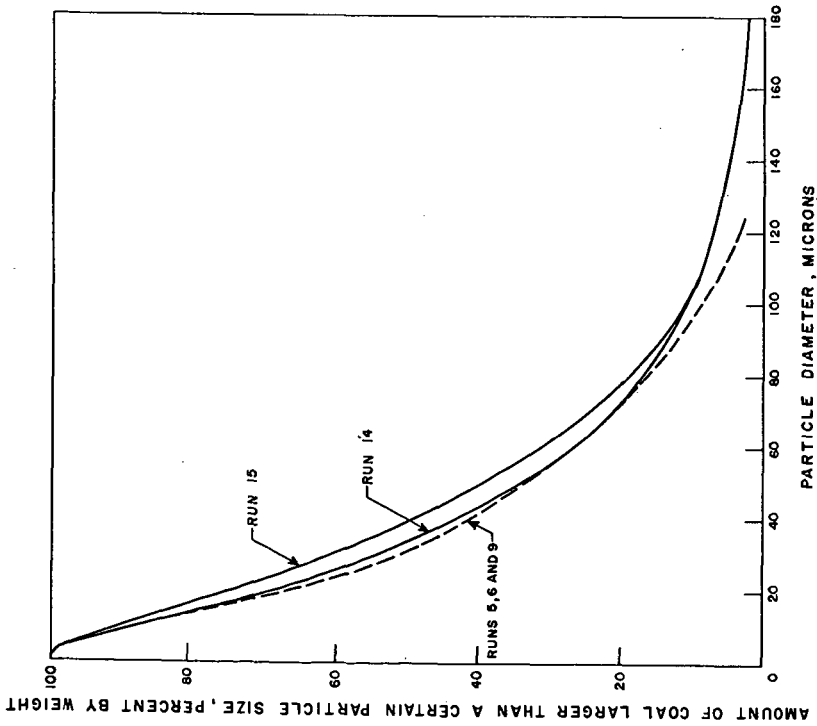


FIGURE 7
SIZE DISTRIBUTION OF COAL USED IN EXPERIMENTAL RUNS

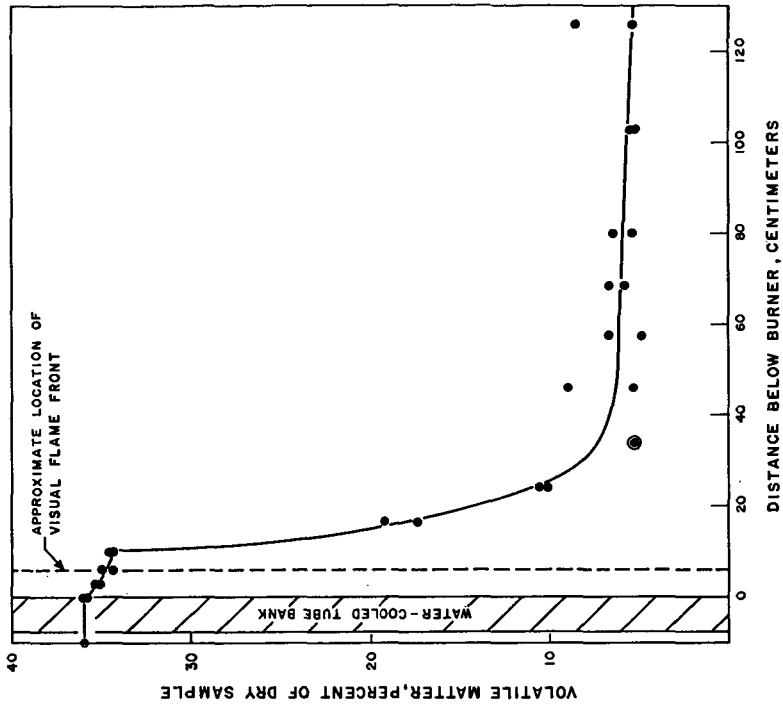


FIGURE 8
VOLATILE MATTER CONTENT OF SOLID MATERIAL DURING
PASSAGE THROUGH FLAME

7. RESULTS

In the following presentation, the data from a single experimental run are used for illustration and can be accepted as a representative example of the data collected in all the runs. Presentation of the data from the other six runs adds no extra value other than illustrating the agreement between runs; this has already been done and the data found to be adequately reproducible. (9)

7.1 Basic Data

The composition of solid material and the temperature of the flame, both measured along the axis of propagation, constitute the basic data obtained (see Figures 8-11). Unexpected observations are that the particles attain a temperature of around 1100°C before either ignition or rapid pyrolysis occurs, and that a significant amount of volatile material exists in the unburned residue leaving the flame. This volatile residue persists over a substantial length of the flame and therefore appears to be a relatively stable component of the original volatile matter. Another significant point to observe is that rapid pyrolysis does not begin until after ignition.

The temperature of the particles begins to rise as they pass through the bank of water-cooled tubes (see Figure 11). Radiation from the flame front first becomes visible to the particles when they are inside the bank; upon emerging from it, their temperature is up to about 480°C. Nevertheless, the composition of the particles remains unchanged until they leave the lower surface of the tubes.

7.2 Useful Arrangement of Data

Since the percentages of volatile material and fixed carbon on a total weight basis are interdependent, a more meaningful arrangement of the data was attained by calculating the two compositions on the basis of their initial values. This allows the contribution to devolatilization of both gaseous evolution and heterogeneous combustion to be studied independently. Also, time is more useful than distance as a kinetics parameter. Accordingly, the basic data can be arranged more usefully as described below.

The conversion from distance to time was made using the known value of the cold flow rate through the combustion chamber and the measured temperature profile. In this calculation it was assumed that the volume change resulting from chemical reaction is small enough to be neglected, an assumption which can be shown to be permissible.

The fractions of the original volatile matter and fixed carbon remaining in the particles at each sampling point were calculated using the ash as a tracer. To achieve this, the following equations, which result from a simple derivation, were employed:

$$\left[\frac{(V. M.)}{(V. M.)_0} \right] = \left[\frac{(\% V. M.)}{(\% Ash)} \right] \left[\frac{(\% Ash)_0}{(\% V. M.)_0} \right] \quad (1)$$

$$\left[\frac{(F. C.)}{(F. C.)_0} \right] = \left[\frac{(\% F. C.)}{(\% Ash)} \right] \left[\frac{(\% Ash)_0}{(\% F. C.)_0} \right] \quad (2)$$

V. M. and F. C. are the weights of volatile matter and fixed carbon remaining in the solid material; %F. C., %V. M. and % Ash are the percentages of the dry material represented by fixed carbon, volatile material and ash; and, the subscript ₀ refers to the original coal. The results of these manipulations of the data are presented in Figures 12 and 13.

The magnitude of the ratio V. M./F. C. at a given point in the flame is indicative of the rate of volatile loss by gaseous evolution relative to the rate of loss by heterogeneous combustion at that particular point. The decay of this ratio with degree of burnout, represented by (F. C.)/(F. C.)₀, is shown in Figure 14.

8. ANALYSIS AND INTERPRETATION

8.1 Qualitative Analysis

8.1.1 Basic Qualitative Behavior - The data presented above furnish a general picture of pyrolysis in the flame. Slow pyrolysis begins when the particles enter the hot combustion chamber at the lower surface of the water-cooled tube bank, and continues for a short time with no accompanying loss of fixed carbon (see Figures 12 and 13). After a period of about 0.05 seconds, heterogeneous combustion, and hence the loss of fixed carbon, begins abruptly with a very rapid rate at a point corresponding to the location of the visually observed flame front (see Figure 13). Soon after ignition, the rate of volatile loss becomes very rapid since volatile matter, in addition to being lost by pure evolution into the gaseous state, is also burned in the

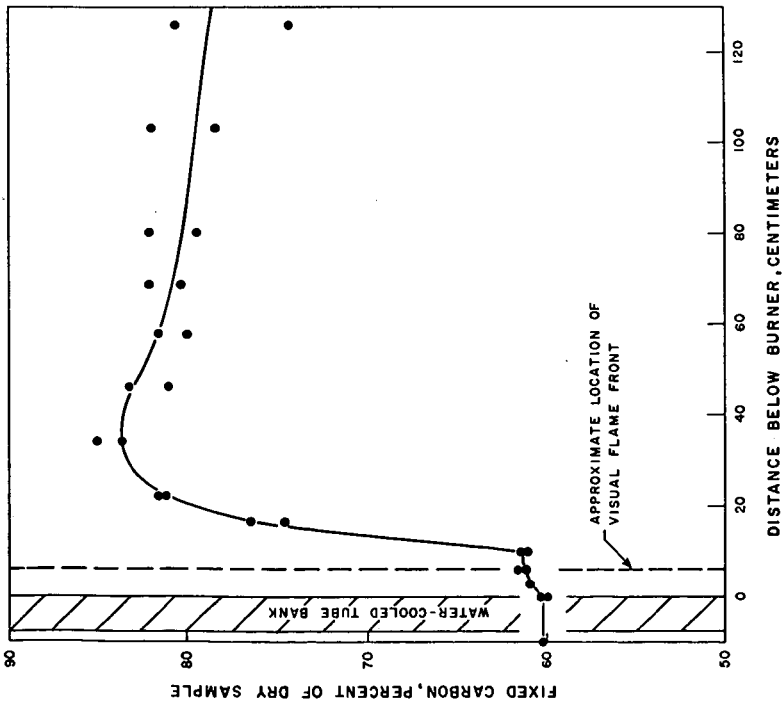


FIGURE 9
FIXED CARBON CONTENT OF SOLID MATERIAL DURING PASSAGE
THROUGH FLAME

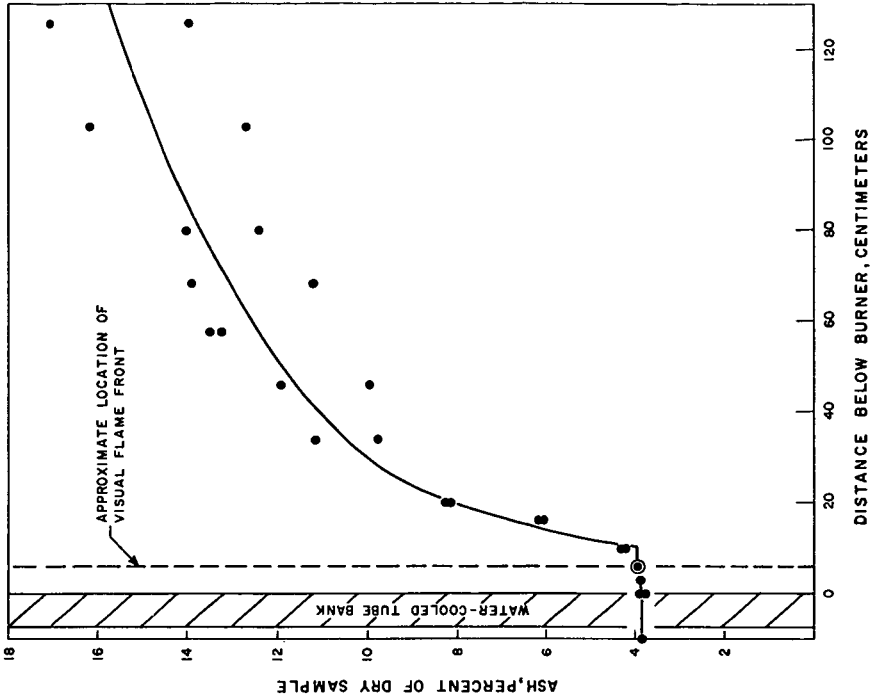


FIGURE 10
ASH CONTENT OF SOLID MATERIAL DURING PASSAGE THROUGH FLAME

solid state along with fixed carbon. Owing to the very small decrease in volatile matter content ahead of the flame front, the rate of combustion of "solid" volatile matter immediately behind the flame front (and before the principal decomposition) would be expected to be as fast as the rate of combustion of the fixed carbon since they are burning together. Furthermore, since the temperature of the particles reaches a substantial value behind the flame front, the rate of evolution increases considerably in that region. After a period of very rapid devolatilization which lasts for about 0.1 seconds, the rate of loss of volatile matter becomes so slow, although about 10 per cent of the original volatile matter still remains in the particles, that about 5 per cent of the original volatile matter is carried from the combustion chamber in the unburned solid residue.

It is instructive to observe the relative amounts of volatile matter and fixed carbon left in the solid material during the combustion process (see Figure 14). During the first 0.05 seconds in the chamber, a small amount of volatile matter is evolved while no heterogeneous combustion occurs; therefore the ratio of volatile matter to fixed carbon drops. Then, heterogeneous combustion begins at such a fast rate that the combustion of solid volatile matter is much faster than the volatile loss by gaseous evolution. Therefore, the ratio of volatile matter to fixed carbon remains essentially constant over a period of about 0.03 seconds while around 10 per cent of the original fixed carbon is burned. Meanwhile, the temperature of the particles becomes so high that the principal pyrolysis reaction, when it finally sets in, is very fast, and the loss of volatile matter by gaseous evolution is much faster than the loss by heterogeneous combustion. Therefore, the ratio of volatile matter to fixed carbon drops rather rapidly over a period of around 0.07 seconds while another 30 per cent of the original fixed carbon is burned. At this point, only about 10 per cent of the original volatile matter is left in the solid material, and the rate of evolution for this last portion is so low that the loss by heterogeneous combustion is again relatively fast and the ratio of volatile matter to fixed carbon decreases very little during the rest of the journey through the flame. This means that the loss of volatile matter in the last 80 per cent of the length of the flame is mainly by heterogeneous combustion.

8.1.2 Qualitative Models - A general, qualitative model, idealizing the progress of pyrolysis, which satisfies these data was selected by eliminating alternative models that were suggested. Of all the models initially proposed for testing, all but two were eliminated because of obvious disagreements or contradictions with the data. The difficulty of choosing between these two survivors required the more detailed analysis outlined below (see Section 8.1.4). Cenosphere formation is not included in these models since the occurrence of cenospheres under the conditions of rapid combustion found in the flame has been shown to be unlikely. (20)

(i) **Model A** is one in which devolatilization is assumed to occur uniformly throughout each coal particle during the whole combustion process. Heterogeneous combustion would be assumed to occur at the surface of the particle so that the particle shrinks as it moves through the flame. Since the volatile material remaining in the particle at any time is uniformly distributed, the rate of combustion of solid volatile matter is always a certain fraction of the rate of combustion of fixed carbon, this fraction being equal to the ratio of volatile matter to fixed carbon, and varying through the flame as shown in Figure 14.

(ii) **Model B** is one which devolatilization is assumed to occur in a thin, moving reaction zone (pyrolysis wave) which is located initially at the surface of the particle; as the particle moves through the flame, the zone moves inward toward the center of the particle. The zone leaves behind a porous matrix which contains the original fixed carbon as well as a component of the volatile matter which is relatively slow to evolve. The unreacted core situated inside the reaction zone is identical in composition to the original coal. Heterogeneous combustion occurs at the surface, and continually shrinks the size of the particle. The proportion of volatile matter being burned in the solid state depends upon the relative speeds of pyrolysis and heterogeneous combustion. If pyrolysis is faster, the pyrolysis zone moves inward so fast that the heterogeneous reaction is left behind at the surface of the porous matrix. In this case, the rate of combustion of solid volatile matter is a constant fraction of the rate of combustion of fixed carbon: the fraction is equal to the ratio of volatile matter to fixed carbon left behind by the devolatilization zone. If the rate of heterogeneous combustion is relatively fast compared to the rate of pyrolysis, the surface of the particle regresses as rapidly as the inward movement of the pyrolysis zone. In this case, both pyrolysis and heterogeneous combustion can occur simultaneously at the surface of the particle, and the loss of volatile matter by heterogeneous combustion can be taken as the total loss of volatiles.

8.1.3 Agreement of Models with Experimental Behavior

(i) **Model A** satisfies the data as follows: In the region of the combustion chamber between the lower surface of the water--cooled tubes and the flame front, pyrolysis occurs uniformly throughout the particle and, since the surface of the particle has not yet ignited, no fixed carbon burns; therefore, the ratio of volatile matter to fixed carbon in the particle drops. Then, the

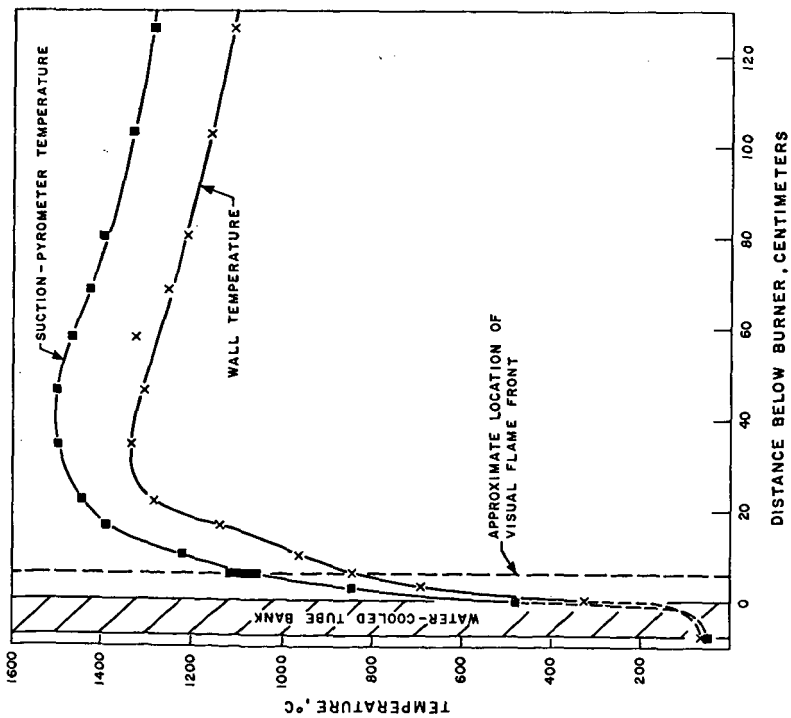


FIGURE 11
 SUCTION-PYROMETER TEMPERATURE OF FLAME AND
 TEMPERATURE OF INSIDE SURFACE OF COMBUSTION
 CHAMBER

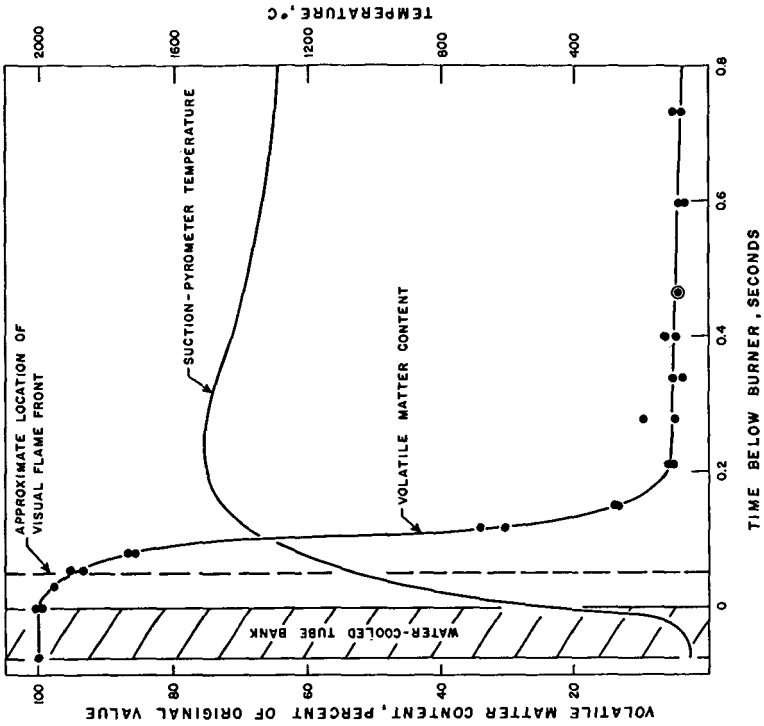


FIGURE 12
 RELATIONSHIP BETWEEN VOLATILE MATTER CONTENT OF
 SOLID MATERIAL, TEMPERATURE, AND TIME

solid particle begins to burn very rapidly while pyrolysis continues at a relatively slow rate; so, therefore, the ratio of volatile matter to fixed carbon remains essentially constant since both materials are burned in approximately the same proportion in which they existed at the onset of heterogeneous combustion. Next, the rate of pyrolysis increases to such an extent that the fraction of volatile matter in the burning particle drops very rapidly while the heterogeneous reaction continues relatively slowly. When only about 10 per cent of the original volatile matter remains in the particle, the rate of pyrolysis becomes so slow that the main source of volatile matter loss is heterogeneous combustion at the shrinking surface of the particle. Therefore, since volatile matter is not completely eliminated from a particle until the solid material is completely burned away, particles which are too large to burn completely in the combustion chamber carry some volatile matter with them as they leave the chamber.

(ii) Model B satisfies the data as follows: The pyrolysis zone starts moving inward as soon as the particle enters the chamber. Until the flame front is encountered, no heterogeneous combustion occurs so the ratio of volatile matter to fixed carbon drops. By the time the surface of the particle begins to burn, the pyrolysis zone is located a certain distance inward from the surface so heterogeneous combustion occurs at the surface of a porous material in which the ratio of volatile matter to fixed carbon is both very small and approximately constant. For a short time immediately following ignition, the regression rates of both the pyrolysis zone and the surface of the particle are such that the ratio of volatile matter to fixed carbon remains approximately constant for the particle as a whole; then the particle becomes so hot that the pyrolysis zone moves sufficiently fast to increase the distance back to the shrinking surface of the particle, to the ratio of volatile matter to fixed carbon decreases. When the pyrolysis zone reaches the center of the particle, the only volatile matter remaining in the solid is the component which is slow to evolve, so the main source of volatile loss in the rest of the combustion process is heterogeneous combustion. Volatile matter and fixed carbon burn together in approximately the same proportion in which they were left by the passing of the pyrolysis zone, since, except for a slow loss of volatile matter by pyrolysis, the ratio of volatile matter to fixed carbon remains approximately constant in the rest of the flame. As in the case of Model A, volatile matter is not completely eliminated from a particle until the solid material is burned away, so large particles can carry volatile matter from the combustion chamber. Qualitatively, therefore, both models are identically comparable with observation.

8.1.4 Tests of Models - According to Model A, pyrolysis occurs uniformly throughout the particle, so the rate of reaction at any time is proportional to the mass (or volume) of unreacted material (volatile matter) still present in the particle, i. e., pyrolysis is a volumetric reaction. Since the total mass (or volume) of material is independent of the size of the particles in which it is contained, this model indicates that pyrolysis should be independent of particle size; therefore, Model A can be disproven if it can be shown that the rate of pyrolysis is dependent upon particle size.

According to Model B, pyrolysis occurs in a thin zone surrounding a solid nucleus in which the volatile matter has not yet reacted. Since the total mass of volatile matter present in such a zone is proportional to the total surface area of the particle, this model indicates that pyrolysis is a surface reaction. Surface reactions are dependent upon particle size; therefore, Model B can be disproven if it can be shown that the rate of pyrolysis is not particle-size dependent.

Model B is considered to be disproven by the following points: (1) The observed time required for pyrolysis is much larger than that predicted from Model B; (2) evidence from the literature (13) indicates there is no influence of particle size on the rate of pyrolysis for particles less than about 60 microns; and (3) calculation of the temperature distribution inside a coal particle in a flame indicates that pyrolysis could not be a surface reaction due to a temperature distribution inside the particle. Each of the above points is amplified below.

(1) Essenhigh (6) found experimentally that the time required to pyrolyze burning coal particles in the size range 0.3 - 5 mm is proportional to the square of the original particle diameter; Essenhigh (6) then showed this result to be in agreement with the proposition that, in the case of particles in the above size range, pyrolysis can be represented by a model in which the rate of devolatilization is governed by diffusional escape of the volatiles from a shrinking reaction zone to the surface of the particle. Model B is effectively identical to Essenhigh's model with regards to the diffusional escape of volatiles, and is therefore suitable for the size range 0.3 - 5 mm.

Assuming that the pyrolysis of particles in the pulverized fuel range (0 - 200 microns) also obeys Model B, two cases are possible: either (1) Model B is obeyed and the rate of devolatilization is controlled by the rate of pyrolysis (chemical control) or (2) Model B is obeyed and the rate of devolatilization is controlled by the rate of diffusion of volatiles to the surface of the particle (physical control). The weight fraction of the original volatile material (V/V_0) remaining in the particle at time (t) is given by the following equations (see Appendix A):

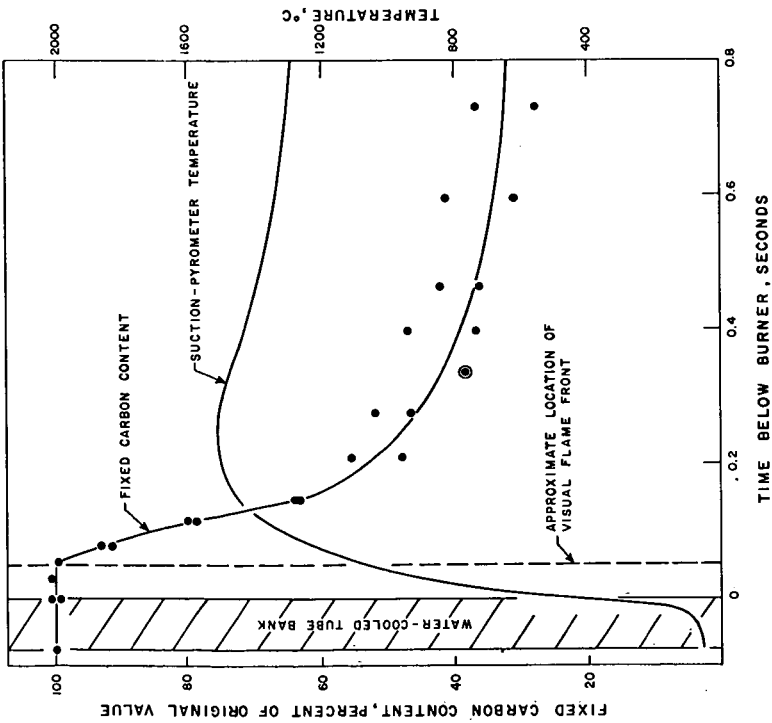


FIGURE 13
RELATIONSHIP BETWEEN FIXED CARBON CONTENT OF
SOLID MATERIAL, TEMPERATURE, AND TIME

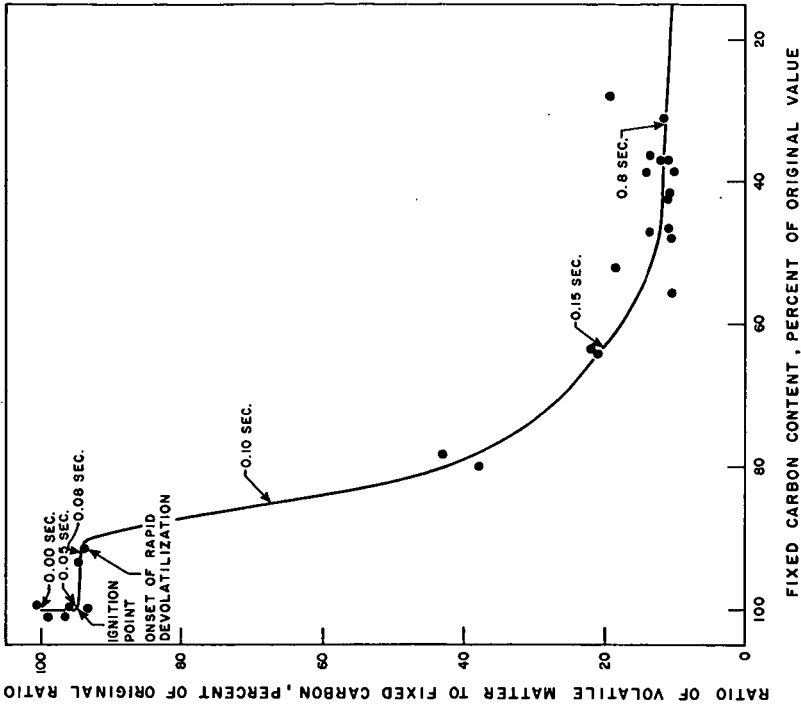


FIGURE 14
VARIATION OF COMPOSITION OF SOLID MATERIAL
WITH DEGREE OF BURN-OUT

$$\text{Case (1), chemical control: } (V/V_0) = (1 - t/t_v)^3 \quad (3)$$

$$\text{Case (2), physical control: } 2(V/V_0) - 3(V/V_0)^{2/3} + 1 = t/t_v \quad (4)$$

where $t_v = K_1 d_0$ for Case (1) and $t_v = K_2 d_0^2$ for Case (2), t_v is the time required to completely devolatilize a particle of initial diameter d_0 , and K_1 and K_2 are constants.

We tested Model B by employing Equations (3) and (4) along with the particle-size distribution (see Figure 7) to calculate the fraction of the original volatile material remaining in the particles at any time after ignition. This was accomplished by separating the particles into several size fractions, analyzing each fraction individually, and then combining the results to construct the total volatile decay curve. Pyrolysis was assumed to begin at the flame front, an assumption which is not far from correct (see Figure 12). Essenhigh's (6) experimental value was taken for K_2 and K_1 was estimated by assuming that chemical rate control is impending in the case of the smallest particles (0.3 mm) studied by Essenhigh (6), thus providing the boundary condition $K_1 d_0 = K_2 d_0^2$ at $d_0 = 0.3$ mm. The results obtained are shown in Figure 15.

The volatile decay rate predicted from Model B is far too large, with the predicted pyrolysis times being about 90-fold too small. This conclusion is the same whether physical or chemical control is accepted, and implies strongly that the dependence of pyrolysis rate on particle size, which is known to occur in the case of particles above 0.3 mm, is not obeyed by particles in the pulverized fuel size range. The extrapolation of results obtained from larger particles down to the p. f. range leads to the prediction of pyrolysis rates which are much too large because, below a certain size, further increase in pyrolysis rate with decreasing particle size is not obtained. Therefore, Model B is unacceptable for particles in the p. f. range.

(2) The above result agrees with the observations of Ishihama (13) who studied the influence of particle size on the lower-limit concentration for inflammability in dusts of several bituminous coals. His results, which are very relevant in the present argument since he studied particle sizes in the p. f. range, show that the influence of particle size upon the concentration required for a lower-limit mixture diminishes as particle size decreases, and below about 60 microns, the effect of particle size becomes inappreciable. Since pyrolysis would be expected to play approximately the same role in inflammability measurements as in a stabilized flame, this observation indicates that pyrolysis rate is independent of particle size when dealing with particles less than around 60 microns. The particle diameters of the coal used in the present investigation were mainly less than this size, so Ishihama's observation should be applicable here.

(3) Information concerning the type of reaction occurring in a coal particle was obtained by calculating the temperature distribution through the particle during the heating process. If the center of the particle is much cooler than the surface, a reasonable assumption would be that the rate of pyrolysis is faster at the surface of the particle and that pyrolysis therefore behaves like a surface reaction. Alternatively, if the temperature distribution is found to be uniform throughout the particle, pyrolysis would seem to be a volumetric reaction. Since the rate of heating is very rapid in a pulverized coal flame, conditions might be expected to be favorable for a nonuniform temperature distribution in which the surface of the particle is much hotter than the center. On the other hand, since pulverized coal sizes are very small, the rate of transport of heat to the center of the particle might be expected to be so fast that the temperature gradient remains rather flat.

The problem of calculating the temperature distribution in a coal particle moving through a flame is one in unsteady state heat transfer and required the consideration of a simplified case in order to avoid mathematical difficulties. The use of this maneuver, although losing generality, still allowed useful results to be attained, particularly of limiting conditions that overestimate the time taken to reach equilibrium.

The case considered is a spherical bituminous coal particle, initially with a uniform temperature profile, suddenly subjected to such rapid heating that the temperature of the surface rises by a certain increment while the inside of the particle remains unchanged. The surface temperature is then held constant while heat flows into the particle; the time required for the temperature of the center to rise by a certain fraction of the initial increment experienced by the surface is indicative of the magnitude of the temperature gradient existing in the particle under real conditions. If the time required for the temperature of the center of the particle to come close to that of the surface is large on the time scale of events in the flame, the temperature of the center of the particle being heated in the flame probably lags behind that of the surface by a significant amount. Alternatively, if the required time is comparatively small, the center of the particle is probably approximately as hot as the surface throughout the heating period.

General mathematical solutions presented graphically in the literature (23) were used, along with physical properties of bituminous coal, in order to obtain a quantitative solution to this

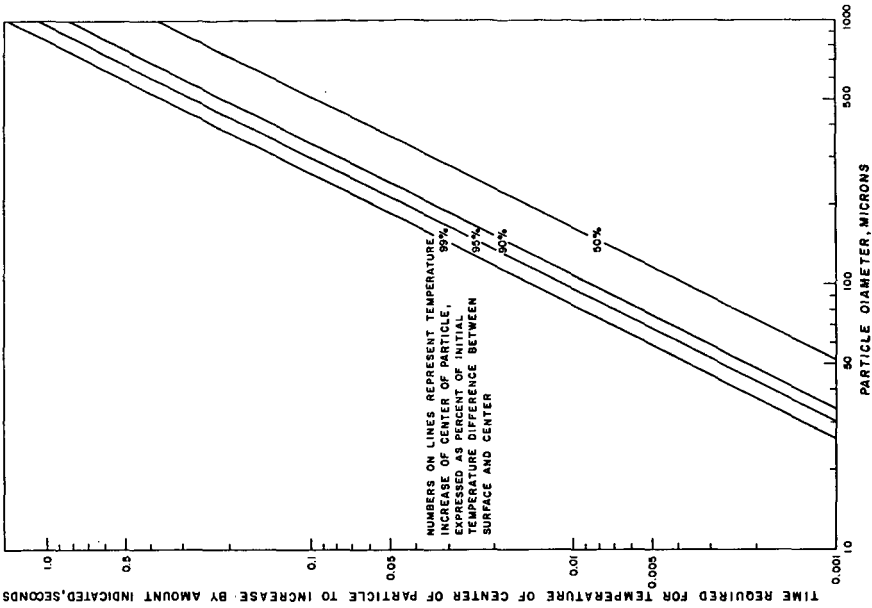


FIGURE 16
INFLUENCE OF PARTICLE SIZE UPON TIME REQUIRED FOR CENTER OF SPHERICAL COAL PARTICLES TO HEAT BY A CERTAIN AMOUNT

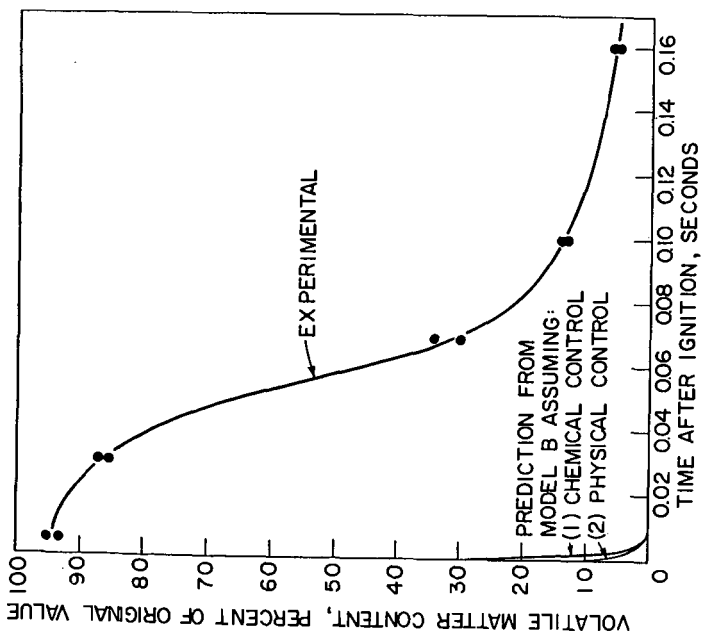


FIGURE 15
COMPARISON OF EXPERIMENTAL VOLATILE DECAY RATE WITH PREDICTION FROM SURFACE REACTION MODEL

problem. The heat absorbed (or generated) by pyrolysis was neglected on the grounds that this has been shown to be a trivial quantity. (14) The results obtained (see Figure 16) indicate that heat transport into the center of the particle is so fast that a significant temperature gradient probably could be neither created nor maintained in particles in the p. f. size range. For example, if the surface temperature of a particle initially at 100°C should suddenly reach 1100°C, about 0.02 seconds would be required for the center to reach 1090°C in the case of a 100 micron particle, and less than 0.001 seconds would be required if the particle size was 30 microns. Both these times are suitably small, especially since the probability of the occurrence of such a drastic temperature gradient is very low and the number of particles as large as 100 microns in pulverized fuel is very small. The conclusion is therefore that pyrolysis is probably not a surface reaction created by a nonuniform temperature distribution.

Data from this and other investigations, as well as the above heat transfer analysis therefore disprove Model B. The inference is that Model A, with the proposition that pyrolysis is a volumetric reaction, is therefore acceptable as there are no experimental grounds for discarding it.

QUANTITATIVE ANALYSIS

9.1 Loss of Volatile Matter

The selection of Model A allows the loss of volatile matter to be described in more detail. The goal of the detailed description is to divide the total loss of volatile matter into two parts, namely, that lost by pyrolysis and that lost by heterogeneous combustion.

At any time t , the total weight of volatile matter lost from the coal is $\Delta(V.M.)$ and can be expressed by the equation

$$\Delta(V.M.) = \Delta V_V + \Delta V_S \quad (5)$$

where ΔV_V and ΔV_S are the weights of volatile matter lost by evolution into the gaseous state, and by heterogeneous combustion, respectively.

According to Model A,

$$dV_S = \int (V.M.)/(F.C.) d(F.D.) \quad (6)$$

where $V.M.$ and $F.C.$ represent the weights of volatile matter and fixed carbon, respectively, and V_S is that part of $V.M.$ which will be lost eventually by heterogeneous combustion. Integration of this equation from the lower surface of the water-cooled tube bank to any point in the combustion chamber provides the following expression for the fraction of the original volatile matter which has been lost by heterogeneous combustion when the coal reaches that point:

$$\int (V_S)/(V.M.)_0 = - \int_1^x \frac{\int (V.M.)/(F.C.)}{\int (V.M.)/(F.C.)_0} \frac{d\int (F.C.)/(F.C.)_0}{\int (F.C.)/(F.C.)_0} \quad (7)$$

where $x = (F.C.)/(F.C.)_0$, $\Delta V_S = (V_S)_0 - V_S$, and the subscript 0 refers to the value of a quantity at the lower surface of the water-cooled tube bank. The negative sign before the integral is necessary since the quantity $d\int (F.C.)/(F.C.)_0$ is negative.

Equation 7 was integrated graphically. It represents the area under a certain portion of the curve formed by plotting $\int (V.M.)/(F.C.) / \int (V.M.)/(F.C.)_0$. An example of this curve has already been discussed (see Figure 14). Values for $(\Delta V_S)/(V.M.)_0$ were thus obtained.

Since the fraction of the original volatile matter which has been lost by both processes is

$$\Delta(V.M.)/(V.M.)_0 = 1 - \int (V.M.)/(V.M.)_0$$

the fraction lost by pyrolysis is, according to Equation 5,

$$\Delta V_V / (V.M.)_0 = 1 - \int (V.M.)/(V.M.)_0 - \int \Delta V_S / (V.M.)_0 \quad (8)$$

This equation was easy to evaluate since values for $\Delta V_S / (V.M.)_0$ were provided by Equation 7, and values for $(V.M.)/(V.M.)_0$ were provided by the data (see Figure 12).

Evaluation of Equations (7) and (8) thus provided a division of the volatile loss into two parts (see Figure 17). It is found that roughly 70 per cent of the original volatile matter is lost by gaseous evolution while about 25 per cent is lost by heterogeneous combustion.

The above analysis provides a basic picture of the process by which volatile matter is lost from the particles, and permits detailed analyses of pyrolysis which would be impossible without this knowledge of the influence of heterogeneous combustion.

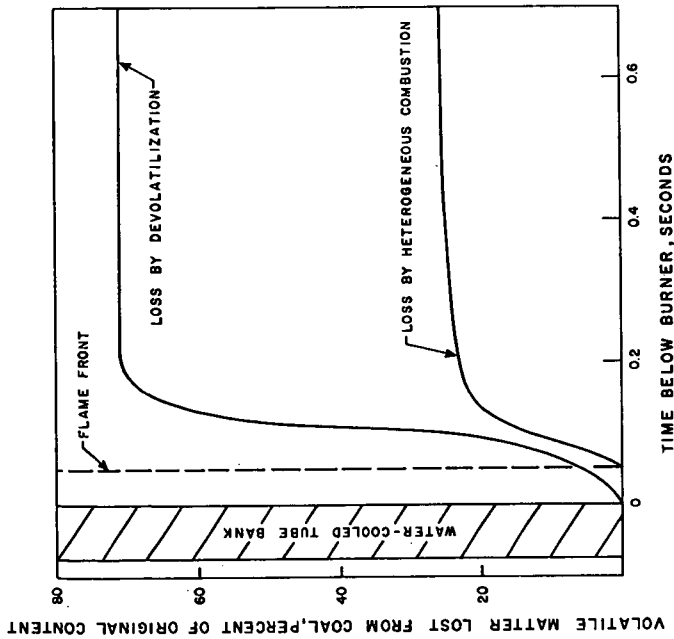


FIGURE 17
LOSS OF VOLATILE MATTER BY HETEROGENEOUS COMBUSTION
AND BY DEVOLATILIZATION

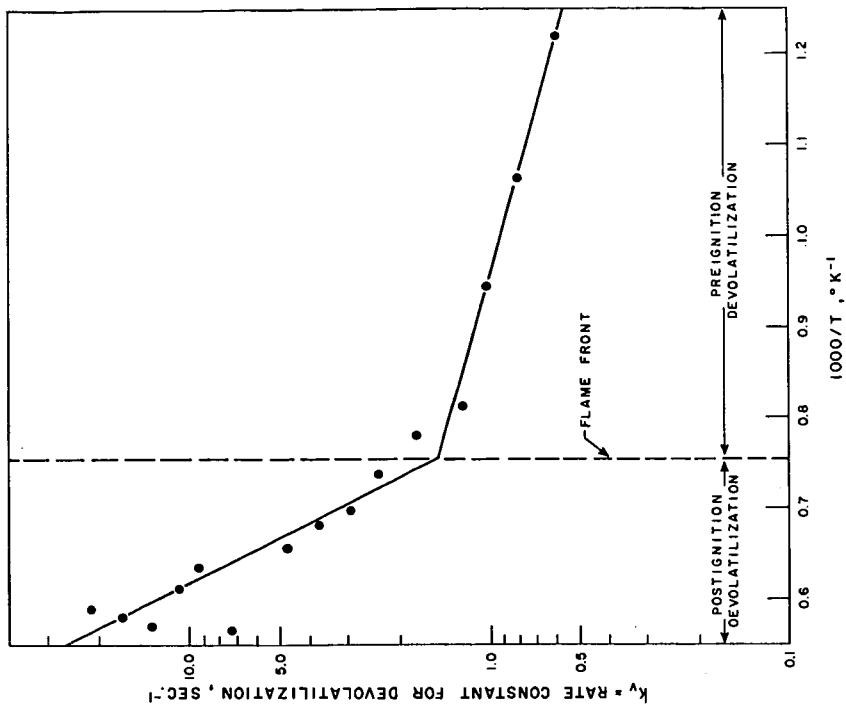


FIGURE 18
ARRHENIUS PLOT FOR EVOLUTION OF VOLATILE MATTER

9.2 Kinetics of Volatile Evolution

Pyrolysis has already been shown to be first-order with respect to the amount of volatile matter left in the solid material (see Section 8.1). The rate of the reaction is therefore given by the expression:

$$d \left[(V.M.) / (V.M.)_0 \right] / dt = -k_v \left[(V.M.) / (V.M.)_0 \right] \quad (9)$$

where $V.M.$ is the weight of the volatile matter left in the solid material at any time t , $(V.M.)_0$ is the initial value of $V.M.$, and k_v is the pyrolysis rate constant. Assuming that pyrolysis is an activated process, we may write

$$k_v = (k_0)_v \left[\exp(-E_v/RT) \right] \quad (10)$$

where $(k_0)_v$ is the frequency factor, E_v is the activation energy, R is the ideal gas constant and T is the absolute temperature.

An attempt to fit the data with Equations (9) and (10) revealed that pyrolysis of the particles in the flame occurs as though the volatile matter exists in the coal in two components, namely, Component I and Component II. Component I decomposes fast enough to be evolved in the flame; but Component II is much slower to decompose, most of it remaining in the solid material after Component I has been evolved. The main loss of Component II is by heterogeneous combustion in the tail of the flame. The volatile matter leaving the combustion chamber in the unburned solid material (see Figures 8 and 12) is part of Component II which, according to these data, represents about 15.5 per cent of the total volatile matter in the original coal. This means that, at the point in the flame where evolution of Component I is essentially completed, the composition of volatile matter in the solid material is about 7.9 per cent of the dry, ash-free material. The devolatilization loss shown in Figure 17 can be taken as a close approximation to the decay of Component I.

The division of the volatile matter into two components has been shown to be in general agreement with the literature. (8) Also, the observation that the slow evolution of Component II allows a significant amount of volatile matter to leave the combustion chamber in the unburned solid residue agrees with the data of Saji (18), who studied flames of pulverized bituminous coal and found that the solid material leaving the furnace contained around 7.5 per cent volatile material. Another point of interest is that the data from the present investigation indicate that the composition of the solid material when the evolution of Component I has just been completed corresponds roughly with the composition at Van Krevelen's (22) carbonization pole.

The experimental data were used to evaluate the activation energy for the evolution of Component I. The rate constant was calculated from Equation (9). The value of the quantity $d \left[(V.M.) / (V.M.)_0 \right] / dt$ at any location in the flame is given by the slope of the devolatilization curve (see Figure 17) at the appropriate point. Values of the quantity $\left[(V.M.) / (V.M.)_0 \right]$ were obtained from a smooth curve drawn through the data (see Figure 12). Since the data give the volatile content of both Component I and Component II, the correct values for this calculation were obtained by subtracting away the amount contributed by Component II.

After obtaining a complete profile of k_v through the flame, E_v was evaluated for Component I by plotting $\ln(k_v)$ against $(1/T)$. According to Equation (10), the slope of the line obtained is $(-E_v/R)$ and the intercept is $\ln(k_0)_v$. The activation energy thus found is different in the preignition and postignition regions of the flame (see Figure 18). The average values found for the different experimental runs are as follows:

$$E_v \text{ in the preignition region} = 6 \text{ kcal/mole}$$

$$E_v \text{ in postignition region} = 28 \text{ kcal/mole}$$

The above values imply that pyrolysis ahead of the flame front is much less temperature dependent than is postignition pyrolysis. The very small activation energy found in the preignition region of the flame indicates that the pyrolysis occurring before ignition involves only very loosely held molecules. Between the burner and the flame front, the major part of the material being evolved probably consists mainly of carbon dioxide and water molecules which were held very loosely in the pores of the original coal.

The activation energy found in the postignition region are about half as large as values which Van Krevelen (21) quotes from the carbonization of coal. This suggests that the pyrolysis reaction occurring in the pulverized-coal flame may be different from that occurring in the relatively slow carbonization process. The activation energy obtained in the postignition zone is for a process occurring in only 0.1 seconds, while Van Krevelen's values are for processes which last for about 1 hour; therefore, different reactions might be expected to occur in the two processes. One possible explanation for the difference is that Component II of the volatile matter is very slow to be evolved because of a high activation energy. In the flame, events are so rapid

that this component is relatively inert with respect to pyrolysis and therefore does not affect the experimental value of activation energy. In slower processes, however, Component II has time to react and therefore could be responsible for the relatively high observed value of the "effective" or "global" activation energy.

10. INFLUENCE OF PYROLYSIS ON IGNITION AND FLAME PROPAGATION

The above data can also be used in a further analysis designed to determine whether ignition in the pulverized coal flame occurs first on the solid surfaces of particles or in gaseous volatiles. The object of the analysis is to evaluate the role of pyrolysis in ignition and flame propagation. If ignition occurs in gaseous material, then the rate of flame propagation is governed by the rate of pyrolysis ahead of the flame front; alternatively, if ignition occurs on the surfaces of solid particles, then the flame speed is independent of the kinetics of pyrolysis. (10) Again, the method of exclusion was employed, the reasoning being that the correct description of the mechanism of ignition can be obtained by disproving its alternative.

10.1 Proposed Models

Two models were constructed for testing: (i) Model C advocates that ignition occurs first on the solid surfaces of particles, with the gaseous material being ignited later following the heterogeneous combustion; (ii) Model D supports the proposition that ignition occurs first in gaseous volatiles, and solid particles are then ignited by gaseous combustion.

Model C can be disproved if it can be shown that the ignition temperature disagrees with accepted values for the ignition temperature of solid surfaces. Model D can be disproved if it can be shown that an inflammable gaseous mixture does not exist at the flame front.

10.2 Test of Models

10.2.1 Complete Mixing Assumed - Before describing the detailed testing of the above models, we should like to point out that the balance of the circumstantial evidence is unfavorable to Model D, thus implying that ignition occurs first on the solid surfaces of particles. Since only a small amount of pyrolysis occurs before ignition (see Figure 8), and since a concentration of combustible gases of only 0.02 per cent by volume was found by using gas chromatography to analyze samples collected from the preignition zone of the flame with a water-cooled gas sampling probe, the existence of a combustible gaseous mixture at the flame front appears unlikely. Assuming complete mixing, an analysis of the data at the flame front shows that the maximum volatile concentration attained before ignition is around 0.0026 grams per grams of air, a value which is short of a combustible mixture by a factor of 10 even if carbon dioxide and water are neglected and all the volatiles are assumed to be methane. If the gas analyses mentioned above are included in the analysis, again assuming well mixed conditions, the maximum concentration of combustible gases before ignition is found to be 300 fold short of an inflammable mixture. However, in spite of this evidence against Model D, the possibility can still exist that the mixing of volatiles into the ambient air is slow enough to permit the establishment of an inflammable gaseous mixture around the surface of each particle by the time the flame front is reached. This possibility is explored below.

10.2.2 Limited Mixing Considered - Although mixing is both diffusional and turbulent, the latter type can be neglected as a first approximation since there should be very little relative motion between the particles and the ambient air in the preignition zone of the flame (Reynold's Number is around 2000). Assuming particles to be spheres, the flow of volatiles away from the surface of the particle can be described by the following equation which was obtained by adapting the standard Stephan flow equation to spherical coordinates, and imposing the condition that the net rate of flow of volatiles away from the particle is equal to the rate of their production by pyrolysis:

$$(P_v)_r = 1 - \int [1 - (P_v)_s] \exp(a^{-1} - r^{-1}) K \quad (11)$$

where

$$K = (RT) \int c_a^3 / 3DPM_v \int [(\% V. M.)_0 / 100] d[(V. M.) / (V. M.)_0] / dt$$

and where: $(P_v)_r$ = partial pressure of volatiles at any distance (r) from the center of the particle; $(P_v)_s = (P_v)_r$ at the surface of the particle; R = ideal gas constant; T = absolute temperature at the location being considered; ρ_c = density of coal; a = radius of the coal particle; D = coefficient of diffusion of volatiles into air; P = total pressure; M_v = average molecular weight of volatiles; $(\% V. M.)$ = percentage of volatile matter in the original coal; $(V. M.) / (V. M.)_0$ = fraction of the original volatile matter remaining in the coal at the location being considered; t = time measured from the lower surface of the water-cooled tubes.

Equation (11) indicates that the profile of the concentration of volatiles around a particle is strongly dependent upon the size of the particular particle being considered, with large particles being surrounded by a higher concentration of volatiles than that around the small ones. This condition is enhanced, but not created, by the selection of Model A since, other things being equal, the flux of volatiles leaving the surface of a particle decomposing by a volumetric reaction increases roughly in proportion to particle size. The implication of this effect is that a relatively large, spherical particle can be visualized as being composed of two concentric, spherical shells, with the common center located at the center of the particle. The inner radius of the smaller shell coincides with the surface of the particle. The common surface of the shells is located at a radial distance where the concentration of volatiles equals the upper limit value for an inflammable mixture. The outer surface of the outside shell is situated at a radial distance corresponding to a lower limit concentration. In the region defined by the smaller shell, the concentration of volatiles is assumed to be so high that no ignition can occur, while the region defined by the larger shell contains an inflammable mixture. Beyond the large shell, the concentration is too low to be ignited.

When this description is applied to extremely small particles, Equation (11) shows that the radii of the hypothetical spheres are equal to (or theoretically less than) the particle radius. This means that no inflammable mixture exists around such particles.

In the case of medium sizes, the outer surface of the larger shell is still maintained away from the particle even though the smaller shell has disappeared. The meaning of this situation is that the material adjacent to the surface of the particle is inflammable, but the location of the lower limit boundary is only a small distance from the surface.

This creates for us the following picture: There exists a critical particle size below which the concentration of surrounding volatiles is too low to support ignition, while, above the critical size, an inflammable mixture is present around the particle, though it is not necessarily adjacent to the surface. The experimental data were used in conjunction with Equation (11) to make a quantitative estimation of the critical size in order to provide evidence for the trial of Model D.

The evaluation of Equation (11) was hampered to a certain extent by insufficient knowledge about boundary conditions. However, by assuming that $(P_V)_r = 0$ when $r \gg a$, the particle radius was found to be

$$a = (K')^{-1/2} \left\{ \ln \left[1 - (P_V)_s / -1 \right] \right\}^{1/2} \quad (12)$$

where

$$K' = (RT \varphi_c / 3DPM_V) \int (\%V.M.)_o / 100 \int \left\{ d \int (V.M.) / (V.M.)_o \int / dt \right\}$$

The critical radius $(a_c)_1$ can be found by imposing the condition $a = (a_c)_1$ when $(P_V)_s = (P_V)_{L.L.}$, where $(P_V)_{L.L.}$ is the partial pressure of volatiles in a lower limit mixture with air. If the volatiles being evolved at the flame front are assumed to be composed chiefly of methane, an assumption grossly in favor of Model D, $(P_V)_{L.L.} = 0.05$. Therefore, when these conditions are substituted into Equation (12), the critical

$$(a_c)_1 = \sqrt{\int (0.153)DPM_V / RT_i \varphi_c \int \left[\frac{(\%V.M.)_o}{100} \right] \left\{ d \int (V.M.) / (V.M.)_o \int / dt \right\}_i dt_i} \quad (13)$$

where the subscript (i) denotes the point of ignition.

The experimental data were used to evaluate Equation (13). The term $d \int (V.M.) / (V.M.)_o \int / dt$ is the slope of the devolatilization curve (see Figure 17) at the point of ignition; T_i is the ignition temperature (see Figures 12 and 13); and since the volatiles are assumed to be methane, M_V is 16 g/mole and D is $0.157 (T_i/273)^{1.75} \text{ cm}^2/\text{sec.}$ (17) if T_i is expressed in Kelvin degrees. The average of the values of $(a_c)_1$ calculated for the different experimental runs is 130 microns. Owing to our neglect of (a) turbulent mixing and (b) the presence of carbon dioxide and water in the volatiles liberated in the preignition zone, this calculated value, though serving as a lower limit, is probably too low by a factor of 2 or 3. Since only a very small fraction of the particles in pulverized fuel is as large as 130 microns, the critical diameter can be regarded as above the pulverized fuel range, thus ruling out the existence of particles surrounded by combustible gaseous mixture.

10.3 Accepted Model (Conclusion)

The conclusion from the above analysis is that the rate of transport of volatiles away from the surface of the particles in the preignition zone of the flame is fast enough to prevent the accumulation of an inflammable gaseous mixture around the particle surfaces. Hence, ignition at the flame front cannot occur in gaseous material, and Model D must be excluded. The strong inference is, therefore, that ignition originates on the solid surfaces of particles; hence Model C

is accepted by exclusion of Model D. Furthermore, the adoption of Model C receives support from the agreement between the ignition temperature observed in this investigation (around 1100°C, see Figures 12 and 13) and values reported in the literature for comparable conditions. (15, 19) The rate of flame propagation can, therefore, be regarded as independent of the rate of pyrolysis.

11. SUMMARY

The pyrolysis of particles in pulverized coal flames was studied by probing a one-dimensional flame. The object of the investigation was to fill a gap which existed in the knowledge of pulverized fuel combustion, and at the same time to improve the understanding of coal pyrolysis. The flame studied was produced in a system employing a new type of "burner", and the water-cooled probes used were developed and tested in this investigation. Measurements were made of the flame temperature and the composition of the solid material in the preignition and postignition regions of the flame as well as in the flame front.

The data thus collected were employed in an analysis designed to formulate a picture of pyrolysis and to evaluate the effect of pyrolysis on flame propagation. The following conclusions were drawn:

(1) The particles attain a temperature of about 1100°C before either ignition or a significant amount of pyrolysis occurs. The rate of pyrolysis does not become significant until after ignition. After a period in which the rate is very rapid, pyrolysis then becomes so slow that about five per cent of the original volatile material leaves the combustion chamber in any unburned solid residue.

(2) Pyrolysis and heterogeneous combustion occur simultaneously, thus making impossible a division of the flame into two distinct zones, one containing only devolatilization and the other containing only solid combustion.

(3) Volatile matter is lost from the particles by both heterogeneous combustion and gaseous evolution; the latter mode of loss accounts for slightly less than 3/4 of the total loss.

(4) Pyrolysis occurs as though the volatile matter in coal is composed of two different components, one of which is evolved very rapidly while the other is much slower to be evolved. The slow-evolving component seems to represent about 15 per cent of the total volatile matter.

(5) Pyrolysis of particles in the pulverized-fuel size range (0-200 microns) is evidently a volumetric reaction occurring uniformly throughout each particle; the rate of pyrolysis in the flame is therefore independent of particle size.

(6) The activation energy of pyrolysis was found to be about 6 kcal/mole in the preignition zone and about 28 kcal/mole in the postignition zone of the flame.

(7) Ignition was found to occur on the surfaces of solid particles instead of in gaseous volatiles; hence the rate of flame propagation is independent of the rate of pyrolysis.

ACKNOWLEDGMENTS

The work described in this paper was carried out in the Combustion Laboratory, Department of Fuel Science, The Pennsylvania State University, University Park, Pennsylvania. We wish to acknowledge joint financial support, and permission to publish, from the Babcock and Wilcox Company (Alliance Research Station) and the State Funds of the Commonwealth of Pennsylvania for Coal Research.

LITERATURE CITED

- (1) Beér, J. M., Ph. D. Thesis, University of Sheffield, Sheffield, England, 1960.
- (2) Beér, J. M., and Thring, M. W., Min. Ind. Exp. Sta. Bull. 75, 1961, p. 25, Pennsylvania State University.
- (3) Beér, J. M., Thring, M. W., and Essenhig, R. H., Combustion and Flame, 3, (1959) 557.
- (4) Berkowitz, N., Fuel, 39 (1960) 47.
- (5) Csaba, J., Ph. D. Thesis, University of Sheffield, Sheffield, England, 1963.
- (6) Essenhig, R. H., J. Eng. for Power, 85, (1963) 183.
- (7) Essenhig, R. H., B. W. K., 12, (1960) 356.
- (8) Essenhig, R. H., and Howard, J. B., American Conference on Coal Science, Pennsylvania State University, 1964, Paper 44 (to be published).
- (9) Howard, J. B., Ph. D. Thesis, Pennsylvania State University, University Park, Pennsylvania, 1965.
- (10) Howard, J. B., and Essenhig, R. H., Combustion and Flame, 9, (1965) 337.
- (11) Howells, T. J., Beer, J. M., and Fells, I., J. Inst. Fuel, 33, (1960) 512.
- (12) Hubbard, E. H., and Pengelly, A. E., Symposium on Flames and Industry, London, 1957, p. A-9, Institute of Fuel, London, 1957.
- (13) Ishihama, W., Eleventh International Conference of Director of Safety in Mines Research, Warsaw, Poland, 1961.
- (14) Millard, D. J., J. Inst. Fuel, 28, (1955) 345.
- (15) Orning, A. A., Trans. A. S. M. E., 64, (1942) 487.
- (16) Pitt, G. J., Fuel, 41, (1962) 267.
- (17) Rohsenow, W. M., and Choi, H. Y., "Heat, Mass, and Momentum Transfer," Englewood Cliffs, New Jersey, Prentice-Hall, 1961, p. 382.
- (18) Saji, K., Fifth Symposium (International) on Combustion, New York, Reinhold, 1954, p. 252.
- (19) Singer, J. M., Ninth Symposium (International) on Combustion, New York, Academic Press, 1963, p. 407.
- (20) Slater, L., and Sinnatt, F. S., Fuel, 3 (1924) 424, 5, (1926) 335, and 6 (1927) 118. McCulloch, A., Newall, H. E., and Sinnatt, F. S., J. Soc. Chem. Ind., 46, (1927) 331T. Sinnatt, F. S., Fuel, 8 (1929) 362.
- (21) Van Krevelen, D. W., and Schuyer, J., "Coal Science." New York, Elsevier, 1957, p. 295.
- (22) Van Krevelen, D. W., Van Heerden, C., and Huntjens, F. J., Fuel, 30, (1951) 253.
- (23) Williams, E. D., and Adams, H. L., Phys. Rev., 14, (1919) 99.

APPENDIX

According to Model B (see Section 8.1), a pyrolyzing spherical coal particle of initial radius r_0 can be visualized as a spherical core (radius = r) of unreacted material surrounded by a spherical shell of thickness ($r_0 - r$). Pyrolysis occurs at the surface of the unreacted core, producing volatile material which diffuses through the surrounding porous matrix to the surface of the particle. The following analysis produces two equations describing the relationship between the weight fraction V/V_0 of the original volatile material left in the particle at time t : one equation describes the case in which the rate of devolatilization is controlled by the rate of diffusion of volatiles out of the particles (physical control), and the other one describes the alternate case in which the rate of pyrolysis is the limiting step (chemical control).

Case I (Physical Control) - According to Essenhig (6), the equation describing the above model under conditions of physical control should be of the form

$$(r - r^2/r_0) dr = - (r_0^2/6t_v) dt \quad (A1)$$

where t_v is the time required for complete devolatilization. Integration of Equation (A1) between the limits $r = r_0$ at time $t = 0$ and $r = r$ at $t = t$, together with the substitution $(r/r_0)^3 = (V/V_0)$, produces the following result.

$$2(V/V_0) - 3(V/V_0)^{2/3} + 1 = t/t_v \quad (A2)$$

Case II (Chemical Control) - In this case, at a given temperature, the rate of devolatilization is proportional to the surface area of the unreacted core, and is expressed as follows:

$$d(V/V_0)/dt = K(r/r_0)^2 \quad (A3)$$

where K is a constant. Since $(V/V_0) = (r/r_0)^3$, Equation (A3) can be integrated between the limits $(V/V_0) = 1$ at $t = 0$ and $(V/V_0) = (V/V_0)$ at $t = t$. When a value is obtained for K by imposing the condition $(V/V_0) = 0$ at $t = t_v$, the resulting expression is found to be:

$$(V/V_0) = (1-t/t_v)^3 \quad (A5)$$

SYMPOSIUM ON PYROLYSIS REACTIONS OF FOSSIL FUELS
PRESENTED BEFORE THE DIVISION OF PETROLEUM CHEMISTRY, INC.
AMERICAN CHEMICAL SOCIETY
PITTSBURGH MEETING, MARCH 23-26, 1966

DISTRIBUTION OF GASEOUS PRODUCTS FROM LASTER PYROLYSIS
OF COALS OF VARIOUS RANKS

By

Fred S. Karn and A. G. Sharkey, Jr.
U. S. Department of the Interior, Bureau of Mines
Pittsburgh Coal Research Center
Pittsburgh, Pennsylvania

Changes in coal and products from coal resulting from thermal treatment have been the subject of many investigations. (1, 6) An extensive bibliography has been included in reference 6. With the exception of the evolution of water and small quantities of light hydrocarbons, coals are but little affected by temperatures up to about 300°C. However, at 500°C as much as 50 percent of some coals can be volatilized. Temperatures of 1,000°C to 5,000°C are of special interest because it is in this range that equilibrium concentrations of acetylene and hydrogen cyanide become significant. Such temperatures can be attained by induction furnaces, plasmas, flash heating, and lasers. (4)

The development of the laser has presented a new opportunity for the study of coal pyrolysis. The laser is a device which compresses light energy three ways: (a) in band width--essentially a single frequency is produced; (b) in time--the energy is delivered in about a milli-second; (c) in area--the beam is approximately the diameter of the laser rod and can be focused. High energy densities and temperatures far exceeding any previously available for the pyrolysis of coals are produced. Temperatures of several thousand degrees centigrade can be attained quickly without sample or product contamination. Laser techniques have been used for the rapid vaporization of metals and graphite at temperatures estimated as 7,000° K to 8,000° K. (7) Light energy from the laser source passes readily through the walls of a glass reaction vessel and can be quickly converted into heat and chemical energy by a dark absorbing medium such as coal. Thus, the laser is a particularly good source of energy for converting coal into gases rich in acetylene and HCN.

Previous attempts at this laboratory to pyrolyze coal at high temperatures using flash and laser techniques have produced more acetylene and less methane than conventional coke oven pyrolysis. (1) Flash photolysis was applied to coals of several ranks by Rau and Seglin and product gases containing up to 16 mole percent of acetylene were reported. (5) Bond has reported acetylene analyses as high as 30 mole percent from the plasma jet irradiation of coal. (6) Arc image techniques have also been applied to the pyrolysis of coal by Rau and Eddinger. (8)

• EXPERIMENTAL PROCEDURE

The following coals were used in this investigation:

<u>Rank</u>	<u>Coal</u>	<u>Source</u>
Anthracite	Dorrance	Pennsylvania
Low Volatile Bituminous	Pocahontas No 3	West Virginia
Medium Volatile Bituminous	Sewell	West Virginia
High Volatile A Bituminous	Pittsburgh	Pennsylvania
High Volatile A Bituminous	Chilton	West Virginia
High Volatile C Bituminous	Rock Springs	Wyoming
Lignite	McLean	North Dakota
Lignite	Sadow	Texas

The coals are listed above in order of decreasing rank according to the American Society for Testing and Materials (ASTM) and International Classifications; that is, according to volatile matter up to 33 percent and according to calorific parameter above 33 percent volatile matter.

Samples (3/8-inch cubes) were sealed in pyrex tubes 10 mm ID and 90 mm long as shown in Figure 1. All samples were heated to 100°C for 20 hours in a vacuum oven, then sealed and irradiated. Five pulses of 1.5 joules of focused energy were impinged on each coal sample. Gaseous products were admitted to the mass spectrometer in five fractions distilling from liquid nitrogen, dry ice, ice water, room temperature, and 60°C baths. The total volume of each fraction was determined and each fraction was analyzed by mass spectrometry. A carbonaceous residue deposited on the wall of the glass tube during irradiation of Pittsburgh seam coal was examined by infrared.

RESULTS AND DISCUSSION OF RESULTS

Gaseous products from coals of several ranks were compared. Analyses of the coals are given in Table 1 and analyses of gaseous products are shown in Table 2. Gas analyses are averages of from two to eight tests on different samples of the same coal. Yields of major components (above 10 percent) in terms of moles/irradiation showed deviations of from 4 to 20 percent from the average; minor components (under 10 percent) showed variations of up to 50 percent from the average. These variations, resulting at least partly from the present state of the experimental technique, do not affect the conclusions.

Atomic C/H Ratios

Figure 2 gives the atomic C/H ratios for the original coals as well as for the gaseous products. For the coals, this ratio decreases rapidly between anthracite and Pittsburgh seam (hvab); little change is shown in the C/H ratio for the hvab coals to the lignites. The gaseous products are richer in hydrogen than their parent coals although this difference is small for the lignites. Since rapid heating occurs in and around the region of irradiation, volatile matter will comprise a large portion of the gas from a high volatile coal (Figure 3). In coals with a low volatile content the laser energy will again release the more volatile components but these gases, comprising less of the coal, will be less characteristic of the whole coal.

Distribution of Gaseous Product

Gaseous products are given in Table 2 as mole percent of total gas and also as moles of gas per irradiation. The distributions of hydrogen, methane, acetylene, carbon monoxide, and carbon dioxide as functions of volatile matter of the coals are shown in Figure 4. Results for coals with volatile contents from 50 to approximately 20 percent were similar to the flash heating results of Rau and Seglin, that is, the younger coals with higher volatile matter show less methane and hydrogen. (5)

This type of plot, however, obscures the fact that many lower rank coals yield three or four times as much gas as higher rank coals such as anthracite. An investigation of the absolute gas yield is now underway. Weight balances obtained in this investigation have not been considered reliable. However, as the same irradiation procedure was used for all samples, an attempt was made to correlate the gas yield with volatile matter, as shown in Figures 5, 6 and 7. The data, while not as reproducible as desired, do give a truer indication of changes in gaseous product with volatile content and coal rank.

The total volume of gas per irradiation on a H₂O, N₂, and O₂ free basis, is shown in Figure 5. The total gas increased as coal rank decreased, showing about a four-fold increase from anthracite to lignite.

Figure 6 shows the moles of H₂, CH₄, and C₂H₂ produced per irradiation as a function of volatile matter. Methane yields were quite low and showed little change with volatile matter. Acetylene from the low rank, high volatile coals exceeded that from anthracite by approximately 15 times while hydrogen increased by a factor of 10 over the same range of volatile matter. These data are similar to those of Aust for the plasma jet heating of coal to extreme temperatures, namely, that acetylene yield is related to the volatile matter. (6)

As expected, yields of CO and CO₂ were higher for the lower rank coals having more volatile matter and a higher concentration of oxygen (Figure 7). The ratio of CO to CO₂ shown in Figure 8 indicates little variation in the ratio for coals from Texas lignite to Sewell (mvb). The oxygen content for these coals ranges from 4.4 percent (Sewell) to 18.6 percent (Texas lignite).

While the yield of water does not follow a consistent pattern, much higher values were obtained for the lower rank coals as would be expected. It is likely that the evacuation method (100°C for 20 hours in a vacuum oven) was only partially successful and that the values include both water from the surface of the coal and product from the reaction. The yield of HCN was low, but did show a trend toward higher values for the lower rank coals. These data indicate that with laser irradiation the maximum yield of hydrogen is obtained from coal of medium rank, that is,

Table 1.- Coal analyses

Coal Rank	Dorrance anthracite	Pocahontas lvb	Sewell mvb	Pittsburgh hvab	Chilton hvab	Rock Springs hvcb	North Dakota lignite	Texas lignite
Proximate, percent maf								
Volatile matter	5.9	18.9	23.7	40.7	40.2	45.4	48.5	51.2
Fixed carbon	94.0	81.0	76.3	59.2	59.7	54.6	51.5	48.8
Ultimate, percent maf								
H	2.8	4.7	5.1	5.5	5.7	5.6	5.0	5.4
C	92.5	89.5	88.4	82.2	79.9	79.2	70.9	72.4
O	2.8	3.8	4.4	8.9	11.3	12.4	21.4	18.6
N	1.0	1.4	1.5	1.7	1.6	1.7	1.1	1.4
S	0.9	0.8	0.5	0.8	1.4	1.1	1.6	2.1
Atomic ratio, C/H	2.75	1.59	1.44	1.24	1.17	1.18	1.18	1.12

coal such as Pittsburgh seam (hvab). The distribution of products is considerably different from that obtained by the vacuum pyrolysis of coals to 450°C. (3) In the 450°C vacuum pyrolysis studies, the hydrogen yields were low and independent of rank. Methane yields were a maximum for the medium rank coals and much higher than the yield of hydrogen. Carbonization at 900°C produces gas with characteristics of both the high-temperature laser irradiation and gas from low-temperature carbonization, that is, high concentrations of hydrogen and methane and a low concentration of acetylene. As reported previously for the flash irradiation of coal, gas from the laser irradiation showed a lower concentration of saturate species such as methane and a higher concentration of unsaturate species, including acetylene, than gas from lower temperature processing.

Infrared Spectrum of Solid Residue

An infrared spectrum was obtained of the solid residue deposited on the walls of the reaction tube during irradiation of Pittsburgh seam (hvab) coal. As shown in Figure 9, most of the bands characteristic of the coal spectrum were absent in the spectrum of the solid residue, indicating that the product was primarily carbon.

Craters Produced by Laser Irradiation

Craters (Figure 3) produced in coals of different ranks differed greatly. A preliminary examination indicated that craters produced in low rank coals such as lignite were much deeper than those produced in high rank coals such as anthracite. It therefore appeared that the energy penetrated deeper in the low rank coals having more volatile matter. Figure 3 also reveals that there was extensive carbonization in the region surrounding the crater.

CONCLUSIONS

Laser irradiation has several advantages over other techniques for studies of the high-temperature reactions of coal: (1) The energy can be focused and directed on specific areas, (2) heating is done by an external source negating contamination, (3) rapid heating of the sample and cooling of the gases occurs. The products obtained in this investigation were similar to those reported previously from flash and argon plasma irradiations. The unsaturated species (primarily acetylene) were much higher and the methane lower than the concentrations found from 900°C carbonization of coal. The lower rank coals not only produced approximately 4 times as much gas as the higher rank coals, such as anthracite, but showed, also, much higher concentrations of acetylene, indicating that further studies of lower rank coals might be fruitful. Infrared studies of the carbonaceous residue indicated that the high temperatures attained with Laser irradiation volatilize a major portion of the components that produce infrared spectra of medium rank coals.

ACKNOWLEDGMENT

The authors gratefully acknowledge the assistance of Anthony F. Logar in the laser irradiation of coal samples.

LITERATURE CITED

- (1) Sharkey, A. G. (Jr.), Shultz, J. L., and Friedel, R. A., Gases from Flash and Laser Irradiation of Coal. *Nature*, v. 202, 1964, pp. 988-989.
- (2) Hawk, C. O., Schlesinger, M. D., and Hiteshue, R. W., Flash Irradiation of Coal, Bureau of Mines Report of Inves. 6264, 1963, 7 pp.
- (3) Sharkey, A. G. (Jr.), Shultz, J. L., and Friedel, R. A., Advances in Coal Spectrometry, Mass Spectrometry, Bureau of Mines Report of Inves., 6318, 1963, 32 pp.
- (4) Ladner, W. R., High Temperatures and Coal, The British Coal Utilization Research Asso., Monthly Bull., v. 28, No. 7, July 1964, pp. 282-299.
- (5) Rau, E., and Seglin, L., Heating of Coal with Light Pulses, *Fuel*, v. 43, 1964, pp. 147-157.
- (6) Aust, T., Ladner, W. R., and McConnell, G. I. T., The Decomposition of Coal at High Temperatures, Preprints of Sixth Intern'l Conf. on Coal Science, Munster, Germany, June 1-3, 1965.
- (7) Honig, R. E., and Woolston, J. R., Laser-Induced Emission of Electrons, Ions, and Neutral Atoms from Solid Surfaces, *Applied Phys. Letters*, v. 2, 1963, pp. 138-139.
- (8) Rau, E., and Eddinger, R. T., Decomposition of Coal in Arc-Image Furnace, *Fuel*, v. 43, 1964, p. 246.

Table 2.- Product gases from laser irradiation of coals

Coal Rank	Dorrance Anthracite	Pocahontas lvb	Sewell mvb	Pittsburgh hvab	Chilton hvab	Rock Springs		North Dakota		Texas						
						hvcb	hvcb	lignite	lignite	lignite	lignite					
Product gas	Moles x 10 ⁷ %															
H ₂	4.3	28.1	22.9	62.9	12.5	57.6	29.8	52.2	31.3	54.1	24.3	34.0	20.6	36.1	19.5	31.7
CO	4.7	30.8	5.1	14.0	3.7	17.1	12.7	22.5	15.3	26.4	25.5	35.7	27.8	48.7	23.9	38.9
CO ₂	4.6	30.1	1.3	3.6	1.9	8.8	5.0	8.7	1.6	2.8	12.5	17.5	5.9	10.4	10.6	17.2
CH ₄	1.0	6.5	0.9	2.5	0.8	3.6	2.9	5.1	2.6	4.4	2.2	3.1	0.6	1.0	0.8	1.3
C ₂ H ₂	0.5	3.2	5.8	15.9	2.6	12.0	6.0	10.6	6.8	11.6	5.8	8.2	1.8	3.1	6.0	9.8
HCN	0.2	1.3	0.4	1.1	0.2	0.9	0.5	0.9	0.4	0.7	1.1	1.5	0.4	0.7	0.7	1.1
O ₂	6.8		3.2		14.4		1.0		3.7		1.2		1.0		1.7	
N ₂	10.9		10.5		42.1		51.4		38.4		11.9		22.3		17.1	
H ₂ O	91.8		33.4		16.3		41.7		34.7		38.6		23.3		29.4	
Total gas, moles x 10 ⁷	15.3		36.4		21.7		56.9		58.0		71.4		57.1		61.5	
CO/CO ₂	1.02		3.92		1.95		2.54		9.56		2.04		4.71		2.25	

1/ H₂O, O₂ and N₂ free.

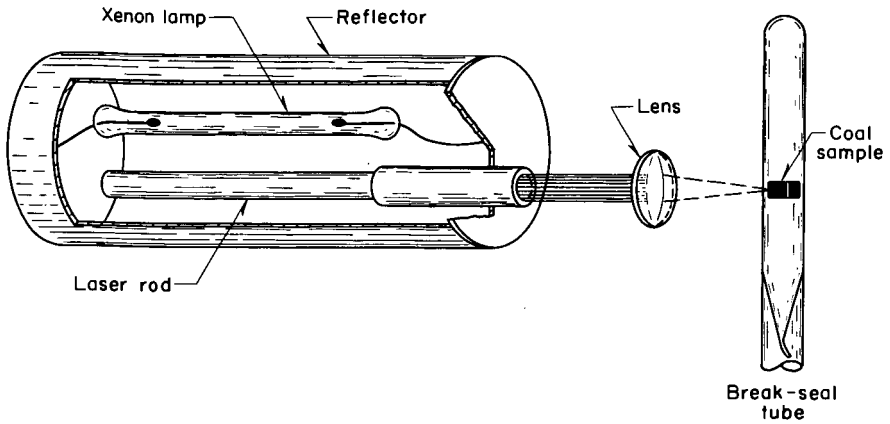


Figure 1.-Laser used for coal irradiation.

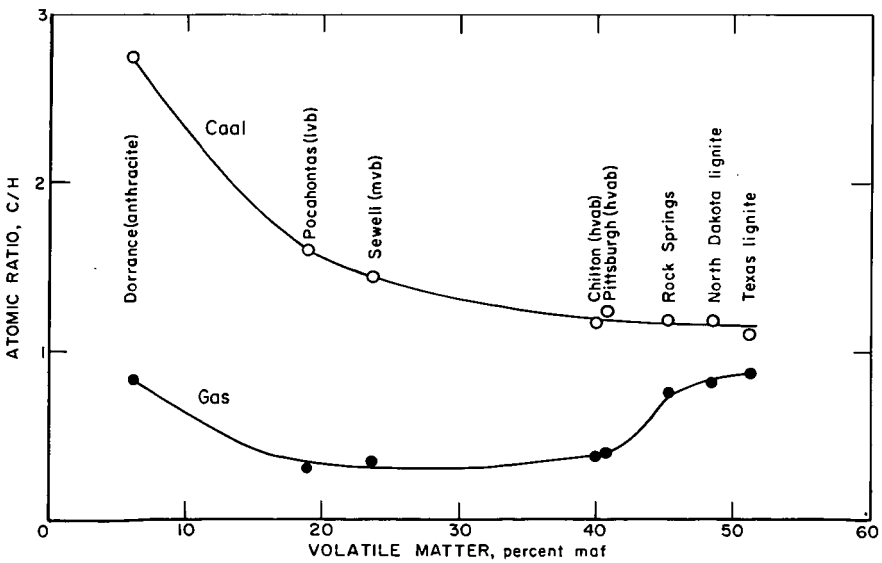


Figure 2.-Atomic C/H ratios of original coals and gases from laser irradiation.



Figure 3.- Coal crater produced by laser irradiation.

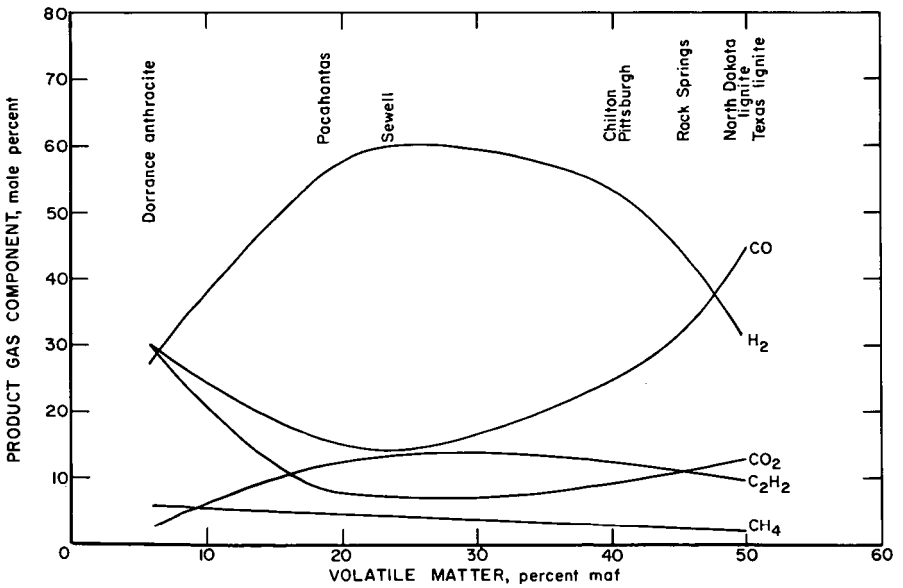


Figure 4.—Product gas as a function of volatile matter in coal

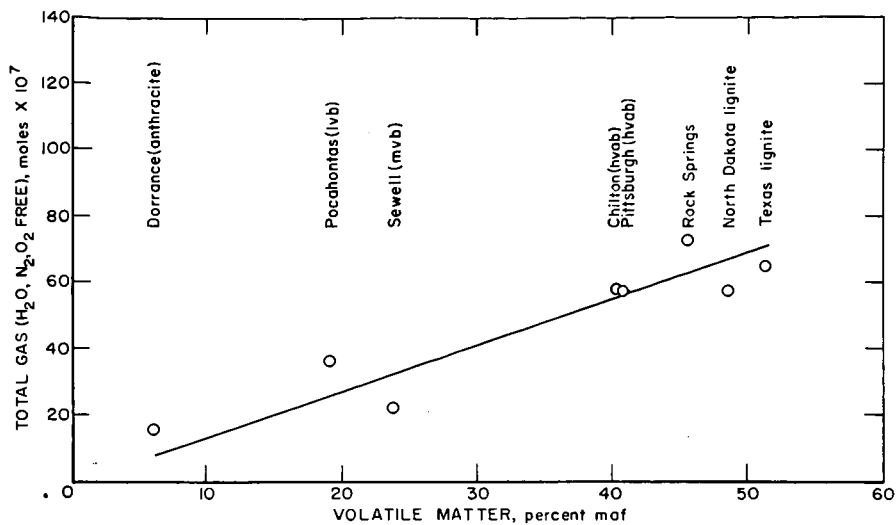


Figure 5.—Product gas as a function of volatile matter in coal.

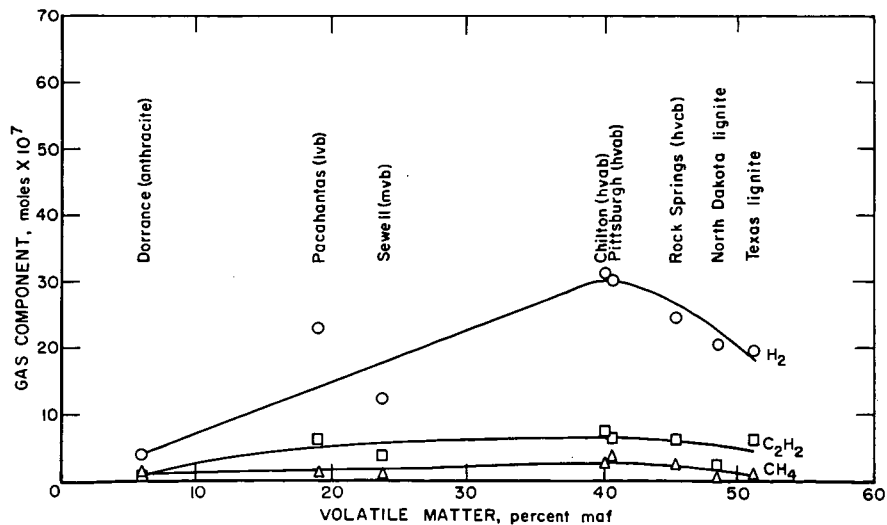


Figure 6.—CH₄, C₂H₂ and H₂ in product gas as a function of volatile matter in coal.

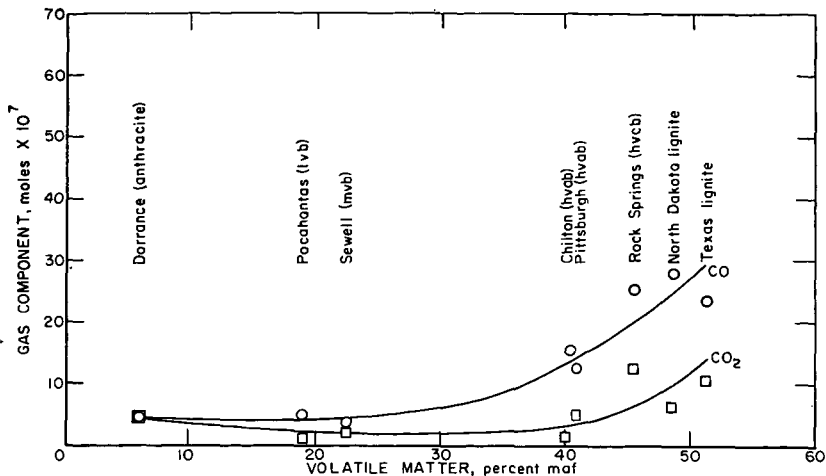


Figure 7—CO and CO₂ in product gas as a function of volatile matter in coal.

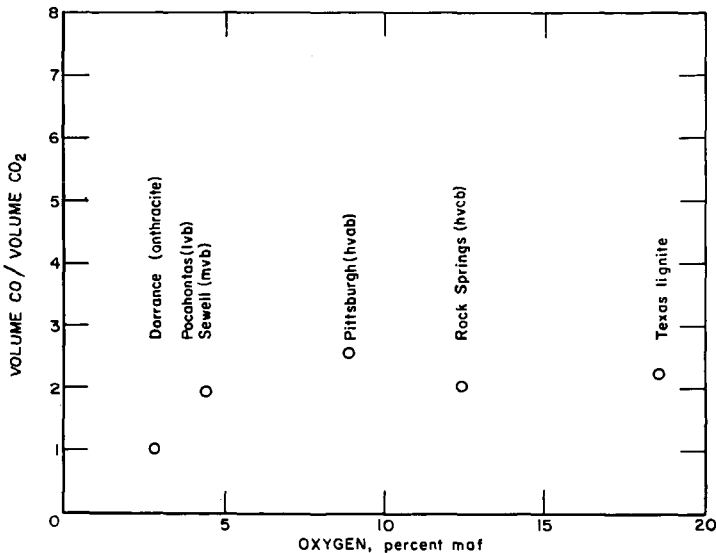


Figure 8.—Ratio of CO to CO₂ in product gas as a function of oxygen in coal.

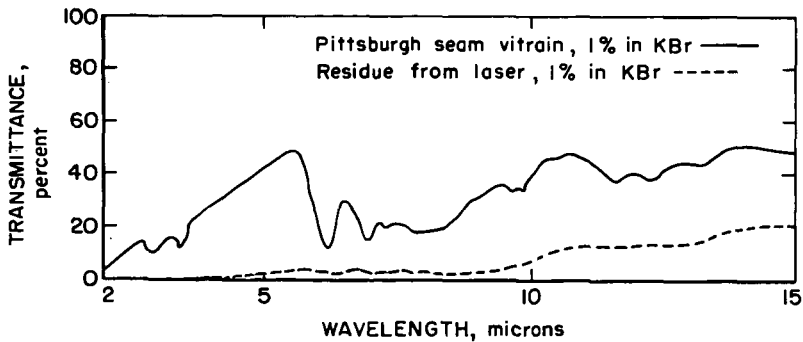


Figure 9.—Infrared spectra of Pittsburgh seam vitrain and residue after laser irradiation.

SYMPOSIUM ON PYROLYSIS REACTIONS OF FOSSIL FUELS
PRESENTED BEFORE THE DIVISION OF PETROLEUM CHEMISTRY, INC.
AMERICAN CHEMICAL SOCIETY
PITTSBURGH MEETING, MARCH 23-26, 1966

USE OF THE LASER-MICROPYROLYSIS-MASS SPECTROMETER
IN STUDYING THE PYROLYSIS OF COAL

By

F. J. Vastola and A. J. Pirone
Department of Fuel Science
Penn State University
University Park, Pennsylvania

INTRODUCTION

The study of the pyrolysis products of high molecular weight organic materials has been a fruitful method of determining their structure. The structural identification becomes more difficult if the pyrolysis products undergo secondary reaction and consequently are not representative of the original structure. In order to minimize secondary reactions the following experimental criteria should be satisfied. To minimize reaction within the solid the heating rate should be high and its duration short. Surface rather than bulk heating would also be advantageous. To minimize gas phase interactions the pyrolysis should take place in vacuo. To insure analysis of materials of low vapor pressure and of free radicals the analysis should take place within one mean free path of the pyrolysis zone. Also, since coal is a highly heterogeneous material the analytical system has to have high sensitivity due to the inherent difficulty in separating large quantities of selected petrographic constituents.

Mass spectrometric techniques of analysis present themselves as a method of satisfying many of the above criteria. Coal (1, 2, 3), as well as coal extracts (4, 5), have been pyrolyzed in mass spectrometers and stable pyrolysis products and coal derivatives have been studied using heated inlet systems (6, 7, 8). However, none of the above techniques have met the requirements of rapid heating and minimum contact of the pyrolysis products with the bulk material.

The development of the laser has made available a compact source that can provide controlled heating fluxes of 10^6 cal./sec./cm.². Focused lasers have been used to vaporize graphite in mass spectrometer sources. (9, 10) The laser has been used also to pyrolyze coal with subsequent analysis of the permanent gaseous decomposition products. (11) Coal because of its low reflectivity is an ideal material to heat by focused laser radiation. When coal is heated by a focused laser beam only a few nanograms are pyrolyzed, but this is a sufficient quantity for analysis if the products are released within the ionization chamber of a mass spectrometer. Since the pyrolysis time is short (ca. 0.4 millisecond) only a time-of-flight mass spectrometer can be used to produce a complete spectrum of a pyrolysis from a single flash. In this type of instrument ions are produced in pulses, accelerated and resolved according to their time of flight down a field free drift tube to a detector. A complete mass spectrum can be recorded for a single pulse of ions. Since the ion pulse width is of the order of 5 microseconds, several spectra can be recorded during the pyrolysis.

If the coal to be pyrolyzed is viewed through the same optical system that is used to focus the laser output the area to be heated can be selected. This capability enables the petrographic constituents of coal to be pyrolyzed in-situ.

EXPERIMENTAL

Figure 1 shows a picture of the complete laser-mass spectrometer. Figure 2 shows a more detailed view of the laser and its microscope optics. Figure 3 is a schematic representation of the laser, ionization chamber and inlet system of the instrument.

The high coherency and low divergence of the light output of a pulsed ruby-laser greatly simplify the design of the optical system needed to produce small areas of intense illumination. A simple lens can concentrate the laser output sufficiently to vaporize carbon. In this application we are faced with two conflicting requirements; in order to achieve maximum light concentration a lens of short focal length is desired, however, in order to obtain a large working distance (lens to target distance) a lens of long focal length is needed. A compromise was made by using a 2X objective lens (Leitz VO) which gave working distance of 75 mm.

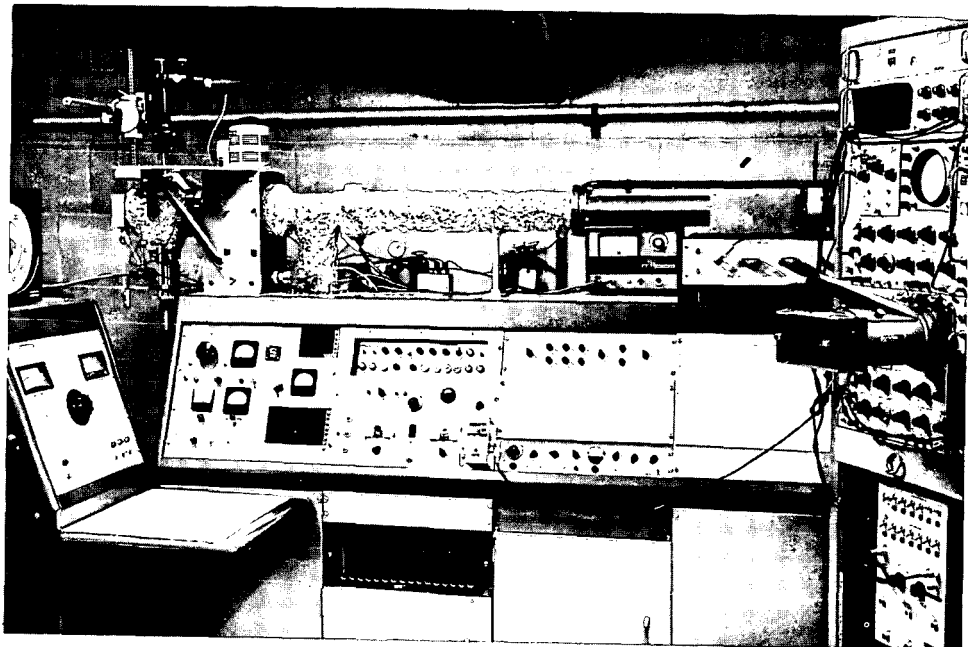


FIGURE 1 - LASER-MASS SPECTROMETER

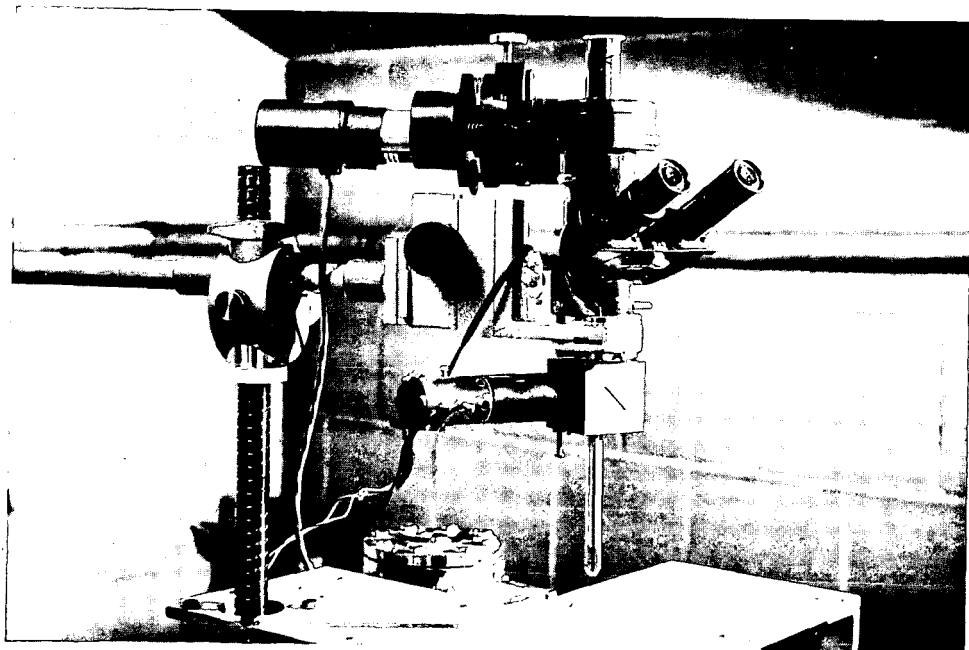


FIGURE 2 - LASER-MICROSCOPE ASSEMBLY

The Laser head consists of a T. R. G. , Inc. , Model 103, Minilaser and Model 153 microscope coupling. The laser is a 6.35 x 38 mm. ruby rod pumped by a helical gas discharge lamp. When the laser is pumped by a 230 joule discharge its output is 100 millijoules. The output pulse length is 0.4 to 0.5 milliseconds in duration. The wavelength of the laser light is 6943Å. The laser concentration and viewing system is constructed around a Leitz binocular-monocular FS microscope head.

The 25 X eye pieces (Leitz periplanatic wide field) in conjunction with the 2X objective give a total magnification of 50 X. The high power eye piece in conjunction with the low power objective degrades image resolution but this solution was necessary due to the problem of working distance mentioned above. However, image quality is sufficient to locate the desired pyrolysis areas. The target is illuminated for viewing by a vertical illuminator. The reflecting surface of the illuminator is a microscope slide mounted permanently in the optical path at an angle of 45 degrees. In order to minimize clearance problems the objective lens was mounted at the end of a 86 by 12 mm. extension tube. The entire optical system is mounted outside of the vacuum system. The flange above the in source in the Bendix model 12-107 TOF mass spectrometer has a 25 by 100 mm. well with an optical flat window at its lower surface. The objective lens can be lowered down this well to reach its proper working distance.

The polished coal sample (12 by 3 mm. surface) is mounted in a positioning clamp and inserted into the mass spectrometer through a modified Bendix model 843A direct inlet port. In position the coal sample is located just underneath the electron beam in the mass spectrometer ionizing chamber.

Figure 4 is a block diagram showing the electrical interconnection of the various units of the spectrometer system. Figure 5 shows the timing of the operating sequence. The master clock (Tektronix Model 180-S1) provides 10Kc. synchronizing pulses as well as 200 and 1000 Kc. reference timing markers. The TOF spectrometer is set to run synchronously with the 10Kc. master clock. When the laser-fire switch is activated the first arriving 10Kc. pulse will fire the flash tube in the laser head and start the delay timer in the oscilloscope (Tektronix model RM45B with type CA preamplifier). At the end of the preset delay time, the spectra can be displayed representing the composition of the pyrolysis product cloud above the coal at various times, in 0.1 millisecond increments, after the laser is fired. This delay is necessary since it may take up to 0.2 milliseconds for the laser to reach its peak output. The single sweep can be adjusted to give a complete mass scan (1 to 2000 AM. U.) or a magnified presentation of a limited mass range. The spectra are recorded on Polaroid Polascope type 410 film. Figure 6 shows a series of craters produced by laser radiation and Figure 7 shows a typical spectrum.

RESULTS

Figure 8 depicts an intermediate molecular weight portion of the pyrolysis products of a high volatile A, Pittsburgh seam bituminous coal.

The spectrum indicates the presence of both aromatic and aliphatic substituted aromatic compounds. Some of the possible assignments are given in Table I, only hydrocarbons are considered.

TABLE I
MASS ASSIGNMENTS

M/e	Ion	Compound
78	C ₆ H ₆ ⁺	Benzene
92	C ₇ H ₈ ⁺	Methylbenzene
106	C ₈ H ₁₀ ⁺	Dimethylbenzene, Ethylbenzene
128	C ₁₀ H ₈ ⁺	Naphthalene
142	C ₁₁ H ₁₀ ⁺	Methylnaphthalene
156	C ₁₂ H ₁₂ ⁺	Dimethylnaphthalene, Ethylnaphthalene

The spectrum in Figure 8 was obtained using an ionization potential of 50eV. The spectra produced by electron bombardment have characteristic fragmentation patterns, in the case of methylbenzene the major peaks will be at mass 92 (C₇H₈⁺) and mass 91 (C₇H₇⁺) with only minor peaks at mass 90 (C₇H₆⁺) and mass 89 (C₇H₅⁺). However, the spectrum produced by laser pyrolysis has major peaks at masses 89 and 90. The intensity of a single peak in a mass spectrum is the sum of the contributions of all species having fragments at that particular mass. For

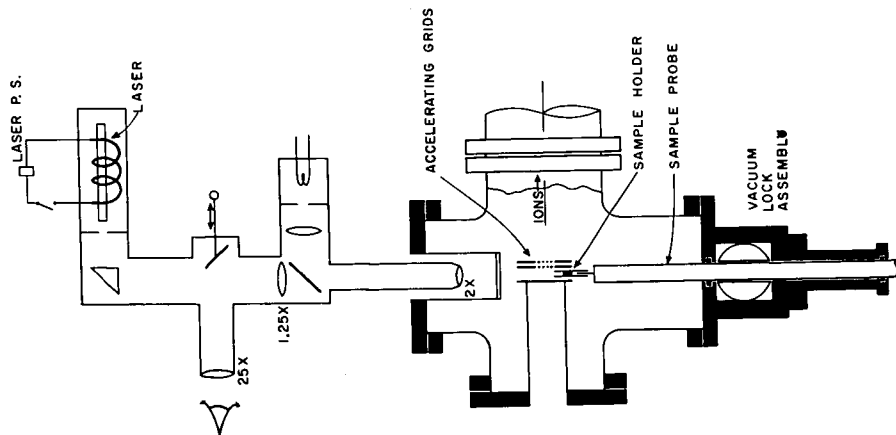


FIG. 3 SCHEMATIC OF SYSTEM

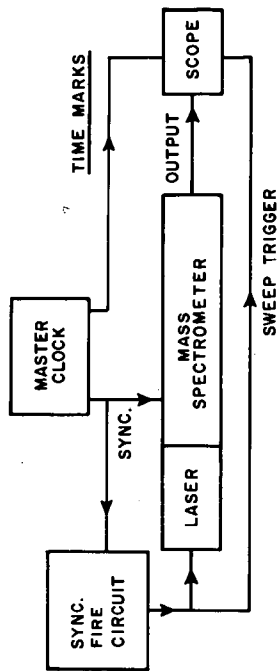


FIG. 4 BLOCK DIAGRAM

EACH INTERVAL EQUALS 100 μ SEC.

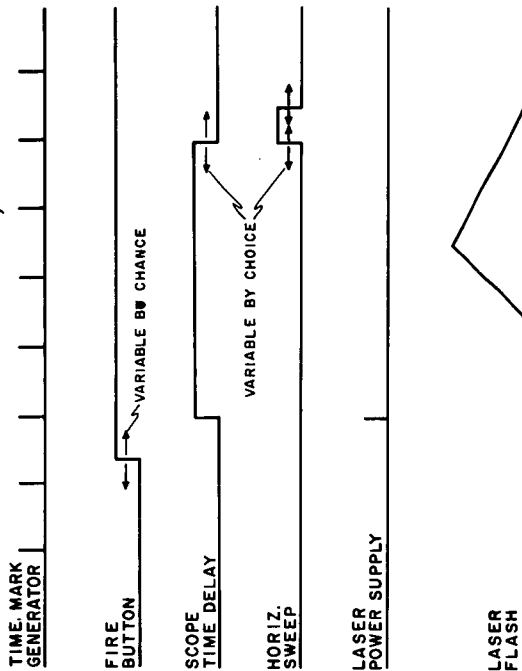


FIG. 5 OPERATIONS SEQUENCE

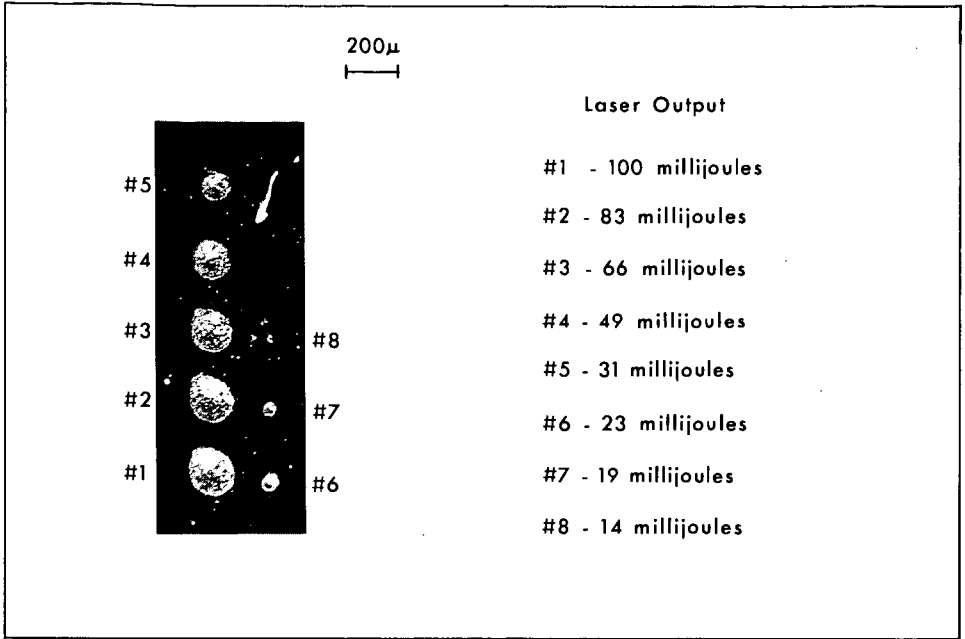


FIGURE 6 - LASER IRRADIATED COAL

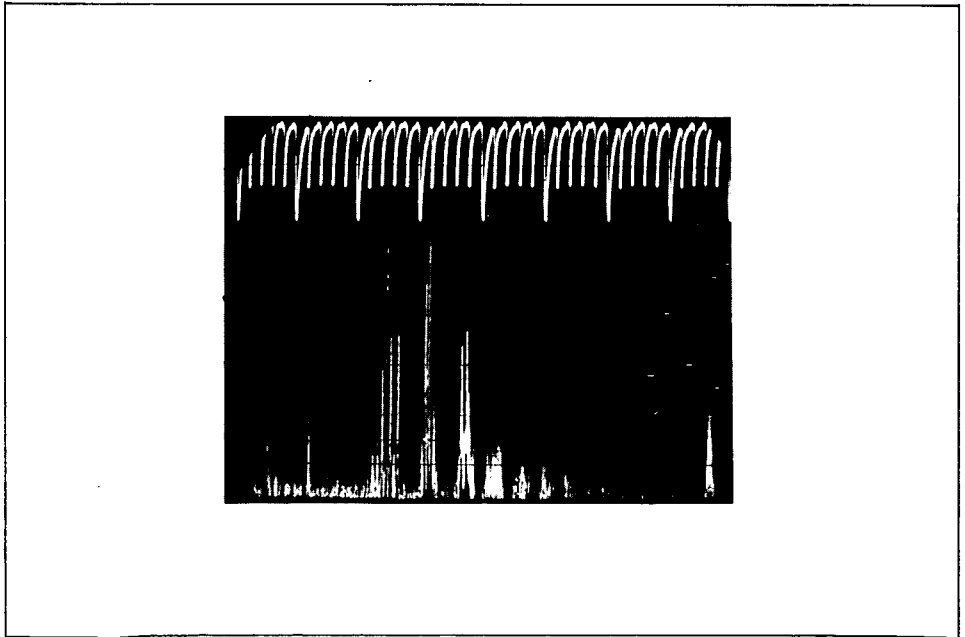


FIGURE 7 - A TYPICAL SPECTRUM

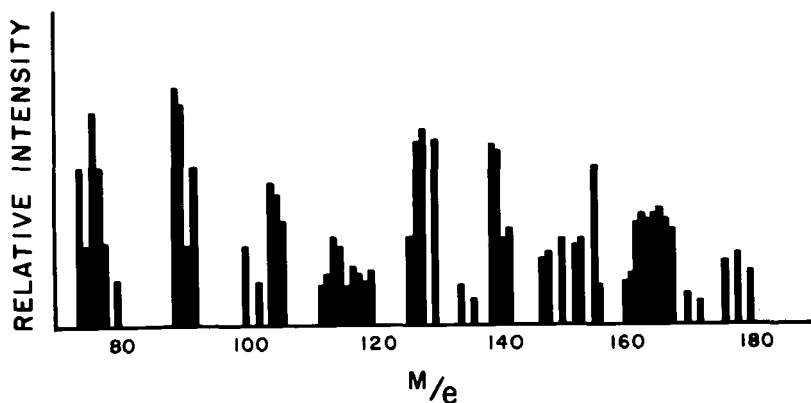


FIG. 8 SELECTED PORTION OF SPECTRA

example, the mass 91 ion is a major constituent of the spectra of other members of the aliphatic substituted series (e. g., dimethylbenzene, ethylbenzene). Since neither mass 89 or 90 is a major fragment in any hydrocarbon spectrum their presence indicates the existence of high concentrations of free radicals in the ionization chamber before electron bombardment. The same abnormal mass distribution, indicative of the existence of free radicals, is found in the benzene, naphthalene, methylnaphthalene and dimethylnaphthalene groupings of the mass spectrum. It therefore appears that the laser-mass spectrometer is capable of detecting primary coal pyrolysis products.

ACKNOWLEDGMENT

This work was supported by a grant from the National Science Foundation.

LITERATURE CITED

- (1) Vastola, F. J., Annual Report NYO-6675, A. E. C. Contract AT(30-1)1442 (1956).
- (2) Holden, H. W., Robb, J. C., *Nature* 182, 340 (1958).
- (3) *Ibid.*, *Fuel* 39, 39 (1960).
- (4) Reed, J., *J. Chem. Soc.* 3423 (1958).
- (5) *Ibid.*, *Fuel* 39, 341 (1960).
- (6) Sharkey, A. G. (Jr.), Wood, G., Shultz, J. L., Wender, I., Friedel, R. A., *Fuel* 38, 315 (1959).
- (7) Sharkey, A. G. (Jr.), Shultz, J. L., Friedel, R. A., *Fuel* 40, 423 (1961).
- (8) *Ibid.*, *Fuel* 41, 359 (1962).
- (9) Honig, R. E., Woolstron, J. R., *Appl. Phys. Letters* 2, 138 (1963).
- (10) Berkowitz, J., Chupka, W. A., *J. Chem. Phys.* 40, 2735 (1964).
- (11) Sharkey, A. G. (Jr.), Shultz, J. L., Friedel, R. A., *Progress in Coal Science*, *Advances in Chemistry Series*, American Chemical Society, in preparation.

SYMPOSIUM ON PYROLYSIS REACTIONS OF FOSSIL FUELS
PRESENTED BEFORE THE DIVISION OF PETROLEUM CHEMISTRY, INC.
AMERICAN CHEMICAL SOCIETY
PITTSBURGH MEETING, MARCH 23-26, 1966

THE DIRECT PRODUCTION OF A LOW POUR POINT HIGH GRAVITY SHALE OIL

By

George Richard Hill, Duane J. Johnson, Lowell Miller and J. L. Dougan
Fuels Engineering Department
University of Utah
Salt Lake City, Utah

The production of shale oil by an in situ process has been long recognized as an important step in the potential utilization of the tremendous Green River Oil Shale reserves in the western United States. For the past several years the Equity Oil Company has sponsored a research project in the Fuels Engineering Department of the University of Utah to test a concept of the late Mr. J. L. Dougan that the energy required to heat the rock and convert the kerogen to a mobile oil could be provided by heated natural gas. The hydrocarbons in the natural gas would serve as a compatible solvent for the oil produced and would penetrate the pores and fissures produced as the converted kerogen moved out of its original sites due to its thermal expansion and volatility. The temperature of the heated natural gas could be high enough to produce the desired kerogen decomposition but low enough to minimize endothermal decomposition of the carbonate minerals of the marlstone matrix and the fusion of these minerals which occurs in combustion type, high temperature processes.

The laboratory experiments confirmed the concept and gave the following results.

Natural gas is a suitable heating medium to effect the desired kerogen breakdown with the production of a low pour point, high API gravity crude oil.

Table 1 lists the operating temperatures, pressures and run durations for a series of typical experiments together with the oil yield and properties. Percent of Fischer Assay yield as determined on the same core samples by the Bureau of Mines at Laramie, Wyoming, are also indicated.

TABLE 1
EFFECT OF TEMPERATURE ON OIL YIELD

Test	Temperature	Pressure	Duration	Oil-Weight Percent		U. of U. % of
				U. of U.	Fischer Assay	Fischer Assay
D-4	331 ^{°C} 628 ^{°F}	atm	550 hrs	4.0	11.9	33.6
D-5	347 657	atm	425	4.8	11.9	40.4
D-19	353 667	atm	159	4.3	11.0	39.1
D-7	364 687	atm	312	6.0	11.4	52.6
D-22	395 743	atm	71	7.6	10.6	71.6
D-16	399 750	atm	86.5	8.0	11.0	72.8
D-17	420 788	atm	38.0	8.8	11.0	80.0
D-10	427 801	atm	37.5	8.9	11.4	78.1
D-14	427 801	1000 psig	14.7	8.6	11.8	72.9
D-1	500 932	atm	13.5	7.6	8.2	92.6

An excellent indicator for the beginning of kerogen decomposition is the appearance in the product gases of hydrogen sulfide. Figure 1 shows the comparative mass spectrometer peak heights of the $m/e = 34$ (H_2S) for a typical run.

Superimposed on the same temperature plot in the figure is a differential weight loss curve from an oil shale decomposition study by Allred. (1) The correspondence between the hydrogen sulfide evolution and the total product evolution during pyrolysis of the kerogen is most striking. Hydrogen sulfide evolution is a good indicator of the total decomposition process.

Figure 2 illustrates the results of a typical run in which the volume of gas produced during a run is the time dependent parameter. The liquid products from these runs were condensed in a freeze out trap cooled by dry ice in acetone. Weighed samples of the oil shale cores from the Piceance Creek Basin in the Green River Formation were the raw materials in both static and

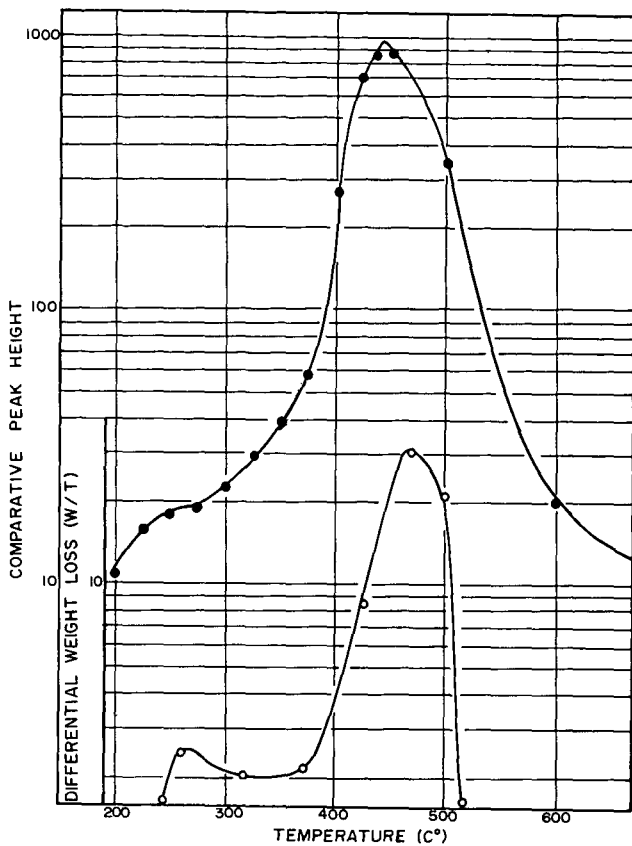
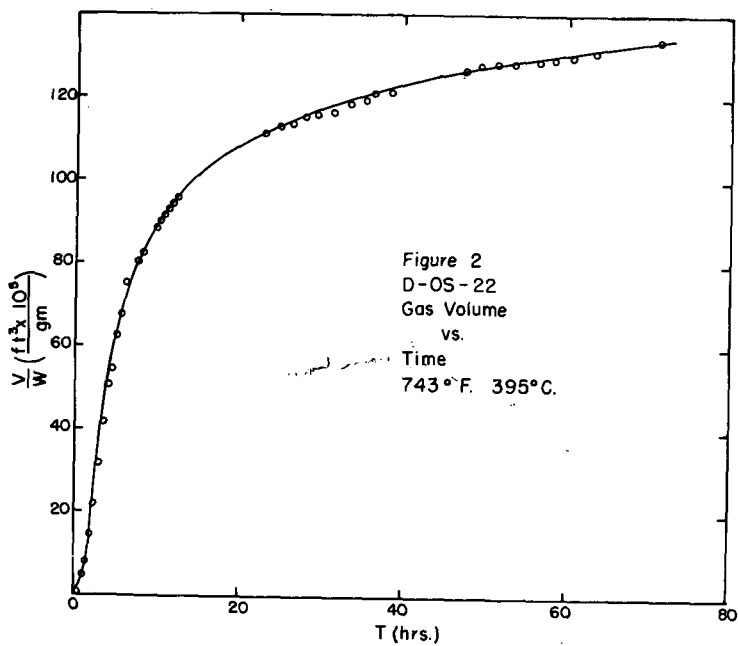


Figure 1. H₂S production (●) and oil production (○) at increasing temperatures.



flow runs. The data obtained on each run included initial and final weights of the oil shale, weight and volume of oil and water and the volume of gas produced. Material balances and product yields were determined for each run.

From the series of gas evolution--time curves at temperatures from 331°C to 427°C the following data can be obtained.

The heat of activation for initial product evolution is 26.7 kcal. During the long term, slower, continuing product evolution an activation energy of 20.5 kcal is calculated. At each temperature oil continues to be evolved at essentially constant rates over periods of up to 550 hours (Figure 3).

Typical analyses of the gases produced from non-flow tests are shown in Table 2 together with the volume of non-condensable gases per gram of original shale.

Data relating to the oil quality as a function of conversion temperature are shown in Table 3.

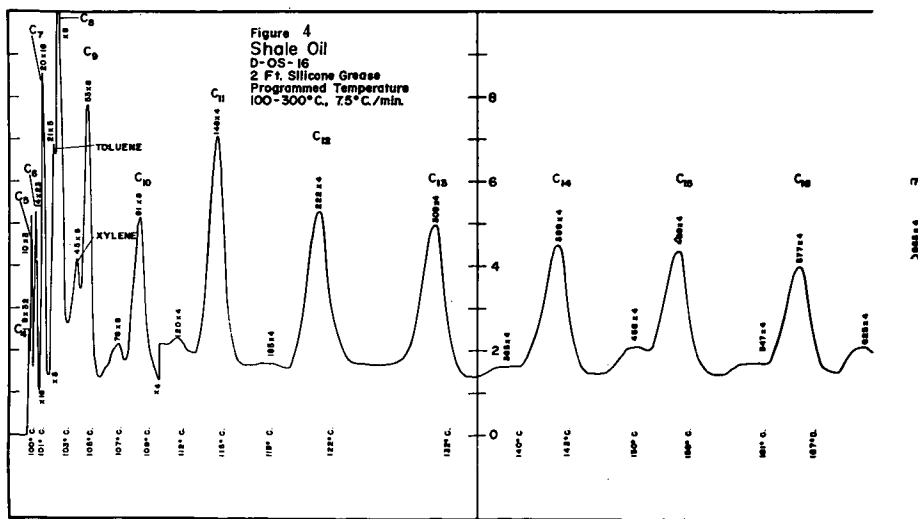
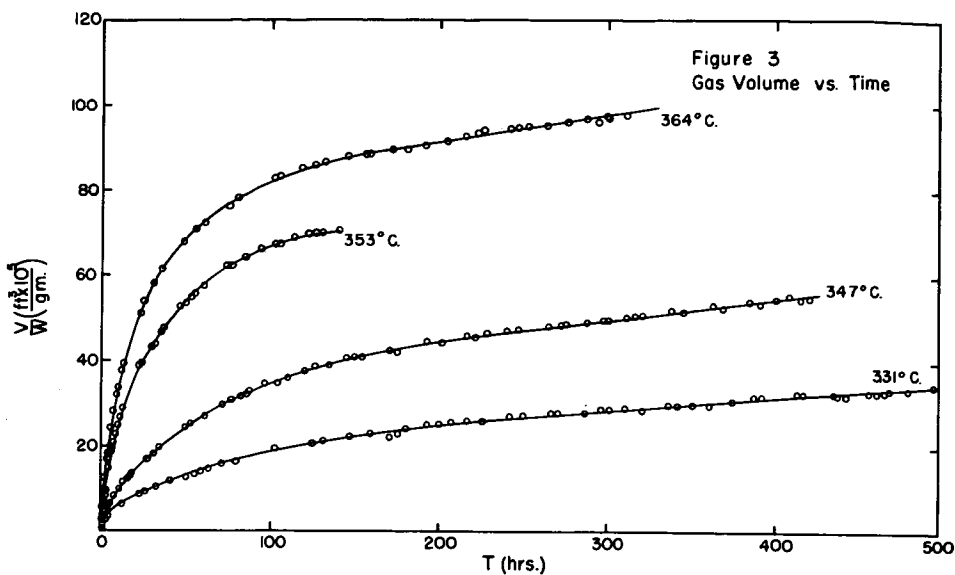
TABLE 2
TEMPERATURE EFFECT ON GAS YIELD AND PRODUCT GAS ANALYSIS

Temperature	Gas Evolved ft ³ x 10 ⁵ /gm	%CO ₂	%CH ₄	%C ₂ H ₆	%C ₃ H ₈	%H ₂ S	%H ₂ +others
170°C	3.21	.27					
300	1.88	30.5	43.6	2.09	3.55		20.3
350	1.7	18.7	15.2	16.3	2.85	.44	46.5
380	2.64	3.8	13.1	4.02	3.40	.90	74.8
404	3.21	3.5	19.2	6.44	4.54	.61	65.7
444	6.61	9.6	28.1	6.92	3.04	.29	52.0
485	6.79	26.7	21.2	1.44	.75		49.9
500	3.58	41.0	9.94	.85	.90		48.2
525	10.7	69.0	4.23	.33			26.4
552	33.4	89.6	2.91				7.5
575	39.6	77.5	1.34				21.2
590	9.25	99.6	.37				

TABLE 3
EFFECT OF TEMPERATURE ON OIL QUALITY

Test	Temperature	Specific Gravity	API Gravity	Pour Point	Fischer Assay Specific Gravity
D-4	628°F 331°C	.822 gm/cm ³	40.7	-40°C	.911 gm/cm ³
D-5	657 347	.823	40.5	-45	.911
D-19	667 353	.828	39.4	-23	.914
D-7	687 364	.817	41.6	-18	.912
D-22	743 395	.838	37.4	-20	.910
D-16	750 399	.828	39.4	-23	.914
D-17	788 420	.832	38.6	-20	.914
D-10	801 427	.888	27.7	-5	.912
D-14	800 427(1000psig)	.814	42.3	-22	.903
D-1	932 500	.852	34.6	10	.907
D-2	968 520	.859	33.5	0	.907

One explanation of the difference in the quality of the oil with temperature is that cracking the kerogen at minimum decomposition temperatures produces relatively low molecular weight primary product molecules of sufficient stability that they do not undergo polymerization. At higher temperatures secondary cracking and polymerization reactions occur producing the usual high pour point, low gravity material. The same difference has long been known between coal oil, a low temperature distillate, and coal tar, a high temperature product. In Table 3 it is noted that there is a general correlation between the temperature of the experiment and the API gravity and the pour point of the oil produced. At temperatures below 420°C, at atmospheric pressure the oils varied from 37 to 41 degrees API and were liquids to below -18°C. Oils produced at higher temperatures were lower in gravity and had a higher pour point.



The oil produced in test run D-14 at 1000 psig and 427°C had an API gravity and pour point characteristic of oils produced at lower temperatures.

The specific gravity of the oil produced in the Fischer Assay of the same samples is given for comparison.

For comparative purposes ultimate analyses of typical high temperature shale oils from approximately the same stratigraphic horizon and from a Pumpherston retort sample are given in Table 4. Most significant here are the lower nitrogen content and the higher hydrogen content of the low temperature product.

TABLE 4
COMPARISON OF U. OF U. SHALE OIL WITH SHALE OILS FROM OTHER SOURCES

Shale Oil	Retort	%C	%H	%N	%S	%O	C/H
Colorado	U. of U.	83.9	12.5	.65	1.15	1.84	6.71
Colorado	N-T-U	84.5	11.3	1.77	.75	1.63	7.48
Kimmeridge, England	Pumpherston	80.9	8.6	1.4	6.5	2.6	9.4

Table 5 gives the ultimate analyses and C/H ratio for a series of oils produced in our laboratory at 300 psi but at increasing temperatures from 370°C to 493°C.

Significantly the nitrogen content was lower in the low temperature samples. The percentages of nitrogen and sulfur appeared to go through maxima. The oxygen content was fairly constant above temperatures of 425°C.

The C/H ratio was lowest in the oils produced at the lower temperatures.

TABLE 5
EFFECT OF TEMPERATURE ON SHALE OIL
ULTIMATE ANALYSES FROM A FLOW STUDY AT 300 PSIG.

Sample	Temp. °C	%C	%H	%N	%S	%O	C/H
HP-14-2	370	83.9	12.5	.65	1.15	1.84	6.71
HP-14-3	400	84.0	12.6	.6	1.16	1.36	6.66
HP-14-4	425	84.8	12.3	.83	1.31	1.08	6.89
HP-14-5	430	84.6	12.6	.91	1.61	1.24	6.71
HP-14-6	450	85.0	12.2	1.11	1.30	1.01	6.96
HP-14-7	480	84.5	12.0	1.46	1.27	1.11	7.04
HP-14-8	485	84.5	12.0	1.41	1.04	1.11	7.04
HP-14-9	490	84.6	11.9	1.01	1.24	1.07	7.11
HP-14-10	493	84.2	11.8	1.08	.96	1.11	7.14

Microscopic examination of the shale residue shows interesting results. As the kerogen decomposes and volatilizes it leaves voids in the otherwise unaltered rock. These voids provide an interconnecting network and an internal porosity in the previously impermeable shale.

Measured values of porosity and permeability before and after thermal treatment at 480°C are shown in Table 6. These results confirm the important findings of Thomas (2) who heated shale plugs ingeneously confined at pressures approximating those to be encountered in in situ heating at depth. He reported comparably high porosities but lower permeability. Our experiments in the laboratory were performed at gas pressures up to 400 psi but without physically confining mechanical pressure.

When Green River oil shale (marlstone) is heated to temperatures used in the Fischer Assay (or other conventional retorting processes) the constituent mineral carbonates decompose. The spent shale is ordinarily partially fused in the process. The carbonate decomposition is endothermic and wasteful of thermal energy. Also the resulting mass is not permeable or porous. Problems resulting from these phenomena have been serious in attempts in situ firing experiments.

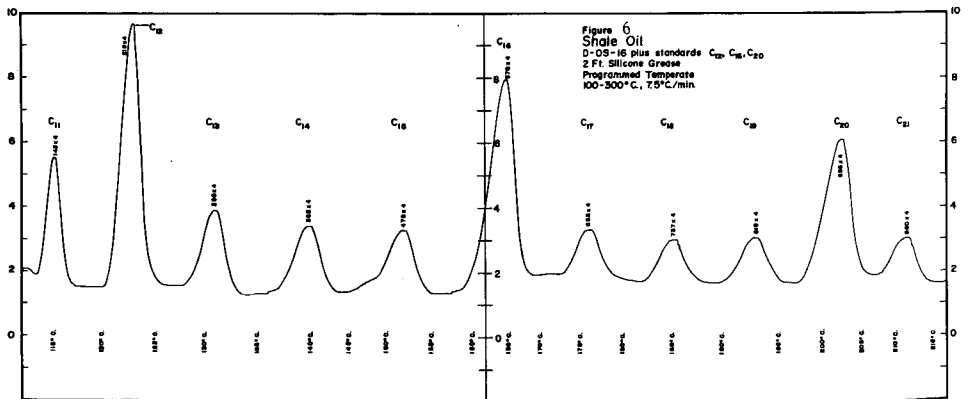
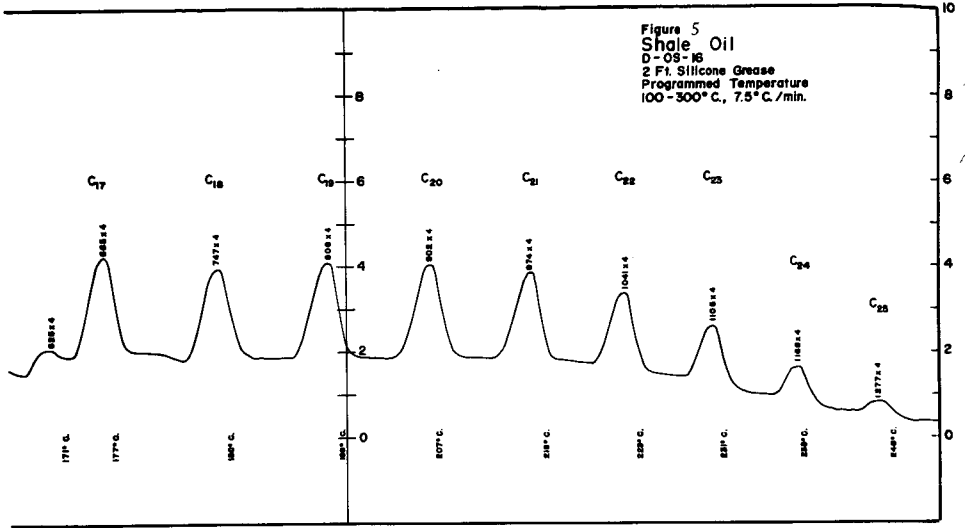


TABLE 6
POROSITY AND PERMEABILITY OF OIL SHALE

Test	Sample Description	Temp. °C	Pressure psig	Permeability		Porosity %
				Horizontal	Vertical	
	Raw Shale			0.0	0.0	0.8
HP-8	Spent Shale Top of Reactor	480	300	125	4.7	44.7
HP-6	Spent Shale Top of Reactor	485	300	5.7	4.3	30.6
	Bottom of Reactor	485	300	14	2.8	41.5

Figures 4 and 5 show the results of a chromatographic column separation of the components of the oil. An F and M model 720 temperature programmed chromatograph was used. The two foot silicone grease column was used. The heating rate was 7.5°C per minute. The temperature range was from 100°C to 300°C. The probable components in the oil are noted on each peak. Normal paraffin hydrocarbons from C₄ to C₂₅ were identified. No paraffins larger than C₂₅ were detected.

To confirm the identity of several components a sample of the oil was spiked with pure samples of normal, C₁₀, C₁₂, C₁₆, and C₂₀. Figure 6 shows the chromatographic analysis record of the spiked sample. The peaks assumed to be C₁₀, C₁₂, C₁₆ and C₂₀ are each increased relative to adjacent peaks. No broadening or doubling of the peaks is noted confirming the identity assignment.

The heating value of three of the shale oils are given in Table 7. They vary from 18,270 to 19,090 Btu per pound.

TABLE 7
HEATING VALUE OF SHALE OILS

Test	Pressure psig	Oil Heating Value Btu/lb
HP	300	18,270
HP	300	18,450
D-7	Atmos.	19,090

In Summary - Green River Oil Shale can be heated by natural gas to temperatures below the mineral carbonate decomposition temperature with the production of a 40°API, low pour point shale oil in approximately 2/3 Fischer Assay yield. The nitrogen content of the oil is one-third to one-half the content of Fischer Assay oil from the same stratum of shale. Hydrogen sulfide evolution provides a convenient indicator of the kerogen decomposition.

The conversion of the kerogen in the shale to oil and its distillation and mechanical removal from the shale by the hot natural gas produces a porous structure which allows the process to continue through the formerly non-porous, impermeable solid oil shale.

The process has been applied in a field test in the Piceance Creek Basin in Colorado and has produced shale oil of the same quality as that produced in the laboratory.

LITERATURE CITED

- (1) Allred, V. Dean, and Nielson, G. J., "Counter Current Combustion - A Process for Retorting Oil Shale," 48th National Meeting of AIChE., August 26-29, 1962.
- (2) Thomas, G. W.; "The Effects of Overburden Pressure on Oil Shale During Underground Retorting." Society of Petroleum Engineers of AIME, Preprint SPE 1272, October, 1965.

SYMPOSIUM ON PYROLYSIS REACTIONS OF FOSSIL FUELS
PRESENTED BEFORE THE DIVISION OF PETROLEUM CHEMISTRY, INC.
AMERICAN CHEMICAL SOCIETY
PITTSBURGH MEETING, MARCH 23-26, 1966

PYROLYSIS OF KEROGEN CONCENTRATE IN THE PRESENCE
OF CALCIUM HYDRIDE

By

J. J. Cummins and W. E. Robinson
Laramie Petroleum Research Center
U. S. Bureau of Mines, Department of the Interior
Laramie, Wyoming

Pyrolytic conversion of oil-shale kerogen to crude shale from which useful petroleum-like products can be made is an established procedure. However, the mechanism of the conversion of kerogen to shale oil, carbon residue, and gas by application of heat is not thoroughly understood. One method to study the mechanism is to pyrolyze kerogen in the presence of a hydrogen donor. The hydrogen donor should stabilize the pyrolytic products as they are formed and should provide primary thermal degradation products. Pyrolysis of kerogen in the presence of a hydrogen donor should minimize, if not eliminate, most polymerization reactions. By utilizing a system of this nature, the thermally degraded products should be more closely related to the kerogen structure and more suitable for composition study.

Pyrolytic reactions of Green River oil-shale kerogen have been studied by various investigators. McKee and Lyder (4) heated oil shale in sealed containers for 1 to 8 hours at 375°C. to 425°C., and they concluded that the kerogen degraded to a bituminous intermediate product. This intermediate product upon further heating decomposed into lower-molecular-weight oils of greater stability and higher saturation. Maier and Zimmerly (3) studied the formation of soluble bitumen by the pyrolysis of kerogen and concluded that bitumen formation was a function of temperature and time of heating. Hubbard and Robinson (2) determined the specific reaction rate for the thermal decomposition of kerogen at temperatures from 350° to 525°C. Bitumen formation increased to a maximum then dropped to zero which indicated that kerogen was converted to bitumen which on subsequent heating was cracked to gas, oil, and carbon residue. Robinson and Cummins (5) thermally extracted kerogen with tetralin, a hydrogen donor, at temperatures from 25° to 350°C. It was found that 95 percent of the kerogen was converted to a soluble product at 350°C. in 144 hours.

In studies where the compositions of thermal degradation products are correlated with the structure of kerogen, it is desirable to obtain primary degradation products that have not had an opportunity to polymerize. Polymerization does occur in unprotected thermal products as evidenced by the increase in amount of high-molecular-weight materials upon standing. Also, preliminary pyrolysis of kerogen directly into the time-of-flight mass spectrometer at this Center showed lower m/e fragment ions than are obtained from retorted shale oil. It was of interest in this study to ascertain if pyrolysis of kerogen in the presence of a hydrogen donor produced more stable products than are produced by the usual pyrolytic methods.

Pyrolysis of kerogen in the presence of calcium hydride was investigated to ascertain if pyrolysis products can be stabilized. Calcium hydride conceivably furnishes hydrogen as hydrogen radicals, hydride ions, or molecular hydrogen. Free radicals produced from kerogen could abstract a hydrogen radical from calcium hydride. Carbonium ions produced from kerogen could abstract a hydride ion from calcium hydride. Any water evolved from the kerogen concentrate as moisture, mineral water, or organic derived water could release molecular hydrogen from calcium hydride. By utilizing calcium hydride as a hydrogen donor in kerogen pyrolysis, the products should be more stable and should be more representative of initial degradation products.

This preliminary report discusses the thermal conversion of kerogen in the presence and absence of calcium hydride under both atmospheric and reduced pressures. The effect of the calcium hydride upon the pyrolysis reaction both at atmospheric and reduced pressures was determined from differences in the composition of the thermal product.

EXPERIMENTAL

Apparatus

The apparatus consisted of a 100 ml. round-bottom flask inverted over a gas trap (Figure 1). A heater surrounded the pyrolysis flask for sample heating. A thermocouple that extended into the flask by means of a small well controlled the temperature within the pyrolysis flask. A dry ice container which served to condense the volatile products surrounded the gas trap. The vacuum source consisted of a diffusion pump backed up by a forepump connected directly to the gas trap.

Samples

The kerogen concentrate, prepared from Mahogany Zone oil shale of the Green River Formation from the Bureau of Mines demonstration mine near Rifle, Colorado, by a method described in a paper by Fester and Robinson, (1) contained 85 percent organic material. Benzene-soluble bitumen, mineral carbonates, and most of the quartz and feldspar were removed by this concentration method. The remaining minerals consisted of about one-half clay and other silicious minerals and one-half pyrite.

Pyrolysis

Two grams of kerogen concentrate or mixtures of 2 grams of kerogen concentrate and 1.5 grams of calcium hydride were placed in the pyrolysis flask. Sufficient quantity of glass wool to fill the flask was added, then the sample and glass wool were agitated until the sample was dispersed uniformly in the glass wool. The apparatus was assembled, flushed out with nitrogen gas, and the cooling container was placed over the gas trap. When using reduced pressure conditions, the system was evacuated prior to heating the pyrolysis flask to the desired temperature. Runs were made at 390°C. for 20 hours. These conditions were chosen because heating kerogen for 20 hours at 390°C. gave significant conversion and permitted consecutive daily runs. All runs made at reduced pressure were at or near 10^{-4} Torr. Runs with calcium hydride present were made with 0.75 grams of hydride per gram of kerogen concentrate because preliminary runs were ratios of hydride to kerogen were varied suggested that this ratio provided an excess of hydride. All mixtures of kerogen concentrate and calcium hydride were ground with a mortar and pestle in a dry inert atmosphere prior to pyrolysis. The distillate material was collected in the gas trap while the soluble-pyrolytic product was extracted from the shale residue with benzene.

Fractionation of Products

Figure 2 illustrates the method used for fractionating the pyrolysis products. The combined products were fractionated into pentane-soluble and pentane-insoluble material with pentane at 0°C. overnight. The pentane-soluble material was fractionated by elution chromatography on alumina into a predominantly hydrocarbon fraction and a polar fraction referred to as resins. In addition to these fractions, a varying amount of material was left on the columns and will be referred to as polar material not recovered. The predominantly hydrocarbon fraction was further fractionated by elution chromatography on silica gel into paraffins, aromatic oil, and polar oil. The paraffins were fractionated into normal and iso plus cycloparaffins on molecular sieves. Duplicate fractionation results checked within ± 2 percent.

RESULTS AND DISCUSSION

The total yields based on soluble products obtained from the kerogen due to pyrolytic conversion at 390°C. for 20 hours are shown in Table 1. The yields include both the materials distilled from the kerogen concentrate and the materials made soluble but not distilled.

TABLE 1
YIELDS OF PYROLYSIS PRODUCT

Conditions		Yield, weight percent of kerogen ^{1/}
Pressure	CaH ₂	
Atmospheric	Yes	59
Atmospheric	No	53
Reduced	Yes	53
Reduced	No	48

^{1/} Fischer assay equivalent 65 percent.

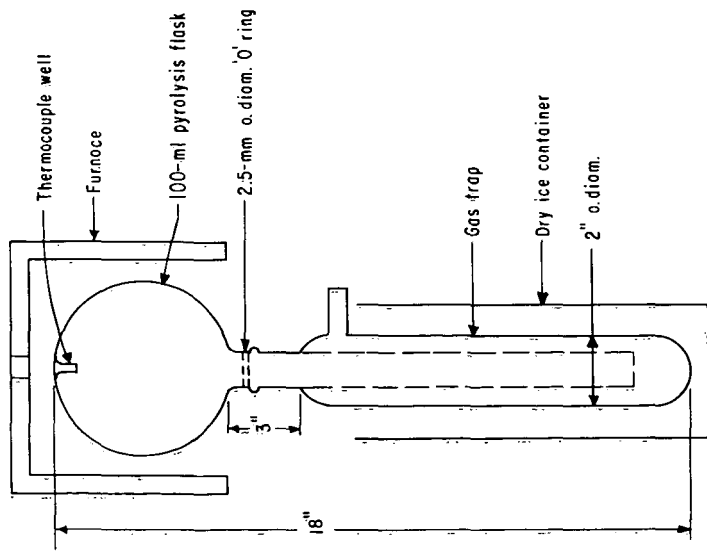


FIGURE 1.-Pyrolysis Apparatus.

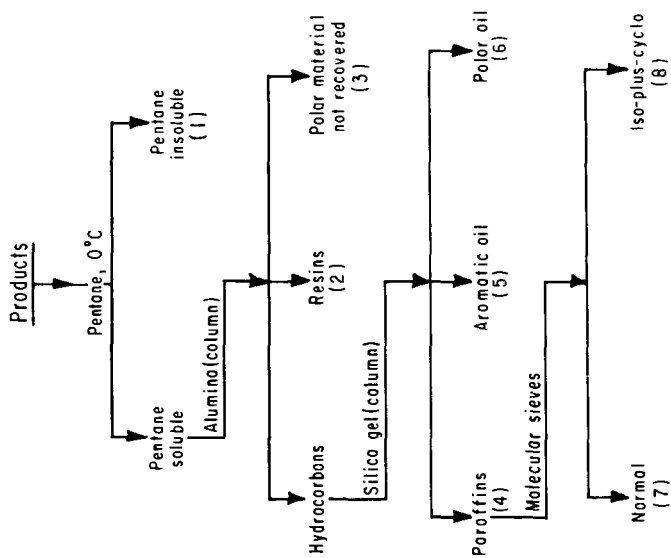


FIGURE 2.-Fractionation of Pyrolysis Products.

The amount of pyrolytic product obtained at atmospheric pressure with calcium hydride was 59 percent of the kerogen compared to 53 percent in the absence of hydride. Likewise the yield at reduced pressures with calcium hydride was 53 percent of the kerogen compared to 48 percent in the absence of hydride. At both pressure conditions, the conversion of kerogen to soluble products tended to be greatest from kerogen in the presence of calcium hydride. Reduced pressure apparently did not increase the conversion of kerogen.

The distillate and the materials made soluble but not distilled were fractionated into paraffins, aromatic oil, polar oil, resins, and pentane-insoluble material. The sum of the paraffins and aromatic oil (fraction 4 plus fraction 5), the sum of the resins and polar oil (fraction 2 plus fraction 6), the polar material not recovered from the alumina column (fraction 3), and the pentane-insoluble material (fraction 1) are shown in Table 2.

TABLE 2
YIELDS OF FRACTIONS OF THE PYROLYSIS PRODUCTS

	Pyrolysis conditions			
	Atmospheric pressure		Reduced pressure	
	With CaH ₂	Without CaH ₂	With CaH ₂	Without CaH ₂
Paraffins + aromatic oil (4 + 5)	25.8	15.3	28.8	19.9
Polar material recovered (2 + 6)	60.4	45.3	61.7	55.7
Polar material not recovered (3)	8.5	32.4	7.2	17.8
Pentane insolubles (1)	<u>5.3</u>	<u>7.0</u>	<u>2.3</u>	<u>6.6</u>
Total	100.0	100.0	100.0	100.0

The maximum amount of paraffins and aromatic oil produced under both pressure conditions was obtained from kerogen in the presence of calcium hydride. At atmospheric pressure the yield of paraffins and aromatic oil was 26 percent of the pyrolysis product when hydride was present compared to 15 percent when hydride was absent. At reduced pressures, the yield of paraffins and aromatic oil was 29 percent of the pyrolysis product when calcium hydride was present compared to 20 percent when calcium hydride was absent. This showed a substantial contribution by the calcium hydride was absent. This showed a substantial contribution by the calcium hydride to the production of more paraffins and aromatic oil. The presence of calcium hydride lowered the amount of polar material produced as shown in Table 2. The sum of the polar material recovered and the polar material not recovered at atmospheric pressure with calcium hydride, represented 69 percent of the pyrolysis product compared to 78 percent without hydride. Similarly, the total polar material, obtained at reduced pressure with calcium hydride, represented 69 percent of the pyrolysis product compared to 74 percent without hydride. Thus, with both pressure conditions smaller yields of total polar material were obtained in the presence of calcium hydride than in the absence of calcium hydride. A more significant difference in the polar material produced in the presence or absence of calcium hydride was the degree of polarity of the material produced in the presence or absence of calcium hydride was the degree of polarity of the material as evidenced by the amount of material not recovered from the alumina column. The amount of material retained on the alumina column was much less for pyrolytic products prepared in the presence of calcium hydride than in the absence of calcium hydride. At atmospheric pressure 9 percent of the product prepared in the presence of calcium hydride was retained on the alumina column compared to 32 percent of the product prepared in the absence of calcium hydride. At reduced pressure the same comparison was 7 to 18 percent. The amount of pentane-insoluble material was also less when calcium hydride was present during the pyrolysis than when calcium hydride was absent (5 percent compared to 7 percent and 2 percent compared to 7 percent).

Apparently hydrogen from the calcium hydride did combine with kerogen fragments to produce more paraffins and aromatic oil, less polar material, less highly reactive polar material, and less high-molecular-weight material in the range of pentane insolubles. Reduced pressure conditions contributed to the production of more hydrocarbons, less pentane insolubles, and less reactive polar materials than atmospheric pressure conditions.

Nuclear magnetic resonance analysis of the iso plus cycloparaffin fraction was conducted to ascertain the extent of cleavage of ring structures and functional groups. Measurement of the methyl/methylene ratio should provide information on the amount of thermal cleavage of this fraction under both pressures and in the presence or absence of calcium hydride. The iso plus cycloparaffin fraction was used for this measurement because it was essentially free of oxygen, nitrogen, and sulfur atoms and provided satisfactory spectra. The results of these determinations, shown in Table 3, suggest that reduced pressure did decrease the the methyl/methylene ratios probably because the products were removed from the pyrolysis zone before further thermal degradation could take place. The lowest methyl/methylene ratio of 0.3 was obtained for the sample heated under reduced pressure conditions in the presence of calcium hydride. No noticeable effect was found with the atmospheric pressure pyrolysis.

The results of these preliminary tests suggest that calcium hydride is a hydrogen donor in the pyrolysis reaction and tends to terminate the pyrolysis reaction by stabilizing the thermal products. Where calcium hydride was present, the pyrolysis product contained more hydrocarbons, less polar material which displayed considerably less reactivity, and less pentane-insoluble material than when calcium hydride was absent. Reduced pressure conditions contributed to the production of more hydrocarbons, less pentane-insoluble material, and less reactive polar material than did atmospheric pressure conditions. Additional work will be required to determine the exact nature of the observed differences and the significance of these differences.

TABLE 3
METHYL/METHYLENE RATIOS OF THE ISO PLUS CYCLOPARAFFIN FRACTION

	Conditions		CH ₃ /CH ₂
	Pressure	CaH ₂	
Atmospheric		No	0.5
Atmospheric		Yes	.5
Reduced		No	.4
Reduced		Yes	.3

ACKNOWLEDGMENT

The work upon which this report is based was done under a cooperative agreement between the Bureau of Mines, U. S. Department of the Interior, and the University of Wyoming, Laramie, Wyoming.

LITERATURE CITED

- (1) Fester, J. I., and Robinson, W. E., *Anal. Chem.* 36, 1392 (1964).
- (2) Hubbard, A. B., and Robinson, W. E., *Bureau of Mines Report of Inv.* 4744 (1950).
- (3) Maier, C. B., and Zimmerly, S. R., *Utah Univ. Res. Inv. Bull.*, 14, 62 (1924).
- (4) McKee, R. H., and Lyder, E. E., *Ind. Eng. Chem.* 13, 613 (1921).
- (5) Robinson, W. E., and Cummins, J. J., *J. Chem. and Eng. Data*, 5, 74 (1960).

SYMPOSIUM ON PYROLYSIS REACTIONS OF FOSSIL FUELS
PRESENTED BEFORE THE DIVISION OF PETROLEUM CHEMISTRY, INC.
AMERICAN CHEMICAL SOCIETY
PITTSBURGH MEETING, MARCH 23-26, 1966

GAS-PHASE PYROLYSIS OF SOME HYDROCARBONS IN FLOW SYSTEMS*

By

H. B. Palmer, K. C. Hou**, R. K. Sharma***, and J. Lahaye****

Department of Fuel Science
The Pennsylvania State University
University Park, Pennsylvania

INTRODUCTION

A series of studies on a variety of hydrocarbons has been undertaken to examine the kinetics of their thermal decomposition in flow systems. In the present work, previous studies of acetylene (1), diacetylene (2), and benzene (3) have been extended to methane, biphenyl, and, in a preliminary fashion, to naphthalene. Methane is considered to be of special interest because of the wealth of literature extant on its pyrolysis, and the conflicts in that literature; at the same time, the aromatic hydrocarbons are interesting because of the paucity of literature on them.

The experimental methods in all of this work have been similar. The apparatus has been described elsewhere. (2, 3) It consists essentially of a hot porcelain tube (5 mm i. d.) with a well-defined temperature plateau, through which hydrocarbon passes at low concentration in helium carrier gas. Analyses are performed by means of gas chromatography. In the studies of biphenyl and naphthalene, the entire inlet, outlet, and analytical systems have been kept at elevated temperature to avoid condensation of starting material.

We have made all calculations of residence times and rate constants on the basis of the temperature profiles as measured with a bare thermocouple under helium flow rates similar to those of the pyrolysis experiments. A detailed analysis of the possible errors due to errors in gas temperature, to lack of thermal equilibrium, or to lack of plug flow has not been carried out (for an excellent treatment of these effects, see Mulcahy and Pethard). (4) However, some calculations have been performed which indicate that such effects should not be important sources of error in this work. Therefore, we believe the rate behavior to be representative of the chemical kinetics of these substances.

RESULTS AND DISCUSSION

One of the hopes in this work has been to find similarities in behavior among some of the hydrocarbons. Therefore we group them, in the following discussion, according to their observed kinetic behavior.

Benzene, Biphenyl, and Naphthalene

In previous work on benzene (3) it was found that the kinetics over times of the order of 20×10^{-3} sec. could be described by mixed first- and second-order processes. The latter was thought to be a four-center reaction to form biphenyl and hydrogen. The first-order process was almost certainly a chain. Its rate was several orders of magnitude larger than any reasonable estimate of the rate of a bond-breaking reaction and its activation energy was low: of the order of 50 kcal. In order to account for the low activation energy it was postulated that one of the chain-carrying steps involved decomposition of phenyl radicals on the wall. It has since occurred to us that it might be possible also to have an important contribution from phenyl radical decomposition on carbonaceous nuclei, or incipient carbon particles, in the gas stream. These nuclei are formed very early, so the associated induction period would not be observed by our methods. Unfortunately, too little is known about the nucleation and growth of carbon particles to allow a quantitative kinetic treatment.

*Work supported in part by the J. M. Huber Corp., in part by the U. S. Atomic Energy Commission under Contract AT(30-1)-1710.

**Present Address: Department of Chemistry, Cornell University, Ithaca, New York.

***Present Address: Department of Chemistry, Birla Inst. of Tech. and Science, Pilani, Ind.

****Supported by a grant from NATO and the C. N. R. S. (France).

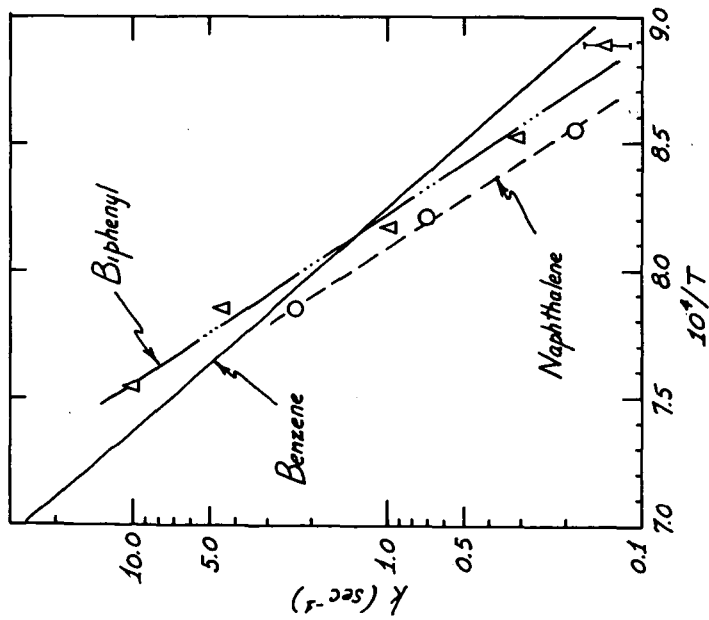


Fig. 1. First-order rate constants for thermal decomposition of benzene, biphenyl, and naphthalene in a flow system.

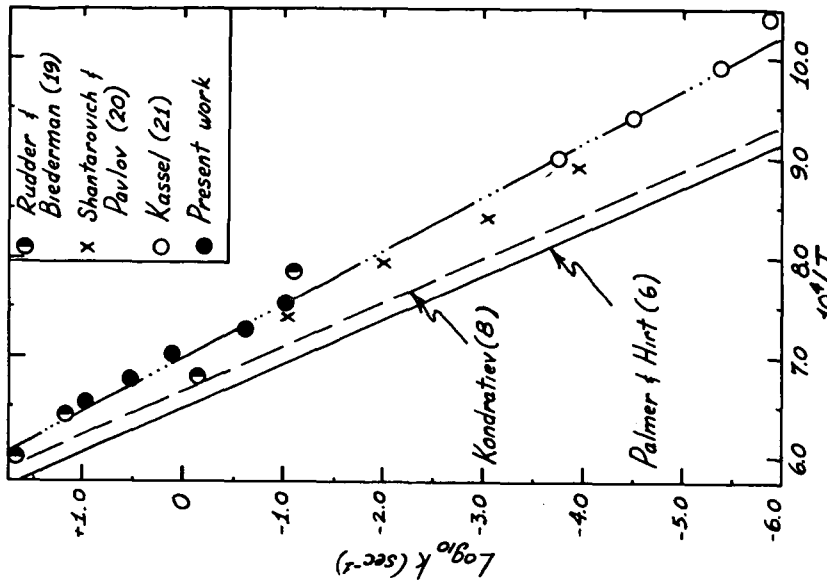
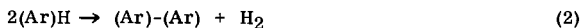


Fig. 2. First-order rate constants for thermal decomposition of methane in the low-temperature regime.

Our knowledge of the kinetics of biphenyl and naphthalene is even less extensive than the rather rudimentary data on benzene. In Figure 1 are presented the previously-determined first-order rate constants for benzene, (3) together with rate constants for biphenyl and naphthalene calculated on the assumption of first-order kinetics. The experimental tests for reaction order in the case of biphenyl have given ambiguous results. The order for naphthalene has not been tested. It is very probable that there is mixed-order behavior, as in benzene, in the case of both biphenyl and naphthalene. Kinney (5), in reviewing the pyrolysis of aromatic hydrocarbons, points out that reactions of the type



occur in all three. Such reactions should be second-order.

However, in the absence of more detailed information, we prefer simply to make a first-order assumption for purposes of comparing rate behavior at comparable concentrations (ca. 1% by volume). Some support for this lies in the observation that benzene is produced from biphenyl in yields up to 20%. It cannot readily be formed in reactions of the type represented by equation 1. Figure 1 shows that between about 1100° and 1300°K, all three compounds decompose at roughly the same rate. Although lines have been drawn through the data, the temperature coefficients for biphenyl and naphthalene are not felt to be of sufficient accuracy to justify extrapolation. One can say that the similarity in rate constants is not surprising, and that they may well maintain similarity over a wide range of conditions. It is interesting to note that, if nucleation phenomena do affect the rates, they too must be similar in all three.

Methane

The decomposition of methane should be completely understood by now. Having published the results of studies of the rate of deposition of carbon films from methane (6) that seemed to settle the question of the correct rate constant, we turned to the flow system for confirmation. To our dismay, we obtained the results shown in Figure 2, which agree very well indeed with the dozens of previous studies in flow and static systems. These have been reviewed by Kramer and Happel (7) and only three of them are shown in the figure. The line through the results from flow- and static-systems is expressed by

$$\log_{10} k = 13.0 - 18.6 \times 10^3/T \quad (2)$$

corresponding to an activation energy of 85 kcal. This is to be compared with the result of Palmer and Hirt (6), based on their carbon deposition rates and shock tube studies:

$$\log_{10} k = 14.6 - 22.5 \times 10^3/T, \quad (3)$$

corresponding to an activation energy of 103 kcal. Kondratiev's (8) recent result is nearly the same as equation 3.

It seems likely that these seemingly irreconcilable results actually express the behavior in two different kinetic situations. In the flow and static systems, residence times are relatively long and there is opportunity for nucleation to occur in the gas phase. These nuclei, which may be thought of as very large free radicals or as a highly dispersed solid with an extremely active surface, can promote direct decomposition of the methane. Tesner (9) has studied the direct decomposition of methane on carbon black (under the electron microscope). The process exhibits an activation energy equal to 78 kcal.

In shock tube studies, times are too short for nucleation, if it occurs at all, to have an appreciable effect. Our flow system studies overlap the temperature regime of Skinner's shock tube work. (10) The decomposition data at the two lowest temperatures (Figure 3) give indications of an induction period. However, even though our rate constants are based upon the decomposition at the shortest times (0.1-0.3 sec.), they are some 10 times greater than the shock tube results. That is, the induction period for the formation of nuclei seems (on the present hypothesis) to be essentially over before 0.1 sec. It is not at all difficult to imagine a rate that commences at the shock tube value and accelerates to the observed value in a time of the order of 0.1 sec. (or less, at the higher temperatures).

The deceleration at long times and large extent of decomposition (Figure 3) is probably due to back reactions. Since these may move not only carbon nuclei and hydrogen but also ethane, ethylene, and acetylene, no quantitative treatment is attempted.

The carbon film deposited on the wall during the pyrolysis of methane is of the vitreous carbon type, very different from carbon black. This is consistent with the low rate constants obtained from measurements of the rate of carbon deposition on the wall. (6) The film carbon seems to be inactive in promoting the direct decomposition of methane, and grows by decomposition of free radicals. Free radicals should also decompose on nuclei, but this should not

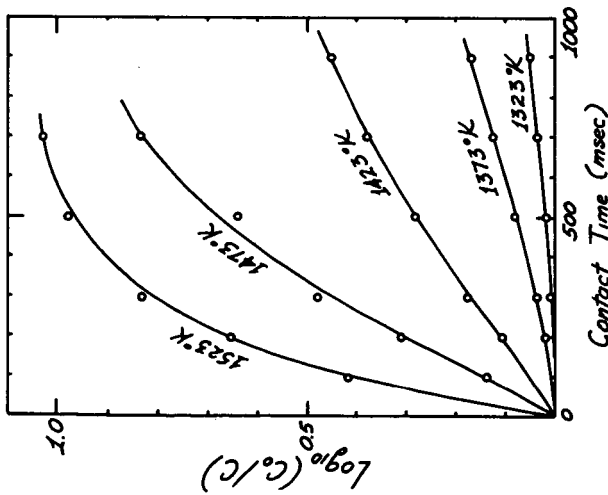


Fig. 3. Experimental data on thermal decomposition of methane in a flow system, at five temperatures.

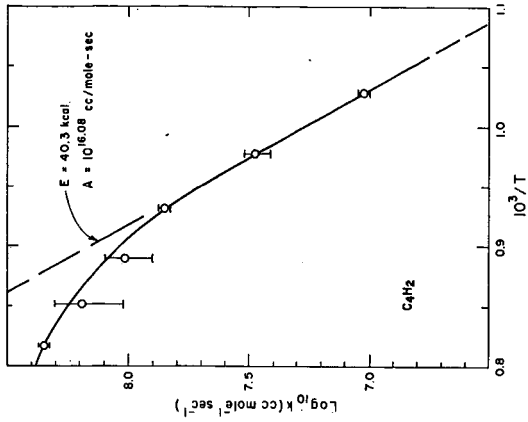


Fig. 5. Second-order rate constants for thermal decomposition of diacetylene in a flow system.

perturb the rate of wall deposition appreciably. The reason is that, at a typical (9,11) particle concentration of $3 \times 10^{10}/\text{cm}^3$ and a diameter of 100A, the total surface area of the particles is less than 1% of the area of the reactor wall. Thus the rate of wall deposition should essentially equal the rate of creation of free radicals if they decompose on the wall with reasonable efficiency. A mathematical analysis of this process is presented elsewhere. (12)

We therefore still believe that equation 3 quite accurately represents the rate of the first step in the pyrolysis of methane. The question as to the identity of this step is still not settled, though it seems very likely that it is C-H bond rupture. The large pre-exponential factor in the rate constant is hardly compatible with splitting-out of H_2 , whereas Skinner (10) has noted that it is quite reasonable if an H atom breaks off.

Acetylene and Diacetylene

We have no new experimental data to report on these compounds. There has, however, been some important new work on acetylene published by Gay, Kistiakowsky, Michael, and Niki (13) that deserves comment in the light of a previous study from our laboratory. (1) Gay *et al* (to be referred to as GKMN) used a time-of-flight mass spectrometer in a shock-tube study of the pyrolysis above 1600°K, and established the following:

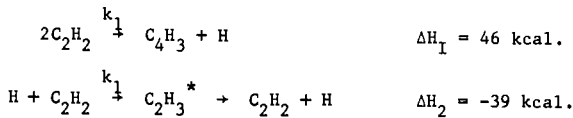
(a) Isotopic exchange between C_2H_2 and C_2D_2 is much faster than the total pyrolysis reaction.

(b) The radical C_4H_3 is formed immediately and very rapidly reaches a steady state.

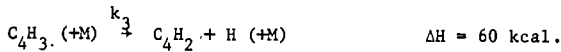
(c) The species C_4H_2 , C_6H_2 , and C_8H_2 form in that time sequence. C_4H_2 appears as early as C_4H_3 .

GKMN note that all these species have been observed in sooting acetylene flames. (11) It may be significant that the species C_4H_4 , which was not found by GKMN, has been identified in the flames.

GKMN then postulate the following mechanism to account for the rapid isotopic exchange:



They suggest that the pyrolysis occurs by reaction 1, followed by



which gives diacetylene, followed in turn by reasonable steps to give higher species.

The second-order rate constants for pyrolysis thus are identified with k_1 . GKMN point out that the mechanism is not flawless. We suggest here modifications that may render it more able to account for all the available evidence on acetylene pyrolysis. In this connection, there is some disagreement between ourselves and GKMN. They examined 76 rate constants from 10 publications, split them into two temperature regimes (620°-1000°K and 1000°-2450°K), formed least-squares Arrhenius expressions for these regimes and also for the whole collection, and observed that all three expressions agreed reasonably well. They concluded that a single rate constant probably governs the decomposition over the entire range, in contrast to our conclusion, from the same data, that there is a transition from long-chain behavior at low temperatures to non-chain behavior at low temperatures to non-chain behavior at high temperatures.

GKMN remark: "The large spread of reported activation energies is but a sad reflection of the difficulties in identifying an activation energy and a pre-exponential rate factor from a limited set of measurements." Our view is that the data on acetylene have nearly become unlimited, and critical attention to each work is necessary if one is to discover what is happening.

There are now some 96 rate constants available. We have plotted them in Figure 4, without attempting to use distinguishing symbols for individual publications. Shock tube data are, however, distinguished from flow- and static-system results. One can put a straight line through all points and obtain an activation energy of 40 kcal; or one can divide them in two, or in three. We have done the last, looking at the regions $10^4/T = 4-8$, $8-12$, and $12-16$. These correspond approximately to the shock tube region, the flow system region, and the static vessel region.

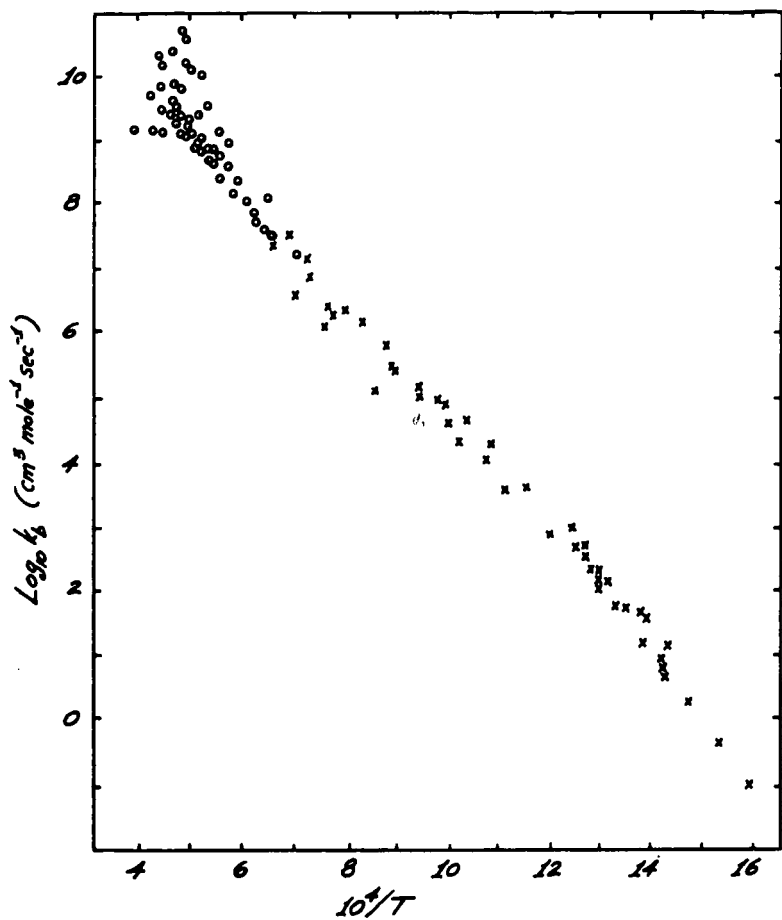


Fig. 4. Summary of all available second-order rate constants for thermal decomposition of acetylene. Circles are shock tube results.

One finds activation energies (excluding some obviously bad points from the shock tube region) of about 48 kcal, 35 kcal, and 48 kcal, respectively. These figures are compatible with transitional kinetic behavior.

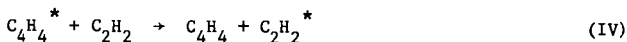
However, there are other arguments that are more compelling:

(a) GKMN do not find C_4H_4 above 1600°K, and their mechanism does not provide for its formation. Nevertheless, the bulk of available evidence supports some mechanism that yields vinylacetylene, C_4H_4 , as the first isolable product at low temperatures, with a shift to diacetylene, C_4H_2 , at high temperatures.

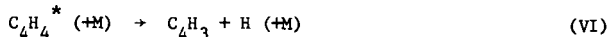
(b) We are quite willing to accept GKMN's conclusion that the chain length in pyrolysis is of the order of unity at high temperatures; but at low temperatures the decomposition is a chain of considerable length (ca. 100).

(c) The "all points" activation energy of about 40 kcal does not appear to be compatible with the estimate (46 kcal) of the ΔH for GKMN's reaction 1. The situation worsens when one considers that the activation energy of the reverse reaction, $H + C_4H_3 \rightarrow 2C_2H_2$, may be appreciable.

We think that a modification of the heuristic mechanism presented by Palmer and Dormish (1) can contribute to reconciliation of the various studies. In that mechanism there were five elementary reactions:



The asterisk denotes a triplet state. For a discussion of the genesis of this mechanism, the interested reader can consult the original paper. (1) The point that we wish to make here is that reaction V may well be in competition with the unimolecular decomposition of $C_4H_4^*$. For simplicity, let us assume that



provides the dominant competition, against reaction IV, for the species $C_4H_4^*$. One notes that neither C_4H_3 nor H will continue the chain; but the H atom provides the necessary species for isotopic exchange, and provides it as soon as reaction commences. C_4H_3 decomposes rapidly at high temperature, yielding C_4H_2 and H, and exhibits a low steady-state concentration. It is possible that at low temperatures, C_4H_3 extracts an H atom from some species and ends up as vinylacetylene.

Failure to observe C_4H_4 at high temperatures requires that its unimolecular decomposition have a large temperature coefficient. The problem of C_4H_4 seems to us to be the least satisfactory feature of the mechanism; but the experimental data are also somewhat unsatisfactory. Skinner and Sokolowski (14) found C_4H_4 in the products at 2000°K, but GKMN did not see it above 1600°K.

A steady-state treatment of the scheme (I-IV, VI) yields a second-order rate constant equal to

$$k_b = k_1(k_3/k_2) \left\{ \frac{[3-k_4[C_2H_2]]}{(k_4[C_2H_2] + k_5)} \right\} / \left[1 + \frac{(k_3/k_2)k_5}{(k_4[C_2H_2] + k_5)} \right] \quad (4)$$

Assuming $k_3 \gg k_2$ at all temperatures, one finds that at low temperatures, where it is expected that $k_4[C_2H_2] \gg k_5$,

$$k_b \approx 2 k_1 (k_3/k_2) \quad (5)$$

At high temperatures, where it is expected that $k_5 \gg k_4[C_2H_2]$,

$$k_b \approx 3k_1 \quad (6)$$

These results at the temperature extremes are the same as were obtained before. (1) There is an interesting difference in the transitional behavior. The larger the concentration of acetylene, the higher the temperature necessary for the condition $k_5 \gg k_4$ [C_2H_2]. Comparison of experimental studies (1, 15, 16, 17) in the 900°K-1500°K region seems to indicate that the chain length does indeed remain moderately large in this region where $p_{C_2H_2}$ is 0.1 atm or more, while with partial pressures of the order of 10^{-2} atm, the reaction appears to have become essentially non-chain by about 1200°K. However, this conclusion is obscured slightly by the probable difference in the nucleation behavior at different concentrations.

As a final remark to connect the pyrolysis of diacetylene with that of acetylene, we reproduce the previously-reported (2) rate constants in Figure 5, and repeat the conclusion that the behavior seems to be very analogous to acetylene. There appear to be long chains at low temperatures and a transition towards non-chain behavior starting around 1100°K. A shock-tube study of C_4H_2 would be most welcome.

CONCLUSIONS

One can use tubular flow systems to gain some kinetic information of practical importance, and to gain some insight into probable mechanisms of decomposition of hydrocarbons. At sufficiently high temperatures, flow systems may yield quite accurate data on homogeneous processes if the rates of these are faster than nucleation rates. However, in such a temperature regime, the shock tube is apt to become a preferable tool. Alternatively, at lower temperatures one may be able to measure the rate of a process that is not affected by gas-phase nucleation. The rate of formation of a carbon film on the wall seems, albeit tentatively, to provide an independent technique of this type in the case of methane, and possibly in benzene. (18)

In the clarity of hindsight it is obvious that, in general, flow systems can yield fundamental data on homogeneous pyrolysis of hydrocarbons only if concentrations can be reduced to extremely low levels, to avoid nucleation problems. The alternative, and one much to be desired, is to use other devices (e. g. shock tubes) to study nucleation and particle growth in such detail that they can be introduced quantitatively into the analysis of flow system data.

LITERATURE CITED

- (1) Palmer, H. B., and Dormish, F. L., *J. Phys. Chem.* **68**, 1553 (1964).
- (2) Hou, K. C., and Palmer, H. B., *J. Phys. Chem.* **69**, 858 (1965).
- (3) Hou, K. C., and Palmer, H. B., *J. Phys. Chem.* **69**, 863 (1965).
- (4) Mulcahy, M. F. R., and Pethard, M. R., *Australian J. Chem.* **16**, 527 (1963).
- (5) Kinney, C. R., The Chemistry of Petroleum Hydrocarbons, Vol. II., Brooks, B. T., Kurtz, S. S., Boord, C. E., and Schmerling, L., eds., Reinhold (1955), Chap. 26.
- (6) Palmer, H. B., and Hirt, T. J., *J. Phys. Chem.* **67**, 709 (1963).
- (7) Kramer, L., and Happel, J., The Chemistry of Petroleum Hydrocarbons, Vol. II, Brooks, B. T., Kurtz, S. S., Boord, C. E., and Schmerling, L., eds., Reinhold (1955), Chap. 25.
- (8) Kondratiev, V. N., Tenth Symposium (International) on Combustion, The Combustion Institute (1965), p. 319.
- (9) Tesner, P. A., Seventh Symposium (International) on Combustion, Butterworths (1959), p. 546.
- (10) Skinner, G. B., and Ruehrwein, R. A., *J. Phys. Chem.* **63**, 1736 (1959).
- (11) Bonne, U., Homann, K. H., and Wagner, H. Gg., Tenth Symposium (International) on Combustion, The Combustion Institute (1965), p. 503.
- (12) Palmer, H. B., *Carbon* **1**, 55 (1963).
- (13) Gay, I. D., Kistiakowsky, G. B., Michael, J. V., and Niki, H., *J. Chem. Phys.* **43**, 1720 (1965).
- (14) Skinner, G. B., and Sokoloski, E. M., *J. Phys. Chem.* **64**, 1952 (1960).
- (15) Munson, M. S. B., and Anderson, R. C., *Carbon* **1**, 51 (1963).
- (16) Towell, G. D., and Martin, J. J., *A. I. Ch. E. J.* **7**, 693 (1961).
- (17) Cullis, C. F., and Franklin, N. H., *Proc. Roy. Soc. (London)* **A280**, 139 (1964).
- (18) Murphy, D. B., Palmer, H. B., and Kinney, C. R., Industrial Carbon and Graphite, Society of Chemical Industry, London (1958), p. 77.
- (19) Rudder, D., and Biederman, H., *Bull. soc. chim.* **47**, 710 (1930).
- (20) Shantarovich, P. S., and Pavlov, B. V., *Zhur. Fiz. Khim.* **30**, 811 (1956).
- (21) Kassel, L. S., *J. Am. Chem. Soc.* **54**, 3949 (1932).

SYMPOSIUM ON PYROLYSIS REACTIONS OF FOSSIL FUELS
PRESENTED BEFORE THE DIVISION OF PETROLEUM CHEMISTRY, INC.
AMERICAN CHEMICAL SOCIETY
PITTSBURGH MEETING, MARCH 23-26, 1966

PYROLYSIS OF OILS DERIVED FROM COAL AND OIL SHALE
IN A FLUIDIZED BED OF CATALYSTS

By

J. F. Jones*, P. L. Barrick, and J. H. Blake**
Chemical Engineering Department
University of Colorado
Boulder, Colorado

INTRODUCTION

For the past several years new reserves of petroleum oil were found at a rate about equal to consumption. Eventually, the supply of good petroleum crude oil may decrease to a point where other sources of oil will be needed to keep up with the demand for gasoline and other oil products. Also, if oil imports were deterred for some reason, other sources of oil would be investigated quite quickly. Some of the other sources of oil which have been investigated, but not used commercially because of the economics of processing are oil shales, tar sands, and coals. Recently, processes have been developed for extracting oil from tar sands in Canada. These processes appear to be competitive locally with the present oil supplies. More recently the government had requested the reopening of the oil shale pilot plant in Rifle, Colorado. This plant is operated by the Research Foundation at the Colorado Schools of Mines and already oil companies are associated with its development. Also, private ventures are under way towards the development of oil shale. In accord with this trend towards developing commercial means for obtaining oil from sources other than petroleum, the newly established Office of Coal Research has let several contracts for investigating processes for converting coal to oil and high Btu gas.

The yield of oil from subbituminous coals varies from 10 to 30 gallons per ton which is similar to yields from oil shale. The higher ranked bituminous coals can yield as much as 50 to 60 gallons per ton. Moreover, coal has an advantage over oil shale in that it is more easily mined and crushed and it is more widely distributed. Also, the spent coal or char from the retorting process is a useful fuel while the spent shale creates a disposal problem.

Oils from coal and oil shale differ in composition from petroleum oils. In addition to the sulfur problem, which is shared also by petroleum crudes, more oxygen and nitrogen are contained in oils from coal and oil shale. Oxygen can be eliminated as water and nitrogen as ammonia by catalytic hydrogenation. (1) However, hydrogen is needed and catalyst life may be short. These are additional costs for the process. Another possible process for removing oxygen from the oil derived from coal is catalytic cracking. Here the oxygen will hopefully be removed as carbon monoxide or carbon dioxide rather than as water. This is desirable since these oils are deficient in hydrogen compared with petroleum. Therefore, the purpose of this investigation was to study the catalytic cracking of low-temperature oils derived from coal with operating conditions similar to those of commercial practice and to compare the results with those obtained with shale oil and petroleum. Successful processing of these new oils would lead to the opening of reserves estimated by many at over a trillion barrels.

EXPERIMENTAL WORK

The catalytic cracking of oils from coal and oil shale was studied by processing the condensed oils in a laboratory, regenerative fluidized-bed reactor. Investigation concentrated on the condensed oils rather than the vapors, because oils from coal and shale would probably first be used in a commercial oil refinery at a distance from the mines. Thus the oils would be transported in the liquid state and then processed. Shale oil and petroleum oil were also catalytically cracked to compare their behavior with that of oils from coal, and to compare the results of the laboratory equipment with those from a commercial plant that uses petroleum.

Sample Preparation

Petroleum oil from Continental Oil Company's refinery in Denver, shale oil from Denver Research Institute, and oil from the pyrolysis of subbituminous coal in a bench-scale fluidized

TABLE I

Cracking of Oil from Coal

Feed Catalyst	Composite		Residuum	
	Silica-Alumina	Filtrol	Filtrol	Silica-Alumina
Temperature, °F.	860	860	950	860
Yield of Liquid Products, wt. %	86.0	69.2	62.8	55.5
Naphtha, wt. %				
In Feed	11.2	11.2	11.2	0
In Product	26.1	36.0	40.8	18
Total Yield	22.4	24.9	29.9	10
Net Yield	11.2	13.7	18.7	10

TABLE II

Cracking of Oil from Shale Oil

Feed Catalyst	Composite			Residuum	
	Silica-Alumina	Filtrol	Filtrol	Silica-Alumina	Silica-Alumina
Temperature, °F.	860	860	950	950	950
Yield of Liquid Products, wt. %	69	69.2	70	70.4	54.0
Naphtha, wt. %					
In Feed	7.5	7.5	7.5	0	0
In Product	17.9	12.4	26.0	21.7	30.0
Total Yield	12.4	8.6	19.2	15.2	16.0
Net Yield	4.9	1.1	11.7	15.2	16.0
Viscosity at 100°F., Saybolt sec.					
Feed			110	184	184
Naphtha Product			40	41	39
Residuum Product			62	53	151

TABLE III

The Performance of the Laboratory Cracking Unit
Compared with that of a Commercial Unit

Unit	Commercial*	Laboratory		
		Petroleum Crude		
Feed Catalyst		Filtrol	Filtrol	Silica-Alumina
Temperature, °F.	860	860	860	860
Feed Rate, w/hr/w	2.0	1.4	1.0	1.7
Yield of Liquid Product, wt. %	75	73	82	73
Yield of Naphtha, wt. %	44	6	10	15

* Refinery of Continental Oil Company at Denver, Colorado.

bed reactor were used as the feeds for the cracking unit. The shale oil and oil from coal were fed both as composite mixtures (containing the original light ends) and as residuums without the light ends. The light ends were considered as all liquids distilling below 410°F. in an atmospheric distillation and were designated as naphtha. Liquids boiling above 410°F. were designated as residuum. The petroleum oil had been previously distilled and contained no light ends.

The laboratory unit for the fluidized bed pyrolysis of coal (Figure 1) consisted of a chamber 2-1/4 inches in diameter and 4 feet long with an enlarged section on top. The bottom was conically shaped for gas distribution. The unit was electrically heated to 1000°F. and wrapped with insulation. The coal was crushed to a size consist of minus 28 to plus 100 mesh and was fed at a rate of about 5 lb./hr. by means of a hopper under a pressure of 15 psig of nitrogen. This pressurized hopper caused the crushed coal to flow in a dense phase through a 3/8-inch tube into the reactor. Natural gas from a laboratory supply line was used to fluidize the coal. This gas was used in lieu of nitrogen or other inert gas. The vapors and gases leaving the retort passed through several condensers. The uncondensable gas was metered and then vented. The spent coal or char was continuously removed through an orifice at the bottom of the reactor.

Fluidized Bed Cracking Unit

The catalytic cracking unit consisted of a regeneration chamber and a reaction chamber as shown in Figure 2. This unit was used previously (2) in cracking studies with shale oil. Each chamber was 2-1/4 inches in diameter and 20 inches long with an enlarged section at the top to prevent catalyst fines from blowing out of the unit and a conical section at the bottom for gas distribution. Heat was supplied electrically and the unit was wrapped with asbestos insulation. Catalyst was circulated by being blown with nitrogen or air through transfer lines as shown in Figure 2. The feed was preheated to about 300°F. and pumped as liquid into the bottom third of the catalyst bed. The catalyst was fluidized with nitrogen, entering at the bottom. The cracked products left the reactor and passed through a series of condensers for oil recovery. The uncondensable gas was metered and then vented. The flue gases from the regenerator were also cooled and then vented. All cracking runs were made at constant feed rate and a constant temperature with either a natural clay catalyst (referred to as Filtrol) or a silica-alumina catalyst. The temperature range studied in the different runs was from 860 to 1000°F. Most of the runs were fed at a space velocity of 1 lb. of feed per hour per pound of catalyst (w/hr/w) which amounted to 8 to 10 cc of feed per minute. Space velocities are on a nitrogen-free basis. The nitrogen added as fluidizing gas and as purge gas amounted to about 0.5 w/hr/w giving an over-all space velocity of 1.5 w/hr/w.

Analytical Procedures

Standard procedures were used for measuring the physical properties of viscosity, specific gravity, and pour point of all liquid products. An ASTM atmospheric distillation to a 410°F. end point determined the light ends. The end point of 410°F. was used because cracking in the distillation flask occurred above this temperature. The gas samples were analyzed with an Orsat apparatus.

RESULTS AND DISCUSSION

Catalytic Cracking of Oil from Coal

Oil from the low temperature pyrolysis of coal is not as aromatic as the high temperature tar from normal coking processes. It contains considerable tar acids and a multitude of various chemicals for which markets are either non-existent or the cost of obtaining pure products is prohibitive. However, low temperature pyrolysis processes can yield over twice the oil than that from high temperature pyrolysis. Thus, it has been suggested (3) that it may be economical to convert the oil from coal to petroleum refinery feedstock or directly to salable petroleum products by catalytic cracking. This investigation studied the feasibility of catalytic cracking oil from coal to obtain a gasoline fraction comparable with that from petroleum oil and shale oil.

The yield versus temperature curves for catalytic cracking a composited oil from coal are shown in Figures 3 to 5. All yields reported in the tables and on the graphs are on a solids- and water-free basis.

The yield of liquid products decreased with temperature from 69 weight percent to 46.5 weight percent between 860 and 1000°F. The naphtha yields (light ends boiling below 410°F.) increased slightly with temperature between 860 and 950°F. and then decreased rapidly. This indicated severe cracking of the light products between 950 and 1000°F. The products showed

TABLE IV

Typical Material Balances for the Cracking Unit

Feed	Residuum from Oil Shale	Residuum from Coal
Temperature, °F.	950	1000
Yields, wt. % of Input		
Oil	70.3	56.0
Gas	4.0	6.3
Carbon Deposited on Catalyst	21.0	30.0
Losses	4.7	7.7
Material Balance	95.3	92.3

TABLE V

Oxygen Balance for Catalytic Cracking of Oil from Coal

Feed	Composite Oil from Coal	Residuum Oil from Coal
Temperature, °F.	1000	1000
Oxygen Content, wt. %		
Feed	9.8	9.8
Liquid Product	5.1	6.9
Amount of Oxygen in Feed Appearing in Liquid Product, wt. %	45	41

TABLE VI

Analyses and Yields of Products from
Pyrolyzing Elkol Coal at 1000°F.

Material	<u>Elkol Coal</u>	<u>Char</u>	<u>Oil</u>	<u>Gas</u>	<u>Liquor</u>
Yield, dry basis, wt. %	-	58.7	14.1	18.0	9.2
Proximate Analysis, dry basis, wt. %					
Volatile Matter	42.2	6.6	-		
Fixed Carbon	54.5	88.2	-		
Ash	3.3	5.2	-		
Ultimate Analysis, dry basis, wt. %					
Carbon	72.0	84.9	80.7		0.2
Hydrogen	5.3	1.7	8.2		-
Nitrogen	1.0	1.2	0.8		0.1
Sulfur	0.8	0.7	0.5		0.02
Oxygen	17.6	6.3	9.8		-
Ash	3.3	5.2	-		-
Gas Composition, Volume Percent					
CO ₂				12.1	
CO				24.9	
H ₂				32.3	
CH ₄				21.9	
C ₂ ⁺				8.8	

a 2- to 4-fold increase in naphtha content over that in the feed (see Figure 5). However, the actual naphtha yield (subtracting the naphtha in the feed) varied from 5 to 15 weight percent based on feed.

A residuum from which the naphtha had been distilled was run to determine the amount of the heavier components of the feed converted to naphtha. The residuum was very viscous and had a pour point of about 200°F. A lower yield of product and naphtha resulted from processing the residuum as shown in Table I. This was probably caused by faster deactivation of the catalyst by more carbon formation with this feed.

A comparison of silica-alumina catalyst with Filtrol catalyst for cracking oil from coal is also shown in Table I. At 860°F. liquid yield was 16.8 weight percent higher with the silica-alumina catalyst than with the Filtrol catalyst. The product obtained with the Filtrol catalyst contained 10 weight percent more naphtha than that from the silica-alumina catalyst, but the naphtha yields were comparable because of the high total yield with the silica-alumina catalyst.

The viscosity of the product from cracking the oil from coal decreased from 81 Saybolt seconds at 100°F. to 45 seconds by increasing the cracking temperature from 860 to 1000°F. as shown in Figure 6. The product and residuum with the naphtha removed were both liquid at 60°F. while the feed had a pour point of 150°F.

Catalytic Cracking of a Shale Oil

Shale oil was cracked in the same laboratory unit to compare its behavior with results from cracking oil from coal.

The yields of naphtha and liquid products as a function of temperature are also shown in Figures 3 to 5 and in Table II for the catalytic cracking of a composite shale oil with a Filtrol catalyst. Both the naphtha content of the product and the naphtha yield based on feed increased to a maximum around 950°F. The curve showing the net yield of naphtha based on feed was obtained by subtracting the amount of naphtha in the feed (7.5 weight percent) from the total naphtha in the product. This left a very small quantity (1 to 10 weight percent) of naphtha that was presumably formed by cracking. However, these calculated values assumed that the naphtha in the feed went through unchanged when actually some of it was probably cracked to uncondensable gases. There was little effect of temperature on the total yield of liquid product between 860 and 950°F., but a decrease of 17 weight percent from the yield at 950°F. was caused by increasing the temperature to 1000°F. (see Figure 3). Based on these data, 950°F. appeared best for the catalytic cracking of shale oil in the laboratory unit.

The yield of naphtha from cracking residuum from shale oil was 15.2 weight percent. This was 3.5 weight percent higher than the yields from cracking the composite feed. This indicated that almost half of the 7.5 weight percent naphtha content of the composite feed was cracked to uncondensable gas and carbon. Thus, the naphtha should be removed from the shale oil before it is cracked to obtain the highest quantity of gasoline-like products. This is commonly done in petroleum oil processing. One run was made with a silica-alumina catalyst at 860°F. Data in Table II show that operating with the silica-alumina catalyst gave about five times more naphtha than that from the Filtrol catalyst. This higher yield with the silica-alumina catalyst was attributed to an inherently greater activity.

The effect of temperature on the viscosity of the products and residues for the catalytic cracking of composite shale oil is shown in Figure 6 and Table II. The viscosity of the feed was 110 Saybolt seconds at 100°F. whereas the viscosities of the products and residues ranged from 35 to 75 seconds. The viscosity of the products decreased about 30 percent as the cracking temperature was increased from 860 to 950°F. This decrease in viscosity was caused by the cracking of the feed to the less viscous naphtha. The viscosity of the products also decreased with increasing naphtha content as shown in Figure 7. An increase in the naphtha content from 7.5 weight percent to 12 weight percent lowered the viscosity by 100 percent, but the effect became less pronounced at higher naphtha concentrations. Also, the residues of the product from which the naphtha had been removed were less viscous than the feed. This indicated that even the more viscous components of the feed were cracked to less viscous products.

Comparison of Data with Catalytic Cracking of a Petroleum Oil

The yield versus temperature curves for the catalytic cracking of a petroleum oil, oil from coal, and a shale oil are compared in Figures 3 and 4. The lowest total yield of liquid products was obtained with the oil from coal. It varied between 63 and 69 weight percent over the temperature range of 860 to 950°F. whereas the yield from petroleum oil and shale oil ranged from 67 to 74 weight percent. The lower yields obtained with the oil from coal may be partly caused by its higher naphtha content which was susceptible to cracking to uncondensable gases and carbon. Also, the oxygen content of the oil from coal was lowered by catalytic cracking as

FIGURE 1
DIAGRAM OF RETORT

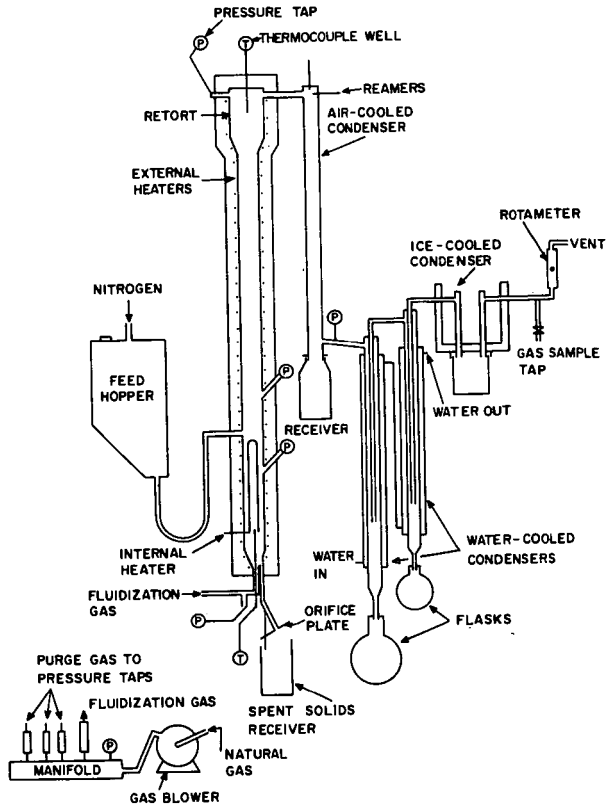
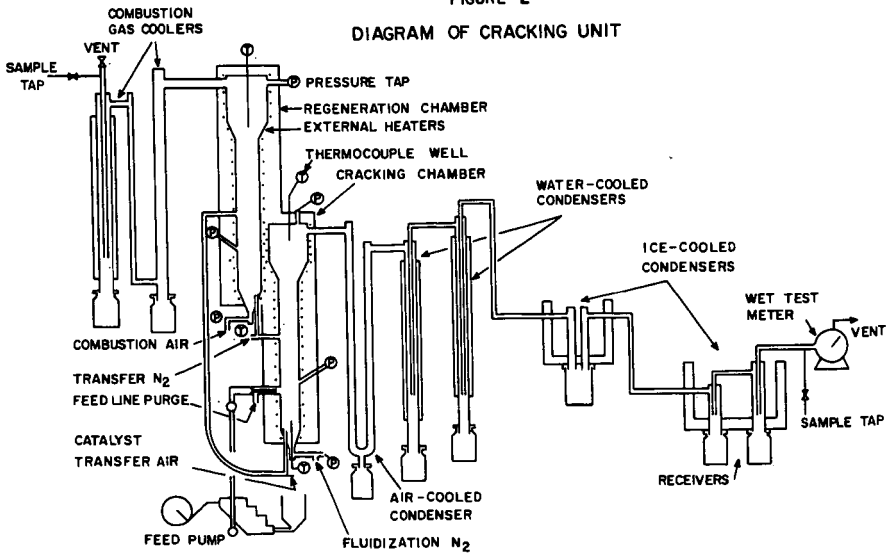


FIGURE 2
DIAGRAM OF CRACKING UNIT



discussed later. The removal of the oxygen would tend to make the yields of product less with the oil from coal than with the petroleum oil and the shale oil which do not contain as much oxygen. At 1000°F., the yields from both the oil from coal and the shale oil decreased about 15 weight percent. Thus, a temperature of 950°F. was the most suitable for cracking in the laboratory unit. This is 90° higher than the temperature used to crack the sample of petroleum oil supplied by a commercial refinery, but is within the range of cracking temperatures used in the petroleum industry. The actual naphtha yields for the petroleum oil fell between those for the shale oil and oil from coal. However, the petroleum oil has no naphtha content and thus the curve curves do not show a direct comparison between the feedstocks.

If the residuum feeds are compared with the petroleum oil, the naphtha yields were 10 weight percent for the oil from coal, 15.2 weight percent for the shale oil, and 14 weight percent for the petroleum oil. Thus, they all fell within a similar range. Therefore, all three feedstocks were cracked with comparable vigor in the laboratory unit, and both shale oil and oil from coal could be used as suitable cracking feedstocks similar to a petroleum oil residuum.

Comparison with a Commercial Refinery

A comparison of the performance of the laboratory unit with that of a commercial unit is shown in Table III, and it is evident that the laboratory unit did not perform efficiently. If the yield of naphtha is taken as a basis of efficiency, then at best the laboratory unit was only about 30 percent as efficient as the large scale unit. The main reason for the lower efficiency was less circulation of catalyst between the reactor and regenerator in the laboratory unit. This rate was difficult to control in the small apparatus. The average carbon level on the catalyst in the reactor was about 10 weight percent compared with about 2 weight percent in the commercial operation. Thus, the recirculation rate of regenerated catalyst was too low in the laboratory and contributed to lower activity of the catalyst. Nevertheless, the laboratory unit proved effective for determining the susceptibility of oils to this refining technique.

Composition of Gas from the Cracking Unit

The gas produced by cracking oil from coal contained about 20 volume percent of carbon oxides, hydrogen from 10 to 20 percent, methane from 40 to 50 percent and 20 to 25 percent C₂⁺ hydrocarbons. The average molecular weight of the gases was 20 to 25. Gas composition changed little over the temperature range of 860 to 1000°F. Gas from cracking shale oil had little carbon dioxide or monoxide, and it contained more methane.

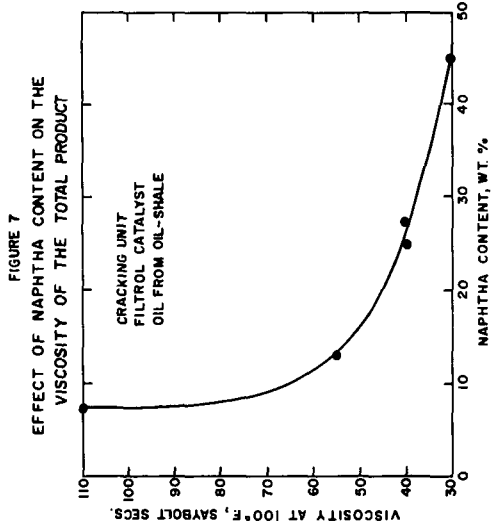
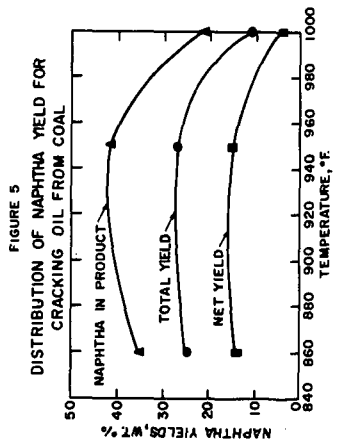
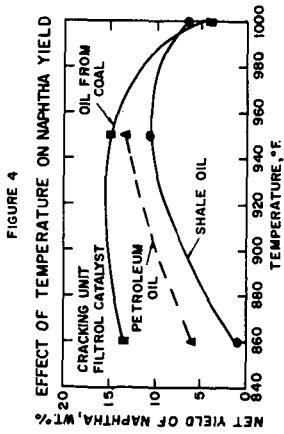
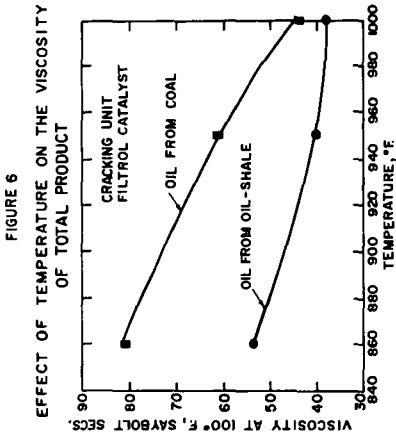
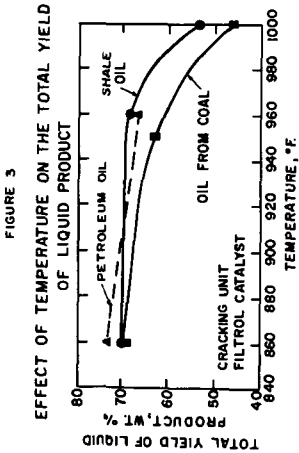
Material Balance for the Catalytic Cracking Unit

The material balances for two catalytic cracking runs are shown in Table IV. Balances ranged from 92 to 95 percent. The carbon on the catalyst was 8.4 weight percent with the run with shale oil and 9.7 weight percent for the run with oil from coal. The carbon yield was defined as the total carbon produced during a run divided by the weight of feed. The carbon formed during a run in this investigation was determined from the carbon on the catalyst left in the reactor at the end of the run and from the amount of catalyst circulated during the run. The circulation rate was about 1 pound of catalyst circulated per pound of feed. The carbon yield as calculated in this manner ranged from 20 to 35 weight percent. This is high and hopefully could be decreased by higher rates of catalyst recirculation.

The purpose of cracking the oil from coal was partially to form useful oil products and to determine if oxygen was removed by this technique. Therefore, an oxygen balance was made to determine the effectiveness of the laboratory cracking unit in removing it. Table V shows oxygen balances for two runs. The composited oil had an oxygen content of 9.8 weight percent. This value was also used to calculate the balance for the residuum oil. The data showed that the oxygen content of the liquid product was less than that of the feed and ranged from 5 to 7 weight percent. Over half of the oxygen in the tar was removed as gas and water. Therefore, even though the laboratory unit operated at the low catalyst circulation ratio of 1 pound of catalyst per pound of feed, 50 to 60 percent of the oxygen was removed from the oil. At a higher circulation rate where more active catalyst is present in the reactor, it is likely that more of the oxygen would be removed.

Pyrolysis of Elkol Coal

The oil from coal used in this work was obtained by the pyrolysis of Elkol coal in a fluidized bed. Feed rate was approximately 5 lb. per hour which gave a residence time for the coal in the reactor of about 20 minutes. The average temperature was 1000°F. but momentary upsets could cause a fluctuation of plus or minus 50°F. Elkol coal is a subbituminous coal and does not agglomerate upon heating. Therefore, it required no special pretreatment before



pyrolysis. Yield and analyses of Elkol coal, and products of pyrolysis at 1000°F. are given in Table VI. A typical material balance for the retorting of Elkol coal at 1000°F. is shown in Table VII. Oil yield was about 14 weight percent.

CONCLUSIONS

1. Oil from coal, shale oil, and petroleum oil were all catalytically cracked with comparable vigor in a fluidized bed.
2. A catalytic cracking temperature of about 950°F. gave the highest naphtha yields with oil from coal and shale oil.
3. Synthetic silica-alumina catalyst promoted the cracking reaction at a lower temperature than a Filtrol catalyst (natural clay) and was considered a more active cracking catalyst.
4. The pour point of oil from coal was decreased from about 150°F. to less than 60°F. by catalytic cracking.
5. The viscosities and gravities of all feeds were reduced by catalytic cracking.
6. Catalytic cracking removed over half of the oxygen from the oil obtained from coal.

ACKNOWLEDGMENT

The authors express thanks to George W. Walpert for his contributions to the design of the equipment and for his work with shale oil.

LITERATURE CITED

- (1) Law, R. D., "The Case for Low Temperature Coal Tar", N.R.R.I., February 1957.
- (2) Walpert, G. W., "Catalytic Cracking of Shale Oil by Direct Coking on a Continuously Regenerated Fluidized Bed", PhD Thesis, University of Colorado, 1953.
- (3) Chilton, C. H., "Chementator" Chemical Engineering, 65, No. 2, 53-54 (1958).

*Present address FMC Corporation, Princeton, New Jersey.

**Present address FMC Corporation, San Jose, California.

SYMPOSIUM ON PYROLYSIS REACTIONS OF FOSSIL FUELS
PRESENTED BEFORE THE DIVISION OF PETROLEUM CHEMISTRY, INC.
AMERICAN CHEMICAL SOCIETY
PITTSBURGH MEETING, MARCH 23-26, 1966

KINETICS OF BUTADIENE PRODUCTION - DEHYDROGENATION OF
MIXED n-BUTANE + BUTENES AT 1/6-ATMOSPHERE PRESSURE
EXPERIMENTAL RESULTS AND EMPIRICAL CORRELATIONS

By

R. E. Sattler and E. W. Pitzer
Phillips Petroleum Company
Bartlesville, Oklahoma

I. INTRODUCTION

In connection with Phillips continuing interest in butadiene production, data were desired for the conversion of n-butene to butadiene in a single stage and at less than atmospheric pressure. Earlier experimental data were limited to the conversion of pure n-butane to butenes + butadiene. For present considerations of this process, data were needed for the conversion of mixed n-butane + butenes (steady-state feed). In addition, data were desired for use in studies of n-butane and butenes dehydrogenation kinetics.

To accomplish these objectives, steady-state feed mixtures were dehydrogenated with 1/70-inch particles of chromia-alumina catalysts at 125 mm. mercury absolute pressure and over the temperature range of 1050 to 1250°F. Product distributions and reaction rates were calculated from the experimental results.

II. EXPERIMENTAL WORK

A. Apparatus and Equipment

The equipment used for the study of low pressure dehydrogenation reaction rates is schematically outlined in Figure 1. The total volume of the system was 8-9 cc and the reactor contained 2.2 cc. The schematic description of the furnace and reactor used for 1/70-inch catalyst particles is shown in Figure 2. Three-way solenoid valves were used to switch instantaneously between hydrocarbon and other gas feeds. Electrically heated furnaces were used to preheat the gases, to heat the catalyst and to produce a "heat seal" at the reactor outlet to minimize heat lost through the exit of the furnace. The preheat and catalyst furnaces were controlled with Wheelco Amplitrol temperature controllers which operated in conjunction with chromelalumel thermocouples located above the catalyst bed (for preheat furnace) and on the external wall of the catalyst zone (for the catalyst zone furnace). The heat-seal furnace was found to give better heat insulation if used in connection with Variac control only. Ceramic orifice gas flowmeters and Ideal needle valves were used to control the gas flows. Pressure control was manual and absolute pressure was measured at the reactor inlet and outlet with mercury manometers. The total effluent was collected and mixed with a Toepler pump. Samples of the total mixture were analyzed by gas chromatography.

B. Materials and Reagents

Catalyst was prepared by impregnating alumina granules with aqueous chromic acid solution, drying, calcining at 1000°F, and preparing a 40-50 mesh fraction by sieving. The catalyst was analyzed and found to contain 29.52 weight per cent Cr_2O_3 and .12 weight per cent Na_2O on dry basis. Surface area by B. E. T. method was found to be 70 square meters per gram.

Gases used for the tests were: (1) pure grade normal butane, pure grade butene-2, research grade ethylene and propylene from Phillips Chemical Company, (2) prepurified nitrogen and cylinder hydrogen from National Gas Company, (3) and building service air which contained 0.0006 grams of CO_2 per liter and approximately 0.0010 grams H_2O per liter.

C. Procedures

A standard procedure was adopted for testing the catalyst to insure reproducibility. When the catalyst was not in use it was usually heated with air going over the catalyst (and in some instances N_2) at a space rate of 1000. Approximately 2.0 cc of 1/70-inch particles were tested.

A test began by treating the catalyst with H_2 at atmospheric pressure for 10 minutes at a space rate equivalent to the hydrocarbon space rate to be used but not going below 1000 space rate. The system was evacuated, checked for leaks for a period of one minute. Immediately after the leak checking period the three-way solenoid on the reactor outlet was activated so there was no possibility of hydrocarbon in the by-pass pressuring back to the catalyst zone. Nitrogen was then turned on over the catalyst at a space rate equal to the hydrocarbon space rate and a moment later the hydrocarbon was turned on and allowed to exit through the by-pass. When the pressure in the reactor built up to the desired pressure of 125 mm Hg absolute (or to atmospheric as in the case of standard butane runs) the reactor outlet solenoid was deactivated so as to commute nitrogen and hydrocarbon below the reactor and control was maintained with one rate valve. The time for this operation was kept to a minimum and usually was accomplished in 2-3 minutes. After all flows and pressures appeared to be steady, a switch controlling the two three-way solenoids above the reactor was activated so that the gas flows were instantaneously reversed (i. e. hydrocarbon started going over the catalyst and nitrogen through the by-pass). An electric clock was connected with this switch so the time measurements were begun simultaneously with the introduction of hydrocarbon. At the same time the switch controlling the solenoids above the reactor was activated, a second switch was activated energizing the solenoid below the reactor. Thus the effluent was conducted into the sample collection system and the pressure in the reactor was manually controlled by a second rate valve. During the dehydrogenation period of three minutes, the by-pass and the reactor were maintained at the same operating pressure to minimize possible leaks through the reactor outlet solenoid. At the end of the dehydrogenation period, the three-way solenoid on the reactor outlet was deactivated and nitrogen was allowed to sweep out any residual hydrocarbon at the same space rate as that used for hydrocarbon. Flushing was conducted long enough to give time for all hydrocarbon to be swept out of the reactor and into the sample collection system. At space rates of 100, flushing was continued for about 7 minutes--the time being measured accurately. After all hydrocarbon was removed from the reactor the sample was "closed in" and the pressure was allowed to build up in N_2 to atmospheric. The sample was removed after the temperature, pressure and volumes were recorded. The sample was replaced with columns of $CaSO_4$ and Ascarite (asbestos impregnated with KOH) connected in series. Nitrogen was turned off and service air was started at 1000 space rate to remove hydrogen and polymer (as water and carbon dioxide) for about one hour.

Temperature measurements were made at six different locations. These are shown schematically in Figure 2. At two of the six locations double thermocouples were used--one for controlling and the other for recording temperatures. Thermocouples were located:

- (1) Externally between the reactor and the core midway down the preheater to indicate how efficiently the gases were heating to reaction temperatures.
- (2) Internally at the preheat outlet or about 1/4-inch above the catalyst bed and inside the thermocouple well. Here also is a second thermocouple used to control the temperature of the preheat furnace.
- (3) Internally at 1/4-inch below the catalyst bed and inside of the thermocouple well.
- (4) Externally between the catalyst reactor and heating core 1/4-inch above the catalyst bed and on the same horizontal axis as (2) above. This thermocouple usually gave lower temperature readings than (2) above because at this point the junction of the narrow preheat furnace and the broader reactor furnace allowed some heat to be lost. Eventually this thermocouple showed signs of radical behavior by giving lower temperature readings. However, it was not replaced because of the danger of dislocating other thermocouples in the process.
- (5) Externally between the catalyst reactor zone and the heating core and midway between the upper and lower catalyst zone. Two thermocouples were located at this position; one for control of the catalyst zone furnace and the other for temperature recordings.
- (6) Externally between catalyst reactor wall and catalyst heating zone core about 3/4-inch below the catalyst zone and at the upper edge of the heat seal reactor. Temperatures were adjusted so as to simulate adiabatic conditions. Before going on hydrocarbon, temperatures at positions 2, 3, 5 described above were maintained within $\pm 5^\circ F$ of the desired reaction temperature. Temperature readings were taken at one minute intervals and the temperature drop recorded. Tables showing temperature recordings therefore represent the average temperatures over the total dehydrogenation period. In actual practice perfect adiabatic conditions were not possible because some heat was supplied through the walls as the endothermic reaction took place.

Analysis of hydrocarbon samples were made by chromatographic procedures at room temperature employing a molecular sieve column for hydrogen, nitrogen, oxygen, methane and carbon monoxide, and a hexamethyl phosphoramine column for the remaining components. The maximum deviation for these analyses was around $\pm 5\%$ of each component which was present in the amount of 10% or less. For components present in larger amounts, the maximum deviation was $\pm 1-3\%$. Typical deviations are usually found to be around $\pm 1\%$ of each component.

TABLE I
RESULTS OF REPRODUCIBILITY STUDIES

<u>Original Procedures</u>		<u>Modified Procedures</u>
<u>Differential Runs</u> ^(b)	<u>Integral Runs</u> ^(c)	<u>Integral Runs</u> ^(a)
<u>Conv.</u> ^(a)	<u>Conv.</u> ^(a)	<u>Conv.</u> ^(a)
3.00	33.9	31.51
3.15	30.4	31.30
5.20	31.6	29.23
2.59	27.7	29.23
3.82	39.0	30.50
1.65	37.4	
2.50		
Mean 3.13	35.0	30.63
Std.Dev. ± 1.13 (+36% of mean)	± 3.6 (+10% of mean)	± 1.06 (+3.5% of mean)

-
- (a) Conversion mols of butane destroyed per 100 mols of feed.
 - (b) Conditions: 1100 F, 1/6 atmosphere absolute pressure, 3 minute dehydrogenation period; feed: the mixture obtained after 20 per cent of the butane is converted in an integral run using a steady state butane-butene mixture.
 - (c) Conditions: 1100 F, 250 GHSV, feed; 60% butane 40% butenes (steady-state); 1/6 of an atmosphere pressure; 3 minute dehydrogenation period.

TABLE II
RANGES OF EXPERIMENTAL CONDITIONS

Pressure, mmHg	760 ^(a) or 125 ^(b)
Temperature, °F	1050, 1100, 1150, 1200, 1250 F
Space Velocity ^(c)	100 - 7000

-
- (a) With n-butane feed only.
 - (b) With mixed n-butane + butene feed only.
 - (c) Volumes of feed (S.T.P.)/volume catalyst/hour

In practice dual analyses were run on each sample and if the deviations were normal they were averaged and these were used for computations.

Catalyst deposits were removed after each run by oxidation with air and measured by absorbing the water formed in a column of CaSO_4 and absorbing the CO_2 formed on Ascarite.

Conversion, yield, selectivity and reaction rate data were calculated with the IBM 7090 computer.

Precision studies were made to determine the reproducibility of results with the equipment and techniques that were employed. Table I presents precision data for differential and integral studies by the original techniques along with data after the equipment and techniques were modified in an attempt to improve reproducibility.

The results of this study show that the precision of integral runs is three times better than that for differential run. This is due to the problem of measuring small changes in reaction products resulting from the low conversions required for differential status. After modifying the procedures and equipment the precision was increased three-fold to a significantly good figure (± 1.06 standard deviation or 3.5% of mean). Precision data were not obtained for the differential runs using the improved techniques, but it is believed that a similar three-fold improvement would be found.

D. Ranges of Experimental Conditions and Data

Table II presents the ranges of experimental conditions used in this study. All possible combinations of these variables were not used; only pure n-butane was used as feed at one atmosphere and it only at a temperature of 1100°F . Sufficient levels of space velocity were used at most temperature levels to establish a butane conversion/space velocity profile. The resulting experimental data and calculated results are quite extensive and are not reproduced here.

Since one objective of the mixed feed runs was to obtain data representative of operation of a plant operating on "steady-state" feed, the feed composition was changed with the temperature level. Feed composition varied from approximately 62 mole % n-butane, 38 mole % butene-2 at 1050°F to 73 mole % n-butane at 1250°F .

III. CORRELATION OF DATA

As a result of using "steady-state" feeds, net butene conversion in all runs was zero plus or minus a few per cent. Therefore, correlation of butene conversion was not attempted.

The complicating feature of the correlation of the dehydrogenation data was the gradual decline in catalyst activity with time. Data taken over a short period of catalyst life, particularly early in the catalyst life, indicated that conversion could be well correlated with space velocity by an equation of the form:

$$x = \frac{f}{a + bf} \quad (1)$$

where

- x = fractional conversion, mols converted per mol of feed.
- f = reciprocal space velocity, ft^3 catalyst-hr per mol feed.
- a, b = empirical constants.

Reciprocal space velocity in terms of mols of feed rather than volume of feed was chosen as the independent variable to give the proper units for the rate of reaction calculated by taking the derivative of x with respect to f.

The normal butane dehydrogenation data obtained at atmospheric pressure and 1100°F . were used to determine the effect of catalyst age on conversion. A number of equation forms were tried; the only acceptable fit of the data was obtained with an equation of the form:

$$x = \frac{f}{a + c\theta d + bf} \quad (2)$$

where

- x = fractional conversion, mols converted/mol feed.
- f = reciprocal space velocity, ft^3 catalyst-Hr/mol feed.
- θ = age of catalyst, days.
- a, b, c, d = empirical constants.

A computer curve fit of the data gave the following values for the constants in equation (2):

- a = 0.13707
- b = 1.26470
- c = 4.18770×10^{-7}
- d = 2.84670

A comparison of the experimental and calculated conversions is shown in Figure 3.

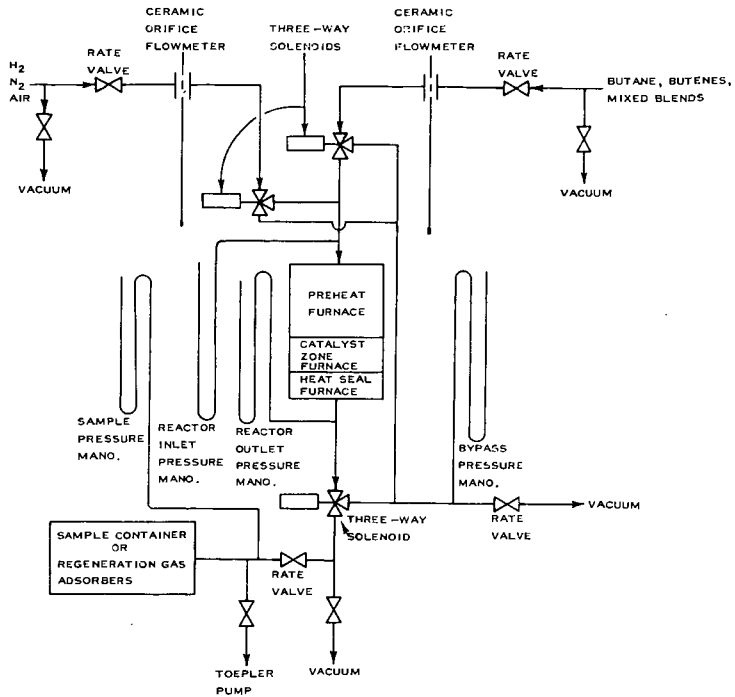


FIGURE 1
ASSEMBLY OF CATALYST TESTING EQUIPMENT

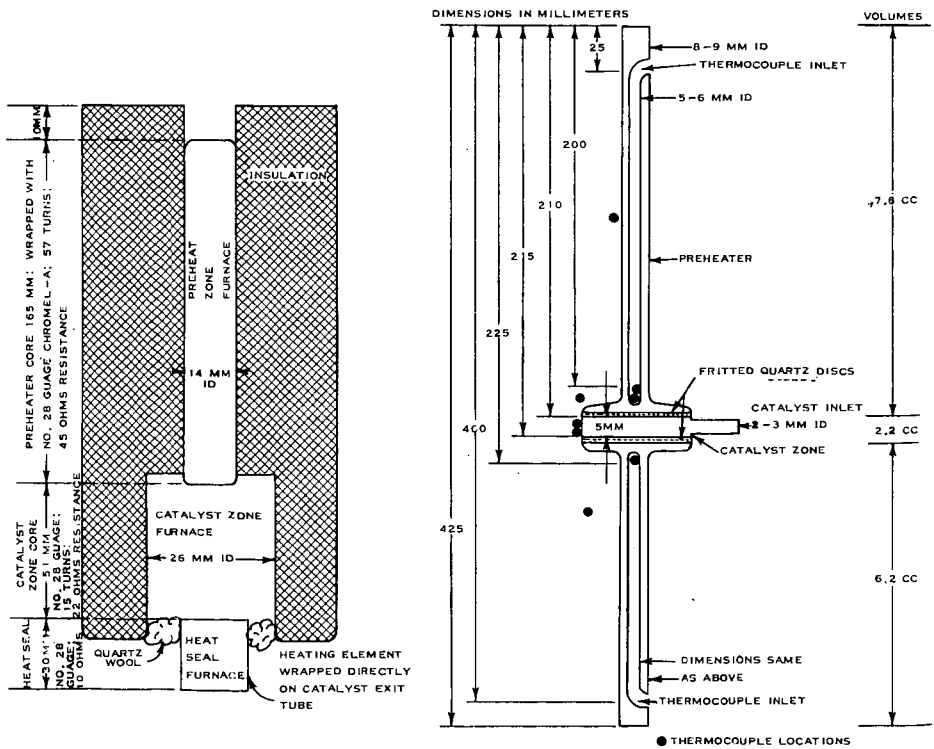


FIGURE 2
REACTOR AND FURNACE ASSEMBLY

There are a number of ways of expressing the activity of one catalyst relative to that of a second (or of the first at a different age). From the standpoint of reaction kinetics work, the preferred method (1) is to express the activity as the ratio of space velocities necessary to obtain the same conversion with the two catalysts. To obtain consistent correlations, it was desired to convert all the data available to their equivalent with a new (zero age) catalyst. For a zero age catalyst equation (2) reduces to:

$$x = \frac{f_0}{a + bf_0} \quad (2a)$$

where f_0 = reciprocal space velocity with zero age catalyst.

To find an expression for the equivalent space velocity with a zero age catalyst, equations (2) and (2a) are equated:

$$\frac{f_0}{a + bf_0} = \frac{f}{a + c\theta^d + bf} \quad (2b)$$

Solving this expression for f_0 in terms of f and θ gives:

$$f_0 = \left(\frac{a}{a + c\theta^d} \right) f \quad (3)$$

The quantity $\left(\frac{a}{a + c\theta^d} \right)$ is, in effect, the catalyst activity factor. Equation (3) was used to correct all the experimental space velocities for the mixed butane-butene feed data to their equivalents at zero catalyst age. In so doing it was tacitly assumed that the constants a , c , and d were not functions of temperature and pressure, or, if they were, that the effect of temperature and pressure were cancelled out by the form of the activity factor relation. It should be emphasized that this relation for activity is strictly empirical and must not be used with any other set of data or calculations without experimental confirmation.

The mixed butane-butene feed data were correlated as follows:

1. The experimental butane conversions, x_1 , where correlated as a function of the equivalent reciprocal space velocities, f_0 , calculated as outlined above in the form:

$$x_1 = \frac{f_0}{a + bf_0} \quad (4)$$

A separate correlation was obtained at each temperature level except 1200°F. At 1200°F. only three data points were available, all at essentially the same space velocity, so that a valid correlation could not be obtained.

2. The logarithms of the values of a and b obtained at each temperature level were plotted against reciprocal absolute temperature, Figure 4. From inspection of these plots, it appeared that the 1100°F points were out of line. These points were ignored and the remaining three points on each plot, representing data at 1050, 1150, and 1250°F., were fit to an equation of the form:

$$\ln a \text{ (or } \ln b) = \alpha + \beta \left(\frac{1}{T} \times 10^5 \right) \quad (5)$$

Evaluation of the constants gave the following results:

$$\ln a = -15.97115 + 0.25232 \left(\frac{1}{T} \times 10^5 \right) \quad (6)$$

$$\ln b = -1.82226 + 0.04281 \left(\frac{1}{T} \times 10^5 \right) \quad (7)$$

where $T = ^\circ R, ^\circ F + 460$.

As a test to justify ignoring the 1100°F. points, equation (6) was used to calculate a at 1200°F. This value of a and equation (4) were then used to calculate a value of b from each of the three data points available at 1200°F. The three values of b were then averaged. This average value of b was identical with the value calculated by equation (7) for 1200°F. It was concluded that ignoring the 1100°F. points was justified since the 1200°F. data had not been used to develop equations (6) and (7).

To check the overall correlation, equations (6) and (7) were used in conjunction with equation (4) to calculate a butane conversion value for each experimental point. Figure 5 shows a plot of observed versus calculated butane conversion and Figure 6 shows the experimental data plotted as conversion versus equivalent reciprocal space velocity; constant temperatures lines are shown calculated from equations (4), (6), and (7). The standard error of estimate for predicting butane conversion is 0.02429, very close to the standard deviation of replicate experimental determinations.

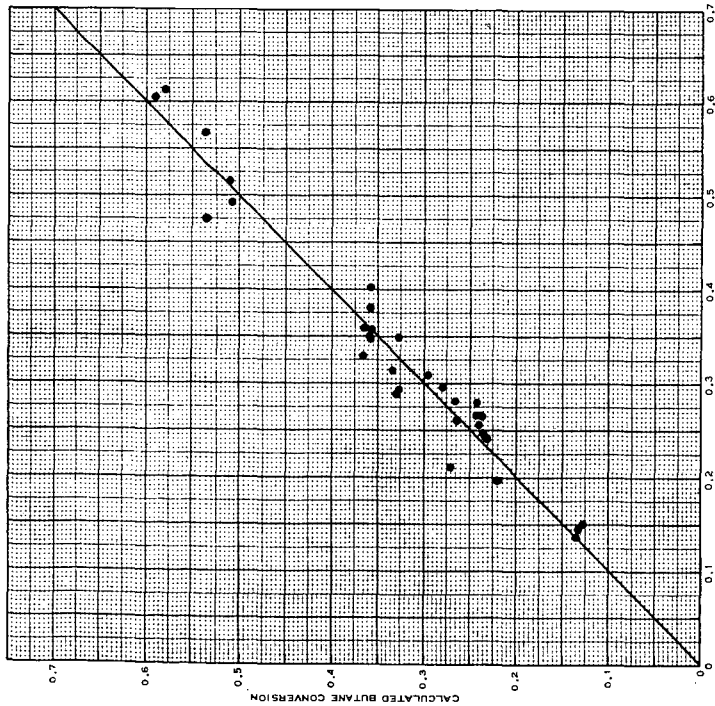


FIGURE 3
CALCULATED VS OBSERVED BUTANE CONVERSION
R - BUTANE FEED, 1100 F., 1 ATM

$X = 0.13702 + 4.10770 \times 10^{-7} f$
 $X = \text{FRACTIONAL BUTANE CONVERSION, MOLES/MOL FEED}$
 $f = \text{RECIPROCAL SPACE VELOCITY, CU. FT. CATALYST - HR/MOL FEED}$
 $\bullet = \text{CATALYST AGE, DAYS}$

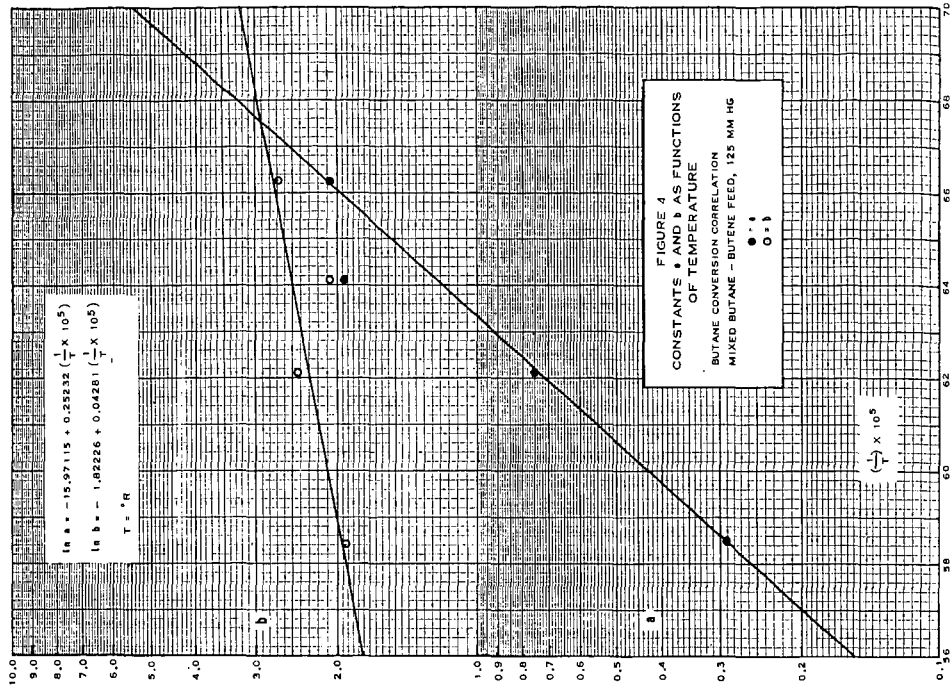


FIGURE 4
CONSTANTS a AND b AS FUNCTIONS OF TEMPERATURE
BUTANE CONVERSION CORRELATION
MIXED BUTANE - BUTENE FEED, 125 MM HG

$\ln a = -15.97115 + 0.25232 \left(\frac{1}{T} \times 10^5 \right)$
 $\ln b = -1.82226 + 0.04281 \left(\frac{1}{T} \times 10^5 \right)$
 $T = ^\circ R$

A similar correlation procedure was used to correlate the data on butadiene appearance. At each temperature level (except 1200°F.), the data were fit to:

$$x_2 = \frac{f_o}{a + bf_o} \quad (4a)$$

where x_2 = butadiene appearance, mols per mol of feed. To be consistent with the result for butane disappearance, the 1100°F. data were ignored, and the a and b values for 1050, 1150, 1250°F. fit as functions of temperature. The results were:

$$\ln a = -13.03794 + 0.19267 \left(\frac{1}{T} \times 10^5 \right) \quad (6a)$$

$$\ln b = -4.48793 + 0.09814 \left(\frac{1}{T} \times 10^5 \right) \quad (7a)$$

Figure 7 shows plots of equations (6a) and (7a) with the data points. A check calculation at 1200°F. confirmed the validity of ignoring the 1100°F. data. Figure 8 shows a plot of observed versus calculated butadiene appearance and Figure 9 shows the experimental data plotted as appearance versus equivalent reciprocal space velocity, with constant temperature lines calculated from equations (4a), (6a) and (7a). The standard error of predicting butadiene appearance is 0.01414.

By differentiating the equation expressing conversion as a function of reciprocal space velocity with respect to reciprocal space velocity, an expression is obtained for the rate. Thus, for butane disappearance the rate is:

$$r_1 = \frac{a}{(a + bf_o)^2} \quad (8)$$

and for butadiene appearance the rate is:

$$r_2 = \frac{a}{(a + bf_o)^2} \quad (8a)$$

where r_1 = mols butane converted/ft³ catalyst-hr.

r_2 = mols butadiene produced/ft³ catalyst-hr.

f_o = equivalent reciprocal space velocity for zero age catalyst, ft³ catalyst-hr/mol feed.

a and b = constants calculated from equations (6) and (7) for butane or (6a) and (7a) for butadiene.

IV. DISCUSSION

In preparation for this study, the two well known methods of obtaining reaction rate data were compared, viz., differential experiments (using various feed mixtures which represent the total product at various locations in the reactor, and a relatively short residence time to give a small conversion), and integral experiments (using a feed mixture which represents the steady-state feed to the reactor, and various residence times to give various conversion levels). Based on this comparison, the integral experimental method was chosen because it gave more precise results than were given by differential experiments. This resulted from the relatively large changes in feed composition which occurred in the integral experiments compared to the relatively small changes in differential experiments.

In this work to obtain data for use in studies of n-butane and butenes dehydrogenation kinetics, temperatures above those normally used with chromia-alumina catalysts were employed. This caused a reduction in catalyst activity and required the use of a catalyst activity index. The value of this index was established at frequent intervals by testing the catalyst for the dehydrogenation of steady-state feed at 1100°F. This index has been used in correlations of these data; however, it may not be entirely satisfactory according to recent tests. These tests with pure n-butane and pure butenes showed that aging or heat-treating the chromia-alumina catalyst reduced its activity for n-butane dehydrogenation but did not affect its activity for butenes dehydrogenation. Data for the 1100°F. profile are questionable because they were obtained before the experimental procedure and equipment were entirely satisfactory. Some of the reasons for the unreliability of the data were: (1) flow rates in the catalyst zone varied widely during each test due to the relatively large volume of the gas handling system, and (2) the product sampling procedure did not insure collection of the total product from a test. These problems affected only the 1100°F. data for the steady-state feed.

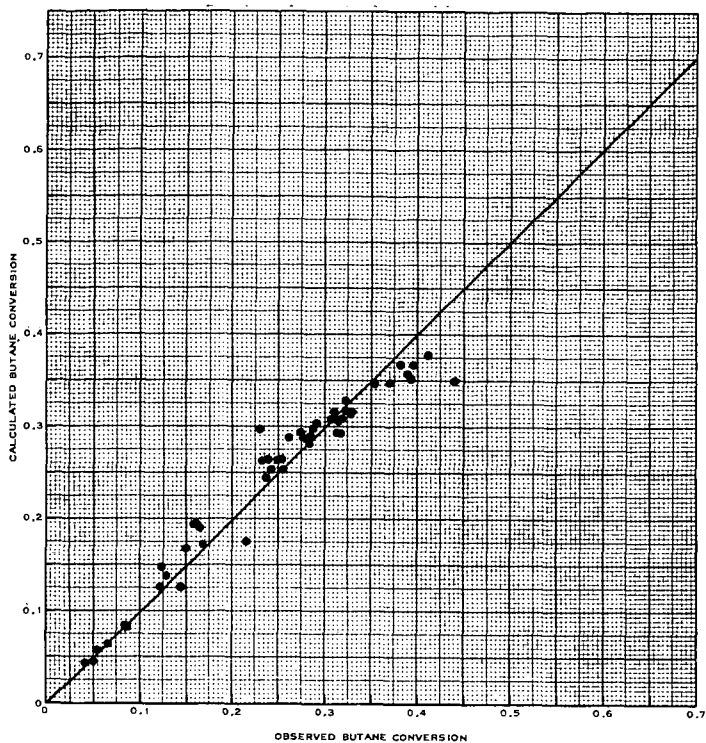


FIGURE 5
CALCULATED VS OBSERVED BUTANE CONVERSION

MIXED BUTANE-BUTENE FEED, 125 MM HG
1050 F, 1100 F, 1150 F, 1200 F AND 1250 F

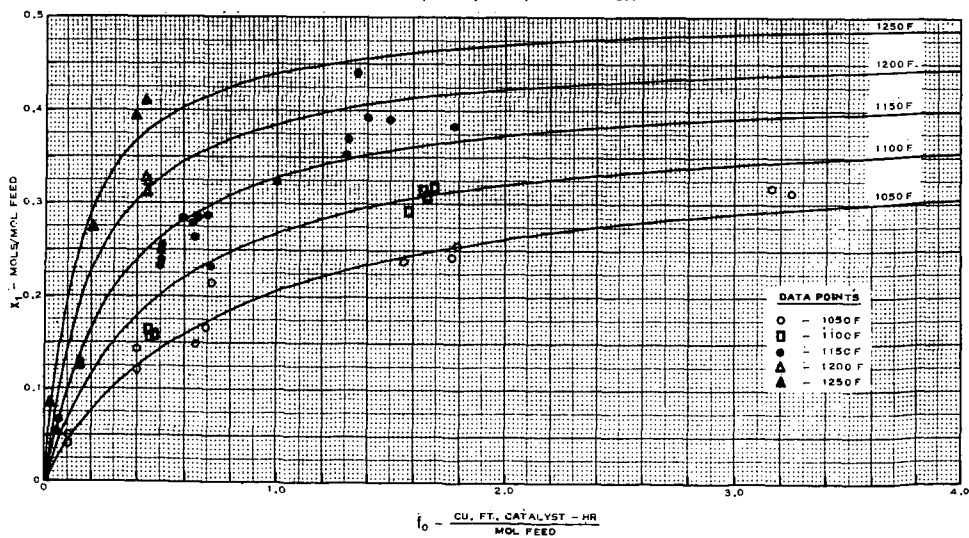


FIGURE 6
BUTANE CONVERSION
VS
EQUIVALENT RECIPROCAL SPACE VELOCITY

The correlations developed appear to fit the data within the experimental accuracy. Figure 3 shows a slight trend toward a breakdown of the butane conversion correlation at high conversion levels.

It must be emphasized that the correlations are empirical and care must be exercised in their use. Within the range of operating variables covered the correlations are adequate for process design work. Their most effective use, however, may be to use them to smooth the experimental data prior to evaluation of reaction mechanism type equations. The use of the correlations in this manner will give an internally consistent set of values for rates to evaluate the constants in reaction mechanism equations.

V. CONCLUSIONS

From the results of this study it is concluded that the conversion of n-butane and the appearance of butadiene in the dehydrogenation of n-butane can be satisfactorily correlated as functions of reciprocal space velocity using a two constant hyperbolic equation. The two constants of this equation can in turn be satisfactorily correlated as functions of temperature by an Arrhenius type equation.

Within the range of the variables studied the resulting equations are suitable for process design work. The equations should also be useful in smoothing the experimental data to obtain rates for a mechanistic type study of the reaction kinetics.

VI. LITERATURE CITED

- (1) Hougen, O. A., and Watson, K. M., "Chemical Process Principles, Part Three, Kinetics and Catalysis", p. 936. John Wiley and Sons, Inc., New York, 1949.

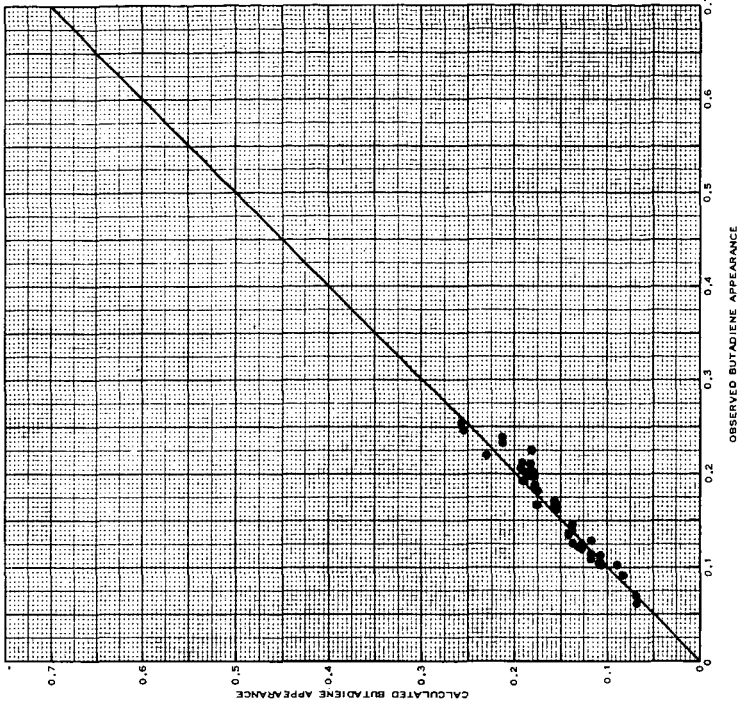


FIGURE 8
CALCULATED VS OBSERVED BUTADIENE
APPEARANCE (MOLS/MOL FEED)

MIXED BUTANE-BUTENE FEED, 125 MM HG
1050 F., 1100 F., 1150 F., 1200 F. AND 1230 F.

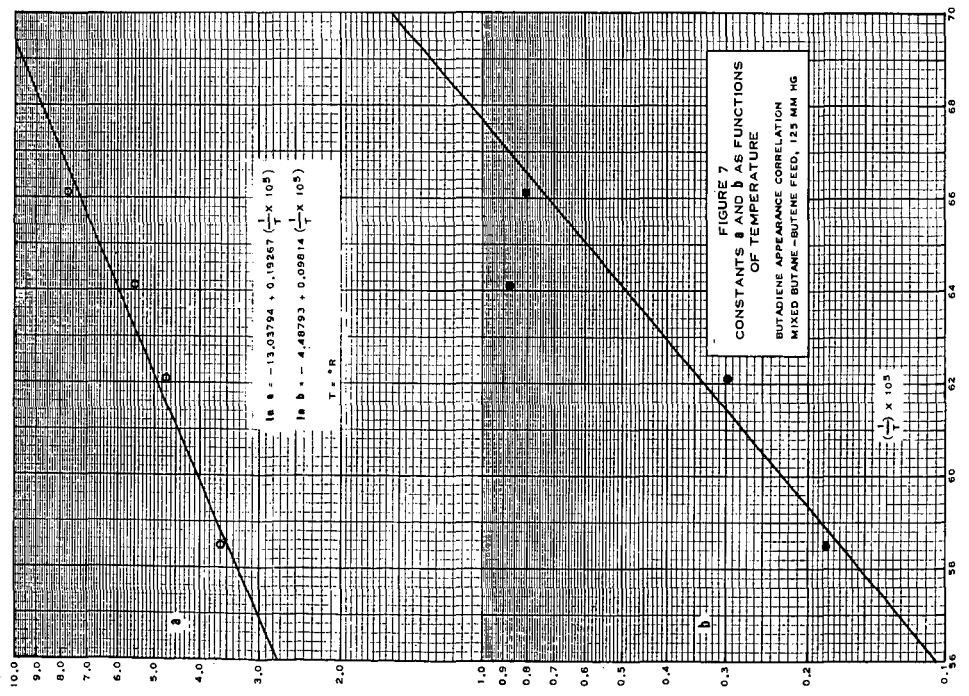


FIGURE 7
CONSTANTS *a* AND *b* AS FUNCTIONS
OF TEMPERATURE

BUTADIENE APPEARANCE CORRELATION
MIXED BUTANE-BUTENE FEED, 125 MM HG

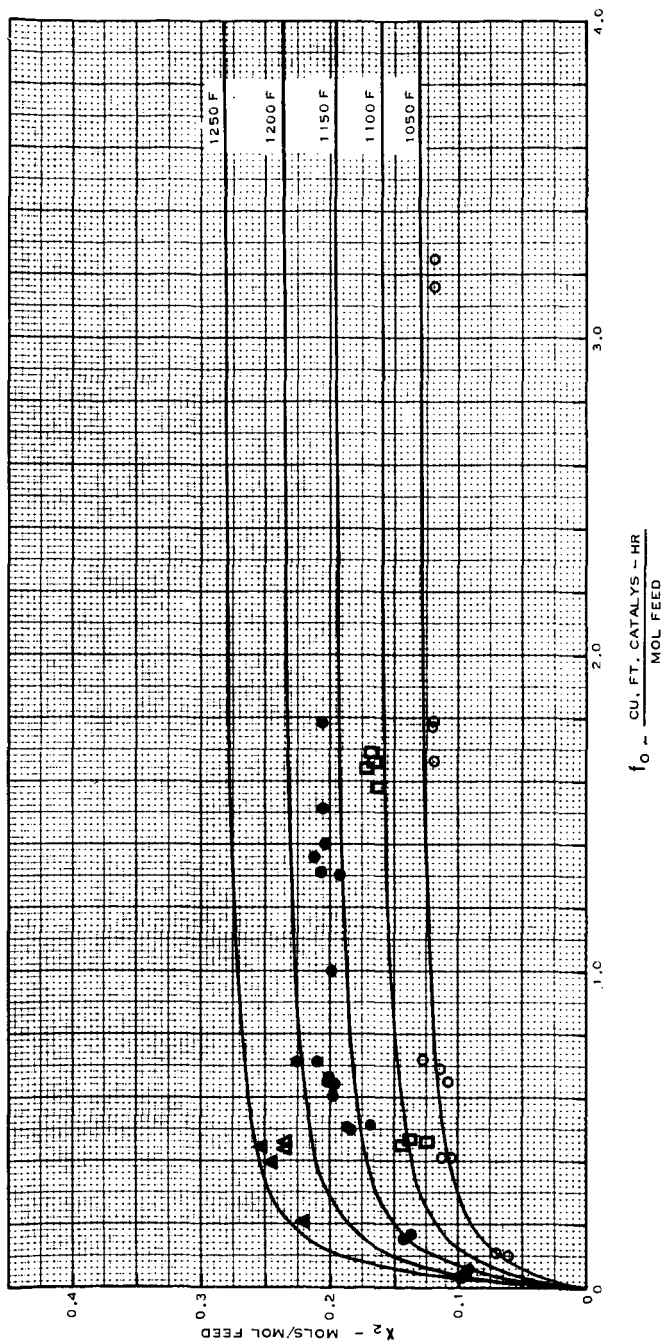


FIGURE 9
 BUTADIENE APPEARANCE
 VS
 EQUIVALENT RECIPROCAL SPACE VELOCITY

SYMPOSIUM ON PYROLYSIS REACTIONS OF FOSSIL FUELS
PRESENTED BEFORE THE DIVISION OF PETROLEUM CHEMISTRY, INC.
AMERICAN CHEMICAL SOCIETY
PITTSBURGH MEETING, MARCH 23-26, 1966

THE EFFECT OF STRUCTURE ON THE RATES OF PYROLYSIS
OF NAPHTHENES

By

A. W. Ritchie and A. C. Nixon
Shell Development Company
Emeryville, California

INTRODUCTION

The Air Force is considering the use of vaporizing and endothermic fuels for cooling high-speed aircraft in the range Mach 3 to about 10. In our work on this problem, as reported in previous papers, (1, 2) we have shown how the endothermic portion of the heat sink can be provided through catalytic dehydrogenation reactions of, particularly, naphthenes. Also, some heat sink can be obtained through thermal cracking reactions. In any event, pyrolysis can be expected to occur in any system in which hydrocarbons are heated up to 1400°F or higher. Accordingly, we have investigated the pyrolytic reactions undergone by all hydrocarbons we have attempted to react catalytically. In this paper we present the results of these studies on naphthenic hydrocarbons. The emphasis here is on the relative rates of the thermal reaction of the various naphthenes rather than the heat sinks obtainable from them.

Methylcyclohexane (MCH), ethylcyclohexane (ECH), the three dimethylcyclohexane (DMCH) isomers, a mixture of the three diethylcyclohexane isomers (DECH), dicyclohexyl (DCH) and a mixture of decalin and methylcyclohexane were tested at 10 atm pressure in the temperature region of 900-1300°F. First-order rate constants were calculated, based on the rate of disappearance of the starting material according to the following equation:*

$$K_{\text{sec}}^{-1} = \frac{\text{LHSV}}{3600} \times \frac{\rho \times 22,412}{\text{MW} \times P} \times \frac{T}{273} \times 2.3 \log \frac{1}{1-f} \quad (1)$$

where

- LHSV = liquid hourly space velocity (i. e., volumes of feed/volumes of "catalyst" per hour)
MW = molecular weight
P = reactor pressure in atmospheres
T = reaction temperature in °K (block temperature)
 ρ = density
f = fraction reacted.

Relative reactivities and activation energies were computed from these first-order rate constants.

Liquid products were analyzed by GLC and were found to be mainly cracked material with small amounts of dealkylated aromatics and unidentified material that was heavier than the feed. The light gas products were analyzed by mass spectrometry and were found to be mainly methane with lesser amounts of hydrogen, ethane, ethylene and C₃ and C₄ hydrocarbons.

The apparatus was a tubular flow reactor equipped with conventional devices for measuring feed flow rates and for collecting liquid and gas products. The reactor was a stainless steel tube (No. 347, 1/2-inch IPS) 32 inches long and was heated by an electric furnace. The complete apparatus was described in detail in the previous papers. (1, 2) For the thermal tests 20 ml of quartz chips (10-20 mesh) were substituted for the catalyst; the "catalyst bed"

*A more intricate method for calculating rate constants for reaction of starting material to gas, liquid, and liquid residues has been proposed by Fabus (3) et al which is particularly applicable to the batch conditions under which they conducted their studies. Our method is patently not strictly accurate since we neglect the volume occupied by the space filler (quartz chips) and ignore the fact that a number of moles of product are generated in the reactor which has the effect of reducing contact time. We also ignore the possibility that reaction can take place before and after the quartz chip bed.

was 3/16 in. annular thickness and about 5 in. long.

Feed materials were:

Methylcyclohexane: Phillips' pure grade passed over silica gel prior to use. Analyzed 99+ % MCH.

Ethylcyclohexane: Matheson, Coleman and Bell, practical grade; passed over silica gel prior to use. Analyzed 97.7% ECH, 2.3% MCH.

Dimethylcyclohexane: The DMCH isomers were prepared by hydrogenation of the corresponding xylenes. The various isomers had the following cis and trans composition:

	<u>1,4-DMCH</u>	<u>1,3-DMCH</u>	<u>1,2-DMCH</u>
% trans	32.1	31.8	40.8
% cis	67.6	68.2	57.8
trans/cis feed	0.475	0.456	0.706
trans/cis equil (1200°F)	1.57	0.645	2.13

Diethylcyclohexane: A Shell Chemical Company preparation containing a mixture of the three isomers and their cis and trans species with the following composition:

	<u>1,4-DECH, %</u>	<u>1,3-DECH, %</u>	<u>1,2-DECH, %</u>
trans	16.2	16.6	6.0
cis	13.4	38.2	9.6
total	29.6	54.8	15.6

Dicyclohexyl: Prepared by hydrogenation of diphenyl. Contained 1.6% phenylcyclohexane.

Decalin: Eastman Kodak practical grade. Contained about 1% of tetralin. Passed over silica gel prior to use.

RESULTS AND DISCUSSION

Conversions as a function of temperature for reaction of the various naphthenes are shown in Table 7, which also shows the yield of liquid and gas products. Complete data for the various naphthenes are shown in Tables 1 to 6, inclusive. Ethylcyclohexane was the most reactive naphthene at 1202°F and over 50% of the starting material was converted compared to 43.7%, 27.3%, and 20.6% for DECH, DMCH (average), and MCH, respectively. First-order rate constants were calculated from the conversions and are also tabulated in Table 7 and plotted as a function of 1/T in Figures 2 and 3. Relative reactivities of the various naphthenes at 1202°F (basis MCH = 1.00) were obtained from these rate constants and are presented in Table 8. Based on these values the relative naphthene reactivities are: ECH > DECH > DCH > DMCH > MCH. This suggests that addition of side chains to the naphthene ring enhances the reactivity for thermal reaction. Further, it appears that naphthenes with side chains containing two carbon atoms are more reactive than those with a side chain containing a single carbon atom.

With DMCH the position of the side chains and their trans-cis arrangement did not appear to influence the reactivity except for the trans 1,3- species. For example, at 1202°F the rate constants for the various isomers and their cis and trans species ranged from 0.091 to 0.10 except for the trans 1,3- species which was 0.053 (Table 3). Further, the evidence is that trans-cis isomerization was not extensive with the 1,4- and 1,2- isomers. This conclusion is based upon the observation that with these two isomers the trans/cis ratios of the feeds and products were about the same and were far from equilibrium (Figure 1, Table 3). For the 1,3- isomer the trans/cis ratios of the feed and product were about the same but were fairly close to the equilibrium value. Hence, no conclusions as to the isomerization rates can be made for this naphthene isomer but they would not be expected to differ much from the other isomers. The equilibrium values were calculated from the data of American Petroleum Institute, Research Project 44.

For DECH the reactivities of the three isomers decreased in the following order: 1,3 > 1,4 > 1,2 (Table 8). For the 1,3 and 1,4 isomers there was no effect of cis-trans arrangement on reactivity for a given isomer (Table 4). For the 1,2- species the trans species was considerably less reactive than the cis. The fact that the trans 1,3-DMCH species and the trans 1,2-DECH species appeared to be more stable than the other species under our conditions is simply an environmental accident, since the fact that their activation energies are higher requires that at some higher temperature they will react more rapidly (in this case this temperature is about 1350°F).

Activation energies were calculated for the various naphthenes and their isomers using the calculated rate constants. These values ranged from 35.0 to 70.0 kcal/mole (Table 8,

Table 1. THERMAL REACTION OF METHYLCYCLOHEXANE

"Catalyst": Quartz Chips
 "Catalyst" Volume: 20 ml
 Reaction Time: 20 min
 Pressure: 10 atm
 LHSV: 20

Run No.	8546-57	9426-51	9426-52
Temperature, °F			
Block	1112	1202	1295
Wall	-	1188	1256
"Catalyst" Bed	1067	1152	1191
Product Components, %			
MCH	88.8	79.4	52.3
Benzene	0.1	0.7	3.1
Toluene	0.2	0.4	2.2
Cracked, liquid	8.2	7.3	13.6
Cracked, gas	-	4.6	17.7
Heavier than Toluene	-	-	0.6
Others ^{a)}	2.8	7.7	10.5
MCH Conversion, %	11.2	20.6	47.7
First-Order Rate Constant, sec ⁻¹	0.04	0.08	0.22

a) Methylcyclohexenes, methylcyclohexadienes.

Table 2. ETHYLCYCLOHEXANE

Pressure: 10 atm
 LHSV: 20
 "Catalyst" Volume: 20 ml
 "Catalyst": Quartz Chips
 Reaction Time: 20 minutes
 Feed: 97.7% ECH, 2.3% MCH

Run No. 8957-	37	38-1	38-3	39
Reaction Time, min	20	20	20	20
LHSV	20	20	20	20
Temperature, °F				
Block	932	1022	1112	1202
Wall	932	1020	1108	1194
Catalyst	932	1020	1106	1188
Product Analysis, %				
Ethylcyclohexane	97.4	91.9	80.1	47.3
Ethylcyclohexene	-	-	-	-
Benzene	0.1	0.3	0.7	3.9
Toluene	-	-	0.1	1.8
Xylene	-	-	0.4	0.9
Ethylbenzene	-	-	-	0.5
Styrene	-	-	0.1	0.6
Cracked Products	2.3	3.7	12.7	25.0
Light gas	-	4.1	6.1	19.8
ECH Conversion, %	2.6	8.1	19.9	52.7
Rate Constant, sec ⁻¹	-	0.012	0.066	0.26

Figure 2). There was no general correlation between reactivity and activation energy, i. e., frequency factors also varied for different naphthenes. These values of the activation energies showed greater spread than was observed by Fabus et al. (4) These workers found that in a static system at 750 to 850°F and at 130 atm pressure most of the activation energies ranged between 60 and 65 kcal.

Curiously, the ethyl derivatives (with the exception of trans 1, 2) and DCH all had energies of activation closer to that of MCH than did the dimethyl derivatives, all of which had E's substantially greater than MCH.

Typical gas-phase product distributions are tabulated in Table 9 for reaction at 1202°F. In all cases the principal product was methane with lesser amounts of hydrogen, ethane, and ethylene. Since with ECH and DECH the sum of the ethane plus ethylene was greater than or equal to the methane formed while with MCH and DMCH the sum of the C₂ components was considerably less than the methane, it is apparent that dealkylation of the side chain is one of the important reactions during pyrolysis of alkyl naphthenes.

CONCLUSIONS

1. The average rate of pyrolysis of naphthenes is $K = 0.1 \text{ sec}^{-1}$ at about 1180°F.
2. The average energy of activation is about 50 kcal/mole, but values range from 37 to 70.
3. Activation energies are generally higher for the dimethyl derivatives than for the ethyl derivatives or MCH or DCH.
4. The highest activation energies are for two trans derivatives, 1, 3-DMCH or 1, 2-DECH.
5. Generally the position of methyl groups does not affect rates while that of ethyl groups does.
6. Both ring and side chain cracking occurs during pyrolysis.

ACKNOWLEDGMENT

This work was done under the sponsorship of the Fuels, Lubricants, and Hazards Branch of the Air Force Aero-Propulsion Laboratory, Wright-Patterson Air Base, Messrs. J. Fultz and C. Johnson, Project Engineers. Permission to publish by the Air Force and by Shell Development Company is acknowledged. We are also happy to thank Dr. R. D. Hawthorn for assistance with the chemical calculations and Mr. D. P. Anderson for contributing laboratory skills.

LITERATURE CITED

- (1) Ritchie, A. W., Hawthorn, R. D., and Nixon, A. C., IEC Product Research and Development 4, 129 (1965).
- (2) Ritchie, A. W., and Nixon, A. C., ACS Div. Pet. Chem. Preprints, 10, 61 (August, 1965).
- (3) Fabus, B. M., Smith, J. O., Lait, R. I., Fabus, M. A., and Satterfield, C. N., Ind. Eng. Chem. Process Design and Development, 3, 33 (1964).
- (4) Fabus, B. M., Kasefjian, R., Smith, J. O., and Satterfield, C. N., Ind. Eng. Chem. Process Design and Development, 3, 248 (1964).

Table 3. THERMAL REACTION OF DIMETHYLCYCLOHEXANE ISOMERS

"Catalyst": Quartz Chips "Catalyst" Bed Thickness: 3/16 in.
 "Catalyst" Volume: 20 ml Pressure: 10 atm
 "Catalyst" Size: 10-20 mesh Reaction Time: 20 min
 IHSV: 20

Run No.	81	82	83-1	83-3	93	94-1	94-3	95	99	100-1	100-3	101
Isomer			1,4-DMCH			1,3-DMCH				1,2-DMCH		
% trans			32.1			31.1				40.8		
% cis			67.6			68.2				57.8		
Trans/cis, feed			0.475			0.456				0.706		
Trans/cis, equil (1200° F)			1.57			0.645				2.13		
Temperature, °F												
Block	932	1022	1112	1202	932	1022	1112	1202	932	1022	1112	1202
Wall	927	1017	1108	1188	927	1017	1108	1190	930	1020	1108	1191
"Catalyst" Bed	898	990	1082	1143	896	986	1076	1141	909	1000	1082	1144
Product Analysis, % ^a												
trans DMCH	31.8	31.9	30.7	22.7	31.1	31.0	30.5	25.4	40.8	40.6	38.4	29.7
cis DMCH	67.9	67.4	64.7	48.5	67.8	67.8	64.8	49.1	57.6	57.2	54.2	40.6
Benzene	0.0	0.0	0.0	1.8	0.0	0.0	0.0	1.1	0.0	0.0	0.6	2.3
Toluene	0.0	0.0	0.0	1.4	0.0	0.0	0.0	1.0	0.0	0.0	0.1	1.8
Xylene	0.4	0.4	0.4	0.7	0.0	0.0	0.0	0.2	0.3	0.3	0.1	0.4
Cracked, liquid ^a	0.0	0.1	2.7	10.5	0.1	0.1	2.4	9.5	1.2	2.0	6.5	16.5
Cracked, gas	0.0	0.0	0.0	10.5	0.0	0.0	0.0	7.9	0.0	0.0	0.0	10.0
Others	0.0	0.2	1.4	3.8	1.1	1.1	2.3	4.5	0.0	0.0	0.3	0.6
Trans/cis, products	0.468	0.473	0.474	0.468	0.452	0.452	0.470	0.518	0.71	0.71	0.71	0.73
Conversion, %												
trans DMCH	0.0	0.6	4.3	29.2	0.0	0.5	2.0	16.8	0.0	0.3	6.0	27.8
cis DMCH	0.0	0.3	4.3	28.2	0.7	0.7	5.0	28.1	0.4	1.2	6.4	30.5
Total	0.0	0.4	4.3	28.5	0.4	0.5	4.0	24.5	0.3	0.9	6.2	28.8
First-Order Rate Constant, sec ⁻¹												
trans	-	-	0.012	0.099	-	-	0.006	0.053	-	-	0.017	0.091
cis	-	-	0.012	0.098	-	-	0.014	0.094	-	-	0.018	0.104
Total	-	-	0.012	0.098	-	-	0.011	0.091	-	-	0.017	0.10

^a) lighter than DMCH.

Table 4. DIETHYLCYCLOHEXANE

Pressure: 10 atm
 LHSV: 20
 Reaction Time: 20 min
 Feed: $\frac{1}{2}$ DECH, %
 16.2 trans
 13.4 cis
 29.6 total

"Catalyst": Quartz Chips
 "Catalyst" Size: 10-20 Mesh
 "Catalyst" Volume: 20 ml

$\frac{1}{2}$ DECH, %
 16.6 trans
 38.2 cis
 54.8 total

$\frac{1}{2}$ DECH, %
 6.0 trans
 9.6 cis
 15.6 total

Reaction Data		125-1	125-2	126-1
Run 8957-		1112	1202	1293
Temperature, °F		1100	1180	1251
Block		1056	1118	1159
Wall				
Catalyst Bed				
DECH Conversion, %		11.8	42.6	72.8
trans-1,4		11.2	43.5	75.4
cis-1,4		11.5	42.9	74.0
Total 1,4		15.2	45.4	75.8
trans-1,3		18.1	46.2	75.1
cis-1,3		17.2	46.0	75.3
Total 1,3		3.4	31.7	65.0
trans-1,2		9.4	40.6	73.9
cis-1,2		7.1	37.2	71.2
Total 1,2		14.0	43.7	74.1
Total DECH				
Rate Constant, sec ⁻¹		0.029	0.133	0.321
trans-1,4		0.027	0.125	0.317
cis-1,4		0.028	0.134	0.345
Total 1,4		0.030	0.145	0.361
trans-1,3		0.046	0.149	0.354
cis-1,3		0.043	0.148	0.356
Total 1,3		0.008	0.054	0.267
trans-1,2		0.023	0.125	0.342
cis-1,2		0.017	0.111	0.317
Total 1,2		0.035	0.136	0.344
Total DECH				

Product Analyses		125-1	125-2	126-1
Run 8957-		1112	1202	1293
Block Temperature, °F		2.7	10.5	17.3
Reaction Products, %		0.0	2.3	5.9
Cracked		0.4	2.5	2.5
Benzene		0.0	1.7	4.4
UI		0.3	0.3	0.5
UI		3.3	4.8	2.9
UI		0.9	1.4	0.9
UI		0.0	0.0	0.8
UI		1.6	2.7	1.8
m,p-Xylenes		1.1	1.9	1.8
UI		0.0	0.3	0.3
UI		0.0	0.0	0.3
UI		0.5	0.0	0.2
DECH, cis-1,3		31.2	20.5	9.5
trans-1,4		14.5	9.5	4.4
trans-1,3		14.0	9.0	4.0
trans-1,2		5.8	4.1	2.1
cis-1,4		11.9	7.6	3.5
cis-1,2		8.7	5.7	2.5
UI		0.3	0.3	0.0
Light gas		0.0	14.8	34.5

a) UI = unidentified product.

Table 6. THERMAL REACTION OF DECALIN-METHYLCYCLOHEXANE MIXTURE

Feed: Decalin, 22.1%
 MCH, 77.9%
 Pressure: 10 atm
 "Catalyst" Bed Thickness: 3/16 in.
 "Catalyst": Quartz Chips
 "Catalyst" Volume: 20 ml
 Reaction Time: 20 min
 LHSV: 20

Run No. 8946-		1022	1112	1202
Temperature, °F		959	1051	1130
Block				
Catalyst				
Liquid Product Analysis, %				
MCH		76.8	74.4	64.0
cis-Decalin		11.8	11.7	8.3
trans-Decalin		8.9	9.0	7.0
Toluene		-	0.1	0.8
Benzene		-	0.1	0.8
Methylcyclohexenes		0.4	2.1	6.7
Naphthalene		-	-	0.1
Cracked, liquid		0.2	0.9	0.1
Cracked, light gas		-	-	4.0
First-Order Rate Constant, sec ⁻¹				
MCH		0.004	0.014	0.0638
Decalin		0.005	0.005	0.0990
Conversion, %				
MCH		1.4	4.5	17.9
Decalin		2.0	2.0	30.8

Table 5: THERMAL REACTION OF DICYCLOHEXYL

Pressure: 10 atm
 LHSV: 20
 Feed: 98.4% DCH
 1.6% PCH
 Quartz chip
 "Catalyst":
 "Catalyst" Volume: 20 ml

Run 9426-	Temperature, °F		Product Analysis, %				DCH Conversion, %	First-Order Rate Constant, sec ⁻¹
	Block	"Catalyst" Bed Wall	DCH	PCH ^{b)}	Cracked, Liquid	Cracked, Light Gas		
15	1022	1015	94.7	1.8	3.5	0.0	3.7	0.007
16	1112	1103	88.1	1.5	10.3	0.0	10.3	0.023
17-1	1202	1186	59.3	1.2	36.8	2.0	40.7	0.116
17-3	1293	1252	31.7	1.4	50.4	14.2	68.3	0.267

a) Unidentified liquid product that emerged after DCH on GLC chromatogram.

b) Phenylcyclohexane.

Table 7. CONVERSION AS A FUNCTION OF TEMPERATURE

Pressure: 10 atm
LHSV: 20

Temperature, °F		Conversion, %	Product Yield, %		First Order Rate Constant, sec ⁻¹
Block	"Catalyst"		Liquid	Light Gas	
Methylcyclohexane					
1112	1067	11.2	11.2	0.0	0.04
1202	1152	20.6	16.0	4.6	0.08
1293	1191	47.7	30.0	17.7	0.22
Ethylcyclohexane					
932	932	2.6	2.6	0.0	-
1020	1020	8.1	4.0	4.1	0.012
1112	1106	19.9	13.5	6.1	0.066
1202	1188	52.7	32.9	19.8	0.26
1,4-Dimethylcyclohexane					
1112	1082	4.3	4.3	0.0	0.012
1202	1143	28.5	18.5	10.5	0.098
1,3-Dimethylcyclohexane					
1108	1076	4.0	4.0	0.0	0.011
1202	1141	24.5	16.6	7.9	0.091
1,2-Dimethylcyclohexane					
1112	1082	6.2	6.2	0.0	0.017
1202	1144	28.8	18.8	10.0	0.10

(Continued)

Table 7 (Contd.). CONVERSION AS A FUNCTION OF TEMPERATURE

Temperature, °F		Conversion, %	Product Yield, %		First Order Rate Constant, sec ⁻¹
Block	"Catalyst"		Liquid	Light Gas	
Dimethylcyclohexane Mixture					
1112	1100	1056	14.0	14.0	0.055
1202	1180	1118	43.7	28.9	0.136
1293	1251	1159	74.1	39.8	0.344
Diethylcyclohexane Isomers ^{a)}					
1,4-DECH					
1112	1100	1056	11.5	-	0.028
1202	1180	1118	42.9	-	0.134
1293	1251	1159	74.0	-	0.345
1,3-DECH					
1112	1100	1056	17.2	-	0.043
1202	1180	1118	46.0	-	0.148
1293	1251	1159	75.3	-	0.356
1,2-DECH					
1112	1100	1056	7.1	-	0.017
1202	1180	1118	37.2	-	0.111
1293	1251	1159	71.2	-	0.317
Dicyclohexyl					
1022	1015	981	3.7	3.7	0.0
1112	1103	1060	10.3	10.3	0.0
1202	1186	1117	40.7	38.2	2.0
1293	1252	1157	68.3	53.6	14.7
Decalin (22% in Methylcyclohexane)					
1202	-	1130	30.8	-	0.099
Methylcyclohexane (76% in Decalin)					
1202	-	1130	17.9	-	0.0638

a) Computed from product analysis of runs with DECH mixture.

Table 8. THERMAL REACTION OF VARIOUS NAPHTHENES

Rate Constants and Activation Energies

"Catalyst": Quartz Chips
 Pressure: 10 atm
 "Catalyst" Volume: 20 ml

Hydrocarbon	Rate Constant, sec ⁻¹ (1202°F)	Activation Energy, kcal/mole	Relative Reactivity (MCH = 1.00; 1202°F)
MCH	0.08	39.3	1.00
1,4-DMCH	0.098	70.0	1.23
1,3-DMCH	0.090	66.0	1.13
1,2-DMCH	0.10	59.4	1.25
ECH	0.26	43.2	3.25
1,4-DECH	0.134	41.0	1.68
1,3-DECH	0.148	37.5	1.85
1,2-DECH	0.111	47.9	1.39
DCH	0.116	46.8	1.45
Decalin ^{a)}	0.099	-	1.24

a) 22% Decalin in MCH.

Table 9. GAS PRODUCTION AND COMPOSITION

Pressure: 10 atm
 Temperature: 1202°F
 LHSV: 20

Feed	MCH	ECH	1,4-DMCH	1,3-DMCH	1,2-DMCH	DECH	DCH	Decalin - MCH ^{b)}
Run No.	51	39	83-3	95	101	125-2	17-2	44
Feed Converted to Gas Products, %	4.6	19.8	10.5	7.9	10.0	14.8	2.0	4.0
Gas Products, %m								
H ₂	24.2	12.5	21.3	18.6	13.6	9.5	20.3	28.7
CH ₄	43.4	26.7	52.3	53.9	55.5	39.3	31.8	39.4
C ₂ H ₄	15.1	19.5	8.4	9.7	12.5	16.2	23.5	14.6
C ₂ H ₆	8.6	20.6	4.8	5.8	7.9	26.4	13.0	8.3
C ₃ H ₆	5.4	5.7	8.4	8.1	6.8	4.3	6.0	5.1
C ₃ H ₈	1.2	2.0	2.3	1.9	1.4	1.1	2.7	1.7
C ₄ H ₆	0.9	0.6	-	0.6	0.7	0.3	0.8	0.6
C ₄ H ₈	1.2	1.7	2.3	2.0	1.5	2.6	1.3	1.2
C ₄ H ₁₀	-	-	0.2	0.1	0.1	0.2	0.1	-
Others ^{a)}	0.2	0.6	-	-	-	0.4	0.4	-

a) Heavier than C₄.

b) 22% Decalin in MCH.

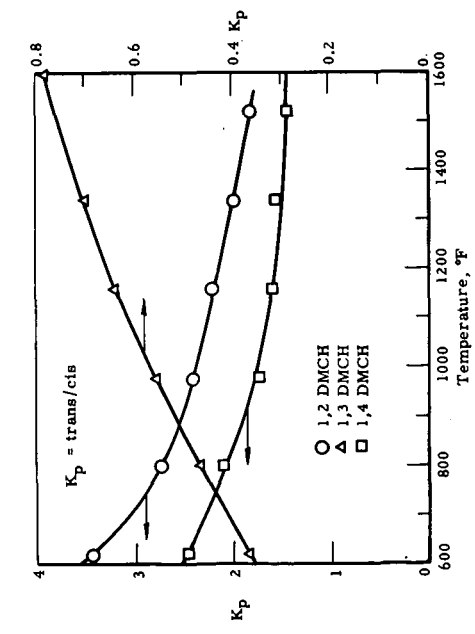


Figure 1. DIMETHYLCYCLOHEXANE TRANS-CIS EQUILIBRIA

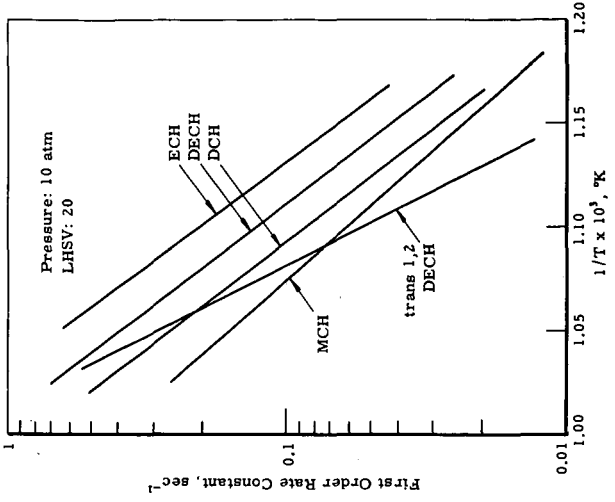


Figure 2. TEMPERATURE COEFFICIENT FOR THERMAL REACTION OF VARIOUS NAPHTHENES

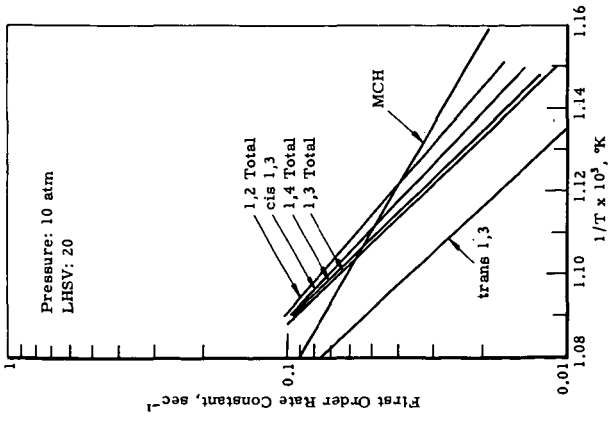


Figure 3. TEMP. COEFF. FOR THERMAL REACTION OF DIMETHYLCYCLOHEXANE ISOMERS

SYMPOSIUM ON PYROLYSIS REACTIONS OF FOSSIL FUELS
PRESENTED BEFORE THE DIVISION OF PETROLEUM CHEMISTRY, INC.
AMERICAN CHEMICAL SOCIETY
PITTSBURGH MEETING, MARCH 23-26, 1966

ON THE KINETICS OF CO AND CH₄ FORMATION DURING COAL PYROLYSIS
AT TEMPERATURES IN THE RANGE 570° - 670°C*

By

W. J. Mullin and N. Berkowitz
Research Council of Alberta
Edmonton, Canada

Following two earlier kinetic studies in which we directed attention to the formation (or, more correctly, the disengagement) of elemental hydrogen and water in the temperature interval between 650° and 850°C (1, 2), we deemed it of some interest to extend the investigations to methane and carbon monoxide which, together with hydrogen, are the principal products discharging from a coal char between 550° and 700°C. This paper reports our findings.

Pending completion of an ancillary study which was suggested by the work here described (an initiated while it was still in progress), we think it inappropriate to offer more than a tentative generalized interpretation of the experimental results. But we would observe that the data obtained in the course of the present investigation are in broad accord with earlier ones in again stressing the role of diffusional processes as rate-controlling mechanisms. Unless coupled with more discriminating methods of experimentation, formal kinetic studies seem to us therefore increasingly unlikely to yield significant information about the chemical transformations associated with coal carbonization.

EXPERIMENTAL

Though somewhat refined in matters of detail, the experimental methods used in this study were essentially those employed in the previous investigations (1, 2), i. e. , test samples were first vacuum-carbonized at 550°C in order to free them from all tarry material and then heated in helium to a pre-selected temperature which was maintained for a sufficiently long period to permit completion of an appropriate gas sampling and evaluation program. Gas samples were in all cases analyzed by gas chromatographic techniques which also allowed automatic recording of gas discharge rates.

The apparatus in which initial carbonization and, later, the kinetic measurements were performed is shown in diagrammatic form in Figure 1 and consisted of an electrically-heated tube-furnace connected to a vacuum system and a suitable g. c. assembly. The latter comprised a gas sampling cell (shown in the diagram) coupled to a 7-ft. long, 1/4 inch dia. column of -42 +60 mesh 13X Linde molecular sieve, a Gow-Mac thermal conductivity cell, and a variable-speed Fisher recorder.

Temperature control was exercised by a Pt-Pt/10% Rh thermocouple whose hot junction was located within the furnace tube, immediately adjacent to the sample holder. The cold junction leads connected with a Beck pulse-time modulation program control unit and a recorder.

To carry out a run, ca. 1 gm. of dry < 48 mesh coal (see below) was placed in a small, open-ended tared quartz tube, and the tube loosely plugged with asbestos, weighed and inserted into the furnace tube. The entire assembly was then repeatedly flushed with dry helium and slowly evacuated for several hours, after which the coal was gradually raised to 550°C and there held for 90 minutes. Throughout this time, a good vacuum was maintained and care was taken to ensure a positive pressure of helium in all non-evacuated lead-lines to the furnace.

When degassing was complete, helium was slowly admitted to the system until atmospheric pressure was restored, the helium flow adjusted to 60 ml. min⁻¹ and the furnace tube switched to connect with the g. c. sampling and detection assembly. Thereafter, the furnace was re-set for, and quickly raised to, the required experimental temperature in the range 570°-670°C. The re-set time represented the experimental "zero point". During heat-up and at the final temperature, gas samples were routinely taken and analyzed at three-minute intervals until gas discharge rates from the char were so small as to be virtually undetectable. When this point had

*Contribution No. 322 from the Research Council of Alberta.

been reached, the power supply was interrupted, the furnace allowed to cool to room temperature, and the sample then removed and re-weighed. Comparison of the char weight loss thus established with a previously constructed w/T curve permitted mass balances to be worked out and also allowed expression of gas yields on a "per gm. 550°C char" basis.

In order to obtain sufficiently detailed data for kinetic evaluation, at least three separate test runs were carried out at each temperature and the gas sampling program so arranged as to overlap. Thus, if in the first run sampling began one minute after "re-set", it was started 2 minutes after "re-set" in the second, and 3 minutes after "re-set" in the third. Figure 2 illustrates this procedure (and the close agreement between data from the different runs) with a composite rate curve representing a complete set.

Initial calibration of the g. c. column and detector was carried out in the usual manner by means of several, carefully prepared CH₄/CO/He mixtures; but in addition, routine calibration checks were also made after each completed set of runs.

To explore the effect of coal type, discharge rates from the three widely different coals were examined. These were (a) a semi-anthracite from the Cascade area of SW Alberta (designated as #1); (b) a bituminous coking coal from the Crownsnest Pass region (designated as #2); and (c) a subbituminous coal from the Drumheller field of C. Alberta (designated as #3). Prior to carbonization, these coals were crushed to < 48 mesh, flotation-cleaned at s. g. = 1.35, extracted with 10% HCl, and finally washed with distilled water and vacuum-dried. The prepared samples were stored under purified nitrogen in gas-tight bottles. Table 1 lists their relevant analytical parameters.

TABLE 1

Coal	Ash, %	Carbon %	d. a. f.		
			Hydrogen %	Sulfur %	Oxygen %
#1	2.33	89.4	4.1	0.7	5.8
#2	4.96	86.8	5.1	0.7	7.4
#3	5.99	73.3	4.8	0.5	21.4

DATA PROCESSING

Conversion of the raw data--i. e., of the chromatograms traced by the recorder--into the forms necessary for kinetic analysis was achieved by a series of individually very simple transforms. In step I, recorded peak heights were changed into areas; where necessary, corrected for attenuation during measurement of discharge rates; and finally recalculated to STP gas volumes gm⁻¹ of 550°C char. Figure 2 shows a typical rate curve thus obtained. In step II, the rate curves were graphically integrated; cumulative yields (y) to various reaction times (t) plotted as functions of t; and the resultant plots transcribed to punched tape which could be computer-extrapolated to t = ∞ to give the total yield (y₀) of CO or CH₄ obtainable at each temperature (T). Plots of y versus ln t were used to estimate the theoretical zero time point and to correct for the non-instantaneous approach to the reaction temperature. (Figure 3 illustrates the procedure.) Finally, in step III, cumulative yields were normalized to take account of the fact that y₀ itself varies with T, and appropriate functions of y/y₀ plotted against t to establish the apparent order of the reaction. For a pseudo-first order--which had been found for the disengagement of hydrogen (1) and water (2)--this meant graphing -ln(1-y/y₀) against t.

RESULTS AND DISCUSSION

The sequence of diagrams reproduced in the following pages summarize the results obtained in this manner. In each diagram, empty circles (○) denote data relating to coal #1, while ● and ⊙ refer, respectively, to coals #2 and #3.

The variation of cumulative yields (y) of methane and carbon monoxide with time (t) at constant temperature (T) is illustrated in Figures 4 and 5 which, near their right hand margins, also contain the estimated final yields (y₀) of CH₄ and CO at each temperature. Figures 6 and 7 show these latter quantities as direct functions of T.

Figures 4 and 5 are, in themselves, quite unremarkable and are here merely placed on record. But some interest attaches to the observation (cf. Figure 6) that over the temperature

interval covered by this study, $y_0(\text{CO})$ is for all practical purposes a linear function of T whose slope is proportional to the oxygen content of the parent (550°C) char. By contrast, $y_0(\text{CH}_4)/T$ assumes a more familiar sigmoid form--although there is, even in this case, a suggestive differentiation between coal #1 on the one hand and coals #2 and #3 on the other. We refer, in particular, to the variation of $y_0(\text{CH}_4)$ with T at $T < 600^\circ\text{C}$ (cf Figure 7).

These matters, however, are of less immediate interest than the information offered by kinetic treatment of the experimental data. As shown in Figures 8-10 (for CO) and 11-13 (for CH_4), test plots of $-\ln(1-y/y_0)$ vs. t indicate not only general conformity to pseudo-first order kinetics, but also suggest the possibility that rates of CO and CH_4 disengagement at temperatures in excess of ca. 600°C may be controlled by at least two mechanisms: in all instances, $-\ln(1-y/y_0)/t$ exhibits a fairly sudden change of slope above some value of y/y_0 , though the point at which this discontinuity occurs appears to vary quite regularly with temperature. Table 2 will serve to illustrate this.

TABLE 2

Coal	Temperature, °C	$y/y_0(\text{CO})$ at "break"	$y/y_0(\text{CH}_4)$ at "break"
#1	612	0.245	0.25
	645	0.525	0.59
	668	0.535	0.675
#2	603	0.28	0.26
	634	0.39	0.51
	663	0.48	0.635
#3	612	0.26	0.31
	641	0.455	0.45
	673	0.60	0.64

The possibility that behavior above the discontinuity in the $-\ln(1-y/y_0)/t$ plot merely connotes some unspecified departure from the norm cannot, perhaps, be dismissed out of hand. And apparent activation energies (E), calculated on that assumption from the initial slopes of each set of $-\ln(1-y/y_0)$ vs. t plots would then suggest that rates of CO and CH_4 disengagement are controlled by processes formally akin to activated diffusion (cf. Table 3).

TABLE 3

Coal	Temperature Range °C	CO Disengagement E , kcal mole ⁻¹	CH_4 Disengagement E , kcal mole ⁻¹
#1	577 - 668	10.1	15.7
#2	577 - 664	7.9	16.5
#3	576 - 673	14.5	17.0

However, bearing in mind the consistently linear variation of $-\ln(1-y/y_0)$ with t above as well as below the "break", it seems fundamentally more reasonable to regard the initial slopes as composites of two superimposed reaction sequences and to resolve them in the manner illustrated in the diagrams (cf. Figures 8-13). The straight lines there designated by the velocity constant k_1 (and drawn to parallel $-\ln(1-y/y_0)/t$ above the "break") reflect one reaction or control mechanism, while those characterized by k_2 (and drawn as the vertical difference between k_1 and the observed rate) indicate the other. That reactions designated by k_2 should in all instances terminate fairly abruptly follows from the form of the discontinuity in the experimental $-\ln(1-y/y_0)/t$ plots.

Apparent activation energies computed on this basis are set out in Table 4 and establish a marked dichotomy. While values of E calculated via k_1 are consistently less than 5 kcal mole⁻¹ (and therefore indicative of simple diffusion control over k_2), those obtained via k_2 are almost large enough to connote some chemical (i. e., reaction) control. They are, in any event, the highest values so far recorded in these laboratories.

TABLE 4

Coal	CO Disengagement		CH ₄ Disengagement	
	E via k_1 kcal mole ⁻¹	E via k_2 kcal mole ⁻¹	E via k_1 kcal mole ⁻¹	E via k_2 kcal mole ⁻¹
#1	2.5	35.1	1.7	55.2
#2	0.5	33.5	3.3	38.1
#3	3.6	22.6	4.4	38.5

Pending completion of a study now in progress, we prefer (as already indicated) to reserve comment on these findings. But it is important to observe that the data in Table 4 do not necessarily imply the operation of two distinctly different rate control mechanisms and that they can, in fact, be more easily and adequately accounted for by several models which only presuppose differential diffusion.

Qualitatively, this is perhaps most conveniently illustrated by considering a structurally isotropic, porous sphere which, at a given temperature T, suffers partial thermal decomposition and thus forms a quantity of gas which derives uniformly from every volume element of the sphere (i. e., $(\partial g / \partial v)_T = \text{constant}$). For the greater part, escape of this gas will be impeded by internal geometry and consequently diffusion-controlled. Superimposed upon this, however, there will also be a substantial quantity of gas which originates in near-surface volume elements and can therefore discharge at rates essentially equal to those at which it forms. And there will be some gas which can disengage from the char at rates intermediate between these two "extremes".

Several restrictions must, of course, be placed upon such a model in order to make it quantitatively conform with the experimental results, and we are currently exploring these in some detail. It is, however, significant that even a generalized model seems capable of accounting for the observation that the "break" in $-\ln(1-y/y_0)/t$ occurs at progressively higher values of y/y_0 as T increases: we note that this would follow from the pronounced temperature-dependence of y_0 and from the relative volumes of near-surface and core elements of a sphere.

LITERATURE CITED

- (1) Berkowitz, N., and den Hertog, W.; *Fuel*, **41**, 507, 1962.
- (2) Neufeld, L. F., and Berkowitz, N.; *ibid.*, **43**, 189, 1964.

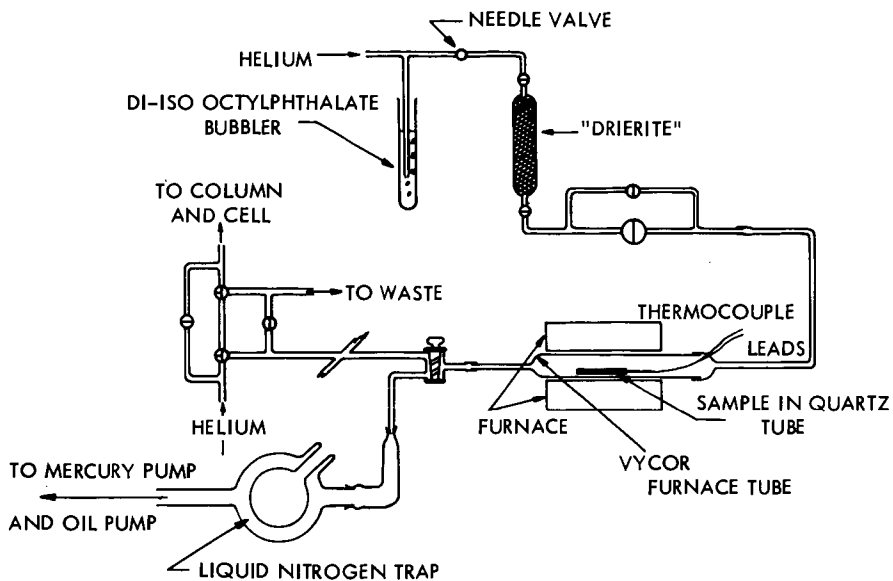
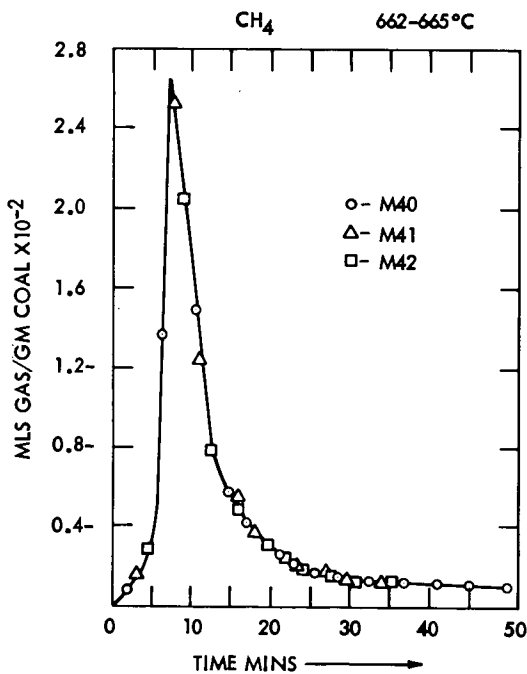
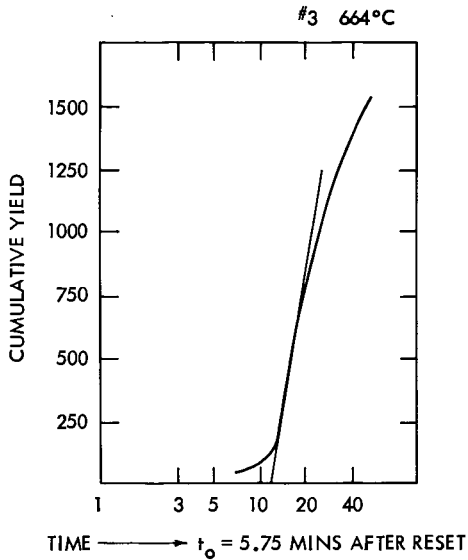


DIAGRAM OF APPARATUS

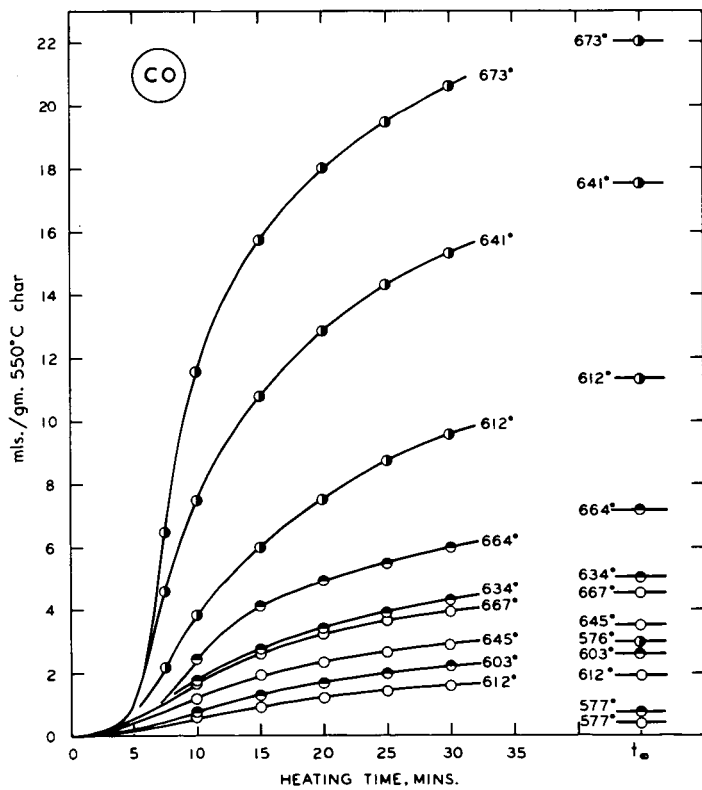
(1)



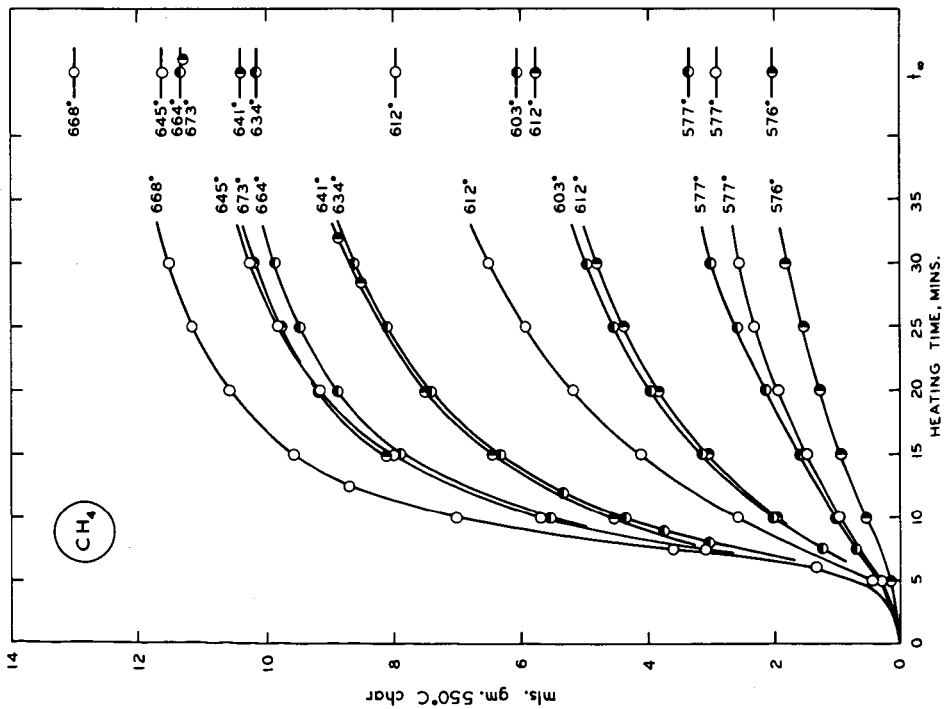
(2)



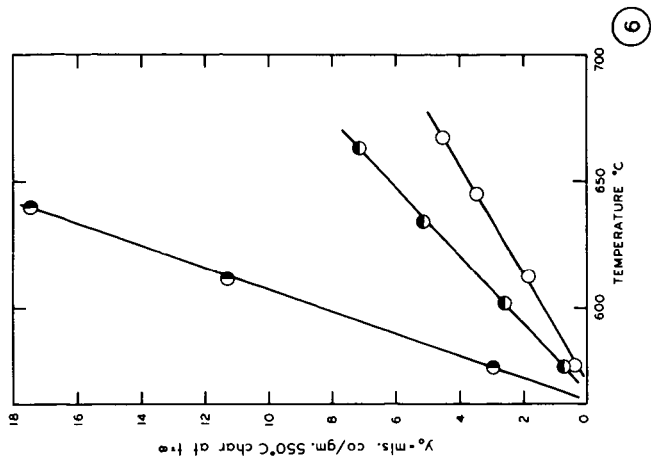
3



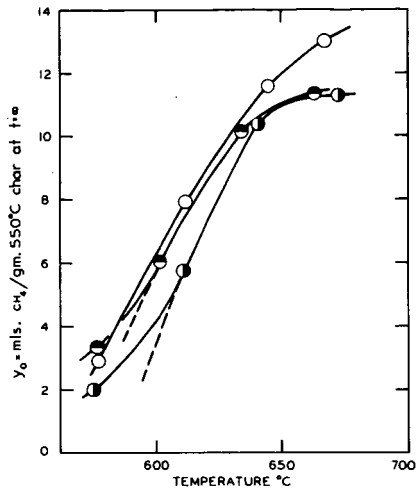
4



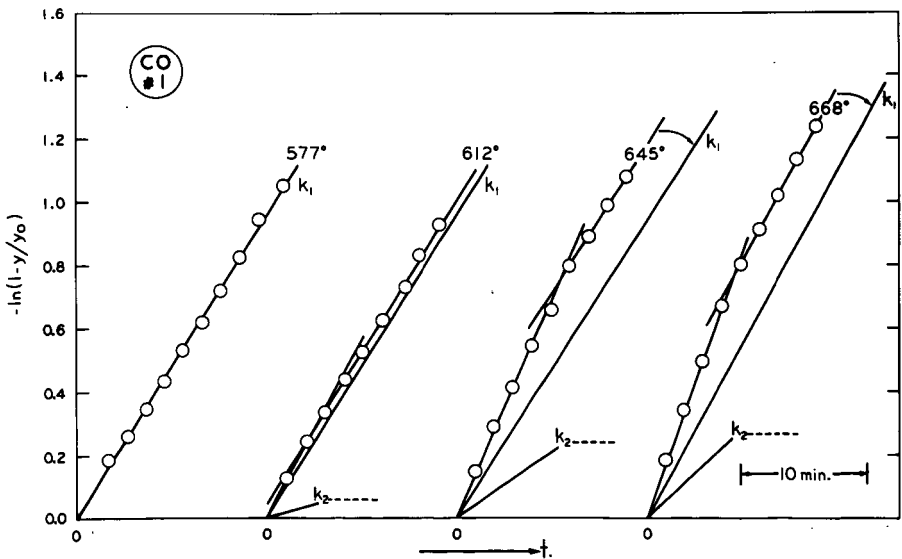
5



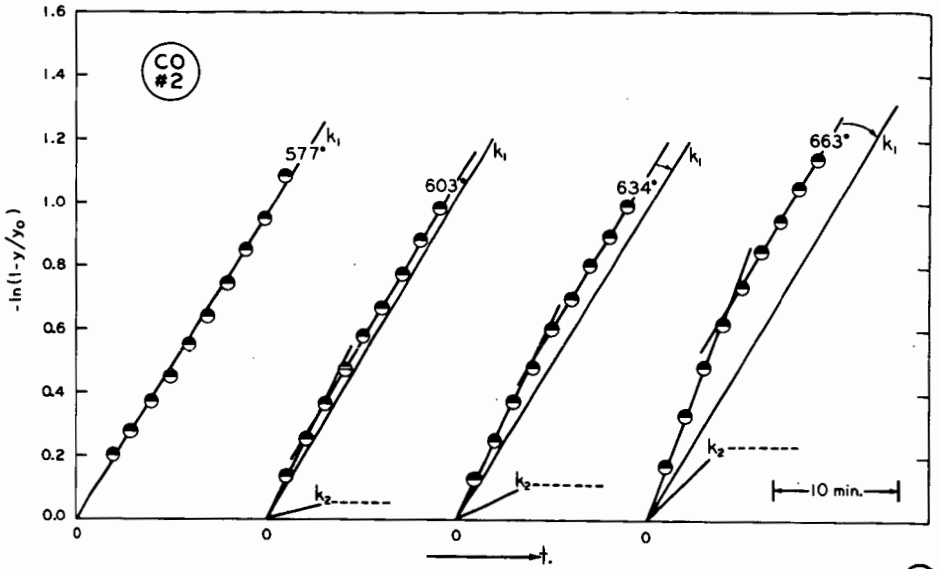
6



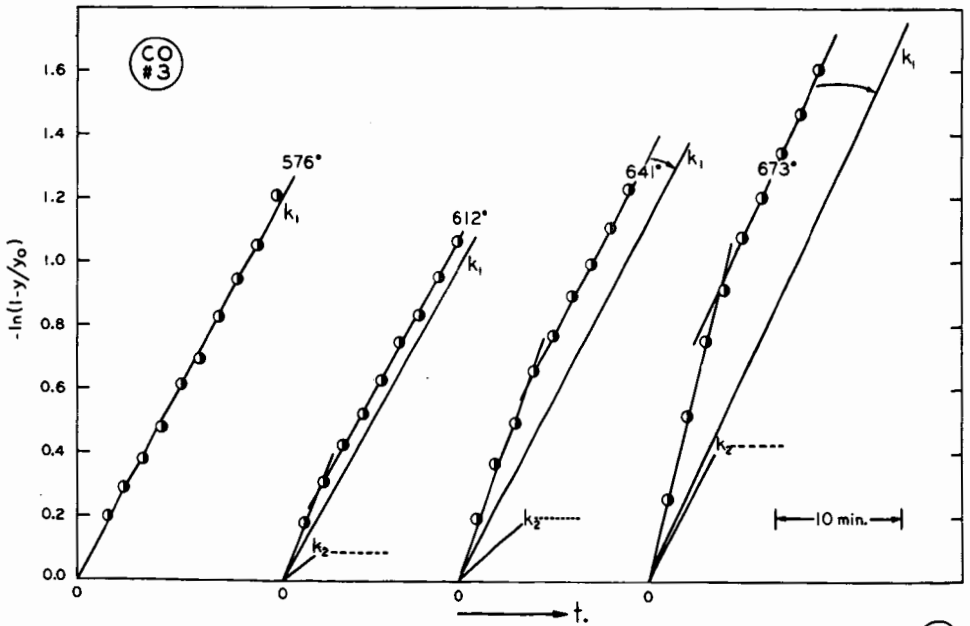
(7)



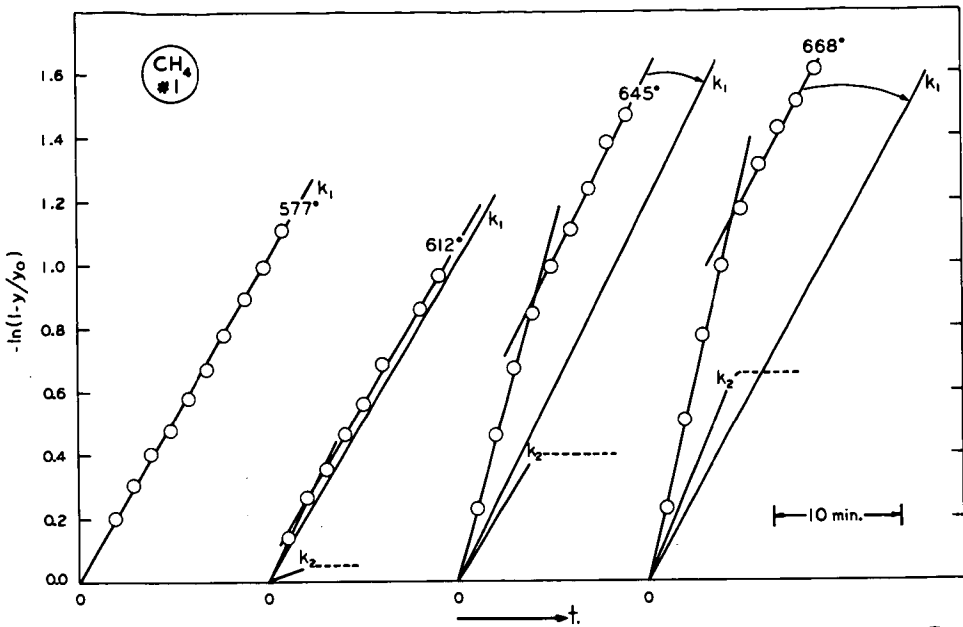
(8)



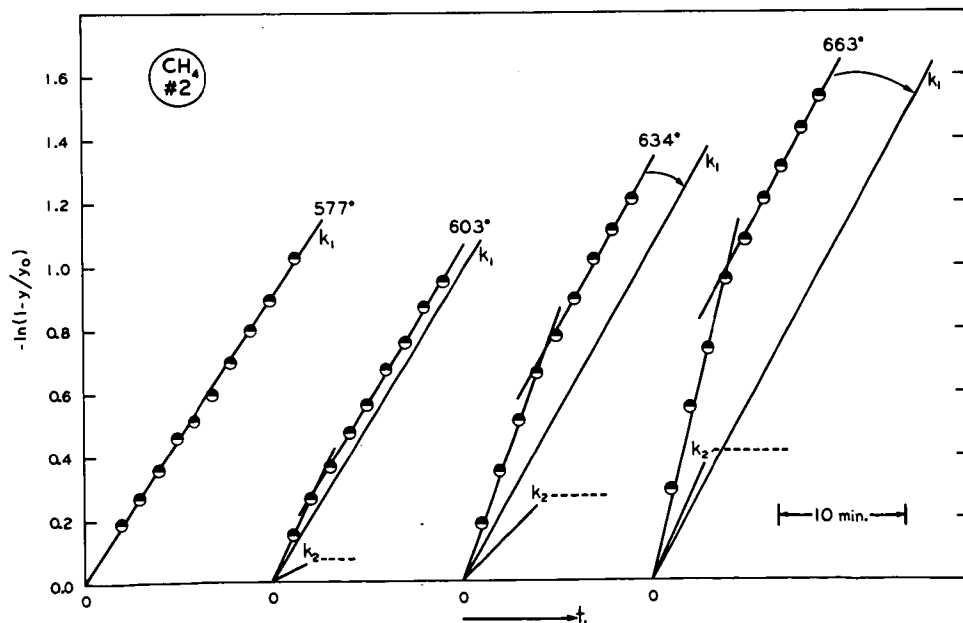
9



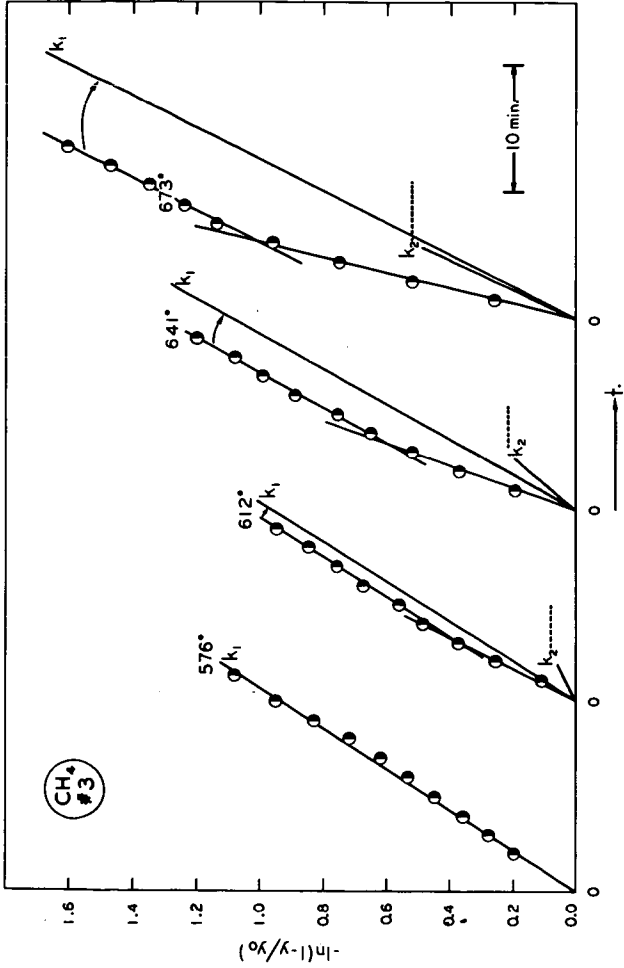
10



11



12



(13)

SYMPOSIUM ON PYROLYSIS REACTIONS OF FOSSIL FUELS
PRESENTED BEFORE THE DIVISION OF PETROLEUM CHEMISTRY, INC.
AMERICAN CHEMICAL SOCIETY
PITTSBURGH MEETING, MARCH 23-26, 1966

A KINETIC STUDY OF THE PYROLYSIS OF A
HIGH-VOLATILE BITUMINOUS COAL

By

Wendell H. Wisler, George Richard Hill, and Norbert J. Kertamus
Fuels Engineering Department
University of Utah
Salt Lake City, Utah

INTRODUCTION

In recent years experimental data from several laboratories have been presented and analyzed in the literature in an effort to arrive at greater understanding of the processes associated with the pyrolysis of coal. Each of these presentations has contributed measurably to an increased understanding, both through the inclusion of experimental data and as a result of interpretations of the data. It is intended that the presentation of experimental data obtained in this laboratory, accompanied by analyses and comparisons with previously reported data, may shed further light upon these very complex processes.

There appear in the literature two basic experimental approaches to this problem:

(1) heating a coal sample to a predetermined temperature where the decomposition processes are studied at constant temperature, and (2) increasing the temperature of the coal sample at a predetermined constant rate. Among those who have pursued their studies at constant temperature, some have heated the coal sample under conditions where the normal coking processes may occur, including the fusion of the sample particles, while others have heated the samples to operating temperatures with the coal particles effectively separated such that attainment of the desired temperature was rapid and fusion of particles was essentially avoided. The results of these various approaches are necessarily varied, but related. The present study is concerned with constant temperature observations of finely divided coal samples under conditions such that fusion of the coal mass may occur in a manner characteristic of coking operations, and at temperatures such that the coal samples pass through the plastic state during the course of the observations.

EXPERIMENTAL PROCEDURE

The equipment used in this study consisted of a vertical tube-type furnace with facility for maintaining constant temperature within $\pm 3^\circ\text{C}$. A stream of nitrogen gas at constant flow rate was admitted at the top of the furnace and flowed downward over the sample. The samples of a Utah high-volatile Bituminous coal, of 47.46 per cent volatile matter on a dry basis, were sized to -40 +60 mesh (particle diameter 417 to 246 microns) and dried at 100°C in a vacuum. Samples of approximately one gram were used in the determinations.

The sample was carefully weighed, then placed in an aluminum foil sample pan and suspended by a nichrome wire from a quartz spring of five gram capacity. A cathetometer measured the deflection of the quartz spring. During the course of pyrolysis, the loss in weight of the sample was recorded, at five minute intervals initially, and at longer intervals after the first 60 minutes. All weight-loss observations, including the initial deflection, were made with a constant flow rate of the nitrogen stream.

RESULTS AND DISCUSSION

Typical fractional weight loss-time curves from this study are shown in Figure 1. It is noted that the later portions of these curves are straight lines, which indicate zero order reaction during these portions, inasmuch as $dx/dt = \text{constant}$. It is noted further that the pyrolysis reaction, as indicated by weight loss of the sample, assumes zero order characteristics at times which decrease in a regular manner from 375 minutes at 409°C to 250 minutes at 497°C , and

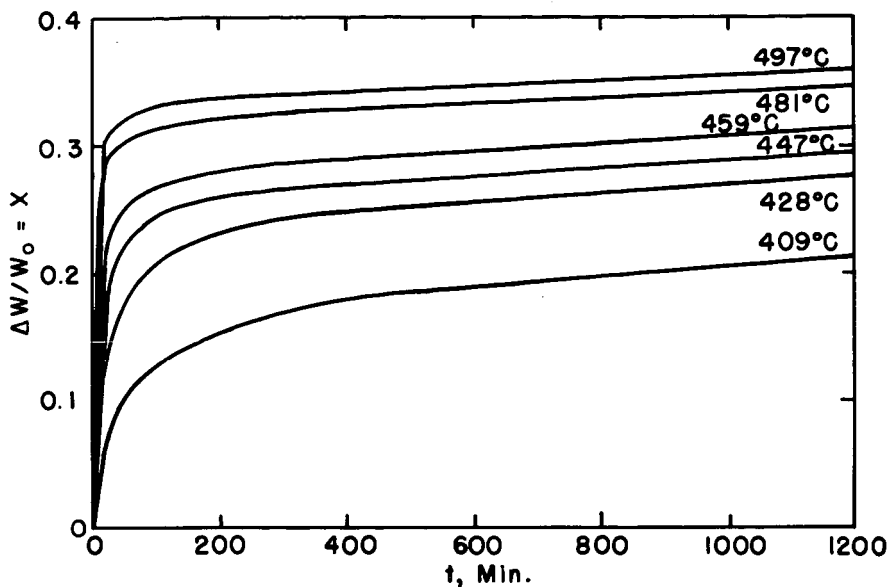


Figure 1. Fractional Weight Loss-Time Curves.

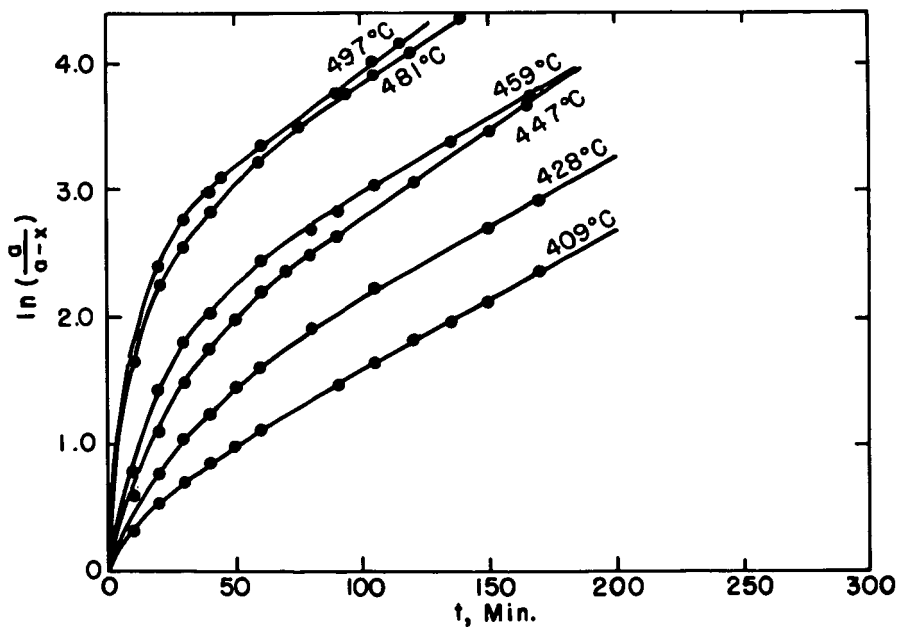


Figure 2. First Order Plot of Data.

continues to be zero order throughout the balance of the determination, which in several cases extends to 1500 minutes. A period of zero weight loss was not attained in any of the determinations.

The analysis of the data for evolution of volatile material for time periods preceding the zero order portions of the curves in Figure 1 involves expressions (e. g. equation 1) wherein the maximum proportion of the coal sample which may ultimately be transformed into volatile products at the temperature concerned must be known or assumed. These quantities were not experimentally observable. Although the nature of the zero order reaction is not known, it is reasonable to assume that it occurs throughout the time of pyrolysis. The reaction velocity constants for this portion of the various curves are determined from the slopes of the straight line portions of the curves in Figure 1, and are observed to be essentially the same for each temperature, with values of the order of 10^{-5} grams per minute. Hence the rate of product evolution, and the quantity of product evolved due to this type of reaction prior to the time when the reaction assumes zero order, are small.

By subtracting the zero order reactions from the weight loss data, values of "a" for the subsequent equations are obtained which characterize the reactions, excluding the slow zero order reaction, occurring to produce most of the volatile material. This was done by extending the straight line portion of the plot of weight loss vs. time to zero time, and subtracting the appropriate quantities, as thus determined graphically, from the observed weight loss values. The intersection of this extended straight line with the ordinate at zero time gives the weight fraction of the sample which would evolve as volatile products if the zero order reaction did not occur, and is thus the value "a" appearing in the differential equations which follow.

To analyze the data prior to the time of over-all zero order reaction, the differential equation is written:

$$\frac{dx}{dt} = k_1 (a-x) \quad (1)$$

where "x" is the observed weight loss at time "t", as a fraction of the initial sample weight, and "a" is the maximum weight loss obtainable (excluding the zero order reaction as explained above). The constant "k₁" is the reaction velocity constant. Integrating equation (1), and evaluating the constant of integration with x = 0 when t = 0, yields

$$\ln \frac{a}{a-x} = k_1 t \quad (2)$$

In Figure 2, $\ln \frac{a}{a-x}$ is plotted versus time. It is noted that the data produce straight lines, and hence are first order, at times above about 90 minutes. The slope of the straight line is equal to "k₁" of equation (2) for that temperature, and over the range of data where the straight line is observed.

For a second order reaction, the following differential equation applies:

$$\frac{dx}{dt} = k_2 (a-x)^2 \quad (3)$$

Integrating and evaluating the constant of integration with x = 0 when t = 0,

$$\frac{x}{a(a-x)} = k_2 t \quad (4)$$

Plotting $\frac{x}{a(a-x)}$ vs. t yields a straight line for the first 60 minutes for some temperatures but a slight curvature at the lower and higher temperatures.

A rate equation of general form is written:

$$\frac{dx}{dt} = k_n (a-x)^n \quad (5)$$

where n ≠ 1 and denotes the order of the reaction. Integrating, and evaluating the constant of integration with x = 0 when t = 0,

$$\frac{a^{1-n} - (a-x)^{1-n}}{1-n} = k_n t \quad (6)$$

This equation is applied to the data for the first 60 minutes, when the larger portion of the product evolution occurs, by selecting values for n at each temperature until a straight line is produced for that temperature over the 60 minute period on a plot of

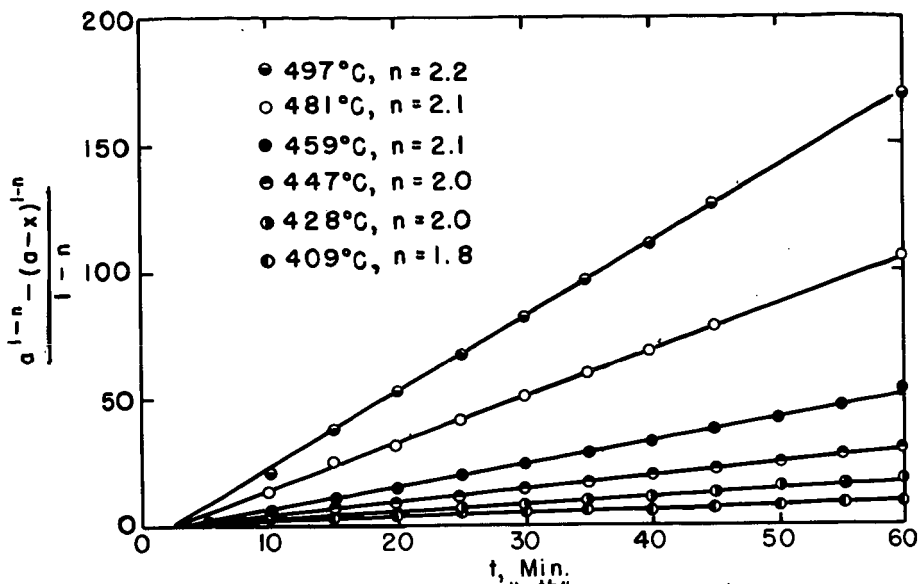


Figure 3. Plot of "n'th" Order Equation.

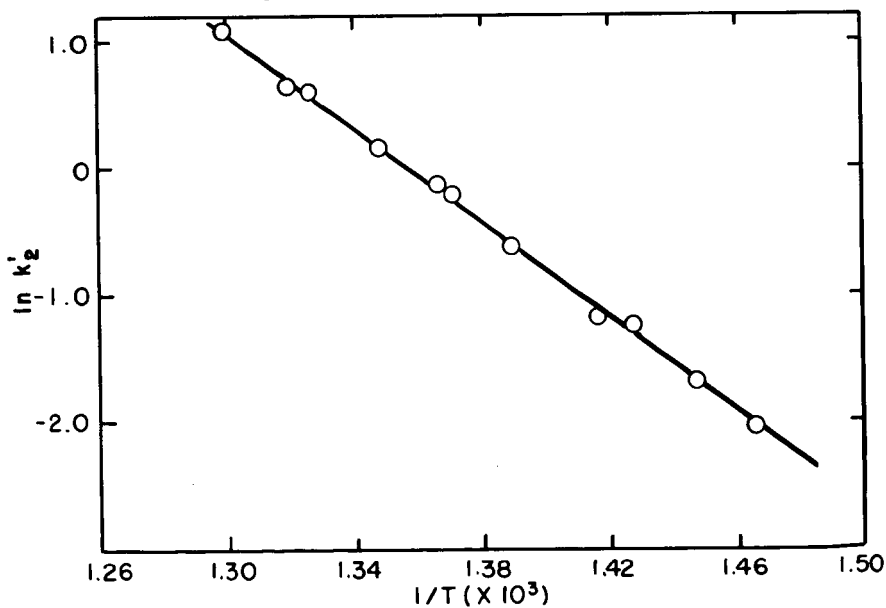


Figure 4. Plot of Arrhenius Eq., First 60 Minutes.

$$\frac{a^{1-n} - (a-x)^{1-n}}{1-n} \text{ vs. } t.$$

The order of the reaction thus determined for the first 60 minutes (with the zero order reaction subtracted, as explained above) ranges from 1.8 at 409°C to 2.2 at 497°C, with a gradual and progressive increase in order noted with increase in temperature. These results are shown in Figure 3. The slopes of the lines in Figure 3 equal " k_n " from equation (6) for each temperature as indicated.

A region of transition from approximately second order to first order is noted, spanning a time of about 30 minutes. A similar region of transition between first order and zero order portions of the data is also observed.

The specific rate of most chemical reactions can be related to the temperature at which the reaction occurs by the Arrhenius equation:

$$k' = Ae^{-E/RT} \quad (7)$$

where E is the energy of activation and A is a quantity which is independent of or varies little with temperature. Over narrow temperature ranges, E and A may be considered to be constant.

Equation (7) may be written in the form

$$\ln k' = \ln A - E/RT \quad (8)$$

A plot of the natural logarithm of the rate constant k' vs. the reciprocal of the absolute temperature should yield a straight line with slope equal to $-E/R$. Figure 4 presents such a plot for the observed reactions of the first 60 minutes. From the slope of the line in Figure 4, an energy of activation of 36.6 kcal. per mole is obtained for the reactions of the first 60 minutes. A similar plot for the first order region yields an activation energy of 5.36 kcal. per mole for that region.

In the use of equation (7), the activation energy, E, varies slightly with temperature, and A involves an entropy term. Strictly speaking, the factor which determines the rate of a reaction is the free energy of activation, ΔF^\ddagger . We may therefore properly write: (4)

$$k' = Ae^{-\Delta F^\ddagger/RT} \quad (9)$$

$$k' = Ae^{-\Delta H^\ddagger/RT} e^{\Delta S^\ddagger/R} \quad (10)$$

where ΔF^\ddagger , ΔH^\ddagger and ΔS^\ddagger are the free energy, heat and entropy of activation, respectively.

The factor "A" in equation (10) is termed the frequency factor, and accounts for the rate of decomposition of the activated complex to form products, which rate of decomposition can be shown to be $\frac{kT}{h}$, where k is the Boltzmann constant, and h is the Planck Constant. Also, it is possible that not every activated complex leads to formation of products. Allowance is made for this possibility by introducing a term, \mathcal{H} , called the transmission coefficient. ($\mathcal{H} \leq 1$, and represents the fraction of activated complexes which does become products.)

For a heterogeneous system such as coal pyrolysis, the number and nature of reaction sites changes with time. Accordingly an expression for the rate of reaction in such a system includes a term of the form:

$$\frac{\text{molar concentration of sites}}{\text{gram}}$$

Equation (10) thereby becomes, for a coal pyrolysis system⁵

$$k' = \frac{\text{molar conc. of sites}}{\text{gram}} \mathcal{H} \frac{kT}{h} e^{-\Delta H^\ddagger/RT} e^{\Delta S^\ddagger/R} \quad (11)$$

which may be written in the form:

$$\ln \left(\frac{h}{\mathcal{H}k} \frac{k'}{T} \right) = -\frac{\Delta H^\ddagger}{R} \frac{1}{T} + \frac{\Delta S^\ddagger}{R} + \ln [C^\ddagger] \quad (12)$$

where $[C^\ddagger]$ denotes the molar concentration of active sites per gram of coal. The transmission coefficient, \mathcal{H} , is usually taken as unity. A plot of

$\ln \left(\frac{h}{\mathcal{H}k} \frac{k'}{T} \right)$ vs. $\frac{1}{T}$ will yield a straight line of slope $-\frac{\Delta H^\ddagger}{R}$ and intercept $\left(\frac{\Delta S^\ddagger}{R} + \ln [C^\ddagger] \right)$.

Such a plot is contained in Figure 5 for the data of the first order region, which yields a value for ΔH^\ddagger of 4.1 kcal. per mole for this region. A similar plot of the data for the first 60 minutes yields a value for ΔH^\ddagger of 35.6 kcal. per mole for that region. The intercepts at $1/T = 0$ yield values for the quantity $(\Delta S^\ddagger + R \ln [C^\ddagger])$ of -12 and -63 for the first 60 minutes and the first order region, respectively.

An expression has been derived by Eyring, et. al. (4) whereby the entropy of activation for a heterogeneous reaction may be calculated from experimentally determined reaction rates and energies of activation:

$$k' = e^{-(\Delta n^\ddagger - 1) \frac{kT}{h}} e^{-E/RT} e^{\Delta S^\ddagger/R} \quad (13)$$

where Δn^\ddagger is the increase in the number of molecules accompanying the formation of the activated complex. The standard state assumed in the use of this equation includes unit concentration of reaction sites. If, as indicated earlier, the reaction during the first 60 minutes is approximately second order, followed by a period of first order reaction, Δn^\ddagger becomes -1 and zero for the two regions, respectively. Equation (13) then yields values of ΔS^\ddagger of -12 e.u. for the first 60 minutes of the pyrolysis reaction, and -63 e.u. for the first order region.

An entropy value of -63 e.u. is unrealistic for the pyrolytic decomposition of coal. Further, it is unlikely that a change in entropy of activation of more than a few (say three or four) entropy units would be observed during the pyrolytic reactions, as an entropy change would reflect a corresponding change in the complexity of the activated complex. Equation (12) demonstrates that the entropy values as determined experimentally, and as calculated from equation (13), include the possible variations in molar concentration of active sites, and reason leads to the conclusion that the concentration of sites is perhaps very different from 1 mole per sq. cm. of surface, as discussed later. Further, the large change in ΔS^\ddagger as determined from equation (12) is perhaps best explained in terms of a change in concentration of active sites.

If it were to be assumed that the entropy does not change during the course of the reaction (which would imply that the nature of the activated complex remains essentially constant), and that the change in apparent entropy is to be accounted for completely by a change in concentration of active sites, combining the expressions

$$\Delta S^\ddagger + R \ln [C_1^\ddagger] = -12 \text{ and } \Delta S^\ddagger + R \ln [C_2^\ddagger] = -63,$$

we get:

$$\frac{[C_1^\ddagger]}{[C_2^\ddagger]} = 10^{11} \quad \text{or} \quad [C_2^\ddagger] = 10^{-11} [C_1^\ddagger] \quad (14)$$

indicating a decrease in concentration of active sites as the reaction proceeds, of the order of 10^{-11} .

It has been observed (2) that the constant "A" in the Arrhenius equation assumes values of the order of 10^{13} for unimolecular reactions, and of the order of 10^{10} for bimolecular reactions. Inasmuch as the apparent order of reaction changes from approximately second order in the initial stages to first order after 90 minutes, allowance may be made in the entropy consideration for a change in "A" of 10^3 (bimolecular to unimolecular). In addition, noting that an entropy change of 4.6 units ($2.3 \times R$) corresponds to a change in concentration of active sites by a factor of 10, we may consider that the entropy decreases by this amount during the course of the reaction. An entropy change greater than this is very improbable. The sum of these two factors for maximum effect would account for a change in apparent entropy of -18 units. Accordingly a decrease in concentration of active sites at least of the order of 10^7 is indicated, corresponding to a change in apparent entropy of -33 units.

As a coal sample is heated at a slow and constant rate a period of rapid evolution of volatile material is observed in the vicinity of 400°C , at temperatures when the fluidity of the coal is rather rapidly increasing. Several investigators (3, 11) have concluded that the plastic state is the result of the decomposition reactions occurring in this temperature range. These initial reactions, at least some of them, appear to be extremely rapid, as indicated by the work of Shapatina, et. al. (9), and of Stone and coworkers (10), where the coal samples were heated under conditions such that the small coal particles remained effectively separated during heating and attained the temperature of the reaction zone very rapidly. The data of Shapatina indicate that the particles attained thermal equilibrium with the reaction zone within 0.5 second after introduction into the heated region. Under these conditions, of the maximum volatile product yield obtainable at 450°C , 32% was evolved during the first 0.8 second after introduction into the heated zone. It should be noted that under the conditions of the experiment escape of the volatile matter in these initial seconds was not impeded by fusion of the coal particles. In contrast to the very rapid heating rates attained by Shapatina, times up to five minutes in length were required to attain thermal equilibrium in the present study, as reported also by Berkowitz (1) in his studies.

Shapatina noted in the initial seconds a rapid evolution of CO_2 , H_2O and CO , accompanied by a somewhat slower and more extended evolution of tar, gaseous hydrocarbons and hydrogen,

with further evolution of CO and CO₂. Previous studies (12) have demonstrated that when a high volatile coal is heated at constant rate, CO₂, CO and H₂O, apparently physically adsorbed within the coal pores, are liberated at temperatures below 200°C. At temperatures approaching 400°C. further evolution of these gases occurs, believed to be associated with chemical decomposition of the coal structure. Kessler (7) noted the occurrence of reactions in this temperature range whereby aliphatic chains were split off and evolved from the coal. Stone, et. al. observed the evolution of appreciable quantities of methane and lesser amounts of other hydrocarbons in this temperature range. Several investigators have noted, as in the present experiments, the appearance of oily products in the volatile matter at temperatures when the coal enters the plastic state. These products have been reported (12) to be initially paraffinic in nature, with naphthenes appearing as the temperature is increased.

It seems probable that during the time of these initial rapid reactions, thermal decomposition is occurring within the coal mass, as well as at sites on the surfaces, both external and internal, which existed in the original coal sample. The products of the primary decomposition, called "fluid coal" by Fitzgerald (3) and "metaplast" by van Krevelen, et. al. (11) being thus dispersed throughout the coal mass, impart a degree of plasticity to it. Whereas in the studies of Shapatina and of Stone the coal particles were effectively separated during this initial period such that the volatile products could rather readily escape from the small particles, in an actual coking operation, as under conditions obtaining in the present study, as well as in the investigations of Fitzgerald, van Krevelen, and Berkowitz, the particles fuse together, inhibiting the escape of the volatile products and resulting in a pressure build-up within the pore spaces within the coal mass. Such a pressure build-up has been extensively discussed by Berkowitz. (1)

Fitzgerald observed that, at 407°C, a state of maximum fluidity in the coal mass was achieved after 25 minutes, following which a decay in the plastic state occurred, with an effective period of plasticity of some 80 to 90 minutes at this constant temperature. Van Krevelen observed that, as the temperature of the test was increased, the time required to attain maximum fluidity was decreased, and the rate of decay of the plastic state increased. It should be noted that the degree of fluidity continues to increase for appreciable times, up to 25 minutes, after the coal has attained the predetermined constant temperature, indicating that some of the primary decomposition reactions are still in progress.

The initial period of 50-60 minutes, during which the over-all reaction order as observed ranges from 1.8 to 2.2, spans the time when the coal manifests a measurable degree of fluidity, and as depicted in the models of Fitzgerald and of van Krevelen, includes the Primary decomposition reactions which produce the plastic or fluid material as well as the secondary reactions which result in the disappearance of the plastic condition. The coal is in a state of measurable fluidity throughout most of this period such that reactions may be considered to occur throughout the coal mass, and not be restricted to sites associated with surfaces. Each of the reactions, considered separately, may be considered as a first approximation to be unimolecular and first order, inasmuch as most decomposition reactions are of such a nature. However the picture of simultaneous occurrence of reactions of both types indicated here becomes further complicated by diffusion problems produced by the appearance and subsequent decay of a plastic state. This combination would not necessarily produce a rate of change in the rate of escape of volatile materials which would follow a first order rate law. The observed gradual increase in reaction order as temperature increases lends support to the proposition that a physical phenomenon, such as diffusion, plays an important role in the processes of this period.

The observed sequence of events of the present study include the following: (1) an initial rapid evolution of volatile products with an observed rate of decrease in the rate of evolution through the first 50-60 minutes such as to approximately fit the equation $\frac{dx}{dt} = k_2(a-x)^2$; (2) a period of changing rate of decrease in rate of product evolution, of approximately 30 minutes duration, whereby the second order rate decays to a first order rate; (3) a period of some 100 minutes wherein the rate of decrease in the rate of product evolution fits the equation $\frac{dx}{dt} = k_1(a-x)$; (4) a second period of decay in the rate of decrease in the rate of

product evolution, of varying duration depending upon the temperature, reaching a period of observed zero order rate; (5) a long period of slow but steady rate of product evolution according to the equation $\frac{dx}{dt} = k$. The series of events, steps (2) through (5), all included, cannot be

conceived to be due to diffusional control throughout, as was proposed by Berkowitz. It is doubtful that diffusion plays a major role in the observed rates of product evolution after the first 90 minutes, or after the observed rate is first order. Rather it is believed that the first order period represents an actual first order reaction, with energy of activation of the order of 5.36 kcal. per mole as observed. It should be noted that in the studies of Shapatina and of Stone

a first order region was observed to follow the period of rapid evolution of volatile products, with energy of activation of 5.3 kcal. per mole in Shapatina's work and 6.7 kcal. per mole in the work of Stone.

It was noted above that the progress of the pyrolytic reaction is accompanied by a change in the quantity $\Delta S^\ddagger + R \ln [C^\ddagger]$, as determined from plotting equation (12), from -12 units in the initial stages to -63 units in the first order region. It has been observed that in a bond-breaking unimolecular reaction the activated complex is often very much like the original reactant, in which case the value of ΔS^\ddagger is zero. If it is assumed that the reactions occurring in the thermal decomposition of coal are of this nature, the value of -12 units must be associated with the concentration of reacting sites.

In using equation (13) to calculate the entropy of activation for the initial 60 minutes of pyrolysis, which also yields a value of -12 units, the assumption was made that the standard state of unit concentration of reacting sites obtained. It is apparent this assumption is not valid. It was observed earlier that an apparent entropy change of 4.6 units was equivalent to a change in concentration of reacting sites by a factor of 10. Hence the value of $\Delta S^\ddagger + R \ln [C^\ddagger] = -12$ could be explained if the actual number of reacting sites is smaller than the assumed value by $\frac{12}{4.6}$ or by a factor of 410. If a model (6) for the structure of coal is examined, one may readily conclude that only a small fraction of the existing bonds would be of such nature as to rupture at the temperatures here indicated, to lead to the products which have been observed to evolve at these temperatures.

The decrease in value for $\Delta S^\ddagger + R \ln [C^\ddagger]$ from -12 to -63 units was observed to represent a decrease in concentration of reacting sites per gram of coal of the order of 10^7 , if the initial period of 50-60 minutes represents a bimolecular reaction, or a decrease of the order of 10^{11} if both periods were characterized by unimolecular reactions. The sites available for the thermal decomposition reactions believed to occur in the initial moments of pyrolysis, associated largely with the plastic state, would be large in number and not restricted to surfaces in existence in the original coal. However the reactions occurring during the first order period, following the resolidification of the coal, would occur only at selected sites upon existing surfaces, internal or external. The large negative value of -63 units, as indicated above, requires that the concentration of reacting sites be low, and this in turn could explain the slow rate of product evolution in spite of the low activation energy of 5.36 kcal. per mole.

Finally it may be noted that observations were made with sample of -200 +250 mesh (74 to 60 microns particle diameter) and the results compared with those from the -40 +60 mesh (417 to 246 microns) used throughout this study. No significant difference in the weight loss-time curves was observed. Decreasing the particle size in the degree indicated would increase the external surface area not more than a factor of 10 in the range 10^{-3} to 10^{-2} square meters per gram. Determinations of the total surface area of coal samples of -40 +60 mesh have yielded values of 50 to 200 square meters per gram. (8) Thus reactions occurring on surfaces or within the mass would not be appreciably altered in this regard. The rate of attaining thermal equilibrium may be increased under certain conditions by decreasing the particle size, thus displacing the curve, but such did not occur in the present study.

ACKNOWLEDGMENT

The Research reported herein was supported by the U. S. Office of Coal Research and by the University of Utah under Contract #14-01-0001-271.

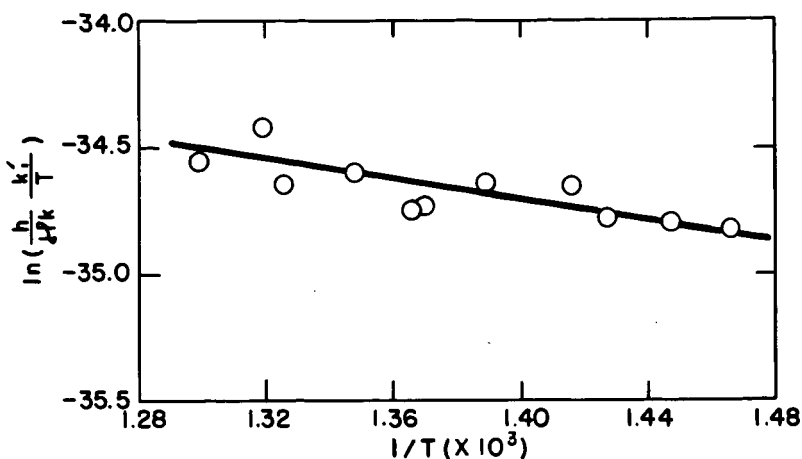


Figure 5. Eyring Plot for Evaluating ΔH^\ddagger and ΔS^\ddagger ,
First Order Region.

LITERATURE CITED

- (1) Berkowitz, N., *Fuel*, **39**, 47 (1960).
- (2) Daniels, F., and Alberty, R. A., "Physical Chemistry", New York, Wiley (1961).
- (3) Fitzgerald, D., *Fuel*, **35**, 178 (1956).
- (4) Glasstone, S., Laidler, K. J., and Eyring, H., "Theory of Rate Processes", New York, McGraw-Hill (1941).
- (5) Hill, G. R., "Experimental Energies and Entropies of Activation--Their Significance in Reaction and Rate Prediction for Bituminous Coal Dissolution", paper submitted for publication in *Fuel*.
- (6) Hill, G. R., and Lyon, L. B., *Ind. and Eng. Chem.*, **54**, 36 (1962).
- (7) Kessler, M. F., and Vecerikova, V., *Brennstoff-Chem.*, **40**, 52 (1959).
- (8) Kini, K. A., *Fuel*, **42**, 103 (1963).
- (9) Shapatina, E. A., Kalyuzhnyi, V. V., and Chukhanov, Z. F., *Doklady Acad. Nauk S.S.S.R.*, **72**, 869 (1950).
- (10) Stone, H. N., Batchelor, J. D., and Johnstone, H. F., *Ind. and Eng. Chem.*, **46**, 274 (1954).
- (11) van Krevelen, D. W., Huntjens, F. J., and Dormans, H. N. M., *Fuel*, **35**, 462 (1956).
- (12) Wilson, P. J., Jr., and Wells, J. H., "Coal, Coke and Coal Chemicals", New York, McGraw-Hill (1950).

SYMPOSIUM ON PYROLYSIS REACTIONS OF FOSSIL FUELS
PRESENTED BEFORE THE DIVISION OF PETROLEUM CHEMISTRY, INC.
AMERICAN CHEMICAL SOCIETY
PITTSBURGH MEETING, MARCH 23-26, 1966

THE MECHANISM OF THE HYDROGEN TRANSFER PROCESS
TO COAL AND COAL EXTRACT

By

George P. Curran, Robert T. Struck and Everett Gorin
Research Division
Consolidation Coal Company
Library, Pennsylvania

INTRODUCTION

A rather vast literature exists on the subject of solvent extraction of coal and excellent review articles are available. (1,4) The bulk of the literature deals with the effect of variation of chemical composition of the solvent and the nature of the coal on results achieved. Much less attention has been accorded to kinetic measurements of the dissolution process. H. P. Oele (5) and co-workers, however, studied in some detail the kinetics of coal dissolution in anthracene and β naphthol solvents. No transfer of hydrogen is involved in the process and the term extractive disintegration was coined to describe it.

A process has been under development for the past several years in the laboratories of the Consolidation Coal Company for the production of synthetic gasoline from coal. The first step in the process is the extraction of coal with a process derived solvent which possesses hydrogen donor properties. The process is thus one which involves transfer of hydrogen from the solvent to coal, similar to that studied by Pott-Broche (6) and others. Some literature data (3) were found relevant to the kinetics of this specific type of extraction process as applied to brown coal but little rate data appears to be available with bituminous coals.

Such data were therefore obtained to aid in the rational development of the process. The data reported here were all obtained with chemically pure solvents in order to simplify interpretation of the measurements and were all obtained in a batch system. Kinetic data were also obtained in a continuous system but this will be reserved for later publication.

The significance of the data to the mechanism of the hydrogen transfer process is discussed in some detail in this paper.

EXPERIMENTAL

The experiments were conducted in a micro-autoclave constructed of 316 stainless steel. The dimensions were 0.625" I. D. and 6" long with an internal volume of 30 ml. The autoclave was shaken vertically at 2300 cycles per minute. The shaking device was driven by an electric motor whose rotary motion was converted to reciprocating motion by means of a crank and cross-head linkage. The shaker was supported above a large fluidized sand bed which could be moved up and down rapidly by means of pulleys to immerse or expose the entire autoclave.

The experiments were conducted by first preheating the sand bed to about 40°F above the desired run temperature followed by rapidly immersing the autoclave in the sand bed. Blank experiments showed that the inner temperature of the autoclave rose to within 3°F of the desired temperature 2.5 minutes after immersing the autoclave in the sand bed. Final temperature control was effected by the addition of a dollop of cold sand to the fluidized bed.

At the end of the desired residence time, the sand bath furnace was lowered and a container of cold water was raised to surround the still shaking autoclave. This cooled the autoclave to essentially room temperature in less than 30 seconds. The reaction times reported are taken as the total time from immersion to quenching less one minute for effective heat up time.

All coal runs were made with a Pittsburgh Seam coal from the Ireland Mine in Northern West Virginia. The coal was crushed and screened to give two fractions, i. e., 100 x 200 Mesh and 28 x 48 Mesh with the analyses shown in Table I-A.

Initial runs showed identical results with the two size fractions so that all further work was carried out with the 28 x 48 Mesh coal.

Each run was conducted with 2 grams of coal while the total amount of solvent was varied between 4 and 8 ml. in individual runs.

No attempt was made to remove air from the autoclave before sealing. The oxygen content of the air above the charge varied between 0.3 to 0.7 wt. % of the coal depending on the filling ratio of the autoclave.

The depth of extraction was measured by the amount of filter cake obtained which was insoluble in xylene at 220°F. The coal conversion was calculated from the weight of dry filter cake and the weight of coal charged as follows:

$$\% \text{ Coal Conversion (MAF)} = \frac{100 (\text{g MAF coal charged} - \text{g dry cake})}{\text{g MAF coal charged}}$$

Experiments were also conducted with a "shallow" coal extract whose composition is given in Table I-B. The extract was prepared by extraction of Ireland Mine coal in a one-gallon stirred autoclave at 650°F for one hour using decalin as solvent. The depth of extraction was 23 percent of the MAF coal.

The bulk of the runs used tetralin as a model for the hydrogen donor liquid, although other pure hydrogen donors were used as will be discussed below.

The amount of hydrogen transferred was determined by analysis of the recovered solvent. The principal product resulting from the transfer of hydrogen to the coal is naphthalene. Appreciable quantities of indane and C₄ benzenes are also formed. Small quantities of cis and trans decalin may also be present.

The weight percent hydrogen in the recovered solvent was determined from the recovered solvent analysis assuming no materials boiling below indane or above naphthalene were formed from the tetralin. The weight of hydrogen transferred was then determined from the difference in weight of hydrogen in the feed tetralin and recovered solvent.

The analysis of the recovered solvent was carried out by first vacuum distilling the product filtrate to recover a cut with a nominal boiling range of 160 x 230°C at 1 atmosphere. The above fraction was extracted with 10% aqueous caustic to remove the tar acids and then analyzed with a Perkin-Elmer Model 154C gas chromatograph.

Separate aliquot portions are analyzed on two different columns as given below:

- Column No. 1 (Polar) - 20% diisodecylphthalate on 60 x 80 M Chromosorb in 1/4" O. D. x 8' stainless steel column at 175°C.
- Column No. 2 (Non-Polar) - 20% DC - Silicone oil on 60 x 80 M Chromosorb in same type column as above maintained at 160°C.

The polar column is used to effect adequate resolution between the naphthalene and tetralin peaks which cannot be achieved with the non-polar column.

Similar gas chromatography analyses were made to define the amount of hydrogen transferred from other pure solvents.

Some experiments were also conducted in either a 300 ml Aminco rocking autoclave or a 1 liter Parr bomb. This was done when the main purpose was not kinetic measurements but to obtain a more complete analysis of the reaction products.

RESULTS AND DISCUSSION

A. Maximum Amount of Hydrogen Transfer

The emphasis in the discussion of the kinetic results will be on measurement of the amount of hydrogen transferred since this is a quantity identifiable with a precise chemical process. Experimental work indicated that there is a "practical" maximum quantity of hydrogen that can be transferred to either coal or extract in a purely thermal process. Some additional hydrogen transfer may be obtained by further treatment at more severe conditions, but little in the way of new useful products are obtained, i. e., very little conversion of asphalt to liquid products occurs. These maximum limits for the coal and extract used in this work are apparently 2.6 and 2.2 wt. % of hydrogen transferred, respectively.

The product distribution resulting from extraction of coal at conditions approaching maximum hydrogen transfer are given in Table II.

B. Basic Nature of Reaction

The hydrogen transfer reaction is first of all a purely thermal process, i. e., attempts to accelerate the reaction with contact catalysts of the hydrofining type (cobalt molybdate on alumina) or with cracking catalysts (silica-alumina) were unsuccessful.

It may be natural to regard the process, also, as a simple second order reaction involving coal or extract molecules and a hydrogen donor molecule.

TABLE II
Hydrogen Donor Extraction of Ireland Mine Coal
at Severe Conditions

	100 x 200 Mesh		Tetralin/Coal, Wt. Ratio	1.5	3.0	1
	28 x 48 Mesh	4.66				
<u>Analysis of Feed Coal</u>						
% by Wt. Dry Basis						
H	4.86	4.66				
C	71.77	70.21				
N	1.25	1.48		10	13	715-750°F
O (diff.)	7.12	6.51		60	60	Hold 750°F
Organic S	2.48	2.25		11	4	750-715°F
FeS ₂	3.70	6.25				
Other Ash	8.82	8.64				
Total Ash	12.52	14.89				
<u>Yields, Wt. % MAF Coal</u>						
H ₂				0.3	0.5	0.1
H ₂ S + CO ₂ + CO				1.6	1.0	0.9
H ₂ O				5.0	3.3	3.5
C ₁ -C ₃ Hydrocarbons				4.5	3.1	1.3
C ₄ x 400°F Distillate				5.4	18.4	14.2
400°F x 750°F Distillate				16.2		
Heavy Oil ⁽¹⁾				26.4	29.0	20.9
Asphaltenes ⁽²⁾				18.4	35.0	42.1
Benzene Insolubles ⁽³⁾				16.6	4.8	10.9
Cresol Insolubles				8.0	7.4	7.5
Total				102.4	102.5	101.4
% H ₂ Transferred				2.4	2.5	1.4

(1) Soluble in cyclohexane.
 (2) Soluble in benzene - Insoluble in cyclohexane.
 (3) Soluble in cresol - Insoluble in benzene.

There are two objections to this point of view. First of all, if this were so the process should follow a simple second order rate law

$$\frac{dH}{dt} = \frac{k(E)(H_T - H)(H_1^0 - H)}{100} \quad (1)$$

The definition of terms used in equation (1) is given in the appendix. The integrated form of equation (1) is

$$kt = \left(\frac{100}{H_1^0 - H_T} \right) \cdot \frac{1}{E} \ln \left[\frac{H_T(H_1^0 - H)}{H_1^0(H_T - H)} \right] \quad (2)$$

where H_T is assigned the value of 2.6 in the case of Ireland Mine coal. The justification for this will be presented later. It should be remembered here that $H_1^0 = 400/132$ (T/E).

It is undoubtedly naive to consider that simple second order kinetics would hold in this case where one is dealing with a non-homogeneous system. However, if the true mechanism is of this type, the second order rate law should hold at least approximately.

The results of such a test of the validity of the second order mechanism are given in Table II. Since the rate constant varies by a factor of 5 over the limited range of conditions tested, it is justifiable to discard the second order mechanism.

Another clue pointing in the same direction is the behavior of different solvents. A true second order reaction would naturally involve very specific stereochemical effects. Thus, it would be expected that only solvents that are very similar in structure would function at all, and that the rate of hydrogen transfer would depend markedly on the chemical structure of the donor.

Data summarized in Table IV again show that these properties of a second order process are not found. A wide diversity of solvents function as hydrogen donors as long as they contain mobile hydrogen bonds. The rate of hydrogen transfer with the more active donors appears to be about the same and independent of their structure.

It would seem, therefore, that the rate of thermal decomposition of the coal determines the extent of hydrogen transfer once a sufficiently reactive donor is used.

These observations would point to a free radical mechanism. The coal is dissociated into free radicals by thermal decomposition which are stabilized by capture of a hydrogen atom from a donor molecule. The hydrogen saturated radicals are now stable molecules and are sufficiently low in molecular weight to be soluble in cresol. Thus, a direct relationship exists between solvent extraction depth and hydrogen transfer. This subject will be discussed in more detail later.

Thus, if donor of sufficient activity or concentration is used, one in effect is studying the rate of thermal decomposition of coal or extract into free radicals.

C. Coal Conversion Kinetics

It is therefore logical to test the above proposition by treating the hydrogen donor extraction process as a first order reaction. The above treatment should apply under conditions where a high ratio of donor to coal is used such that change in concentration of donor during the course of the reaction may be neglected. Such a series of kinetic runs were made using a ratio of 4 cc tetralin per gram coal.

Figure 1 shows a first order rate plot for these runs for coal conversion where $\log \left(\frac{1}{1-\alpha} \right)$ is plotted against time. It is noted that the points of longer residence times fall reasonably well onto a straight line, but that short time points fall well below the line.

The treatment of coal conversion per se as a first order process assumes that only a single thermal decomposition process occurs with a characteristic rate constant. As a matter of fact, it appears more reasonable to assume that two or more decomposition processes occur simultaneously with different rate constants. The rate of coal pyrolysis on this model is given by the expression

$$C_T - C = \sum_{i=1}^n C_i e^{-k_i t} \quad (3)$$

where C_i is the weight percent of the coal which decomposes with the characteristic rate constant k_i .

After a relatively long reaction time, all terms with the higher rate constants decay rapidly such that only the last or slowest rate remains important. The coal conversion rate under these conditions reduces to

$$C_T - C = C_n e^{-k_n t} \quad (4)$$

TABLE III
Second Order Rate Constants in
Hydrogen Transfer to Coal at 730°F

Vol. % Tetralin in Solvent	$E \left(\frac{\text{gms MAF Coal}}{\text{cc}} \right)$	(T/E)	H_0	H_T	H	t (min.)	$k \text{ (min.}^{-1} \text{ cc gm atoms}^{-1}\text{)}$
100	0.178	4.5	13.6	2.6	0.48	10	0.85
↓	↓	↓	↓	↓	0.71	20	0.67
↓	↓	↓	↓	↓	1.22	60	0.36
25	0.178	1.12	3.39	2.6	0.16	5	2.12
↓	↓	↓	↓	↓	0.32	20	1.12
↓	↓	↓	↓	↓	0.47	60	0.56

TABLE IV
Comparison of Hydrogen Donor Activity of
Various Organic Substances
 Ireland Mine Coal Used in All Cases

Solvent	Temp., °F	Residence ⁽¹⁾ Time, Min.	% Hydrogen Transferred to MAF Coal
A - Perhydrophenanthrene	716	60	0.21
Decalin	734	↓	0.28
Indane	716	↓	0.33
o-Cyclohexylphenol	716	↓	0.98
Tetralin	716	↓	1.12
Dihydrophenanthrene	716	↓	1.21
<hr/>			
B - Tetralin	620	60	0.22
Cyclohexanol	620	↓	0.42
<hr/>			
C - 50% Tetralin-50% Decalin	800	20	1.36
50% Isopropanol-50% Decalin	800	↓	1.14

(1) Excludes heat-up time.

Equation (4) may be rearranged to the form

$$\ln \frac{1}{1-\alpha} = -\ln \left(\frac{C_N}{C_T} \right) + k_N t \quad (5)$$

Thus, in a first order plot such as shown in Figure 1, the slope is the value k_N of the smallest rate constant and the intercept $-\ln (C_N/C_T)$ may be used to determine the weight fraction of the coal (C_N/C_T) which decomposes at the low rate.

The above treatment leads to values of .52 and 0.38 for the ratio C_N/C_T at 670 and 730°F, respectively. It is clear that this ratio must be constant and not a function of temperature if it represents the true physical picture.

A more accurate analysis of the situation was made on the analog computer. It was assumed here, as shown in Figure 2, that one is dealing here with only two first order rates occurring in parallel, i. e., a relatively fast and a relatively slow rate. The best fit, which is the one shown in Figure 2, was made on the assumption that $\gamma = 0.50$, i. e., half the coal decomposes at a fast rate.

The fit obtained with this model is eminently satisfactory. The values of the rate constants obtained from the analog computer are given in Table V. It is seen that the high conversion rate is of the order of ten times the slow rate.

D. Relationship Between Coal Conversion and Hydrogen Transfer

The kinetic treatment of the coal conversion process is far from rigorous, since it is not possible to identify it with a precise chemical change. The above kinetic treatment presupposes that in essence two types of coal co-exist, i. e., refractory and labile material.

Hydrogen transfer can on the other hand be identified with a more definite chemical process. On the basis of the free radical picture outlined above, each gram mole of hydrogen transferred can be identified with the dissociation of a specific chemical bond into two free radicals.

The relationship between coal conversion and hydrogen transfer, therefore, might be helpful in throwing some light on the mechanism of the coal extraction process itself. The graphical relationship between the two quantities at 670 and 730°F is shown in Figure 3 and 4, respectively. In this work the solvent consisted of pure tetralin, or tetralin diluted with various quantities of another solvent of which decalin, paraffin hydrocarbons and xylene were used. Surprisingly enough, the coal conversion from these data alone appears to be little affected by the composition of the solvent and is determined primarily by the amount of hydrogen transfer. It is seen that the first 50 percent coal conversion is obtained with very little hydrogen transfer, i. e., < 0.2 wt. %. On the other hand to approach the ultimate possible coal conversion C_T which is approximately 91%, a relatively large amount of hydrogen transfer, i. e., 1.4% is required.

No substantial difference in the above relationship is apparent as the temperature is changed from 670 to 730°F. The 670°F data do, however, indicate a somewhat higher coal conversion at the same level of hydrogen transfer for the more polar solvents.

E. Kinetics of Hydrogen Transfer to Coal

The hydrogen transfer process was treated kinetically in the same fashion as coal conversion. As was pointed out above, there is less uncertainty in this case in identifying the process with a definite chemical change. The kinetic treatment can therefore be more rigorously applied.

It is necessary, in the kinetic treatment of the hydrogen transfer process, to assign a value to the maximum amount of hydrogen that can be transferred, i. e., H_T . A value of $H_T = 2.6$ was assigned. This is based on the fact that experimentally one approaches the same level of H_T under widely different conditions with 100 percent tetralin solvent as cited below:

<u>% H Transferred</u>	<u>Time, Minutes</u>	<u>Temperature, °F.</u>	<u>Unit</u>
2.0	120	730	Kinetics
2.5	60	800	Kinetics
2.4	94*	825	Batch Autoclave

*Total time above 700°F.

The first order type of rate plot is illustrated in Figure 5. The same tendency of the early time points to fall below the straight line remarked earlier in the case of coal conversion is noticed here likewise. Again, an initial first rate followed by a slow rate is indicated. The general kinetic treatment as a series of simultaneous first order reactions applies here likewise.

TABLE V
Summary of Rate Constants Derived from
Analog Computer

Temp., °F	Process	γ	First Order Constants, Min. ⁻¹	
			K ₁	K ₂
616	Coal Conversion	0.50	0.0089	--
670	" "	↓	0.248	0.0167
730	" "	↓	0.895	0.0916
<hr/>				
670	H ₂ Transfer to Coal	0.12	0.047	0.0013
700	"	↓	0.096	0.0040
730	"	↓	0.248	0.0084
800	"	0.149	1.85	0.0437
<hr/>				
670	H ₂ Transfer to Extract	0.15	0.0050	0.0008
700	"	↓	0.0135	0.0018
730	"	↓	0.0195	0.0043

TABLE VI
Energies and Entropies of Activation in Coal
Conversion and Hydrogen Transfer Rate Processes

Process	Energy of Activation, Kcal/Mole		Entropy of Activation, e.u.	
	Mean Value	Prob. Error	Mean Value	Prob. Error
Coal Conversion - - Fast Rate	28.1	1.4	-23.5	2.0
Hydrogen Transfer to Coal - Fast Rate	45.1	1.4	-4.6	2.0
- Slow Rate	41.7	1.5	-21.0	2.1
Hydrogen Transfer to Extract				
- Fast Rate	33.8	5.7	not calculated	
- Slow Rate	47.4	1.2	-9.2	1.7

$$H_T - H = \sum_{i=1}^n h_n e^{-k_n t} \quad (6)$$

The extrapolation technique based on the long time points leads to the expression

$$\ln \left(\frac{1}{1-\alpha} \right) = -\ln \left(\frac{h_n}{H_T} \right) + kt \quad (7)$$

The ratio h_n/H_T here is the fraction of the total hydrogen which is transferred at the slow rate.

Again, a model was chosen based on only two types of bonds, one relatively strong and the other relatively weak. The extrapolation technique as applied in Figure 5 leads to values of the fraction h_n/H_T varying from 0.96 at 670°F to 0.89 at 730°F.

A more accurate appraisal of the dual first order model was made on the analog computer as illustrated in Figure 6. The fraction of weak bonds present γ was assigned the value $\gamma = 0.12$ which appeared to give the best fit. A value of $\gamma = 0.149$ was assigned to the 800°F. points although in the strict sense of the word γ should be independent of temperature.

The rate constants derived from the analog computer are given in Table V. It is seen from Table V that the fast hydrogen transfer rate corresponds roughly to the slow coal conversion rate though it is 2-3 times higher.

The above identification is reasonable since the fast coal conversion rate is associated with little or no hydrogen transfer. The fast hydrogen transfer rate apparently takes over in the coal conversion range of 50-90 percent which corresponds to the slow coal conversion rate. The slow hydrogen transfer rate corresponds in all likelihood to continued transfer of hydrogen to coal extract.

F. Kinetics of Hydrogen Transfer to Extract

The extract used in this work was a shallow extract, i. e., obtained with decalin solvent at 650°F with total coal conversion of only 23 percent.

The kinetic treatment followed the pattern set forth for the coal work. The first order rate plots are shown in Figure 7. The values of γ calculated by the extrapolation technique show that γ ranges from .09 to .13 at 730°F. The analog computer treatment is illustrated in Figure 8. In this case a value of $\gamma = 0.15$ gave the best fit.

The rate constants from the analog computer are given in Table V. It might be expected that the slow rate in the case of coal would correspond to the fast rate in the case of extract. This is seen not to be the case since the fast extract rate is of the order of 3 to 4 times greater than the slow coal rate. The lack of agreement is partly due to the fact that shallow rather than deep extract was used where the comparison would be more valid. Data obtained with deep extracts were insufficient for calculation of rate constants but showed that the rate is indeed slower.

G. Activation Energy, Entropy of Activation in Coal Conversion and Hydrogen Transfer to Coal and Extract

The activation energies were derived by a least squares analysis of the standard Arrhenius type plot as shown in Figures 9 and 10. The resulting equations of the line and the values of the activation energies are given on the figures. The probable error in the activation energy is listed, also.

The activation energies and entropies of activation are summarized in Table VI. Insufficient data are available to estimate the activation energy corresponding to the slow coal conversion rate.

The entropy of activation was estimated by use of the Theory of Absolute Reaction Rates. (2)

$$\text{Rate Constant} = e \left(\frac{kT}{h} \right) e^{-E_{\text{exp}}/RT} e^{\Delta S^\ddagger / R} \quad (8)$$

where ΔS^\ddagger is the entropy of activation.

The exact quantitative value of ΔS^\ddagger is of little significance but its sign and order of magnitude is significant relative to the structure of the activated complex and hence the mechanism of the process.

The low activation energy for the high coal conversion rate of 28 Kcal/mole is well below that of most "reasonable" chemical bond strengths. Thus, it appears doubtful that the reaction involves rupture of a conventional covalent bond. This is consistent with the fact that the fast rate (approximately half of the total conversion) occurs with no significant hydrogen transfer. The energy of activation likely may be attributed to the breaking of non-valence bonds, i. e., hydrogen bonds and the like. The high negative value of the entropy of activation indicates

Figure 1

COAL CONVERSION VS TIME

1st Order Rate Plots

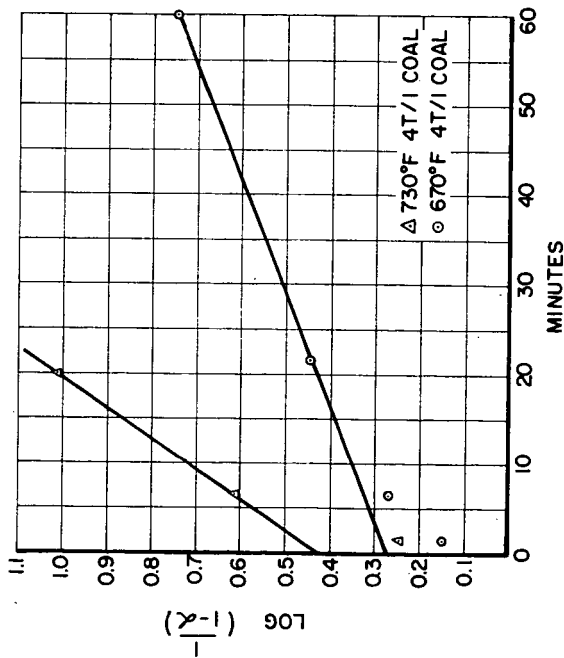
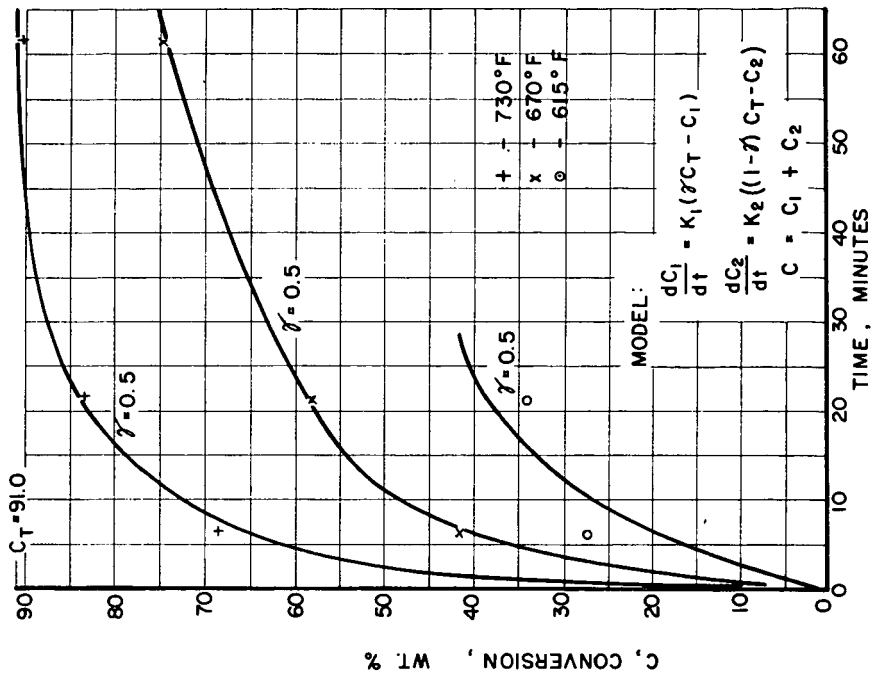


Figure 2

RATE PLOTS - COAL CONVERSION



a much more ordered structure in the activated complex than in the original coal molecule. This may be rationalized as meaning that the surrounding coal molecules must be oriented in a very specific manner to permit escape of the small coal molecule into the surrounding solvent medium.

The hydrogen transfer rates for both coal and extract were also treated in the same manner. The values of the energies and entropies of activation for the initial fast rates is probably of little significance since the accuracy of determination of the characteristic rate constants is not high.

The accuracy for determination of the values for the slow rates is much better since this corresponds to 85-90 percent of the total observed reaction.

The activation energy of the slow rate in the case of extract is higher than in the case of coal. This is to be expected since somewhat stronger bonds are involved. The energy of activation in both cases is somewhat low, however, i. e., ca. 45 Kcal/mole for most normal covalent bonds. The heat of dissociation of carbon-carbon bonds for example varies for most simple molecules between 65-85 Kcal/mole. The low value is indicative of a highly resonating structure in the free radicals produced by bond rupture which stabilizes them. This is analogous to the well-known stable free radicals of organic chemistry such as triphenyl methyl which are stabilized by the same mechanism.

The entropies of activation are again negative. In the case of simple known unimolecular reactions where dissociation to free radicals is involved a positive entropy of activation is usually observed. Thus, in this particular instance the proposed model does not appear to be wholly consistent with the facts.

H. H₂ Transfer Rate as Effected by Tetralin Concentration and Tetralin/MAF Coal Ratio

The above kinetic treatment applies only to the case where high solvent to coal and/or extract ratios are employed and where high tetralin concentrations are used. The hydrogen transfer rate falls off when either of the above quantities are reduced, although it is much more sensitive to a reduction in the latter than to the former quantity. A wholly consistent kinetic model must predict the effect of variation of the above parameters.

Experimentally only sufficient data are available in the case of coal for testing the applicability of kinetic models. Even here most of the data revolves about variation only of the tetralin concentration. The testing of kinetic models in the case of coal is difficult as mentioned above since the system is not truly a homogeneous one.

A number of models were considered to represent the kinetics, but the one given below was chosen by reason of simplicity.

This model considers that the extract or MAF coal has built in hydrogen donor structures which compete for the radicals produced in thermal dissociation. Thus, the kinetic model consists of the following sequence of reactions:

<u>Reaction</u>	<u>Rate Constant</u>
$E \rightarrow 2R$	k_0
$R + T \rightarrow RH + T^-$	k_1
$R + E \rightarrow RH + E^-$	k_2
$R + T^- \rightarrow RH + D$	k_3
$R + E^- \rightarrow RH + DE$	k_4

where T⁻ and E⁻ in the above correspond to radicals produced by abstraction of a hydrogen atom from tetralin (tetralyl radical) and extract, respectively. D and DE are, respectively, dihydro naphthalene and the corresponding dehydrogenated structure derived from extract.

Dihydro naphthalene is undoubtedly a much more reactive hydrogen donor than naphthalene itself, and rapidly undergoes similar reactions wherein it is converted to naphthalene. It thus is present in a very small steady-state concentration such that its activity for hydrogen transfer is equivalent to that of tetralin. From the kinetic point of view it is appropriate to disregard its presence. Experimentally, we have at the present time no definite evidence for or against the presence of dihydro naphthalene. Dihydro naphthalene boils between naphthalene and tetralin and thus is likely difficult to separate even on a gas chromatograph. It would, however, be of interest in the future to prove definitely the presence or absence of this compound as an intermediate.

The above mechanism can be used to derive an expression between the amount of hydrogen transferred from tetralin H₁ and the total amount of hydrogen transferred by all

Figure 3

COAL CONVERSION
vs
PERCENT H TRANSFER AT 730°F

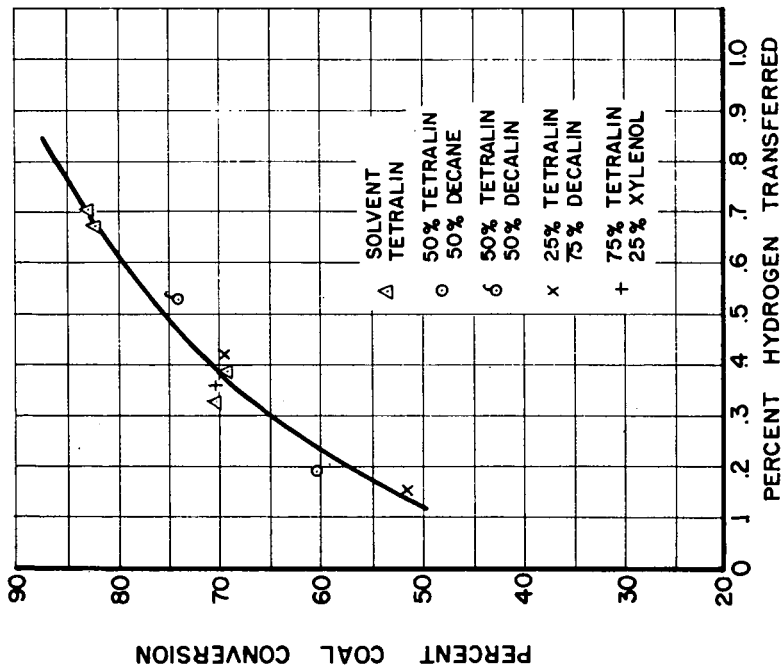
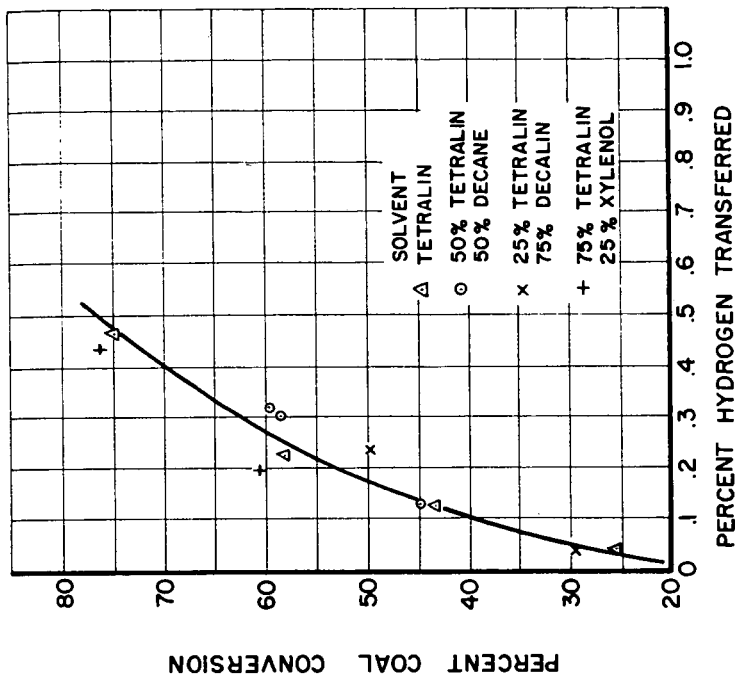


Figure 4

COAL CONVERSION
vs
PERCENT H TRANSFER AT 670°F



mechanisms H as shown below:

$$\frac{dH_1}{dH} = \frac{(H_1^0 - H_1)}{(H_1^0 - H_1) + k \{H_E^0 - (H - H_1)\}} \quad (9)$$

where $k = (k_2/2 k_1)$

Integration of equation (9) leads to the equation

$$\left(1 - \frac{H_1}{H_1^0}\right)^k = 1 - \left(\frac{H - H_1}{H_E^0}\right) \quad (10)$$

The left hand side of equation (10) may be expanded by the binomial theorem. As an approximation only the first term of the expansion is used since $H_1/H_1^0 < 1$. The result, after rearranging and collecting terms and noting that $H_1^0 = 400/132 (T/E)$, is

$$\frac{1}{H_1} = \frac{1}{H} \left[1 + C \left(\frac{E}{T}\right)\right] \quad (11)$$

where

$$C = kH_E^0 \left(\frac{132}{400}\right)$$

Experimental data obtained at 670°F and 730°F using 4 cc total solvent/gm coal were used to test equation (11). The test consists of plotting $1/H_1$ versus E/T . Each series of points at constant temperature and residence time should lie on a straight line. The slope (C/H) divided by the intercept $(1/H)$ should be a constant, i. e., C for each residence time series at constant temperature.

The tests for validity of equation (11) at 670 and 730°F are shown in Figures 11 and 12. Constant values of $C = 3.7$ and 4.2 were used for all the 670°F data and 730°F data, respectively.

The fit to the experimental data is quite good for 21.5 and 61.5 minute points but is poor for the 6.5 minute points. The accuracy of the experimental data points themselves are poor at the shorter times, however, due to the small amount of hydrogen transferred.

The equations derived above must be regarded as semi-empirical and are useful for estimating the effect of tetralin concentration at constant total solvent-to-coal ratio. They cannot be safely used to estimate hydrogen transfer rates at lower solvent-to-coal ratios.

Equation (11) predicts that the amount of hydrogen transfer obtained should be the same at the same tetralin-extract ratio irrespective of the tetralin concentration in the initial solvent. The experimental facts are not in accord with this, since the amount of hydrogen transfer increases at constant (T/E) with increasing tetralin concentration.

A few data points, for example, are available at 730°F and a lower solvent/coal ratio, i. e., 2 cc/gm. The experimentally determined amount of hydrogen transfer as compared with that estimated by means of equation (11) is shown below:

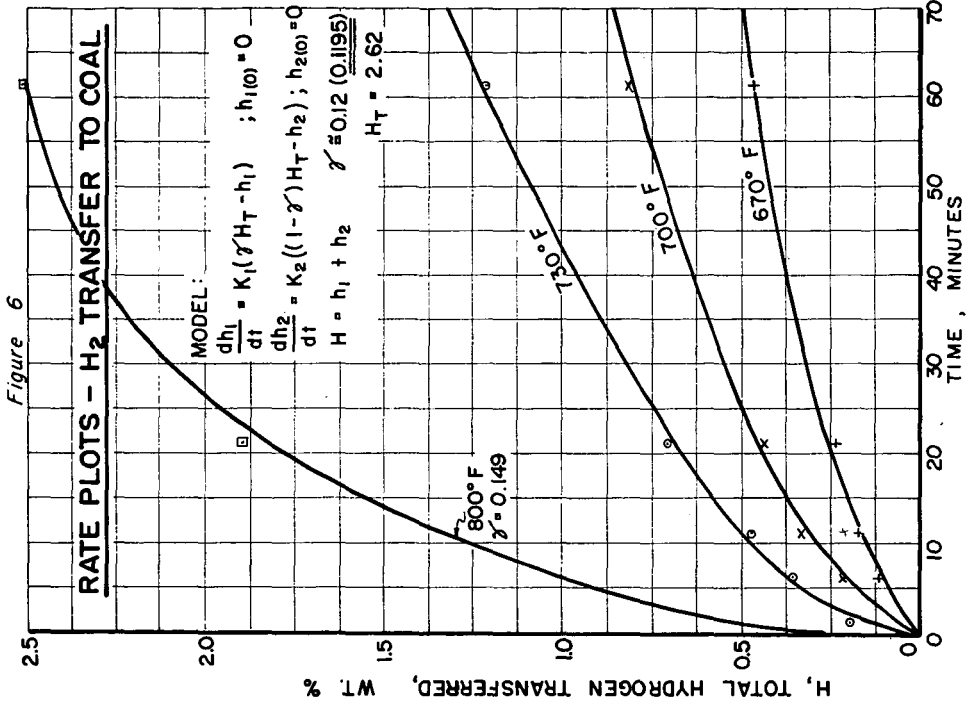
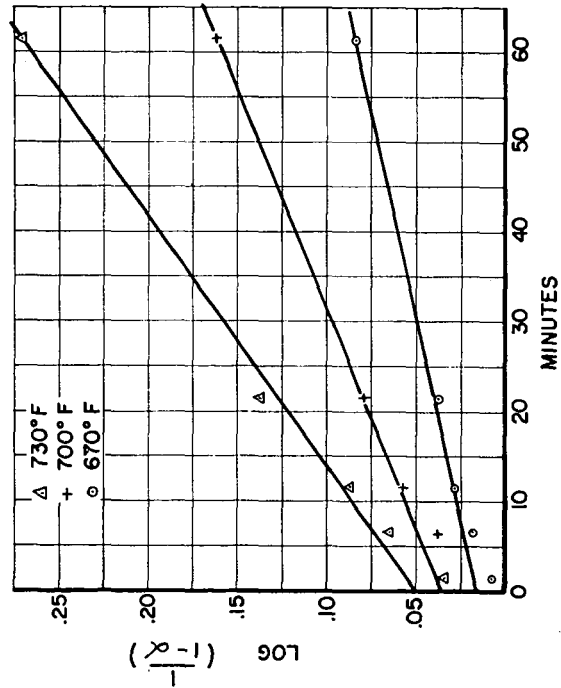
Res. Time Minutes	Solvent/Coal cc/gm	Volume % Tetralin	Hydrogen Transfer	
			Observed	Predicted
6.5	2	100	.33	.26
21.5	2	100	.68	.52

J. Evolution of Free Hydrogen

It has been observed under severe operating conditions, i. e., high temperatures and/or long residence times, that a considerable fraction of the hydrogen released from the tetralin appears as free hydrogen (cf. Table II). Under mild operating conditions little free hydrogen is produced. These facts are also in accord with the general mechanism outlined above. The mechanism at high tetralin concentrations where the recombination of radicals and hydrogen donor properties of the acceptor may be neglected may be written as follows:

Reaction	Rate Constant
$E \rightarrow 2 R$	k_0
$R + T \rightarrow RH + T^-$	k_1
$R + T^- \rightarrow RH + D$	k_3
$T^- \rightarrow D + H$	k_5
$H + T \rightarrow T^- + H_2$	k_6

Figure 5
H₂ TRANSFER TO COAL VS TIME
 1st Order Rate Plots



Thus, molecular hydrogen may be formed by thermal decomposition of the tetralyl radical by way of reactions 5 and 6. High operating temperatures will favor this reaction since reaction 5 will have a higher activation energy than reactions 1 and 3. This is seen from the differential equation corresponding to the above reaction sequence.

$$\frac{dH_2}{dH_1} = \frac{k_1 k_5}{2 k_0 k_3} \left[\frac{\left(\frac{T}{E}\right) \frac{400}{132} - H_1 - 2 H_2}{(HT - H_1)} \right]$$

where H_2 corresponds to moles of free hydrogen produced and H_1 corresponds to gram atoms of hydrogen actually transferred to the extract.

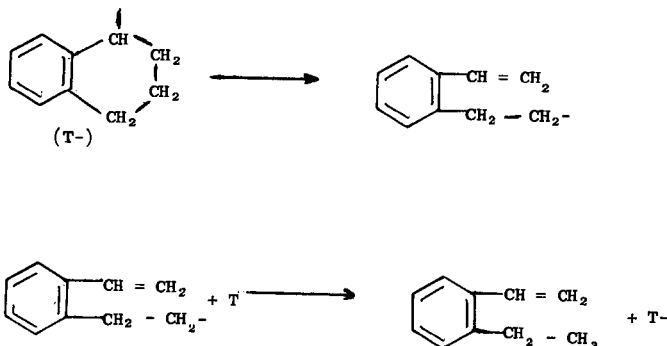
Equation (12) likewise predicts that the relative proportion of free hydrogen will increase at constant temperature with increasing residence time due to decrease in rate of production of free radicals from the coal or extract. This is also in accord with other experimental data which will be presented in a future publication.

K. Sensitized Thermal Decomposition of Tetralin

It has been observed that decomposition of tetralin is enhanced when it is used as a hydrogen donor. This is illustrated by the data in Figure 13 where the decomposition products as a function of time at 800°F are plotted. The tetralin decomposition products other than naphthalene are found largely in two peaks in the gas chromatograph which are labeled arbitrarily as C_4 benzenes and indane, respectively. These do not necessarily correspond to actual compounds produced since these were not definitely identified. The peaks in the gas chromatograph labeled as C_4 benzenes and indanes have, however, the same retention time as those of the corresponding pure compounds.

Thus, unsaturated compounds such as o-ethyl vinyl benzene and o-methyl allyl are not excluded as possible major decomposition products.

Increased yields of these decomposition products would be expected as a result of thermal decomposition of the tetralyl radical produced from the coal radicals as follows:



LITERATURE CITED

- (1) Dryden, I. G. C., "Chemistry of Coal Utilization", (Ed. H. H. Lowry), Supplementary Vol., 237, John Wiley and Sons, New York, 1962.
- (2) Glasstone, Samuel; Laidler, A. J., and Eyring, Henry, "Theory of Rate Processes", McGraw Hill, New York, 1941.
- (3) Jostes, F., and Siebert, K., Oel, Kohle, Erdoel, Teer 14, 777-83 (1938).
- (4) Kiebler, M. W., "Chemistry of Coal Utilization", (Ed. H. H. Lowry), I, 715, John Wiley and Sons, New York, 1945.
- (5) Oele, H. P., Waterman, H. I., Goedkoop, M. L., and Van Krevelen, D. W., Fuel 30, 169 (1951).
- (6) Pott, A., and Broche, H., Fuel 13, 91-5, 125-8, 154-7 (1934).

Figure 7

H₂ TRANSFER TO EXTRACT
1st Order Rate Plots

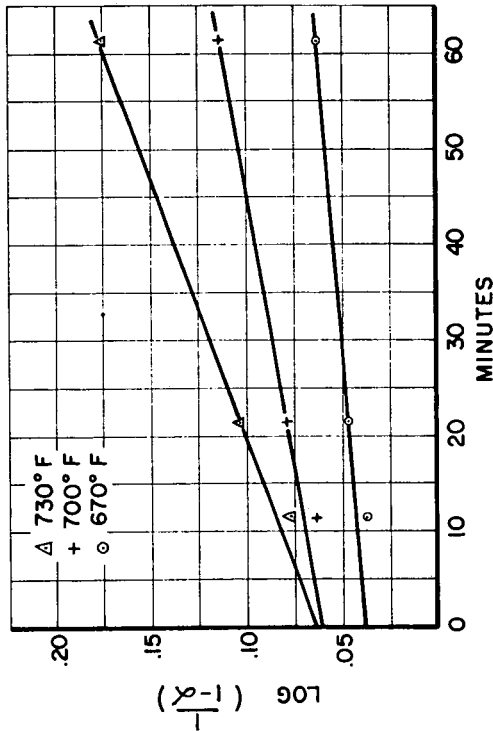


Figure 8

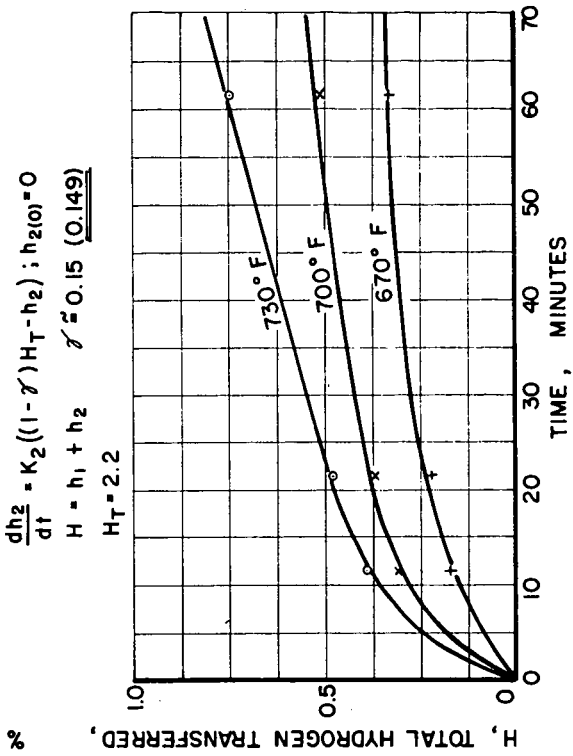
RATE PLOTS - H₂ TRANSFER TO EXTRACT

$$\frac{dh_1}{dt} = K_1(\gamma H_T - h_1) \quad ; \quad h_{1(0)} = 0$$

$$\frac{dh_2}{dt} = K_2((1 - \gamma) H_T - h_2) \quad ; \quad h_{2(0)} = 0$$

$$H = h_1 + h_2 \quad \gamma \approx 0.15 \quad (0.149)$$

$$H_T = 2.2$$



APPENDIX

Definition of Terms

- T = gms Tetralin/cc reaction mixture.
- E = gms Extract or MAF coal/cc reaction mixture.
- H₁ = gm atoms of H transferred from tetralin/100 gm extract or MAF coal.
- H = gm atoms of H transferred from all sources/100 gm extract or MAF coal.
- H_E = gm atoms of H transferred from extract/100 gm extract or MAF coal.
- H_T = Total gm atoms H transferred at infinite time/100 gms extract or MAF coal due to rupture of all bonds.
- H₁^o = Hydrogen transfer capacity of tetralin in gm atoms/100 gms extract or MAF coal.
= 400/132 (T/E).
- H_E^o = Hydrogen transfer capacity of extract in gm atoms/100 gms extract or MAF coal.
- γ = Fraction of "weak" bonds in coal or extract.
- C = Coal conversion in percent of MAF coal.
- C_T = Coal conversion in percent of MAF coal achieved at ∞ time.
- α = Fraction of ultimate conversion.
- α = C/C_T for coal conversion.
- α = H/H_T for hydrogen transfer.
- R = Free radical concentration, moles/cc.
- T- = Concentration of tetralyl radical, moles/cc.
- H₂ = gm moles free hydrogen produced/100 gms of extract or MAF coal.

Figure 9

ARRHENIUS PLOTS

A.) HYDROGEN TRANSFER RATES TO COAL
B.) COAL CONVERSION RATE

A) \circ $\text{LOG } K_1 = 14.362 - 9.879 \times 10^3/T$ $E_1 = 45.1 \pm 1.4 \text{ K Cal/mol.}$

+ $\text{LOG } K_2 = 11.717 - 9.134 \times 10^3/T$ $E_2 = 41.7 \pm 1.5 \text{ K Cal/mol.}$

B) Δ $\text{LOG } K'_1 = 9.230 - 6.147 \times 10^3/T$ $E_1 = 28.1 \pm 1.4 \text{ K Cal/mol.}$

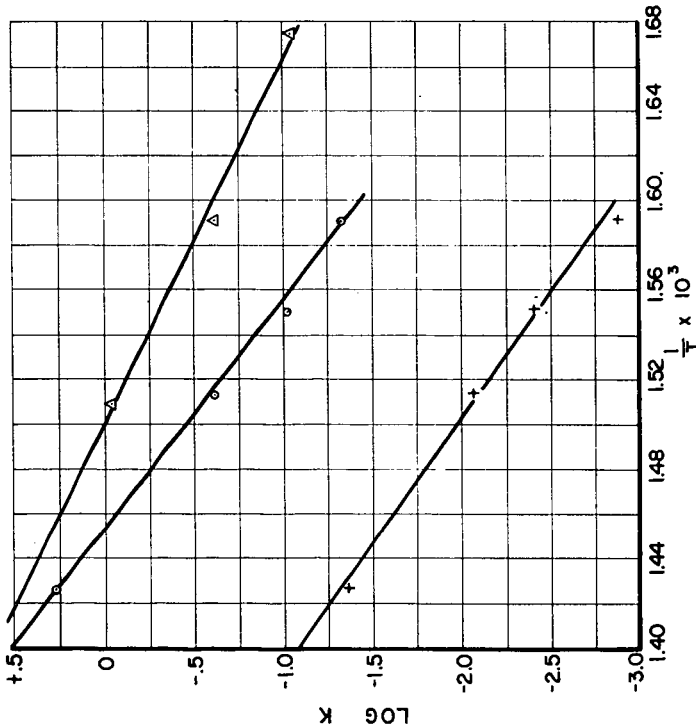


Figure 10

ARRHENIUS PLOTS FOR HYDROGEN TRANSFER RATES TO EXTRACT

+ $\text{LOG } K_1 = 9.532 - \frac{7.402 \times 10^3}{T}$ $E_1 = 33.8 \pm 5.7 \text{ K Cal/mol.}$

\circ $\text{LOG } K_2 = 13.348 - \frac{10.38 \times 10^3}{T}$ $E_2 = 47.4 \pm 1.2 \text{ K Cal/mol.}$

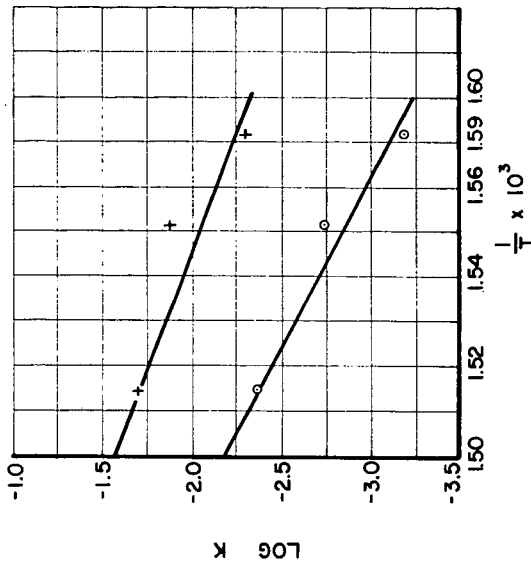


Figure 12

HYDROGEN TRANSFER RATE AT 730°F
AS AFFECTED BY MAF COAL/TETRALIN RATIO

cc Total Solvent/gm MF Coal = 4.0

$$\frac{1}{H_1} = \frac{1}{H} [1 + c(E_T)]$$

C = 3.7

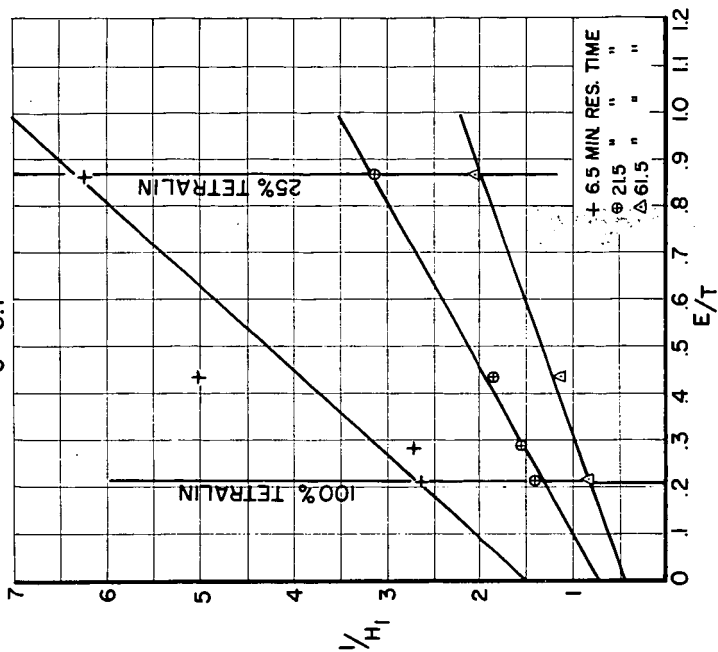


Figure 11

HYDROGEN TRANSFER RATE AT 670°F
AS AFFECTED BY MAF COAL/TETRALIN RATIO

cc Total Solvent/gm MF Coal = 4.0

$$\frac{1}{H_1} = \frac{1}{H} [1 + c(E_T)]$$

C = 4.2

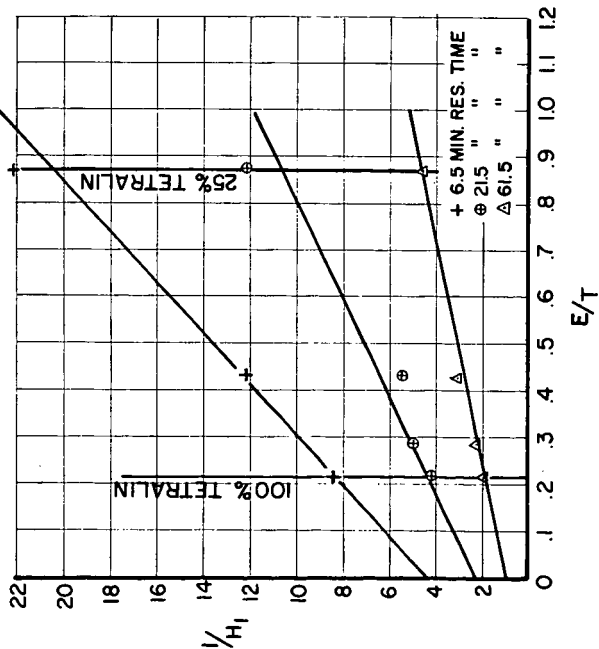


Figure 13

**THERMAL DECOMPOSITION OF TETRALIN
AT 800° F**

